Bursting and Spalling in Pretensioned U-Beams

by

David Andrew Dunkman, B.S.C.E.

Thesis

Presented to the Faculty of the Graduate School of

The University of Texas at Austin

in Partial Fulfillment

of the Requirements

for the Degree of

Masters of Science in Engineering

The University of Texas at Austin

December 2009

Bursting and Spalling in Pretensioned U-Beams

Approved by
Supervising Committee:

Oguzhan Bayrak, Supervisor

James O. Jirsa

Acknowledgements

First and foremost, I am grateful for the support of the Texas Department of Transportation, for providing the opportunity to gain practical, hands-on experience as I learn the research trade. Meetings with members of the TxDOT Project Monitoring Committee (including Dean Van Landuyt, Amy Eskridge, John Holt, Graham Bettis and David Hohmann) have proved both technically instructive and personally gratifying.

Additional support from the Cockrell School of Engineering was appreciated.

Thanks are due to a number of people at Ferguson Structural Engineering Laboratory. I am particularly grateful for the efforts of my advisor, Dr. Bayrak. His guidance and willingness to put in long (and odd) hours have greatly improved this work. Dr. Jirsa (co-Principal Investigator of Project 5831) and Dr. Wood have contributed mightily: with technical insight on structural behavior, and at other times, a hand marking cracks during a structural test.

I am thankful to the fellow graduate-student researchers on this project, Catherine Hovell, Andy Moore and Alejandro Avendaño, for sharing in the glories and the pains (e.g. 40 days per summer surpassing 100°F in an un-air-conditioned lab) of a long-term research effort. Staff at the Ferguson Lab deserve mention: Barbara Howard and Jessica Hanten, for keeping so many administrative tasks off my radar; Eric Schell and Mike Wason, for rescuing me when I got lost in a tangle of wires; and Blake Stasney, Dennis Fillip and Andrew Valentine, without whom nothing would get done on the lab floor.

Lastly I would like to thank family and friends for their continuous support throughout sometimes trying times.

14 August 2009

Bursting and Spalling in Pretensioned U-Beams

David Andrew Dunkman, M.S.E.

The University of Texas at Austin, 2009

Supervisor: Oguzhan Bayrak

Under Texas Department of Transportation (TxDOT) Research Project 5831, an experimental program was conducted at the Ferguson Structural Engineering Laboratory of The University of Texas at Austin to investigate the tensile stresses that develop in the end regions of pretensioned concrete U-beams at transfer of prestress. Understanding the effect of these "bursting" and "spalling" stresses is essential in order to design standard details that might lead to reliably serviceable end regions.

Two full-scale U-beam specimens, designed to be worst-case scenarios for bursting and spalling, were fabricated. Each beam had one square and one highly skewed end. To study the beam end regions, extensive instrumentation, including strain gages on transverse and lateral reinforcing bars, was employed. Experimentally determined bursting and spalling stresses in the end-region bars were compared to results of projects from the literature, which investigated I-beams and inverted T-beams.

Preliminary recommendations are made for changes in the standard reinforcing details for U-beam end regions. These details will be tested in the upcoming phase of Research Project 5831.

Table of Contents

CHAPTER 1: Introduction **1**

1.1 Impetus for Study of End-Region Stresses in U-Beams 1

1.2 Overview of TxDOT Research Project 5831 3

1.3 Thesis Organization 4

CHAPTER 2: Literature Review **6**

2.1 Overview 6

2.2 End-Region Tensile Stress Terminology 8

2.3 Bursting & Spalling Analysis in Prestressed Beam End Regions 13

2.3.1 General Approaches to Analysis 13

2.3.1.1 Elastic Analysis of Beam End Regions 14

2.3.1.2 Inelastic Analysis of Beam End Regions 17

2.3.1.3 Plastic Analysis of Beam End Regions 19

2.3.2 Effect of End Blocks 21

2.3.3 Analysis of U-Beams 23

2.4 Experimental Studies of Bursting & Spalling Effects 24

2.4.1 Studies of End-Region Surface Strains 24

2.4.1.1 Base, 1958 25

2.4.1.2 Zieliński & Rowe, 1960 & 1962 27

2.4.1.3 Marshall & Mattock, 1962 32

2.4.1.4 Gergely, Sozen & Siess, 1963 34

2.4.1.5 Arthur & Ganguli, 1965 36

2.4.1.6 Krishnamurthy, 1970 38

2.4.1.7 Uijl, 1983 39

2.4.1.8 Summary 41

2.4.2 Studies of End-Region Transverse-Reinforcement Strains 42

2.4.2.1 Marshall & Mattock, 1962 43

2.4.2.2 Gergely, Sozen & Siess, 1963 48

2.4.2.3 Itani & Galbraith, 1986 51
2.4.2.4 Tuan et al., 2004 53
2.4.2.5 Crispino, 2007 57
2.4.2.6 O'Callaghan, 2007 60
2.4.2.7 Smith et al., 2008 64
2.4.2.8 Summary 64
2.5 State of Practice 64
2.5.1 Field Experience with End-Region Cracking 64
2.5.2 Best Practices for Minimizing End-Region Cracking 70
2.5.3 Acceptable End-Region Cracking Criteria 72
2.6 Design Code Requirements 73
2.6.1 AASHTO Provisions 74
2.6.2 ASCE-ACI 323 Tentative Recommendations 79
2.6.3 ACI 318 Provisions 80
2.6.4 PCI Recommendations 81
2.6.5 CEB-FIP Recommendations 82
2.7 DOT Standards for U-Beams 82
2.7.1 Texas U-Beam 83
2.7.2 Florida U-Beam 88
2.7.3 Colorado U-Girder 89
2.7.4 Washington Trapezoidal Tub Girder 90
2.7.5 Comparison of End-Region Reinforcement 92
2.8 Summary 96
CHAPTER 3: Experimental Methods 97
3.1 Overview 97
3.2 Specimen Design 97
3.2.1 Prestressed Beam Theory 97
3.2.1.1 Linear and Nonlinear Stress Distributions 98
3.2.1.2 Elastic Shortening of Beam 99
3.2.1.3 Transfer Length of Prestressing Strand 100

3.2.2 U-Beam Design....101
3.3 Concrete Properties....104
3.3.1 Concrete Mixture Design....104
3.3.2 Concrete Mechanical Testing....106
3.3.3 Temperature-Match Curing....108
3.4 Steel Reinforcement Properties....111
3.4.1 Reinforcing-Bar Mechanical Testing....112
3.4.2 Prestressing-Strand Mechanical Testing....114
3.5 Instrumentation....119
3.5.1 Strain Gages on Reinforcing Bars....119
3.5.2 Strain Gages on Prestressing Strands....123
3.5.3 Data-Acquisition Systems....125
3.5.4 Thermocouples in Concrete....127
3.6 Beam Fabrication....130
3.6.1 Beam Casting at Precast Concrete Plant....130
3.6.2 Pretensioning Facility....133
3.6.3 Strand Tensioning....137
3.6.4 Beam Casting....140
3.6.5 Transfer of Prestress....145
3.6.6 Moving the Beam....146
3.7 Summary....147

CHAPTER 4: Results & Discussion....148

4.1 Overview....148
4.2 Experimental Results from Research Project 5831....148
4.2.1 Stresses Inferred from Measured Strains....148
4.2.2 Beam 1 Results....150
4.2.2.1 Beam 1: Cast & Release....150
4.2.2.2 Beam 1: Strand Stresses....153
4.2.2.3 Beam 1: Transverse-Bar Bursting & Spalling Stresses....155

4.2.2.4 Beam 1: Lateral-Bar Bursting Stresses 156
4.2.2.5 Beam 1: End-Block Temperature Profile.....157
4.2.3 Beam 2 Results 158
4.2.3.1 Beam 2: Cast & Release.....158
4.2.3.2 Beam 2: Strand Stresses 160
4.2.3.3 Beam 2: Transverse-Bar Bursting & Spalling Stresses 163
4.2.3.4 Beam 2: Lateral-Bar Bursting Stresses 164
4.2.3.5 Beam 2: End-Block Temperature Profile.....164
4.3 Database of Bursting & Spalling Stresses in Transverse Bars of Pretensioned Beam End Regions.....167
4.3.1 Studies of Bursting & Spalling 168
4.3.2 Assembly of Database.....169
4.3.3 Total Bursting/Spalling Force in the Beam End Regions.....171
4.3.4 Maximum & Average Bursting/Spalling Stresses in Beam End Regions.....173
4.3.5 Contributing Factors to High Maximum Bursting/Spalling Stress.....176
4.3.6 Evaluation of AASHTO LRFD & PCI Design Equations.....179
4.3.7 Concluding Remarks on Database Analysis.....181
4.4 Recommendations.....181
4.4.1 Recommended Texas U-Beam Reinforcing Details for Testing.....182
4.4.2 Special Considerations for Bursting Reinforcement.....184
4.5 Summary.....186
CHAPTER 5: Conclusions.....**188**
5.1 Summary of Research Program 188
5.2 Conclusions.....189
5.3 Recommended Future Research 191

APPENDIX A: Database of Transverse-Bar Bursting & Spalling Stresses in Pretensioned Beam End Regions 192

APPENDIX B: Calculations of Code-Required End-Region Reinforcement for U-Beam Specimens 207

B.1 AASHTO LRFD 207

B.2 PCI Design Handbook 207

B.3 CEB-FIP Model Code 207

APPENDIX C: Specimen Design Calculations 215

APPENDIX D: Concrete & Reinforcement Mechanical Test Results 219

D.1 Concrete Strength Results 219

D.2 Reinforcing-Bar Modulus & Strength Results 226

D.3 Prestressing-Strand Modulus & Strength Results 227

APPENDIX E: End-Block Temperature Profiles 228

REFERENCES 232

VITA 242

List of Tables

Table 2.1 *Range of stresses & total force reported for transverse reinforcement (Marshall & Mattock, 1962)* *45*
Table 2.2 *Causes of end-region cracking from improper technique per PCI report* *71*
Table 2.3 *Other causes of end-region cracking per PCI report* *71*
Table 2.4 *Causes of cracking summarized from national survey of bridge design/construction professionals conducted by Tadros et al., 2007* *72*
Table 2.5 *Typical DOT practice for repair of cracks in pretensioned concrete beams (Tadros et al., 2007)* *73*
Table 3.1 *Concrete mixture proportions* *105*
Table 4.1 *Beam 1 as-measured prestress* *151*
Table 4.2 *Beam 1 applied prestressing force compared with target value* *151*
Table 4.3 *Beam 2 as-measured prestress* *159*
Table 4.4 *Beam 2 applied prestressing force compared with target value* *160*
Table 4.5 *Specimens examined in past studies of bursting and/or spalling stresses* *168*

List of Figures

Figure 1.1 *Cross section of pretensioned concrete U-beam* 2
Figure 1.2 *DEF damage in end block of dapped trapezoidal box beam (after 13 years exposure)* 2
Figure 1.3 *U-beam end-block design alternatives for skewed ends* 3
Figure 2.1 *Severe cracking in a pretensioned concrete beam end region (Marshall & Mattock, 1962)* 7
Figure 2.2 *Convention for end-region stress direction* 10
Figure 2.3 *Development of splitting stress (Uijl, 1991)* 10
Figure 2.4 *End-region stress terminology (after Sanders, 1990)* 12
Figure 2.5 *Bursting & spalling stress distributions (after Lenschow & Sozen, 1965)* 12
Figure 2.6 *Effect of bursting & spalling stresses through exaggerated deformations of beam with discontinuities (after Hawkins, 1966)* 13
Figure 2.7 *Analytical approaches for prestressed beam end regions* 14
Figure 2.8 *Symmetrical prism method of Guyon for a beam under eccentric prestress (Sanders, 1990)* 15
Figure 2.9 *Symmetrical prism method of Guyon for a beam subject to multiple lines of prestress (Sanders, 1990)* 16
Figure 2.10 *Gergely-Sozen analysis model (Gergely & Sozen, 1967)* 18
Figure 2.11 *STM of Davis, Buckner & Ozyildirim (2005)* 20
Figure 2.12 *Transverse reinforcement required for Virginia bulb tee based on STM (after Davis, Buckner & Ozyildirim, 2005)* 21
Figure 2.13 *Effect of end blocks of various lengths on bursting force distribution (after Yettram & Robbins, 1971)* 22
Figure 2.14 *Shear stress distribution in Florida U-beam under prestress load only (Huang & Shahawy, 2005)* 23
Figure 2.15 *Bursting & spalling strains in Base rectangular beam* 26
Figure 2.16 *Spalling strains in Base IT-beams* 27
Figure 2.17 *Concrete prism with extensive surface gaging (Zieliński & Rowe, 1960)* 28
Figure 2.18 *Analytical stress at various locations compared to Zieliński & Rowe's experimental results (Yettram & Robbins, 1969)* 30
Figure 2.19 *Specimen with failure near flange/web junction (Zieliński & Rowe, 1962)* 31
Figure 2.20 *Surface instrumentation & strains at beam end (after Marshall & Mattock, 1962)* 33
Figure 2.21 *Surface instrumentation & strains over beam length (after Marshall & Mattock, 1962)* 33
Figure 2.22 *Prestressing force & spalling strains for a rectangular beam (after Gergely, Sozen & Siess, 1963)* 35
Figure 2.23 *Pretensioning frame at Glasgow (Arthur & Ganguli, 1965)* 37
Figure 2.24 *Mechanical gage points on I-beam specimen (after Arthur & Ganguli, 1965)* 37

Figure 2.25 *Mechanical gage points on I-beam specimen (after Krishnamurthy, 1970)* 39
Figure 2.26 *Typical bursting/splitting crack in hollow-core ribs (Uijl, 1983)* 40
Figure 2.27 *"Internal cracking" viewed in saw-cut specimen (Uijl, 1983)* 41
Figure 2.28 *I-beams studied by Marshall & Mattock* 44
Figure 2.29 *Typical transverse tensile strain variation (after Marshall & Mattock, 1962)* 45
Figure 2.30 *Linear regression analysis forming basis of Marshall & Mattock design equation (after Marshall & Mattock, 1962)* 47
Figure 2.31 *Actual spalling stress variation & uniform stress variation assumed for design* 48
Figure 2.32 *Stirrups serving as both transverse & confining reinforcement (Gergely, Sozen & Siess, 1963)* 49
Figure 2.33 *Typical transverse-bar strain gage locations (Itani & Galbraith, 1986)* 52
Figure 2.34 *Typical strain-gage location for I- & IT-beams* 55
Figure 2.35 *Strain-gage location for 43-in. I-beams* 55
Figure 2.36 *Typical crack pattern in Virginia bulb tee (after Crispino, 2007)* 58
Figure 2.37 *Typical gage locations (after Crispino, 2007)* 60
Figure 2.38 *Typical gage locations (O'Callaghan, 2007)* 62
Figure 2.39 *Typical crack pattern with widths (O'Callaghan, 2007)* 63
Figure 2.40 *Wide IT-beam monitored by Smith et al.* 64
Figure 2.41 *Beam with two strand groups (Fountain, 1963)* 65
Figure 2.42 *Prevalence of crack patterns noted in pretensioned I-beams (after Gamble, 1997)* 67
Figure 2.43 *Cracking in Texas U-beam, one week after release (Barrios, 1994)* 68
Figure 2.44 *Confining reinforcement details tested by Barrios (1994)* 69
Figure 2.45 *Confining reinforcement provided at end of beams with both details shown in Figure 2.44* 70
Figure 2.46 *Common cracks in pretensioned beams (PCI, 1985)* 71
Figure 2.47 *Required splitting reinforcement for a trapezoidal tub girder (after AASHTO LRFD, 2008, Interim)* 78
Figure 2.48 *U-beam as replacement for two I-beams (Ralls, Ybanez & Panak, 1993)* 83
Figure 2.49 *Texas/Florida U-beam section properties (54 in. standard)* 84
Figure 2.50 *Two- & three-strand-row design standards for 54-in. Texas U-beam (Ralls, Ybanez & Panak, 1993)* 84
Figure 2.51 *End-block design alternatives for Texas U-beam (minimum end-block dimensions drawn for maximum skew)* 86
Figure 2.52 *Skewed end-block dimensions for extreme cases* 86
Figure 2.53 *Additional transverse reinforcement near center of end block* 87
Figure 2.54 *Colorado U-girder section properties (48 in. deep, pretensioned standard)* 89
Figure 2.55 *Curved pretensioned/post-tensioned Colorado U-girder (Endicott, 2005)* 90
Figure 2.56 *Washington trapezoidal-tub-girder section properties (54 in. standard)* 91

Figure 2.57 *Harped strands in webs of Washington trapezoidal tub girder (Tadros, 2005)* 92
Figure 2.58 *Transverse reinforcement in end region of WSDOT trapezoidal tub girder (after AASHTO LRFD, 2008, Interim)* 93
Figure 2.59 *Transverse reinforcement in the end block of a Texas U-beam, divided into that provided within the projected areas of the void & the webs* 94
Figure 2.60 *Standard end-region reinforcement for U-beams (54 in. deep, 78 – 0.5-in. strands) vs. code requirements (counting all transverse reinforcement in end block)* 95
Figure 2.61 *Standard end-region reinforcement for U-beams (54 in. deep, 78 – 0.5-in. strands) vs. code requirements (neglecting transverse reinforcement within projection of void in end block)* 95
Figure 3.1 *Elastic stress trajectories in a post-tensioned concrete beam, illustrating the division into D- and B-regions (after Schlaich, Schäfer & Jennewein, 1987)* 98
Figure 3.2 *Concrete modulus equations from ACI 318 & 363* 100
Figure 3.3 *Tension-zone longitudinal reinforcement* 103
Figure 3.4 *Beam 1 & 2 design summary* 103
Figure 3.5 *U-beam end-block design alternatives for skewed ends* 106
Figure 3.6 *Cylinder compressive-strength testing* 107
Figure 3.7 *Schematic for splitting tensile-strength test (after Tuchsherer, 2007)* 108
Figure 3.8 *Maturity-age concept (Kehl & Carrasquillo, 1998)* 109
Figure 3.9 *Sure Cure temperature-match-curing system (Tuchsherer, 2007)* 110
Figure 3.10 *Reinforcing bar used in U-beam specimens* 112
Figure 3.11 *Reinforcing-bar tension testing in 60-kip test machine* 113
Figure 3.12 *Extensometer on reinforcing-bar sample* 113
Figure 3.13 *Failure modes for Grade 60 rebar & deformed wire* 114
Figure 3.14 *Typical strain-gage installation along pitched wire within strand (O'Callaghan, 2007)* 115
Figure 3.15 *Extensometer & strain gage on strand sample* 116
Figure 3.16 *Strands epoxied into black pipe for tensile-strength testing* 117
Figure 3.17 *Typical strand failure mode* 118
Figure 3.18 *Setup used for Beam 2 elastic-modulus testing for strand* 119
Figure 3.19 *Crack map for Beam 0, as received five months after cast & release* 120
Figure 3.20 *Typical strain-gage placement in beam end-region* 121
Figure 3.21 *Instrumentation for transverse reinforcement within end block* 122
Figure 3.22 *Strand strain-gage installation process (Beam 2, 45°-skewed end)* 124
Figure 3.23 *Completed strand strain gaging (inset from O'Callaghan, 2007)* 124
Figure 3.24 *Strand strain-gage locations (Beam 2)* 125
Figure 3.25 *Interface board used to connect strain-gage leads to quarter-bridges* 126
Figure 3.26 *Heuristic for checking quarter-bridge channels* 126
Figure 3.27 *Heuristic for checking half-bridge channels* 127
Figure 3.28 *Typical thermocouple instrumentation (Beam 2)* 128
Figure 3.29 *Typical thermocouple data (after Tuchscherer, 2007)* 128

Figure 3.30 *Thermocouple placement in small skewed end block (Beam 1)* *129*
Figure 3.31 *Placing concrete using sidewinder (concrete buggy)*..... *131*
Figure 3.32 *Consolidating bottom-flange concrete using internal vibrators & external form vibrators (not shown)* *131*
Figure 3.33 *Installing the interior-void form*..... *132*
Figure 3.34 *Filling the webs and end blocks around the interior-void form, held in place with hangers* *132*
Figure 3.35 *Finishing the top surface* *133*
Figure 3.36 *FSEL pretensioning bed (O'Callaghan, 2007)*..... *134*
Figure 3.37 *Wider bulkhead in place at stressing end*..... *135*
Figure 3.38 *Special tapered side form fabricated by Hamilton Form*..... *136*
Figure 3.39 *U-beam formwork in pretensioning bed*..... *136*
Figure 3.40 *Modifications to beam header* *137*
Figure 3.41 *Strands installed, tensioned to nominal stress for instrumentation*..... *138*
Figure 3.42 *Linear potentiometers (circled) used to monitor strand elongation*..... *139*
Figure 3.43 *Slump testing*..... *141*
Figure 3.44 *Cylinder molds set out for beam cast* *141*
Figure 3.45 *Placing concrete in the bottom flange*..... *142*
Figure 3.46 *Consolidating bottom-flange concrete using internal vibrators & external form vibrators* *142*
Figure 3.47 *Moving interior void into position after bottom flange is cast*..... *143*
Figure 3.48 *Positioning interior-void hangers* *143*
Figure 3.49 *Casting end block (and webs) around the interior void*..... *144*
Figure 3.50 *Placing concrete in large triangular end block (Beam 2, 45°-skewed end)* *144*
Figure 3.51 *Removing interior void form in preparation for transfer*..... *145*
Figure 3.52 *Detensioning by gradually decreasing pressure in stressing rams*..... *146*
Figure 3.53 *Lifting Beam 0 from delivery truck*..... *146*
Figure 4.1 *Strain time histories for two gages*..... *149*
Figure 4.2 *Beam 1 cast & release timeline with key events*..... *150*
Figure 4.3 *Beam 1 transverse-bar bursting & spalling stresses, with cracking from transfer* *152*
Figure 4.4 *Beam 1 prestress losses in instrumented strands, after transfer*..... *154*
Figure 4.5 *Beam 1 effective prestress & distance from beam end, after transfer*..... *154*
Figure 4.6 *Beam 1 lateral-bar bursting stresses*..... *156*
Figure 4.7 *Beam 1 end-block temperature profiles, at transfer of prestress* *157*
Figure 4.8 *Beam 2 cast & release timeline with key events*..... *159*
Figure 4.9 *Beam 2 transverse-bar bursting & spalling stresses, with cracking from transfer* *161*
Figure 4.10 *Beam 2 prestress losses in instrumented strands, after transfer*..... *162*
Figure 4.11 *Beam 2 effective prestress & distance from beam end, after transfer*..... *162*
Figure 4.12 *Beam 2 lateral-bar stresses*..... *164*
Figure 4.13 *Beam 2 end-block temperature profiles, at transfer of prestress* *165*

Figure 4.14 *Temperature time variation with temperature limits (Beam 2)..... 166*
Figure 4.15 *Temperature profiles for two end-block alternatives for skewed ends at time of maximum temperature differential (Beams 1 & 2)..... 167*
Figure 4.16 *Proportion of database in which bursting & spalling behaviors were examined..... 169*
Figure 4.17 *Transverse reinforcement within the U-beam end block..... 170*
Figure 4.18 *Total transverse-bar bursting/spalling force & prestressing force..... 171*
Figure 4.19 *Total transverse-bar bursting/spalling force & prestressing force, with section geometry for beam end-region specimens emphasized..... 172*
Figure 4.20 *Assumed end-region transverse-bar stress distributions & associated maximum-to-average stress ratios..... 174*
Figure 4.21 *Maximum transverse-bar bursting/spalling stress compared with average within h/4 design region..... 175*
Figure 4.22 *Contribution of high average bursting/spalling stress in transverse reinforcement to high maximum bursting/spalling stress..... 176*
Figure 4.23 *Contribution of reinforcement provided within end h/4 region (normalized by that required by AASHTO LRFD) to high maximum transverse-bar bursting/spalling stress..... 177*
Figure 4.24 *Contribution of bottom-fiber stress near beam end to high maximum transverse-bar bursting or spalling stress..... 178*
Figure 4.25 *Relation between total transverse force & prestressing force [AASHTO LRFD]..... 180*
Figure 4.26 *Relation between total transverse force, divided by beam height-to-transfer-length ratio, & prestressing force [PCI]..... 180*
Figure 4.27 *Proposed end-region detail (cross-section)..... 183*
Figure 4.28 *Proposed end-region detail (elevation)..... 184*
Figure 4.29 *Design of bursting & spalling reinforcement in a U-beam with debonded strand..... 187*

CHAPTER 1

Introduction

1.1 IMPETUS FOR STUDY OF END-REGION STRESSES IN U-BEAMS

During the development of Texas Department of Transportation (TxDOT) standards for a new line of pretensioned concrete bulb tees (Tx girders), O'Callaghan (2007) conducted an experimental study of end-region stresses (bursting and spalling stresses) acting in these beams at transfer of prestress. Finding high stresses in transverse reinforcing bars stemming from long cracks in the bursting zone, he recommended changes to the standard end-region reinforcing details for the beams. Heavy reinforcement was continued out to one transfer length (36 in.) from the beam end, rather than one-third that distance.

Pretensioned U-beams (shown in cross section in Figure 1.1) were standardized by TxDOT in the early 1990s without the aid of experimental testing in the laboratory. Transverse-reinforcement detailing and concrete dimensioning (notably for web widths and end-block lengths) were developed based on common practice. The amount of transverse reinforcement in U-beam end regions, however, is small compared to that in the end regions of Tx girders. In light of the results of O'Callaghan (2007), comprehensive study of bursting and spalling in U-beams was warranted.

In addition, detailing for large concrete end blocks, notably the size, deserves re-examination. Large masses of concrete such as that found in an end block can cause high internal temperatures during curing, which in turn can lead to materials problems such as delayed ettringite formation (DEF). An example of severe DEF-related cracking causing the structural disintegration of a dapped trapezoidal box beam (a predecessor to the U-beam) with a 60 in. long end block is shown in Figure 1.2.

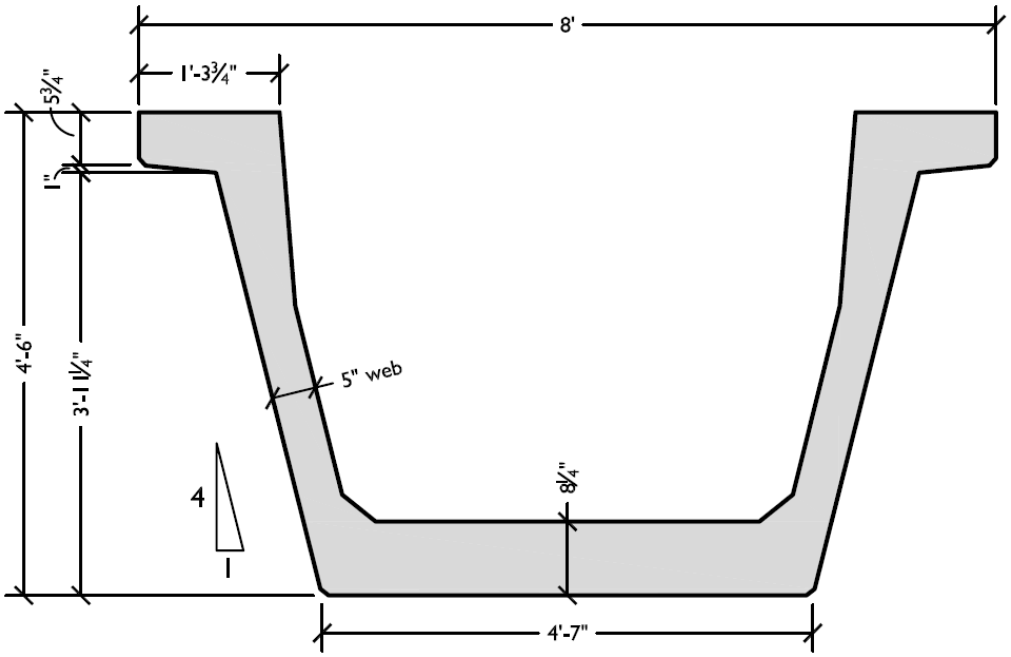

Figure 1.1 Cross section of pretensioned concrete U-beam

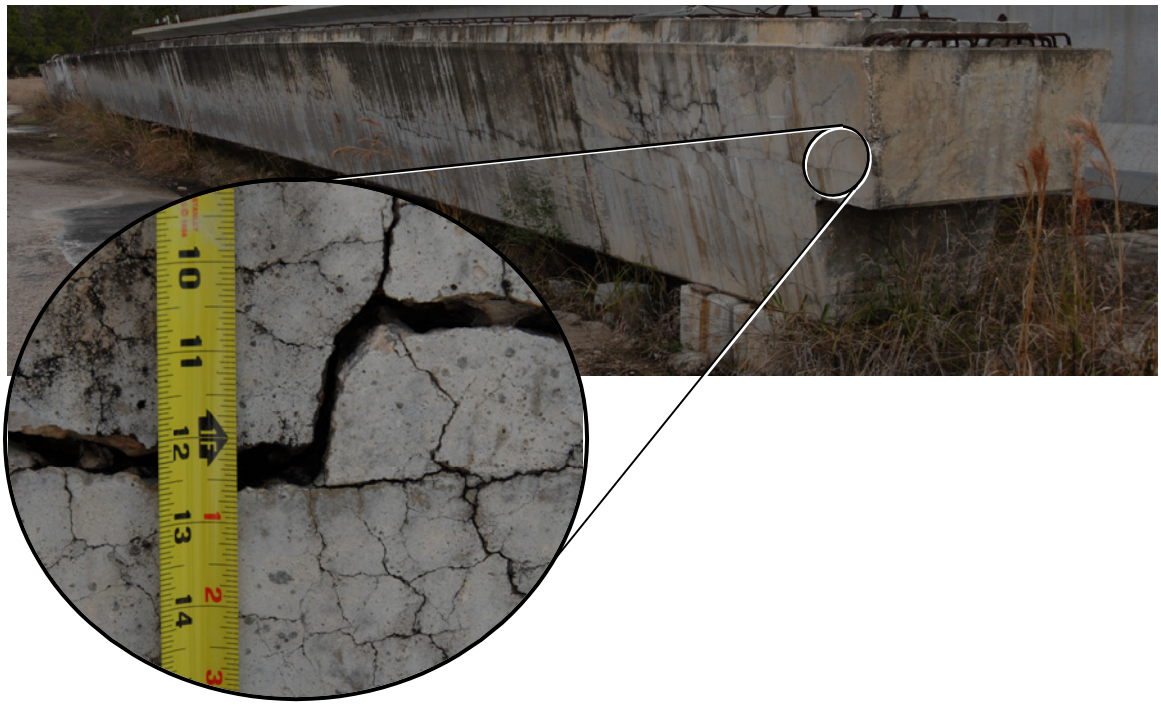

Figure 1.2 DEF damage in end block of dapped trapezoidal box beam (after 13 years exposure)

1.2 OVERVIEW OF TXDOT RESEARCH PROJECT 5831

In TxDOT Research Project 5831, concerns over the U-beam end-region detailing (reinforcement and concrete) are examined through a two-part study of behavior at prestress transfer (bursting and spalling forces) and under shear loading (service loads and overloads). This thesis focuses on bursting and spalling behavior; later reports will address results from shear testing.

Square and skewed U-beam end regions were examined. For skewed end regions, two end-block design alternatives are shown on the standard drawings. These alternatives provide for very differently sized end blocks, especially at large skews. Figure 1.3 shows the two end-block alternatives for the maximum permissible skew (45º). Should the smaller skewed end block (Figure 1.3-b) have the same characteristics as the larger triangular end block (Figure 1.3-a) in terms of bursting/spalling and shear behavior, the smaller end block might be considered preferable for the reduced temperature demands and decreased DEF vulnerability associated with its lower volume of concrete.

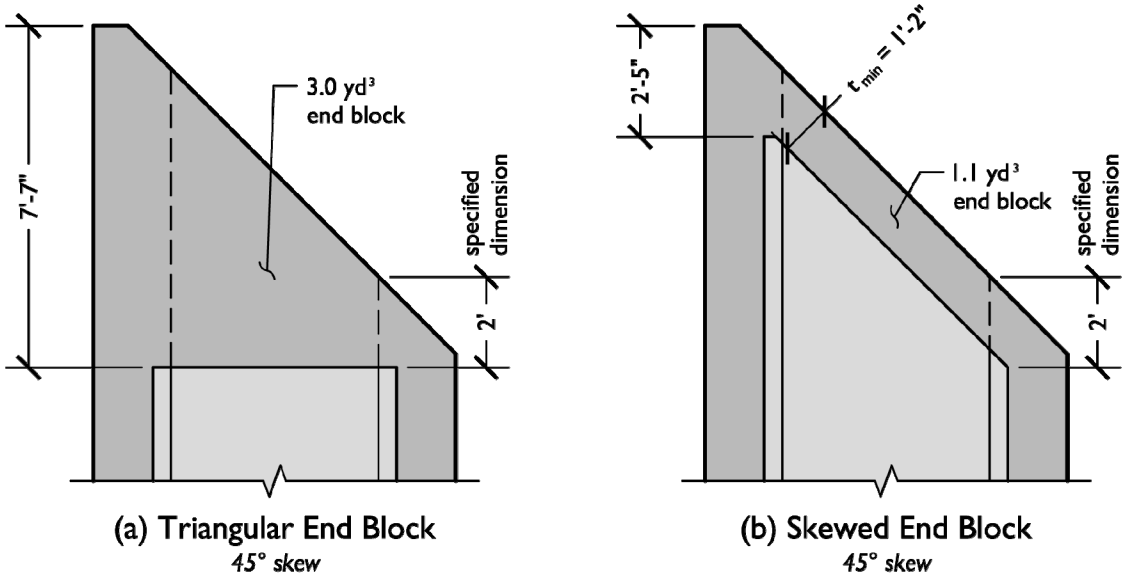

Figure 1.3 U-beam end-block design alternatives for skewed ends

At present, current end-region details, both in terms of reinforcement and concrete, have been tested for square and 45º-skewed end regions. With the understanding gained from this experience, proposed end-region details are in development, and soon will be tested at transfer and under shear loading. Later phases of the project will address similar issues (bursting/spalling and shear behavior) in pretensioned concrete box beams.

1.3 THESIS ORGANIZATION

After this brief introduction, results of a thorough review of literature are presented (Chapter 2). The review focuses on experimental studies of bursting and spalling in pretensioned concrete beams, both those in which surface strains were measured and those—like this study—in which reinforcement strains were measured. Standard practice regarding end-region effects is assessed through discussion of field investigations, Department of Transportation (DOT) beam-acceptance criteria and design code provisions. Lastly U-beam standard designs from other state DOTs are examined.

The experimental methods used to quantify bursting and spalling effects are discussed in Chapter 3. First specimen design is presented, followed by procedural aspects of instrumenting the beam end regions with strain gages on reinforcing bars and prestressing strands, and thermocouples in concrete end blocks. Lastly attention is paid to beam fabrication techniques, as employed at a precast concrete plant and in the laboratory.

Results from the two U-beam specimens are presented in Chapter 4. These results are discussed in the context provided by past studies of transverse-bar stresses at prestress transfer (bursting and spalling stresses) from the literature. Though past studies have mainly examined I-beams, general trends from the database of test results are still of

interest. Preliminary recommendations for U-beam end-region detailing are made at the close of the chapter.

In Chapter 5, a summary of the work reported in this thesis is presented, and conclusions made from the experimental results summarized.

CHAPTER 2

Literature Review

2.1 OVERVIEW

Prestressed concrete bridge construction was introduced in the United States after World War II, and became commonly used as the federal government began the ambitious public works of the Interstate Highway System. Early on, practice preceded code development – the first set of American Concrete Institute (ACI) recommendations regarding prestressed concrete design and construction (Tentative Recommendations for Prestressed Concrete) were not published until 1958, a year by which over 10% of the highway bridge inventory was prestressed concrete (Lin & Burns, 1981).

Field experience with unacceptably wide and long horizontal cracks forming in the end region at prestress transfer (Figure 2.1) brought prestressed concrete design engineers to a bifurcation: the problem of cracking could be approached theoretically from both the stress side and the strength side. Stress-side attempts to minimize end-region cracking included such prescriptions as adding end blocks (increasing the concrete area over which the bursting and spalling forces would act) and distributing the prestressing force more uniformly at the member end.

Integral to the stress-side approach was accurate estimations of the bursting and spalling tensile stresses a beam would experience. A variety of analytical solutions toward this end were developed in the 1950s and before. Most analytical methods were developed on the basis of two-dimensional elastic analysis for rectangular beams or other simple sections. Contemporary engineers recognized that adapting these methods for the general case (any beam cross section) would be *"either impossible or too complicated to attempt"* (Thorson, 1955, p. 658).

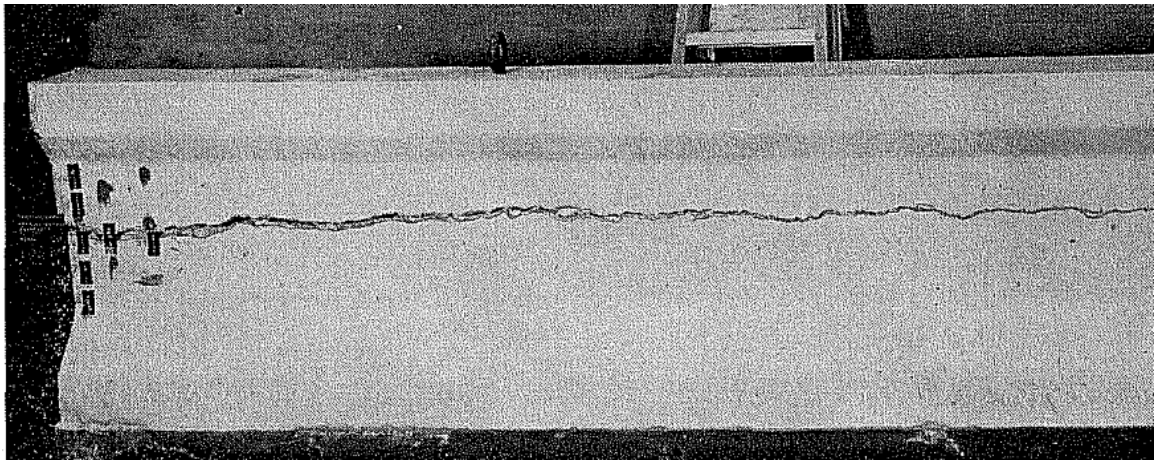

Figure 2.1 Severe cracking in a pretensioned concrete beam end region
(Marshall & Mattock, 1962)

The fundamentals of some analytical methods are presented in this chapter for their historical influence; however, the focus of this literature review is on experimental research. Despite million-fold advances in computational power since the days of hand calculations, modern-day methods are not significantly more accurate when it comes to predicting what matters most to bridge engineers: the location and extent of cracking.

The strength-side approach arose from the high degree of uncertainty apparent even in state-of-the-art analyses. Gergely, Sozen and Siess (1963) saw the debate between approaches based upon "what starts a crack" (stress side) or "what stops a crack" (strength side) as trivial: only the latter approach could be translated into intelligible design guidance. The prevailing winds in the early 1960s blew toward *"a more pragmatical treatment"* of the problem:

> *It has now been established that instead of treating the problem as a stress concentration problem in a homogeneous elastic body, it should be handled as an equilibrium problem of free bodies produced by the formation of cracks. The width and length of cracks became to be of concern. Therefore, the analytical and experimental methods are equally important. The question is not of distribution,*

extremes and averages of stresses under concentrated loads, but rather it is about the formation and extent of cracks (Gergely, Sozen & Siess, 1963, p. 120).

Around that time, two landmark studies were completed at the laboratories of the Portland Cement Association (Marshall & Mattock, 1962) and the University of Illinois (Gergely, Sozen & Siess, 1963). Both studies examined, among other items, the amount of transverse reinforcement necessary to control end-region cracking. The Marshall and Mattock end-region reinforcement design procedure, in a simplified form, was immediately incorporated into the American Association of State Highway Officials (AASHO) Standard Specifications (1961, Interim), and later adopted more directly for the Precast/Prestressed Concrete Institute (PCI) Design Handbook (1999). The analytical treatment of beam end regions first proposed by Gergely, Sozen and Siess (1963) has proved influential in the prestressed concrete research community.

The organization of this literature review is as follows. First, terminology relevant to end-region tensile stresses is defined. Discussion then touches on analytical techniques and findings before moving on to experimental studies. Experimental studies reviewed include those in which surface strains were measured and those, like the present study, in which strains in transverse reinforcement were measured. Results from field investigations and surveys of Department of Transportation (DOT) and other bridge design/construction professionals are presented. Current code provisions and their history are examined, followed by discussion of standard U-beam designs in Texas and three other states.

2.2 END-REGION TENSILE STRESS TERMINOLOGY

As stated by Lin and Burns (1981), the purpose of prestressing is to *"counterbalance undesirable strains and stresses"* (p. 12). In a typical prestressed concrete beam, the flexural tension zone (lower portion of the beam) is precompressed

through use of tensioned, high-strength steel reinforcement. By prestressing, an engineer can reduce or eliminate the longitudinal tensile stresses to be experienced by the precompressed tension zone under service loads.

Not all tensile stresses are reduced by prestressing, however. In the end regions of prestressed beams, tensile stresses are *induced* by the spread of the prestressing force, concentrated in the bottom, and often top, portions of the beam, to the entire cross section. This spread of forces occurs nonlinearly—i.e. the end region experiences a disturbed state of stress or in strut-and-tie terminology, is a D-region.

The direction, location and magnitude of end-region tensile stresses are highly dependent on section properties (e.g. prestressing force level and distribution, beam section geometry) and local variations in material properties (e.g. concrete tensile strength). End-region stresses are often categorized based on their direction and location. The direction of the stresses can be categorized as longitudinal (horizontal), transverse (vertical) or lateral (out-of-plane), as shown in Figure 2.2. Longitudinal stresses are primarily compressive, though along the top edge, tensile stresses may exist. Lateral stresses are often small as the strand pattern for most beams is symmetric about the beam vertical axis (y-axis in Figure 2.2). The strand pattern for a highway beam is rarely symmetric about the z-axis, however, making the transverse tensile stresses the most significant—and the most studied—of the end-region tensile stresses.

Based on their location, end-region stresses acting at transfer of prestress can be classified as bursting or spalling stresses. Bursting stresses occur along or near the line of action for the prestressing force, and typically reach their peak some distance into the beam. Bursting stresses are caused by equilibrium: the spreading of the concentrated prestressing force to the rest of the section. Cracks due to bursting stresses are typically horizontal.

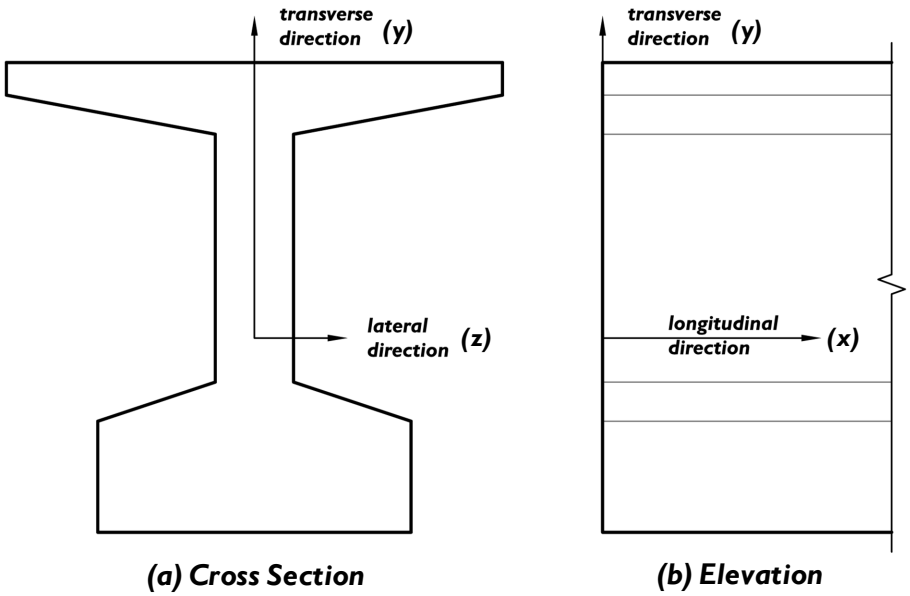

Figure 2.2 Convention for end-region stress direction

Some European researchers (e.g. Uijl, 1983) subdivide the near-prestress-axis stresses into bursting and splitting stresses. Though both result from equilibrium, splitting stress is a more localized phenomenon. In the area immediately surrounding a prestressing strand, splitting stress develop circumferentially in reaction to radially directed compressive bond stresses (Figure 2.3).

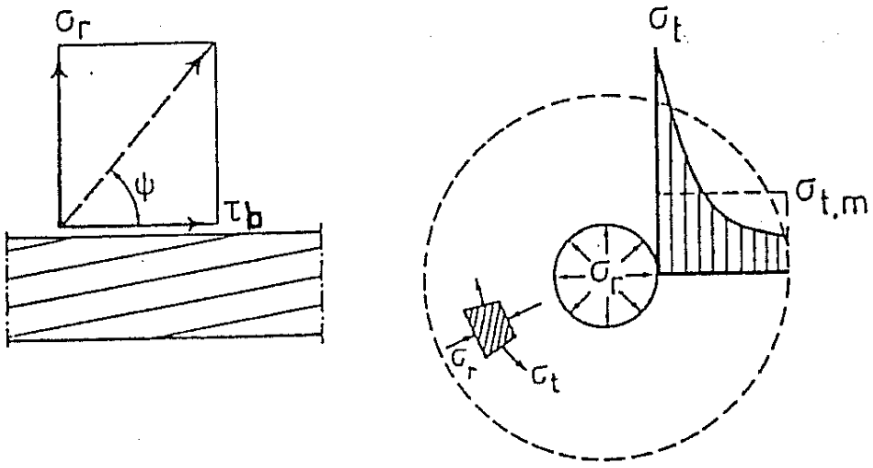

Figure 2.3 Development of splitting stress *(Uijl, 1991)*

As splitting stress is bond-related, it affects only pretensioned members. Bursting stress is a member-level phenomenon related to load spreading, and occurs in both pretensioned and post-tensioned members. Since *"bursting and splitting occur in the same region… their effects must be superimposed"* for design (Uijl, 1983, p. 99). In this spirit, bursting and splitting stresses are considered in a superimposed sense for the purposes of this thesis. The term "bursting stress" is used for tensile stresses resulting both from bond effects and load spreading, unless otherwise noted.

Spalling stresses occur away from the prestressing-force line of action, along the member end. Such forces can be caused by deformation compatibility, prestress eccentricity or division of the prestress into multiple strand groups. Cracks due to spalling stresses are horizontal or diagonal (oriented in the opposite direction of shear cracks).

In Figures 2.4 through 2.6, these distinctions between end-region stresses are illustrated. Figure 2.4 differentiates stresses based on their location for a beam with multiple anchorages (or strand groups); Figure 2.5 gives examples of bursting and spalling stress distributions, considering two sections of a post-tensioned beam; and Figure 2.6 shows their effect through exaggerated deformations.

Comparing research studies investigating end-region effects in prestressed beams through the 1980s and recent U.S. codes of practice, it can be observed that inconsistent terminology is used to describe stresses in the end region. This thesis largely adopts the terminology from the earlier research studies, but the American Association of State Highway and Transportation Officials Load and Resistance Factor Design Bridge Design Specifications (AASHTO LRFD) has neglected the "bursting" and "spalling" stress designation in favor of referring to transverse tensile stresses in general, using the term "bursting" first (1994 to 2007), then "splitting" (since 2008).

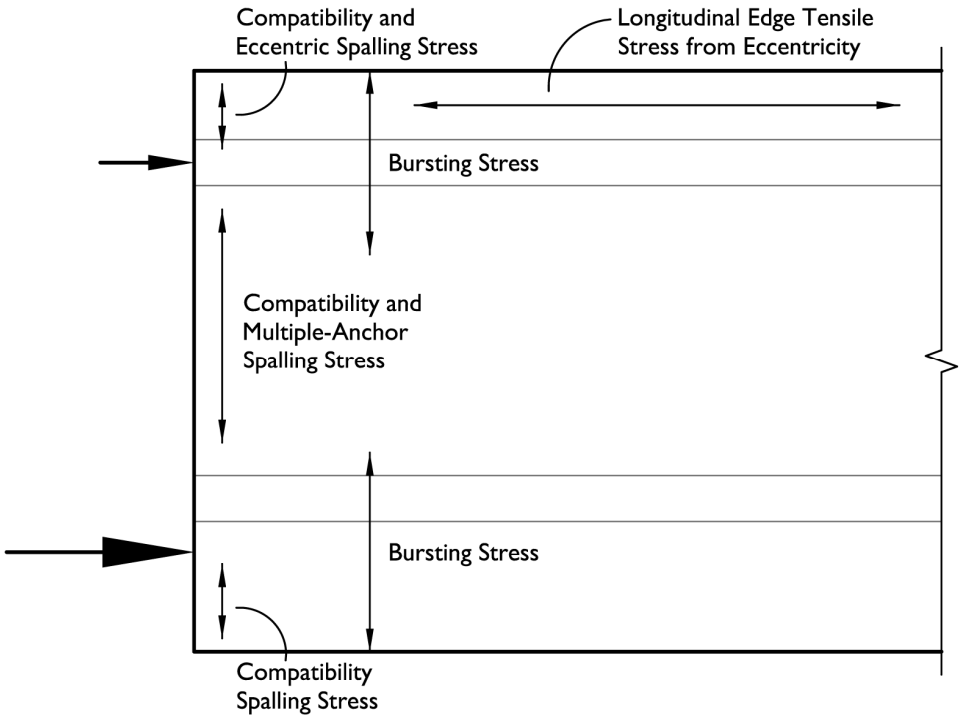

Figure 2.4 End-region stress terminology *(after Sanders, 1990)*

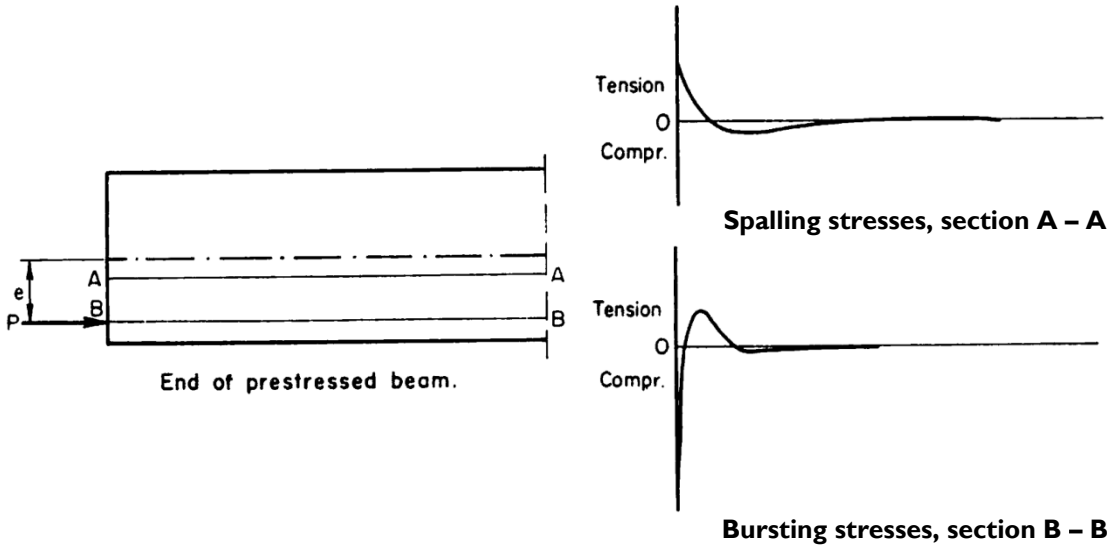

Figure 2.5 Bursting & spalling stress distributions *(after Lenschow & Sozen, 1965)*

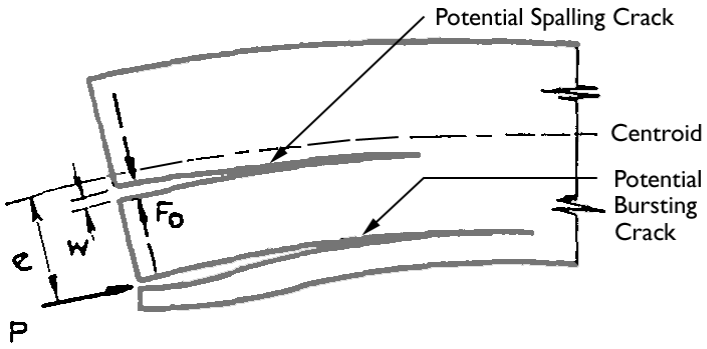

Figure 2.6 Effect of bursting & spalling stresses through exaggerated deformations of beam with discontinuities *(after Hawkins, 1966)*

2.3 BURSTING & SPALLING ANALYSIS IN PRESTRESSED BEAM END REGIONS

The general framework of several analytical techniques are described in this section. For more thorough coverage, the reader is directed to Iyengar (1962), Gergely, Sozen and Siess (1963) or Hawkins (1966). After this general treatment, analytical results germane to two topics (the role of end blocks and the behavior of U-beams at transfer of prestress) are presented.

2.3.1 General Approaches to Analysis

The general approaches to analysis of end-region behavior in prestressed concrete beams are outlined in Figure 2.7. These analytical approaches lie in three domains: elastic approaches, inelastic approaches and plastic approaches.

Figure 2.7 Analytical approaches for prestressed beam end regions

2.3.1.1 Elastic Analysis of Beam End Regions

Elastic approaches are typically based on the assumption that the concrete acts as a continuous homogeneous, isotropic medium. For the concrete to act in this manner, no cracks can have formed. Elastic analyses are done by solving a set of differential equations, whether at the member level, as in traditional two-dimensional theory-of-elasticity approaches; or at the level of a subdivided element, as in two- or three-dimensional finite element analyses (FEA). Solutions may be highly dependent on the chosen boundary conditions.

Slightly different handling of boundary conditions by different researchers stand chief among the reasons that so many different elastic approaches were developed in the 1950s and earlier (Hawkins, 1966). Many of these approaches are approximate solutions to the two-dimensional Airy stress function (F), as presented in Equation 2.1:

$$f_x = \frac{\partial^2 F}{\partial x^2},\ f_y = \frac{\partial^2 F}{\partial y^2},\ t = \frac{\partial^2 F}{\partial x \partial y} \text{ subject to } \nabla^4 F = 0 \qquad \textbf{Equation 2.1}$$

where:

$f_{x,y}$ = *principal stresses (in x- and y- directions as defined in Figure 2.2-b)*
t = *shear stresses*

Solutions were developed using infinite series (Bleich, 1923; Guyon, 1955; Sievers, 1956; Iyengar, 1962) or finite differences (Sargious, 1960; Gergely, Sozen & Siess, 1963). In general, there was an agreement among these solutions on the order of

magnitude of the end-region transverse tensile stresses (Gergely, Sozen & Siess, 1963), though there were differences in some particulars.

The symmetrical prism method developed by Guyon (1955) deserves more extensive treatment due to its historical importance, especially in the development of European codes of practice. Like other investigators, Guyon developed an analytical method based on the theory of elasticity, but uniquely, he believed that *"it is not necessary to examine the complete elastic state of the stresses in the beam end, but simply the stresses on the most unfavourable planes"* (p. 120). The "symmetrical prism" is a prism of concrete defined by the applied prestressing force, the top or bottom edge of the member, and the reflection of this edge about the line of prestress (Figure 2.8). If the prestress applied to the beam end is separated into multiple anchorages (strand groups), analysis should be conducted on more than one symmetrical prism (Figure 2.9).

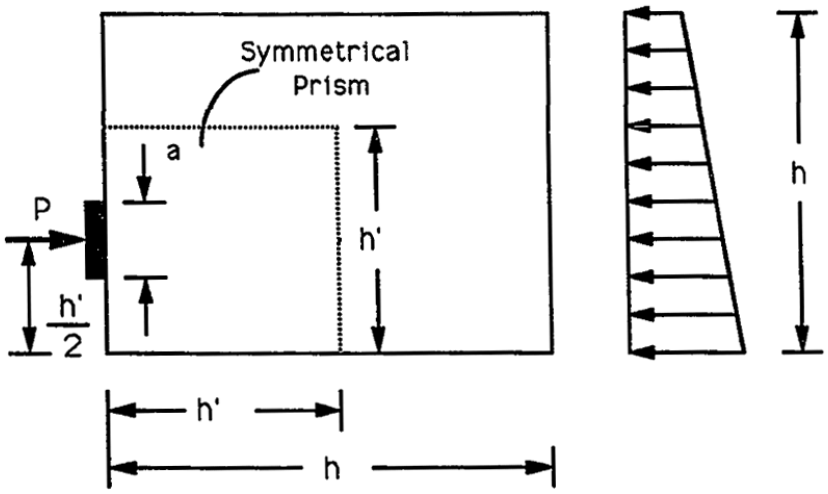

Figure 2.8 Symmetrical prism method of Guyon for a beam under eccentric prestress *(Sanders, 1990)*

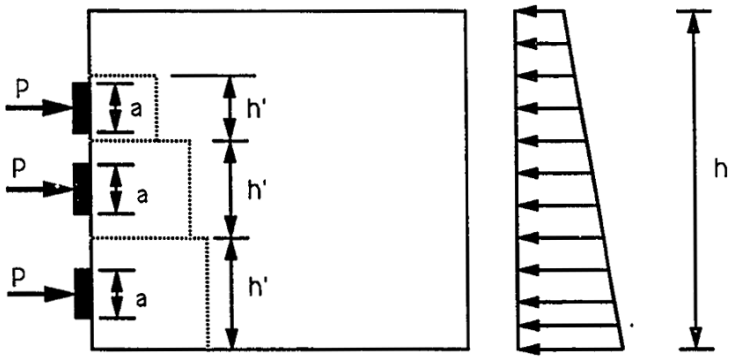

Figure 2.9 Symmetrical prism method of Guyon for a beam subject to multiple lines of prestress *(Sanders, 1990)*

Since, in the symmetrical prism method, only the zone immediately adjacent to the applied prestressing force is examined, bursting stresses (but not spalling stresses) can be estimated. Guyon's method has been found conservative for bursting in pretensioned members (Gergely, Sozen & Siess, 1963; Uijl, 1983), though not for post-tensioned members with thin webs or inclined tendons (Stone & Breen, 1984).

Finite element analysis (FEA) is the method of elastic analysis currently preferred by structural engineering researchers. FEA has proven useful to visualize the flow of forces within a prestressed concrete beam with complicated geometry (Breen et al., 1994). It also has been used to predict cracking loads, though such work is more difficult in the case of pretensioned beams due to variability associated with the gradual transfer of prestress to the section. A major advantage to FEA over traditional approaches is its ability to solve three-dimensional problems. As noted by Uijl (1983), certain phenomena such as splitting are by definition three-dimensional and cannot be addressed in two-dimensional analyses.

FEA can readily output color maps of elastic principal stresses and strains within a section, but it is important to remember that an underlying assumption of the analysis (that of an uncracked medium) is often invalidated in real beams.

> *The usefulness of [elastic methods] has to be examined in view of the structural performance of the member. One may be primarily interested in the magnitude and the position of the maximum transverse stress in order to predict crack initiation. However, the stress distribution can be obtained, at best, only under idealized conditions. The initiation of a crack can be estimated only if the tensile strength of the concrete, under the complex conditions of stress, is known. This is especially important in the case of the spalling stresses that are confined to a small area. Also, frequently there are initial (mainly shrinkage) cracks or differential shrinkage stresses in the member that invalidate the "elastic" analysis. For these reasons, the usefulness of the purely elastic stress approach is limited in practice* (Gergely & Sozen, 1967, p. 48).

2.3.1.2 Inelastic Analysis of Beam End Regions

The primary method of inelastic analysis is a design method developed by Gergely, Sozen and Siess (1963). For simplicity and ease of use, this method is a solution of equilibrium only (rather than the triumvirate of compatibility, constitutive laws and equilibrium used in elastic techniques). In Gergely-Sozen analysis—so called based on the 1967 PCI paper that publicized the method—an initially cracked medium is assumed: a crack has formed at the beam end face and extends some distance into the beam. The end-region transverse tension is taken by steel stirrups provided near the end face; as such, the method can be used to detail spalling reinforcement.

The transverse tension in the end region is calculated on the basis on the beam's linear stress distribution. As previously noted, the end-region stress distribution is nonlinear, even when the end region is not cracked. Gergely-Sozen analysis, then, takes the stress state at some distance into the beam (L in Figure 2.10), and projects its effect back onto the end region. A crack is assumed to occur at an arbitrary height, c; the prism

below this crack is considered. The longitudinal-force unbalance on this prism—between the external loading (applied force *P*) and the internal stresses integrated over the prism area—leads to a moment *M* acting on the section. To preserve static equilibrium, this moment must be resisted along the top edge of the prism, as a couple between a compression force *C* acting near the crack tip and the tensile force *T* provided by the transverse reinforcement close to the beam end (spalling reinforcement).

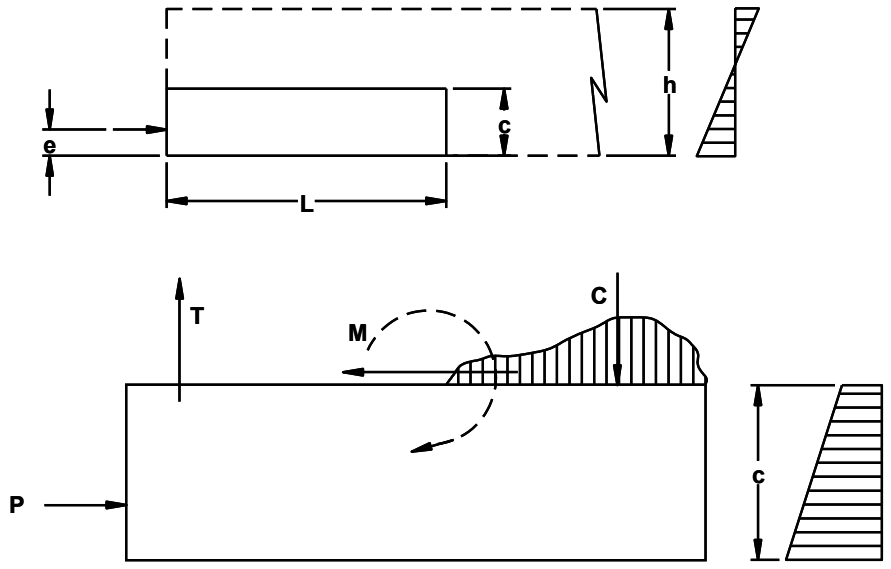

Figure 2.10 Gergely-Sozen analysis model *(Gergely & Sozen, 1967)*

As different crack locations (i.e. prism heights) are assumed, the moment varies. Gergely, Sozen and Siess assumed that the crack was most likely to form at the location where the moment is maximized. For many pretensioned beams, this location is just below the section centroid in the spalling zone. While the Gergely-Sozen method deals with spalling forces, due to its basis in equilibrium (only), the method cannot be used to predict spalling forces arising from compatibility.

2.3.1.3 Plastic Analysis of Beam End Regions

The primary plastic method of analysis used is strut-and-tie modeling (STM). An advantage to this method is its versatility: it can be used to provide a rational basis for transverse reinforcement placed anywhere in a beam end region, not just very close to the beam end. However, in order for the reinforcement to become effective, cracking must develop. If the transverse reinforcement is placed far from the regions of maximum tensile stress from elastic analysis, cracking may be extensive before the rebar is engaged.

As the primary purpose of transverse-tension analyses since Gergely, Sozen and Siess (1963) has been to provide sufficient transverse reinforcement to ensure serviceable end regions, the applicability of a method that assumes the plastic behavior of highly cracked concrete may seem limited. The use of STM for conservative predictions of ultimate capacity in post-tensioned concrete beams (Sanders, 1990) does not immediately lend itself to pretensioned beam serviceability.

That said STM has been applied to pretensioned concrete beams by Castrodale et al. (2002) and Davis, Buckner and Ozyildirim (2005). As the latter model was experimentally investigated by Crispino (2007), it is outlined below.

The goal of the STM developed by Davis, Buckner and Ozyildirim is to provide a rational basis for dimensioning transverse reinforcement beyond the near-end region handled by AASHTO LRFD in hopes of controlling long diagonal spalling cracks often seen in Virginia bulb tees. The prestressing force in these beams is typically separated into two groups, one applied to the top of the web and the other to the bottom flange. While in an actual pretensioned concrete beam, the prestressing force is applied to the section gradually over the strand transfer length, the model assumes the prestressing force to act as concentrated load at the member end (like in a post-tensioned beam). The more

sudden transfer of force is considered conservative in terms of bursting and spalling forces imparted to the section.

The STM is actually two smeared-tie models, and is shown in Figure 2.11. The "smeared tie" designation refers to the assumption that tie width need not be restricted by the width of compressive struts. In the upper STM, the compression from the top strand group is translated to its equilibrium position (assuming a linear stress distribution); in the lower STM, the same is done with the primary (bottom) strand group. The flow of forces from the bottom strand group is used to determine the transverse reinforcement required close to the beam end; that from the top strand group is used to detail reinforcement further into the beam. The transverse-bar design stress used for this model is less than the 20 ksi assumed by AASHTO LRFD (discussed further in Section 2.6.1).

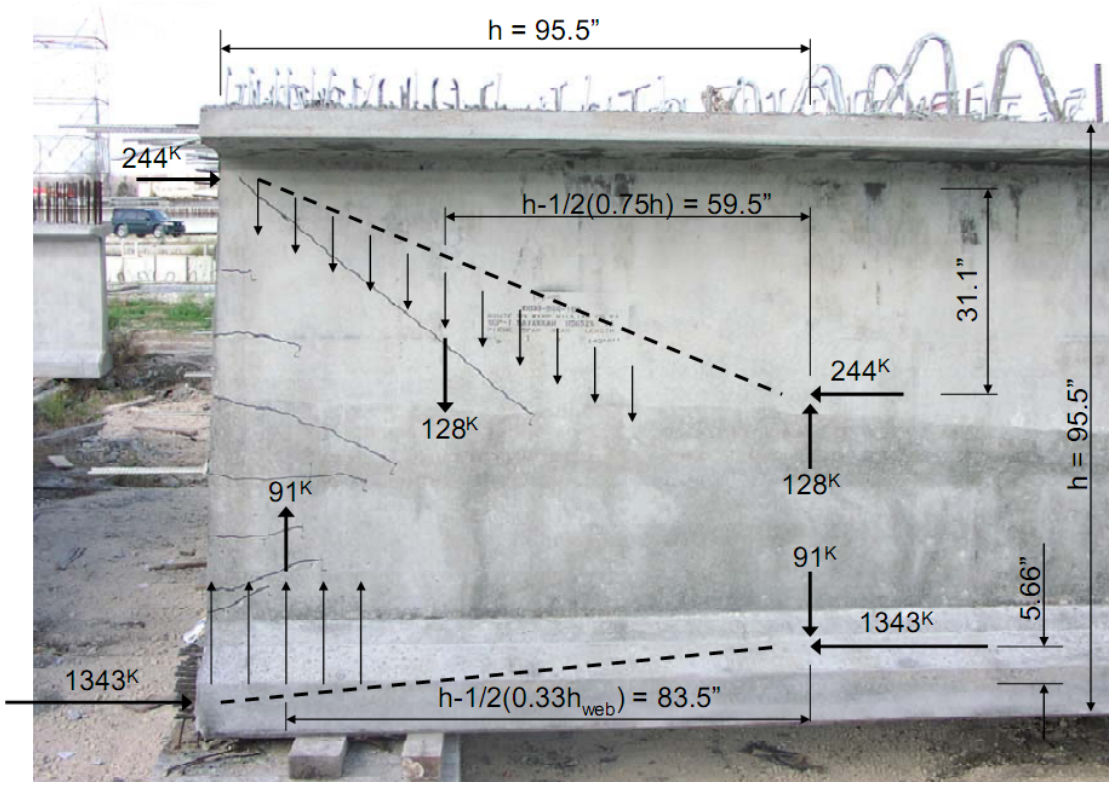

Figure 2.11 STM of Davis, Buckner & Ozyildirim *(2005)*

The effect of this model on the transverse reinforcement distribution is dependent on the beam depth (Figure 2.12). AASHTO LRFD requires enough transverse bars to resist 4% of the applied prestressing force, P_i, within $h/4$ from the end of the beam. Comparing the reinforcing requirements of the STM with that required by the code, it can be seen that, within the $h/4$ region, the STM requires 75 to 100% of the stirrups required by AASHTO. The STM requires additional reinforcement beyond $h/4$, in an amount of 75 to 150% what AASHTO prescribes for the end $h/4$.

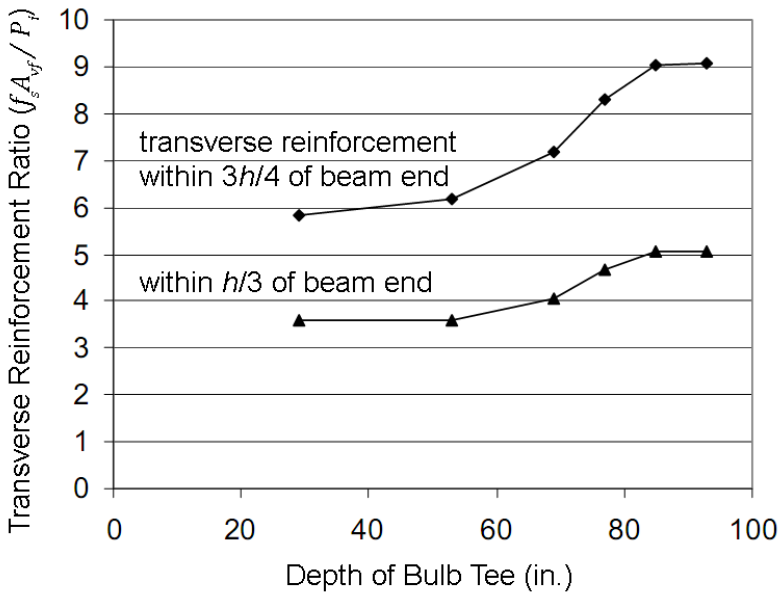

Figure 2.12 Transverse reinforcement required for Virginia bulb tee based on STM
(after Davis, Buckner & Ozyildirim, 2005)

2.3.2 Effect of End Blocks

Various researchers have conducted linear elastic FEA to assess the effect of end blocks on bursting and spalling; most studies have been conducted on post-tensioned concrete I-beam models. If an end blocks is provided, the transverse tensile force distribution is distorted in the beam end region. If an end block is provided, the bursting

force can increase by 400% (Yettram & Robbins, 1971; Uijl, 1983), as shown in Figure 2.13, and the spalling force by 100% (Sarles & Itani, 1984). Because the end block provides additional concrete area over which bursting and spalling forces may act, transverse-force increase does not lead to a corresponding increase in the transverse tensile stresses. In fact, modest decreases in transverse tensile stress (on the order of 25%) for beams with end blocks have been shown in analyses conducted by Uijl (1983) and Sarles and Itani (1984).

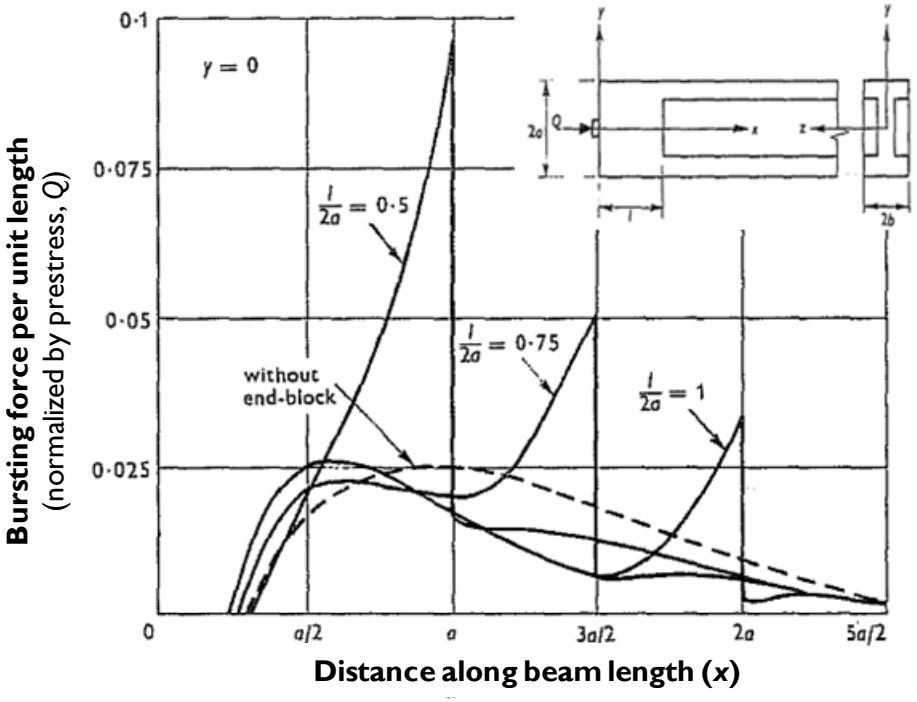

Figure 2.13 Effect of end blocks of various lengths on bursting force distribution
(after Yettram & Robbins, 1971)

In addition to decreasing transverse tensile stresses slightly, providing an end block may offer advantages in the area of constructibility. Yettram and Robbins (1971)

claim that end blocks allow for a *"three-fold increase in reinforcement [in I-beams] without increasing congestion"* (p. 39).

2.3.3 Analysis of U-Beams

Huang and Shahawy (2005) conducted linear elastic FEA on pretensioned Florida U-beams. The analysis was prompted by a field case of shear cracking under dead load for the U-beam pedestrian bridge (the first U-beam bridge constructed in Florida). The modeling included gradual transfer of prestress, a feature unique to this analysis among those reviewed here. Though their focus was the in-service condition, Huang and Shahawy reported principal and shear stresses caused by individual loads. Under the effects of the prestress, their model predicted shear stresses in excess of 500 psi to act near the bottom flange/web junction (in the bursting zone), as shown in Figure 2.14.

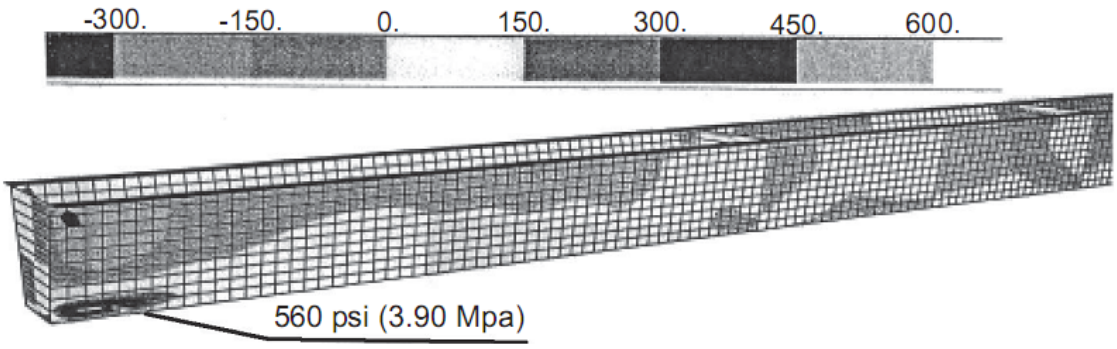

Figure 2.14 Shear stress distribution in Florida U-beam under prestress load only
(Huang & Shahawy, 2005)

2.4 EXPERIMENTAL STUDIES OF BURSTING & SPALLING EFFECTS

Over the past 50 years, researchers have used two distinct experimental approaches for the study of bursting and spalling. In one of these, strains on the surface of a concrete specimen have been measured through use of photoelastic materials or mechanical gages (e.g. Demec or Whittemore). Such experiments have proved useful in checking analytical solutions based on the theory of elasticity or examining the probability of cracking in members for which transverse reinforcement is rarely provided (e.g. hollow-core slabs). However, attempts to extend these tests' results to design recommendations been largely unsuccessful.

The other approach involves the measurement of strains in provided transverse reinforcement. The experimental database of studies of this sort is highly skewed toward I-beams, though some rectangular and inverted T-beams are included. (No U-beams, nor beams of any cross section with an end block, have been tested.) Such an approach is not useful for checking theoretical solutions for end-region stresses because in order for the reinforcement to be engaged, cracks (visible at the surface or not) must form, taking the specimen into an inelastic region of response. That said, studies taking this approach (measuring reinforcement strains) have been able to develop empirical equations for the design of transverse reinforcement adequate for control of end-region cracks to reasonable widths and lengths. The equation developed by Marshall and Mattock (1962) forms the basis of the U.S. code provisions relevant to bursting and spalling effects in pretensioned concrete members.

2.4.1 Studies of End-Region Surface Strains

In the 1940s and earlier, limited photoelastic studies were carried out by a number of researchers as experimental justification of their two-dimensional theoretical solutions for end-region stresses. The results of many of these studies are reported by Guyon

(1955), and are not reported here. As pointed out by Hawkins (1966), a *"major disadvantage"* of the photoelastic method is that it can yield only elastic stresses. The photoelastic method, then, can be used as a check for elastic analysis, but cannot examine the actual state of stress in a prestressed concrete beam. Another limitation to photoelastic studies, discussed by Yettram and Robbins (1969), relates to a property of photoelastic materials. The Poisson's ratio of most photoelastic materials is very different from that of concrete (0.50 compared to 0.20, nominally). Due to this difference, the transverse tensile stress distribution measured by the photoelastic method is distorted, with "*the general effect [of increasing] the external stresses at expense of those internally"* (p. 109) and thus to increase measured transverse-force values.

From the 1950s to the 1980s, the preferred experimental method for determination of surface strains in pretensioned concrete beams at transfer was direct measurement using mechanical or electrical-resistance (foil) strain gages. The data on bursting and spalling surface strains and observed cracking in prestressed concrete beams collected in these studies represent significant contributions to the literature.

2.4.1.1 Base, 1958

Base collected the first set of surface transverse tensile strain data for pretensioned concrete beam end regions. As part of a study examining transmission length (transfer length), Base took measurements of concrete strains using a mechanical gage on target points epoxied to the beam surface. The majority of the beams studied by Base were instrumented with one line of gages at the depth of the prestress centroid, but a set of three trial specimens were more extensively instrumented. These beams had multiple lines of gage points at various heights, enabling transverse strains to be measured between adjacent lines of gage points.

The trial specimens included one 40 in. deep rectangular beam and two 22 in. deep inverted T-beams, prestressed with 0.08 in. or 0.20 in. wires. Seven-wire strand, though developed almost ten years before (Scott, 2004), was still making its way into standard practice at this time.

As shown in Figure 2.15, the rectangular beam showed strains of 150 microstrain or greater in both the bursting and spalling zones. This level of strain is approximately that which would be expected to cause cracking.

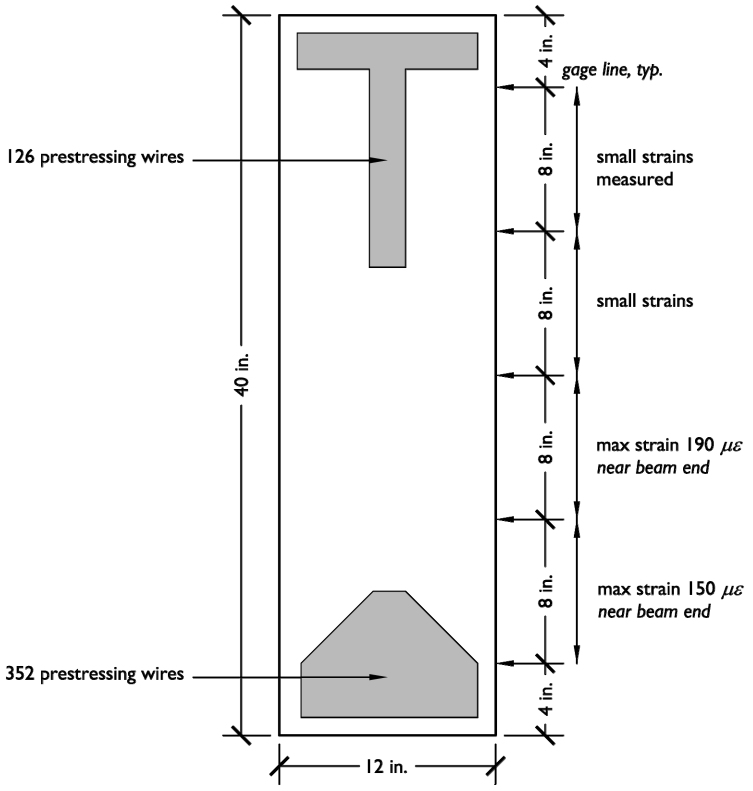

Figure 2.15 Bursting & spalling strains in Base rectangular beam

For the inverted T-beams (IT-beams), transverse tensile strains were measured between the gage lines on the web (Figure 2.16), i.e. in the spalling zone. The two IT-beams differed significantly both in the provided end-region transverse reinforcement

(2 – #3 equivalents at 2 in. for the first beam, and 2 – #3 at 6 in. for the second) and in the measured transmission length (four times larger for the first beam). Base measured a 300-microstrain maximum spalling strain near the end face of the first IT-beam, but did not note any cracking. For the second beam, a crack formed—causing the measured strain to surpass 1500 microstrain near the beam end. For the two beams, spalling effects dissipated within 12 in. (h/2) from the beam end.

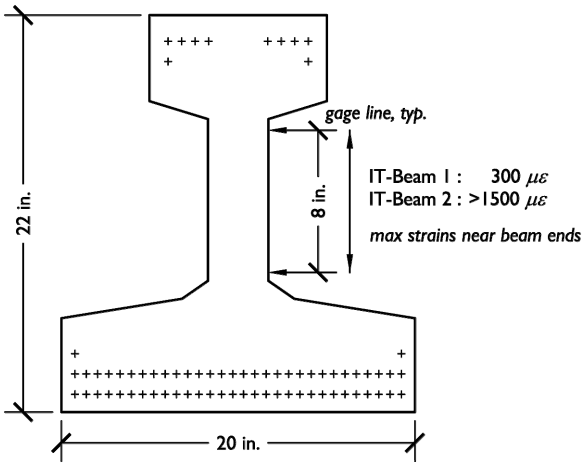

Figure 2.16 Spalling strains in Base IT-beams

Though Base measured bursting strains directly for only one beam, he did comment on their effects more generally. Referring to all the beams in his study (more than 200), Base stated: *"Horizontal cracks at the ends of beams just above the main block of stressing wires are by no means uncommon… particularly in I or inverted T beams"* (p. 4). The area "just above" the bottom group of prestressing wires can be considered the upper portion of the bursting zone.

2.4.1.2 Zieliński & Rowe, 1960 & 1962

Zieliński and Rowe (1960) measured transverse tensile strains in 63 concrete prisms (both reinforced and unreinforced) subject to concentric loading using a small

mechanical gage (2 in. gage length) and closely spaced gage points. These specimens (one shown in Figure 2.17) represented anchorage zones of post-tensioned concrete members. As the strains measured were located near the axis of prestress, they should be classified as bursting strains.

While the applicability of their study to the present work is indirect at best, their study is mentioned for the *very* high bursting stresses and forces reported by the researchers. Zieliński and Rowe reported bursting forces of 20 to 35% of the applied prestressing force, 50 to 100% higher than those predicted by the available theories. *"Mainly because they indicate tensile stresses far in excess of the theoretical two-dimensional values,"* noted Yettram and Robbins (1969), the results of this experimental study were *"widely accepted by designers"* (p. 104).

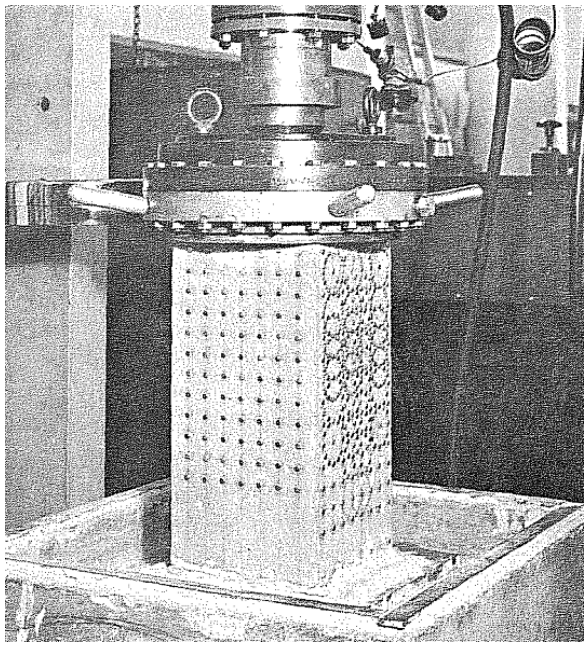

Figure 2.17 Concrete prism with extensive surface gaging *(Zieliński & Rowe, 1960)*

It is now understood (Gergely, Sozen & Siess, 1963; Yettram and Robbins, 1969) that the magnitude of the bursting stresses reported by Zieliński and Rowe were likely exaggerated due to inelastic deformations (e.g. microcracking). Zieliński and Rowe had converted their measured strains to the stress domain assuming that the concrete surfaces had behaved as linear elastic plates.

The level of prestress (longitudinal stress) corresponding to reported stress data in Zieliński and Rowe's study was 10 to 20% of the cube strength. While members subject to uniform compression of this magnitude respond elastically, the same cannot be said for members under a general state of stress. Gergely, Sozen and Siess (1963) found inelastic action at low levels of prestress in a study of post-tensioned beams (Section 2.4.1.4).

Yettram and Robbins (1969) also challenged the general approach of measuring concrete surface strains. Through linear elastic FEM studies of specimens similar to those tested by Zieliński and Rowe, they found disparities in the stress conditions at the surface of the beam compared to the interior. The surface stresses were higher for most realistic loading conditions (majority of beam width loaded). It is clear from Figure 2.18, however, that increases in stress from the surface-measurement technique cannot account for the entire discrepancy between the experimental and analytical results.

In summary, the maxim put forward by Hawkins (1966) should not be ignored: *"Care taken in instrumentation and observation is vital… particularly for calculations of transverse tensile stress"* (p. 198, emphasis added).

In a second study completed by Zieliński and Rowe (1962), 20 eccentrically post-tensioned I-beams were examined. Most I-beams had rectangular end blocks; many had two or more anchorages; and none had transverse reinforcement. As in their previous study, mechanical strain readings were taken using a 2-in. gage.

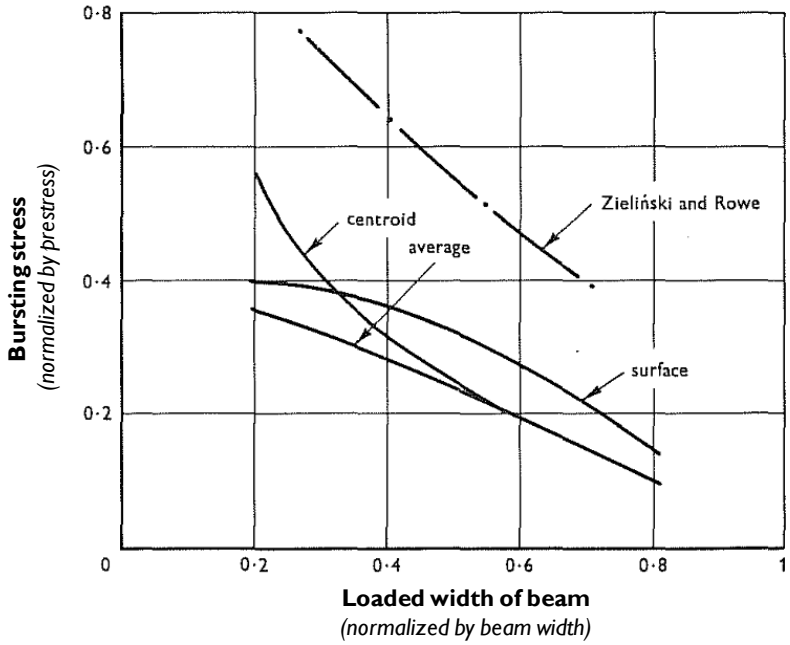

Figure 2.18 Analytical stress at various locations compared to Zieliński & Rowe's experimental results *(Yettram & Robbins, 1969)*

The specimens showed bursting-dominated behavior: maximum transverse tensile stresses occurring along lines of prestress at approximately *h*/3 into the beam. Spalling strains were measured, and were lower than bursting strains; such behavior was considered verification of the symmetrical prism approach of Guyon (1955).

The behavior of several individual specimens is of interest for the present study. First in a direct comparison between two beams with similar prestressing patterns but different end conditions (end block provided or not), the beam *without* the end block was able to sustain more prestressing force (by 17%) before failure (i.e. losing the capacity to carry force due to extensive cracking).

Also interesting was the failure of one beam due to cracking at the flange/web junction (Figure 2.19). The prestressing force for this beam was applied concentrated

near this junction, and the maximum transverse strains developed just above the bottom flange. Referring to this specimen, Hawkins (1966) wrote:

> *For I-sections with the applied load close to the junction of the web and flange, cracking has also been observed to originate at this junction, several inches beyond the end of the member. This type of cracking led to the failure of [one] I-section… These results indicate that for an I-section there can be a zone at the junction of the web and flange for which the principal tensile stresses are higher than those in either the bursting or spalling zones* (p. 200).

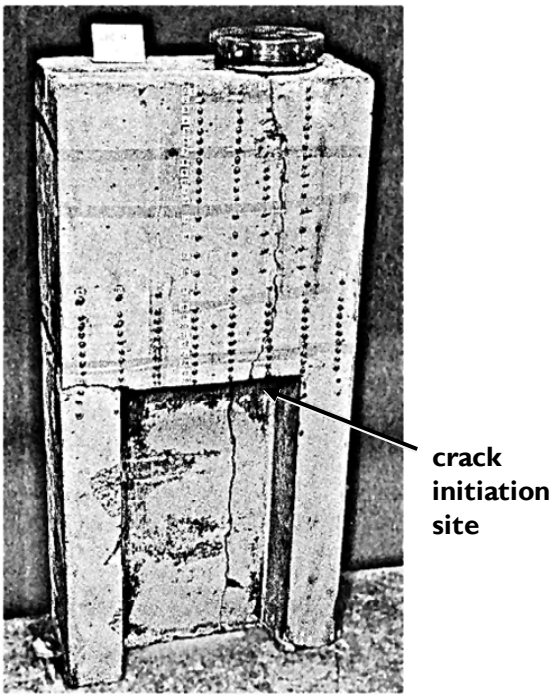

Figure 2.19 Specimen with failure near flange/web junction *(Zieliński & Rowe, 1962)*

Though Hawkins referred to this cracking as occurring neither in the bursting or spalling zones, the definition of "bursting" used in this thesis (near the line of prestress rather than necessarily along it) allows the term to be used. Since the Zieliński and Rowe study, failure in other post-tensioned beams due to bursting has been observed (Stone & Breen, 1984; Sanders, 1990). However, such behavior is tied to the performance of

proprietary post-tensioning anchors and thus is of limited applicability in the case of pretensioned beams (in which the prestressing force is developed by bond, not anchors).

Similar to their previous study, Zieliński and Rowe observed cracking to occur at higher levels of prestress than those predicted considering splitting tensile strength data. In this case, however, the difference was much smaller—beams cracked at strains 30 to 50% higher than expected. The researchers offered the following explanation:

> *In end-blocks, by virtue of the complex stress system that exists, the stress-strain relation of the concrete in tension is modified, the strain capacity before cracking being greater than in normal bending tension* (p. 39).

In a later study, also of eccentrically post-tensioned I-beams, Breen et al. (1994) offered verification of the above hypothesis. Comparing their experimental results to results from FEA, the researchers found that a concrete tensile-strength model incorporating the effects of *"the complex stress system"* could predict observed cracking loads with greater accuracy, though less conservatism, than a model assuming a nominal tensile strength.

2.4.1.3 Marshall & Mattock, 1962

Though their major contribution to the area of bursting and spalling behavior lay in a study of end-region reinforcement strains (discussed in Section 2.4.2.1), Marshall and Mattock were involved in a preliminary study in which concrete surface strains were measured for 10 pretensioned I-beams of 23 in. depth. Foil strain gages were applied to the beam end over the depth of the web, and along the beam length at the height of the section centroid. Typically, the maximum transverse tensile strain was found at the end face near the centroid (Figure 2.20), and the tensile strains decayed to negligible levels approximately $h/3$ from the member end (Figure 2.21).

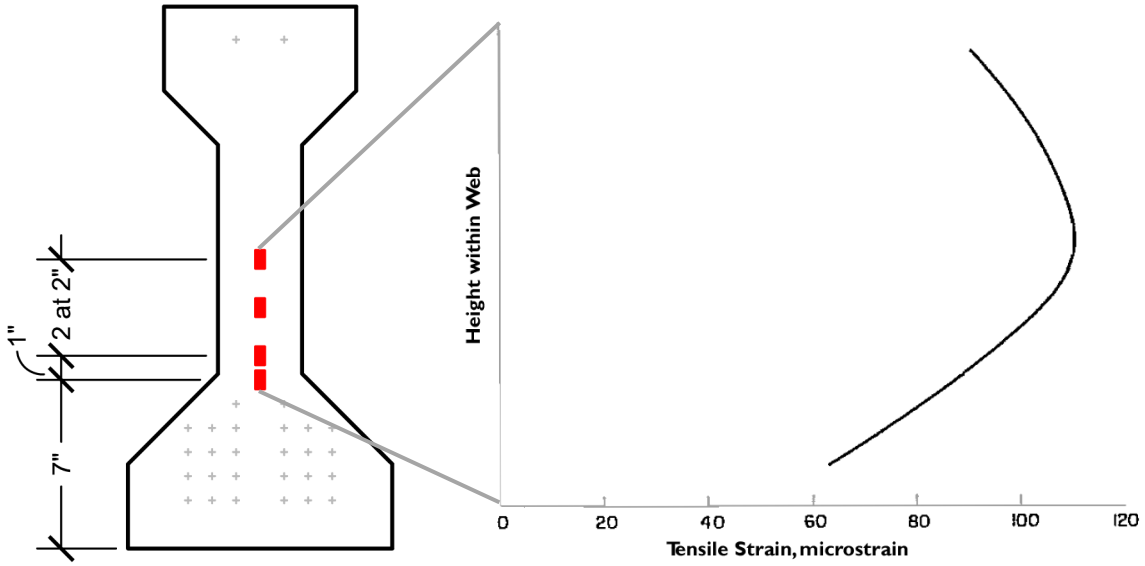

Figure 2.20 Surface instrumentation & strains at beam end
(after Marshall & Mattock, 1962)

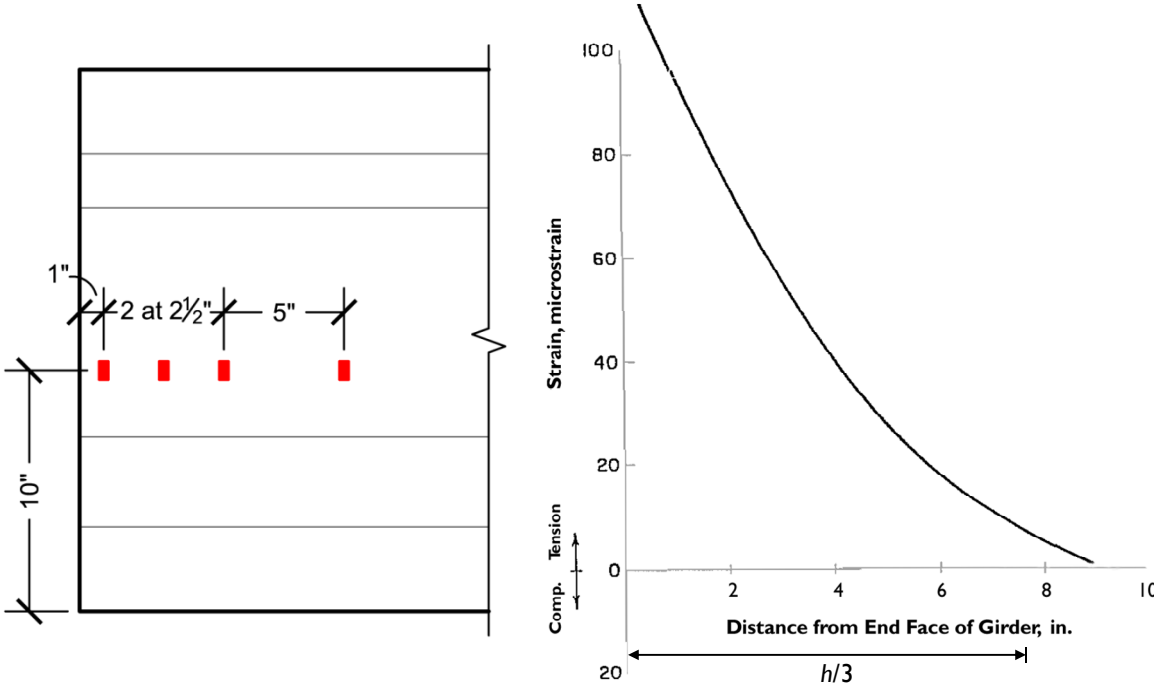

Figure 2.21 Surface instrumentation & strains over beam length
(after Marshall & Mattock, 1962)

Though Marshall and Mattock placed some strain gages at various depths (Figure 2.20), such gages were applied only to the end face of the member. As bursting strains do not reach their maximum value until some distance into the beam, it can be surmised that only spalling strain variation was measured.

2.4.1.4 Gergely, Sozen & Siess, 1963

Gergely, Sozen and Siess, also noted for their contributions to the understanding of end-region behavior using other methods, studied surface strain distribution and crack propagation in 10 eccentrically post-tensioned beams. The beams were of both rectangular and I-section, were small-scale (6 in. maximum breadth, 12 in. deep), and were unreinforced in the transverse direction. Transverse tensile strains were measured using foil strain gages applied to the concrete surface at 0.5 in. spacing. Instrumentation was placed along the line of prestress, at the section centroid and in between; both bursting and spalling effects were measured.

Typically, as prestress was applied, beams would crack in both their bursting and spalling zones. Bursting cracks would form 1 to 2 in. from the beam end face. Spalling cracks would propagate from the end face just below the centroid. Beams also experienced flexural cracking along their top edge, but such cracks occurred far enough from the ends not to affect the transverse strain readings.

Transverse strains were observed to vary nonlinearly with applied prestressing force at very low levels of prestress (25% of the prestressing force at observed cracking). The behavior of the spalling strains for lines along the section centroid was interesting. These strains would typically increase with load, but if a crack should form at another location (e.g. in the bursting zone, or just below the gage line), the strains would decrease, sometimes becoming compressive. This behavior is shown in Figure 2.22.

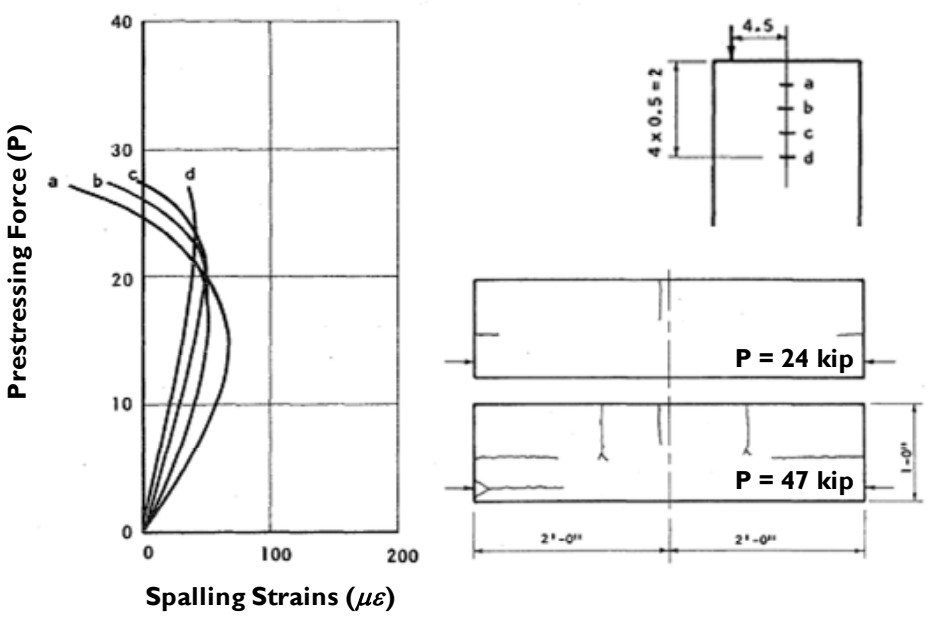

Figure 2.22 Prestressing force & spalling strains for a rectangular beam
(after Gergely, Sozen & Siess, 1963)

While the presence of a bursting crack affected the strains measured in the spalling zone, the converse was not true. The researchers recommended the use of the symmetrical prism approach for bursting-zone design. In this method, the behavior of the beam outside the bursting zone is ignored, consistent with the experimental observation that *"cracking in the spalling zone has little effect on [behavior] in the bursting zone"* (p. 15).

Gergely, Sozen and Siess observed lower bursting and spalling strains in I-beams than in rectangular beams, except at high loads. It was theorized that load spreading occurred differently for the two shapes. In the I-beams, though the prestressing force would eventually spread to the entire beam, for some distance it was confined to the bottom flange. Surface strain readings at low loads indicated that *"the web portion of the end block close to the end face [was] stressed less than the corresponding area of the*

rectangular beam" (p. 21). At high loads, the damage in the rectangular beam due to spalling cracks led to load redistribution away from the middle portion of the beam (i.e. web). These findings especially convinced the researchers that initial irregularities (e.g. shrinkage cracks) would have large impacts on the strain distribution in prestressed beam end regions. The transverse stress distribution was thus found to be more random (and more difficult to capture with an analytical method) than thought by the elastic analysts discussed in Section 2.3.1.1.

Upon this observation, Gergely, Sozen and Siess moved to study the effect of transverse reinforcement in containing cracks (discussed in Section 2.4.2.2) rather than continue work on strain distribution.

2.4.1.5 Arthur & Ganguli, 1965

Before the controversy surrounding the high reported bursting stresses of Zieliński and Rowe (1960) was resolved, Arthur and Ganguli completed a set of tests on 19 pretensioned concrete I-beams at the University of Glasgow—the university that employed Mattock when he was not a visiting fellow at the Portland Cement Association (PCA). Their tests are noteworthy for their primacy: the tests were the first with the primary aim to measure the end-region transverse strains on surfaces of pretensioned concrete beams, and the first in which multi-wire tensioning and gradual detensionsing was employed in a laboratory setting (Figure 2.23).

The beams of this study were small-scale (12 in. deep with 2 to 3 in. thick webs) and employed neither web reinforcement nor end blocks. Though beam end regions were extensively instrumented (Figure 2.24), surface strains seem only to have been measured in the spalling zone. At the beam end, the prestressing force was separated into two groups of 0.2-in. wires, with 20 or 50% of the strands located in the top flange.

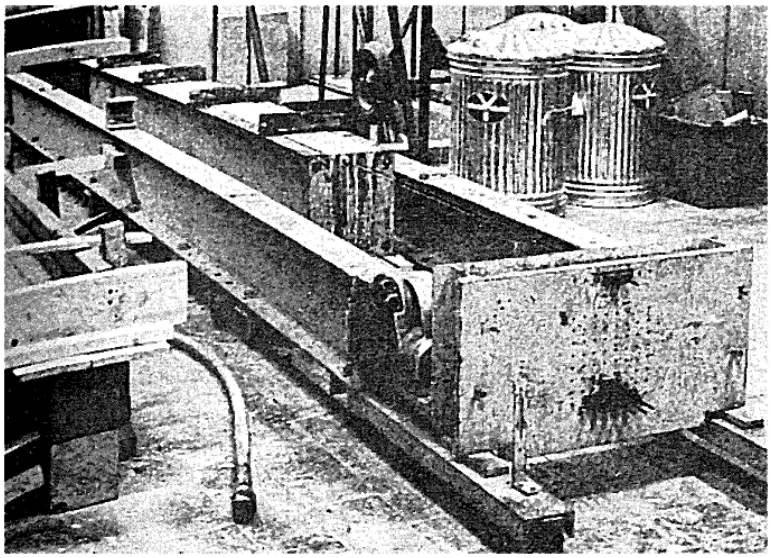

Figure 2.23 Pretensioning bed at Glasgow *(Arthur & Ganguli, 1965)*

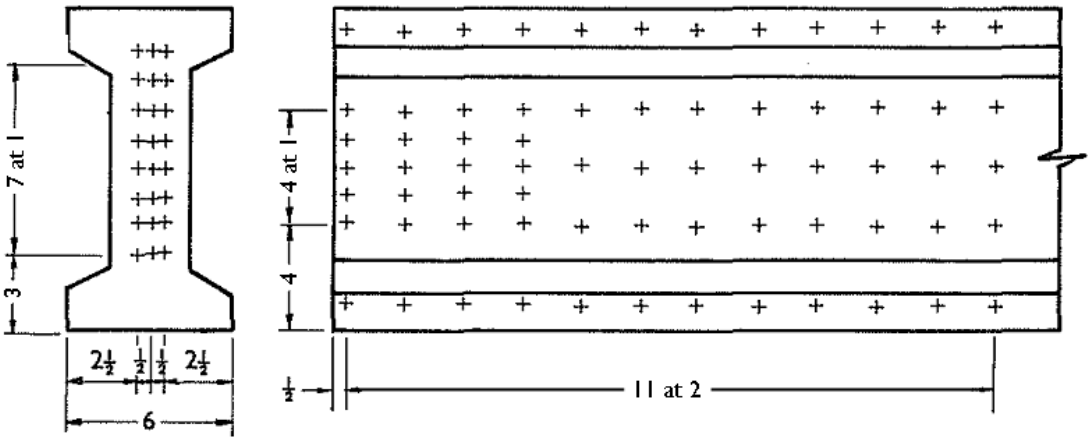

Figure 2.24 Mechanical gage points on I-beam specimen
(after Arthur & Ganguli, 1965)

After transfer of prestress, half of the beam end regions were observed to crack. This proportion was similar for both the fixed ends (9 of 19) and the stressing ends (9 of 18, with one end region not reported). Cracks were 15 in. long on average, with two that were much longer, *"virtually [splitting] the beam in two and [rendering] it of no practical use"* (p. 92).

Most beams observed to crack did so near the section centroid (in this case, mid-depth), at which height maximum spalling strains were measured at the beam end. Interestingly, a number of beams cracked at top flange/web junction (40% of the beams with observed cracking, 7 of 18), perhaps due to bursting effects from the prestressing force applied to the top flange.

The maximum spalling strain in each end region was reported by the researchers. It can be observed that the mean of the maximum spalling strains in "uncracked" beams (370 microstrain) was strikingly similar to that for the "cracked" beams (380 microstrain). The spalling strains for beams without observed cracking ranged from 170 to 900 microstrain; all were above the nominal 150-microstrain cracking strain. As Arthur and Ganguli stated, *"Some of these strains are so high that it is suspected that cracking had in fact occurred, although there was no evidence of it"* (p. 95).

Unlike other studies, Arthur and Ganguli also reported time-dependent behavior of their measured strains. From measurements made immediately after prestress transfer, 24 hours after transfer and 48 hours after, the researchers reported that strains had a tendency to decrease (100 microstrain over 48 hours) *except* at locations of web cracking. Where gages spanned cracks, strains increased with time.

2.4.1.6 Krishnamurthy, 1970

Krishnamurthy performed a similar study to that Arthur and Ganguli, also at Glasgow. Krishnamurthy's study investigated the effect of detensioning method (i.e. time spent detensioning) on transverse tensile strains and transfer length in 12-in. I-beams. Strains were measured on the concrete surface with a small mechanical gage, whose target points covered the spalling zone: the middle portion of beam, within $h/2$ of the beam end (Figure 2.25).

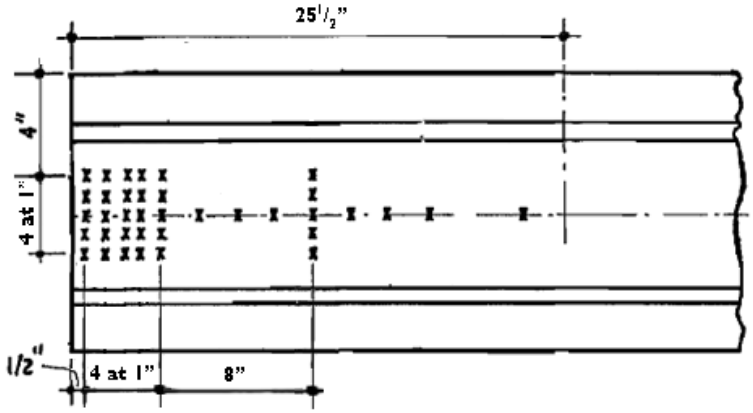

Figure 2.25 Mechanical gage points on I-beam specimen *(after Krishnamurthy, 1970)*

The finding from this study was that the more sudden prestress was transferred, the longer the transfer length (by 15% on average) and the higher the spalling strains (by 40%). While greater transverse tension resulting from more sudden transfer is not surprising, the correlation of longer transfer lengths and higher spalling strains is—as it contradicted the prevailing view (Guyon, 1955; Base, 1958; Marshall & Mattock, 1962) that *shorter* transfer lengths should lead to increased bursting and spalling effects.

2.4.1.7 Uijl, 1983

In addition to his analytical work, Uijl completed tests measuring concrete surface strains in 11 pretensioned I-shaped members representing the ribs of hollow-core slabs. Per standard practice in the hollow-core industry, the specimens had no transverse reinforcement. Uijl noted that for most beams of other section geometries, in which sufficient transverse reinforcement can be easily provided to resist end-region cracking, *"it is of minor interest at what stress level cracks occur. In hollow-core slab, on the contrary, it is of vital importance to know whether the occurring tensile stresses remain smaller than the tensile strength of the concrete"* (p. 21).

The behavior of these beams was dominated by bursting. In the spalling zone, measured strains were typically less than 150 microstrain (8 of 11 beam end regions below this value) and no cracks were observed. Extensive cracking, on the other hand, formed in the bursting zone (Figure 2.26). While their widths were fine, the cracks typically extended 10 to 20 in. long, and grew in length with time. Most cracks started 2 to 3 in. from the end face.

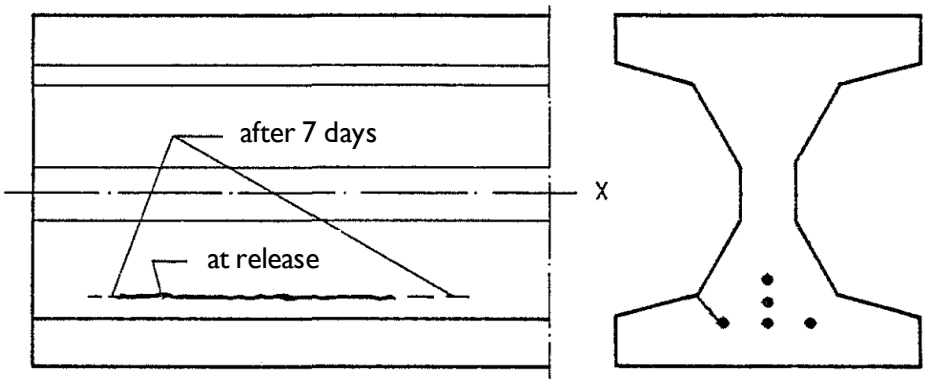

Figure 2.26 Typical bursting/splitting crack in hollow-core ribs *(Uijl, 1983)*

Uijl hypothesized that the combination of bursting (spreading) and splitting (bond-related) stresses caused the cracking, as analysis stresses (done by the symmetrical prism method or FEA) did not yield bursting stresses sufficient to cause cracking. In an effort to see the state of internal cracking, one specimen was saw-cut and examined using a fluorescent spray and UV lighting. The observed cracking seemed to originate from the prestressing strands, in a manner consistent with splitting, as shown in Figure 2.27. It is unclear whether some of these splitting cracks may have formed as a result of the cutting process (and subsequent strand draw-in at this section).

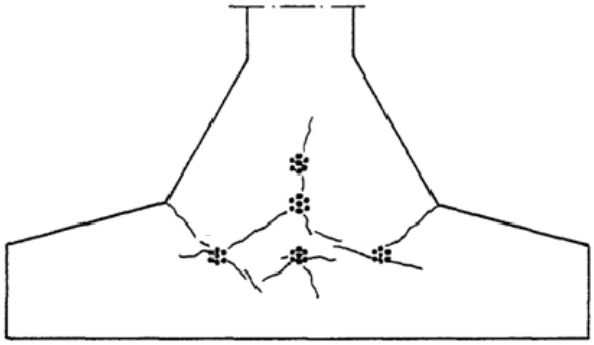

Figure 2.27 "Internal cracking" viewed in saw-cut specimen *(Uijl, 1983)*

Uijl had some success correlating the average cover provided per strand with the presence or absence of cracking, but by and large, the best predictor of cracking was the number of strands in a given beam (i.e. applied prestress).

2.4.1.8 Summary

In summary, the reviewed studies of concrete surface strains have tended to focus on spalling behavior. Bursting, though, has been responsible for cracking in a number of studies examining prestressed concrete beams (Base, 1958; Zieliński & Rowe, 1960 & 1962; Gergely, Sozen & Siess, 1963; Uijl, 1983). Bursting has also been associated with structural deficiency in post-tensioned beams (Zieliński & Rowe, 1962; Stone & Breen, 1984; Sanders, 1990).

The correlation between high measured surface strains and cracking is imperfect, likely due to experimental difficulties in observing of very fine cracking and/or microcracking. If transverse reinforcement is not provided in a pretensioned concrete member, very long cracks due to spalling (Arthur & Ganguli, 1965) and bursting (Uijl, 1983) may form, rendering the beam unusable.

2.4.2 Studies of End-Region Transverse-Reinforcement Strains

> *Of the two important questions: "What starts a crack?" and "What stops a crack?", the first one cannot be answered with sufficient ease and accuracy. The new approach… [is] more concerned with the second question. It [attempts] to find the effects and the propagation of the anchorage zone cracks… [leading] to the examination of the role of the transverse reinforcement in confining the crack (Gergely & Sozen, 1967, p. 48).*

The *"new approach"* taken by experimental researchers in the 1960s was to measure strains of transverse reinforcement in the end region. While bursting and spalling effects often cause pretensioned concrete beam end regions to crack, they rarely cause the transverse bars there placed to yield. Hence, while the concrete in the end regions cannot be said to respond elastically, the steel placed there can, and conversion of transverse tensile strains to stresses proceeds without errors due to inappropriately assumed elastic behavior.

Since the early 1960s, five significant studies have examined end-region behavior of pretensioned concrete beams at transfer of prestress by means of measuring transverse-bar strains. (Another study, examining post-tensioned concrete beams, is also reviewed in this section.) As with studies of surface strains, these studies have focused on I-beams (80% of the specimens reporting transverse stress variation, i.e. 37 of 45 beam end regions). The experimental methods and findings of these studies are detailed in this section. Data from these studies have been compiled along with that from the present study into a database. Findings based on analysis of this database will be described in Section 4.3; figures showing the results of the individual studies are provided in Appendix A.

The key for interpretation of these studies' findings lies in the placement of the strain gages. Strain gages placed far from crack locations are likely to return low strains as the adjacent uncracked concrete will aid in resisting the transverse tensile stresses.

Early studies often examined beams in which up to 50% of the prestressing force was concentrated in the upper flange. Spalling may be critical for such beams due to "multiple-anchor spalling stresses" (shown previously in Figure 2.4), and as such, the beams were primarily instrumented in the spalling zone. Some later studies have copied this instrumentation approach uncritically, placing gages only in the spalling zone for beams in which bursting may be critical (e.g. bulb tees with a large prestressing force applied to the bottom flange). As such, the experimental database is more complete with regard to spalling than bursting behavior.

2.4.2.1 Marshall & Mattock, 1962

The first study of end-region reinforcement strains was completed by Marshall and Mattock at the PCA laboratory in 1962. The primary purpose of the study was prescriptive rather than descriptive: to develop design criteria for the transverse reinforcement in the end regions of pretensioned beams. To broaden the applicability of the findings, the 25 I-beams examined for the study (Figure 2.28) had a number of variables, including

- Size and pattern of the prestressing strand;
- Magnitude of prestressing force;
- Web thickness; and
- Size of transverse reinforcement (#2 or #3 stirrups).

Transverse reinforcement was provided within $h/3$ of the beam end and was instrumented along the centroidal axis (just below mid-depth). In the case of beams reinforced with #3 stirrups, the transverse reinforcement provided in the beam end region was approximately double that currently required by the AASHTO LRFD. For beams with #2 stirrups, the reinforcement was 80 to 120% of that now required by AASHTO.

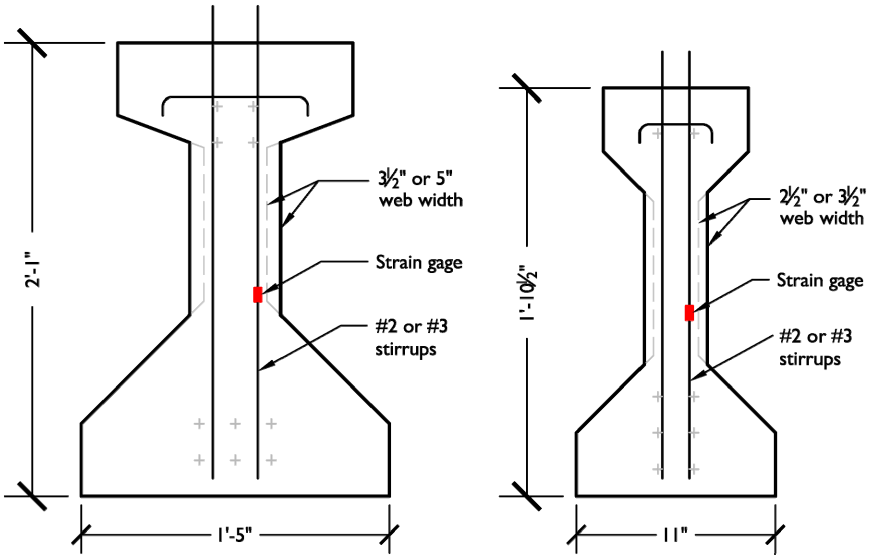

Figure 2.28 I-beams studied by Marshall & Mattock

Prestress was transferred by flame cutting. Immediately after transfer, 18 of the 25 beams were determined to crack by visual observation or measurement of reinforcement strain. The cracking typically occurred near the section centroid at the end face of the beams and extended a 2 to 4 in. into the beam. Because the cracks were so fine (0.004 in. wide or less), cracks length were reported as the distance at which the measured strains decreased to an assumed cracking strain (125 microstrain). Up to the end of the crack, spalling strains decreased approximately linearly with distance from beam end (Figure 2.29). The extent of cracking observed in all beams was judged acceptable.

Separating the prestressing force into two relatively equal strand groups (in the top and bottom flanges) was found to contribute to observed cracking. Beams in this study had 10 to 50% of the total strands in the top flange. Every beam with more than 25% of the strands in the top flange cracked; half of those (7 of 14) with fewer strands at the top did not crack.

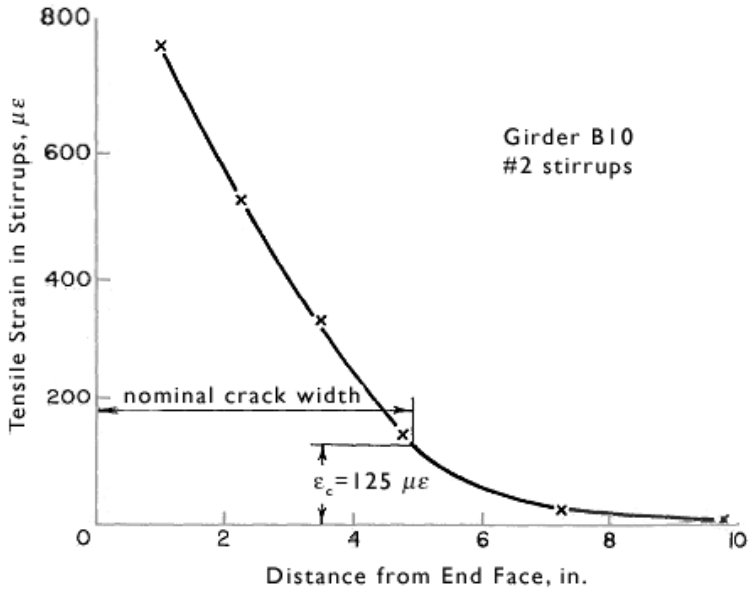

Figure 2.29 Typical transverse tensile strain variation *(after Marshall & Mattock, 1962)*

Of the cracked beams, four cracked at locations distant from the strain gages. For the remaining 14 cracked beams, the maximum stress and total force in the end-region transverse reinforcement were reported (Table 2.1). The later of these was also reported as a percentage of the applied prestressing force.

Table 2.1 Range of stresses & total force reported for transverse reinforcement
(Marshall & Mattock, 1962)

Parameter	**Range**	**Mean**
Maximum spalling stress	9 to 24 ksi	14 ksi
Total spalling force	1.0 to 3.4 % of P_i	1.8 %

As noted previously, two transverse reinforcing details (#2 or #3 stirrups at 1.25 to 2.5 in. spacing) were tested. Beams reinforced with #3 stirrups experienced higher

transverse forces compared to those with #2 stirrups (by 20%) due to the significant increase (120%) in provided bar area. The #3 stirrups were more lightly stressed, however (also by 20%). Cracks in beams with #3 bars were both shorter and finer than those with #2 (by 17%). The correlation between stress in a reinforcing bar engaged by a crack and the crack width seen here has been widely reported (e.g. in the studies summarized by ACI 224, 1972). Given this correlation and the primary goal of the end-region reinforcement being crack control, it seems reasonable to consider the maximum bursting/spalling stress in transverse reinforcement as an indication of the performance of a given set of end-region reinforcing details. The application of such a criterion would rank the behavior of beam end regions reinforced with #3 transverse bars superior to that of those reinforced with #2 bars.

The performance of the beams with #2 transverse bars was judged *"satisfactory with respect to cracking"* (p. 68), however, so Marshall and Mattock used the data from these beams (10 beams of the 14 that cracked near stress-measurement locations) to derive a design equation for transverse reinforcement. The first step of this derivation was to reduce the measured data into a single function, presenting the influence of three factors—prestressing force, member depth and strand transfer length—on the measured spalling force. Linear regression analysis (Figure 2.30) yielded Equation 2.2.

$$\frac{P_r}{P_i} = 0.0106\frac{h}{l_t} \qquad \textbf{\textit{Equation 2.2}}$$

where:

P_r = *force in transverse reinforcement (S in Figure 2.30)*
P_i = *prestressing force (T in Figure 2.30)*
h = *member depth*
l_t = *strand transfer length*

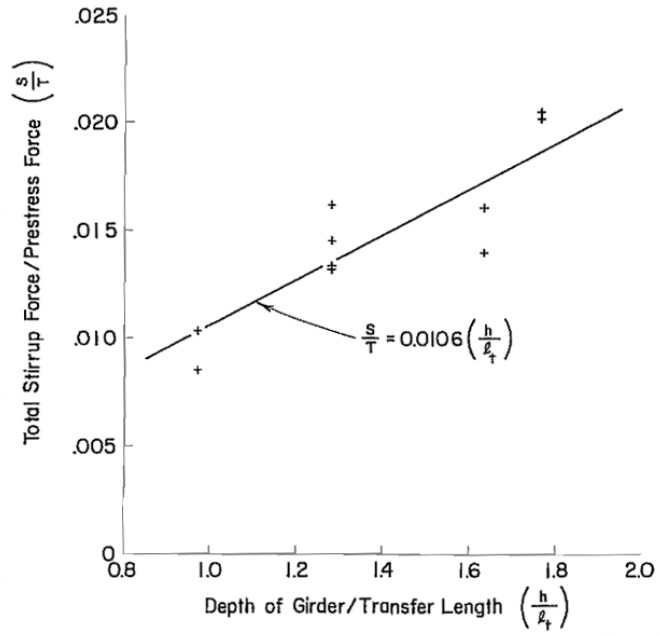

Figure 2.30 Linear regression analysis forming basis of Marshall & Mattock design equation *(after Marshall & Mattock, 1962)*

The actual variation of spalling stress with distance from beam end is approximately linear, as previously shown in strain terms (Figure 2.29). However, for their design procedure, Marshall and Mattock used a uniform design stress for transverse reinforcement in the end region. *"If f_s is the maximum allowable stress in the stirrups, then the average stress will be very nearly $f_s/2$"* (p. 72). The difference, then, between the actual spalling stress variation and that assumed for design is shown in Figure 2.31.

The resulting design equation is shown as Equation 2.3. Marshall and Mattock recommended distributing this reinforcement required by this equation uniformly over the end *h*/5 of a beam.

$$A_r = 0.021 \frac{P_i}{f_s} \frac{h}{l_t} \qquad \textbf{Equation 2.3}$$

where:

f_s = *maximum allowable stress in reinforcement*

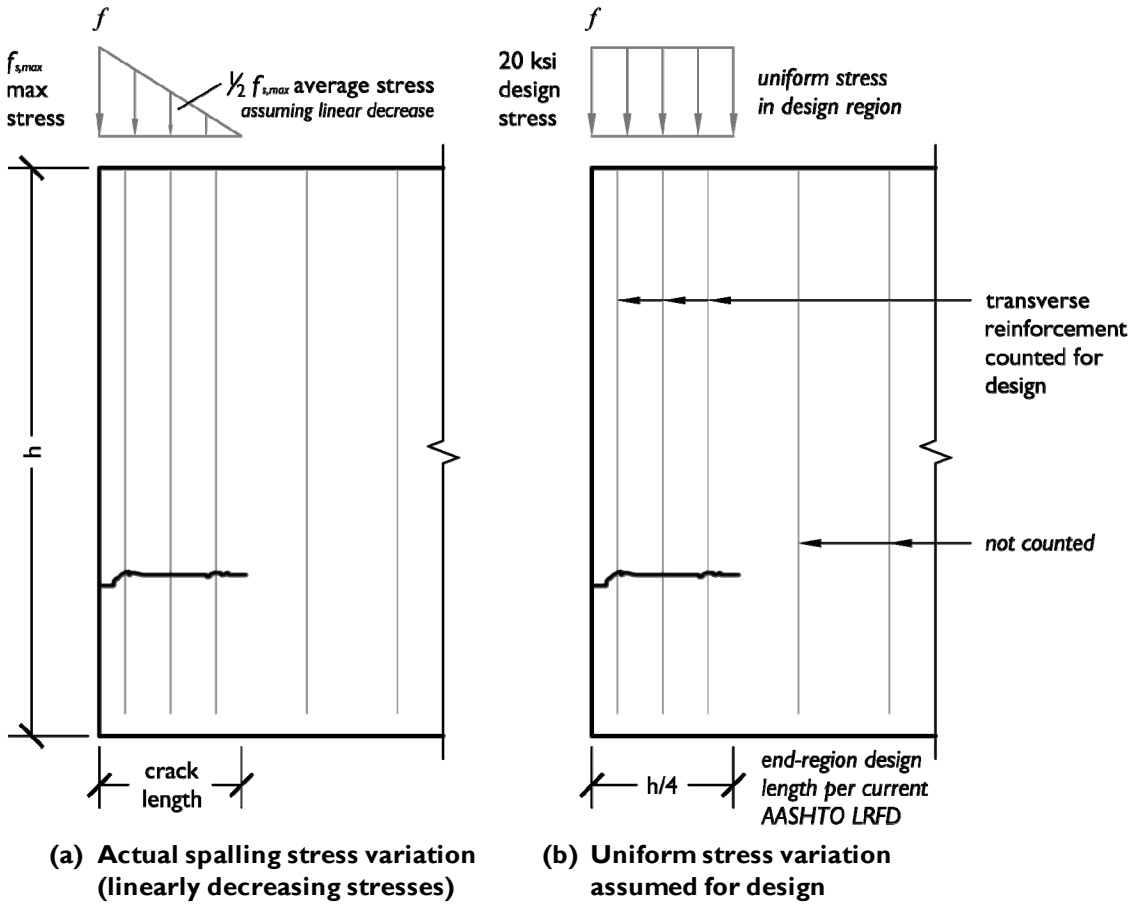

Figure 2.31 Actual spalling stress variation & uniform stress variation assumed for design

2.4.2.2 Gergely, Sozen & Siess, 1963

Experience measuring surface strains (discussed in Section 2.4.1.4) led Gergely, Sozen and Siess to study the effects of transverse reinforcement in crack control. A total of 25 post-tensioned beams were included in their study, but of these, the six rectangular and seven I-beams that were instrumented with strain gages on transverse bars are most relevant to the present study. Transverse reinforcing in these specimens was relatively light, consisting of one or two stirrups. The stirrups were fabricated of either 7-gage wire

or #2 deformed bar. Due to the detailing of this reinforcement, in addition to controlling horizontal cracking, the stirrups served to confine the prestressing force (Figure 2.32).

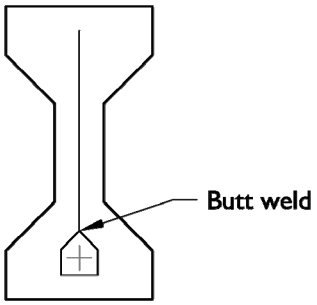

Figure 2.32 Stirrups serving as both transverse & confining reinforcement
(Gergely, Sozen & Siess, 1963)

Stirrups were instrumented along one line, which represented the height of the crack predicted by Gergely-Sozen analysis (previously described in Section 2.3.1). As this height was just below the centroid, spalling behavior was measured.

Strains in transverse reinforcement increased with applied prestress. Interestingly, Gergely, Sozen and Siess reported that the opening of cracks had *"no noticeable effect"* on the forces carried by the transverse reinforcement (p. 29). This finding either indicates that reinforcement is much more effective at preventing cracking than previously (or since) supposed, or it confirms the finding from the surface strain section that fine cracks (or microcracks) are very difficult to observe in the laboratory. The widest cracks observed in the absence of stirrup yielding were on the order of 0.003 in.

Beams reinforced with two stirrups (rather than one) saw the total spalling force split relatively evenly over the stirrups, with each bar taking approximately 75% of that seen in single-stirrup beams. This uniform contribution from each transverse bar counters Marshall and Mattock's observation (Section 2.4.2.1) that spalling stresses decreased linearly with distance from beam end face; however, it should be noted that all of the

stirrups in Gergely, Sozen and Siess' beams were placed very close to the beam end (within $h/6$). Stirrups in Marshall and Mattock's beams were more spread out (extending to $h/3$ from the end face).

Using cracks widths and lengths as indications of the performance of end-region detailing, the researchers concluded that 7-gage wire stirrups were ineffective as transverse reinforcement. Wire stirrups yielded at approximately 60% of the maximum applied prestressing force. While additional prestressing force could be taken by these beams after the stirrups yielded, horizontal cracking was no longer controlled. Yielding was thus seen as a limit state for effective end-region transverse reinforcement. Such experimental observation of inadequate transverse reinforcement is especially valuable—it can be recalled that, in of Marshall and Mattock's study, every beam was judged to perform adequately.

Though the wire stirrups performed poorly and the deformed-bar stirrups well, the difference in behavior is not necessarily due to bar type (i.e. deformation pattern and bond behavior). The wire used had less cross-sectional area and lower yield strength, which both contributed to a yield force one-third that of the deformed bar.

Comparing the behavior of the two different beam shapes yields interesting results. Beams with inadequate transverse reinforcement (e.g. those with one wire stirrup) were found to behave similarly regardless of their shape. For both rectangular and I-beams, severe cracking in the spalling zone was experienced at moderate levels of prestressing force, and effectively prevented the beams' webs from resisting the prestressing force.

I-beams with adequate transverse reinforcement were found to behave similarly to unreinforced rectangular beams based on surface strain data, which was also collected for some beams. This finding indicated that, if reinforced adequately, I-beam webs were

capable of resisting the prestressing force. Unreinforced I-beam webs (discussed in Section Section 2.4.1.4) were unable to sustain such behavior above low levels of prestressing force, due to extensive cracking.

2.4.2.3 Itani & Galbraith, 1986

After the two pioneering studies of transverse reinforcement strains conducted in the early 1960s, recommendations for pretensioned beam end-region design entered design codes (as detailed in Section 2.6). No similar experimental work was undertaken until the 1980s, when the Washington State DOT (WSDOT) sponsored research with the desired end of removing from their pretensioned I-beams rectangular end blocks. While the AASHTO code had ceased to prescribe end blocks 20 years before, WSDOT officials were reticent to remove them from their beams, which had thinner webs than the standard AASHTO shapes (5 in. as compared to 8 in.).

Itani and Galbraith (1986) studied a total of three end regions in 58 and 74 in deep I-beams constructed without end blocks. The transverse steel in these end regions was extensively instrumented (Figure 2.33). While multiple lines of strain gages were present at each instrumented section, only the *maximum* tensile stress for each transverse bar was reported. This method of reporting can be considered design-focused—a given bar must be designed to resist the maximum stress, regardless of the height at which the stress occurs—but frustrates attempts to separate bursting and spalling effects.

One of the two ends of the 74-in beam was lightly reinforced in anticipation of future shear testing. As a result, a direct comparison of two different end details can be made. The lightly reinforced end contained 10% less transverse reinforcement than required by AASHTO LRFD (2009) while the heavily reinforced end contained nearly

50% more reinforcement than required. The instrumented end of the 58-in. beam had an intermediate amount of transverse reinforcement (20% more than the code requirement).

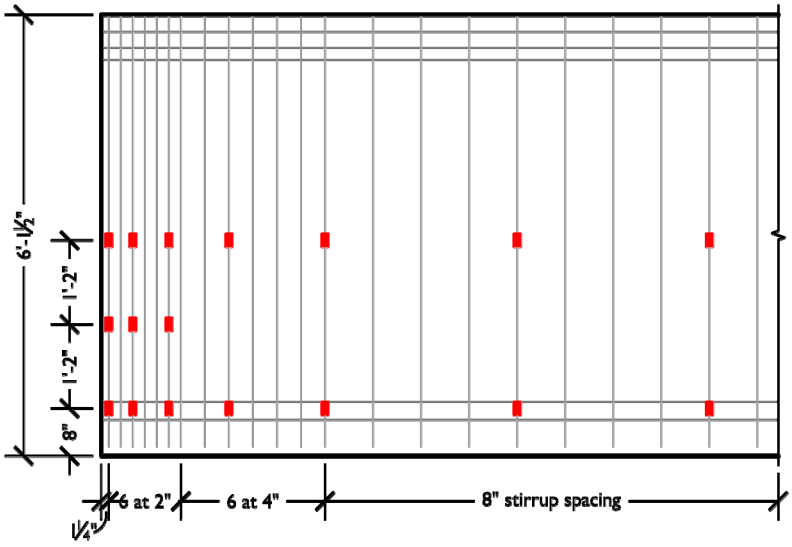

Figure 2.33 Typical transverse-bar strain-gage locations *(Itani & Galbraith, 1986)*

Transverse-bar stresses at prestress transfer deceased from their maximum values, at stirrups closest to the beam end, to nominal levels within *h*/3. One bar exceeded the AASHTO stress limit (20 ksi); the bar was located in the lightly-reinforced end. Stresses in transverse bars were measured twice after transfer of prestress: immediately after transfer, and after the beams were moved from the pretensioning bed (a few house after transfer). Stresses were slightly higher after moving, on the order of 10%. It is unclear whether the beam-lifting process or the passage of time led to the increase in bar stresses.

End-region cracking was well-controlled by transverse reinforcement. The end region with the least reinforcement (the lightly-reinforced end of the 74 in. deep I-beam) experienced the most extensive cracking. In this end region, cracks 10 to 15 in. long and 0.004 in. wide were noted. The more heavily-reinforced end regions experienced fared

better. No cracking was observed in the heavily-reinforced beam end region, and a single 0.004 in. wide crack was seen in the 58-in. beam (moderately-reinforced).

Limited surface-strain measurements were also taken at transfer of prestress using strain rosettes. Maximum tensile principal strains were found in the bursting zone: *"near the bottom flange and slightly in from the end of the girder"* (p. 53). Though no cracking was observed in the region, tensile strains exceeded nominal cracking strain values by 800%. Such data was interpreted as evidence of microcracking.

As Itani and Galbraith performed testing both at prestress transfer and under shear loading on their 74 in. deep I-beam, they could comment on the structural effects of bursting and spalling stresses and associated cracking (from transfer). At shear testing, bursting and spalling cracks from transfer closed up under applied load; their effect was judged negligible. No long-term monitoring of reinforcement strains (i.e. between transfer and shear testing) was conducted, however, due to concerns that the foil strain gages used were ill-suited for this purpose. Beyond the first few hours, *"[strain] readings are significantly distorted by ... drift of the strain gages and measuring equipment"* (p. 41).

2.4.2.4 Tuan et al., 2004

Tuan et al. completed a study of pretensioned beam end-region reinforcement in which a total of 26 beams were tested, including 10 with a new reinforcing detail favored by the authors. This study represents the largest contribution—in terms of number of specimens—to the spalling behavior database.

The impetus for this study was a reported difficulty among bridge design professionals with fitting the transverse reinforcement required by AASHTO LRFD within its allotted zone (i.e. the end $h/4$). Through the use of 0.6-in. strand and high-

strength concrete, increasingly high prestressing forces have been applied recently to sections standardized years ago (Nickas, 2004). This increase in prestressing force may approach 50% for some sections (Nolan, 2004). With higher prestressing force comes a higher transverse reinforcing requirement, which must be balanced with constructibility concerns.

The beams reinforced with standard details included inverted T-beams (IT-beams) of 17 and 25 in. depth and I-beams (NU bulb tees) of 43, 63 and 70 in. depth. Tested with the proposed detail were 17-in. IT-beams and 43- and 63-in. I-beams. Transverse reinforcement in all beams was instrumented at one depth, that consistent with the crack location predicted by Gergely-Sozen analysis. This location was typically in the spalling zone just below the section centroid (Figure 2.34), though for one set of I-beams the line of instrumentation ran closer to the bottom flange/web junction (Figure 2.35). Instrumentation was limited to the end $h/4$ in I-beams and $3h/4$ in IT-beams. Approximately 90% of the installed strain gages functioned after transfer.

It should be noted that the strain-gage location was for this project chosen based on analysis rather than on insight gained from field evaluation. Tuan et al. did conduct such evaluations, however, for they report on typical crack patterns in the same paper:

> *Cracks… frequently observed at the ends of pretensioned concrete members at the time of prestress transfer… are commonly horizontal and occur near the junction of the bottom flange and web. Some diagonal cracks are also observed higher up on the web* (p. 68, emphasis added).

It can be conjectured that in some cases (e.g. the deep I-beam in Figure 2.34-a), the gages may have been positioned too high to measure the maximum strains at transfer.

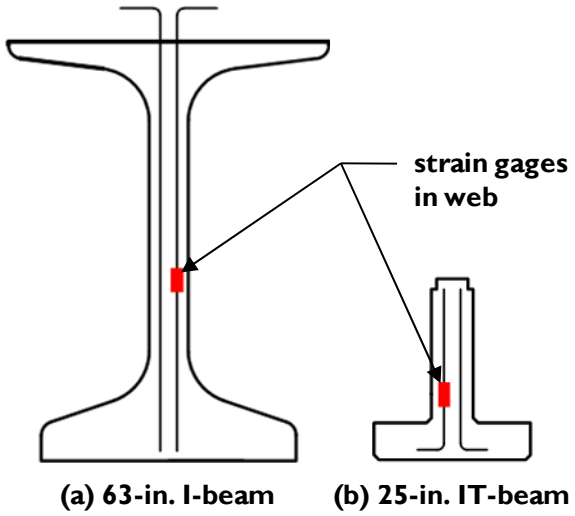

Figure 2.34 Typical strain-gage location for I- & IT-beams

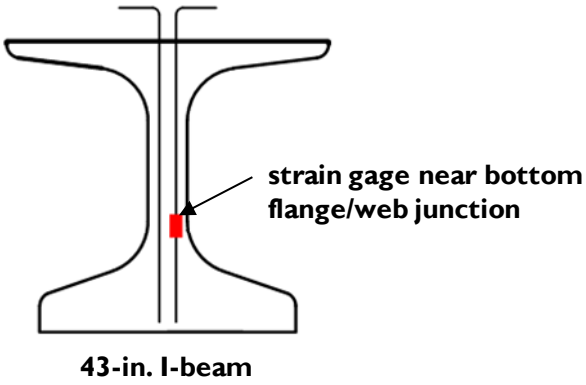

Figure 2.35 Strain-gage location for 43-in. I-beams

Beams reinforced with standard details performed well. For I-beams, several fine cracks typically extended up to 12 in. from the beam end. These cracks were reported to occur *"near the theoretically anticipated location"* (p. 73). Minimal cracking was observed for the IT-beams. All measured stresses in the transverse reinforcement for beams with standard details were below the AASHTO stress limit of 20 ksi, though two I-beams had bars less than 1 ksi below the limit. Stresses decreased approximately linearly with distance from the beam end, leading the researchers to observe that *"only*

the reinforcement located within the end h/8 of the member experienced significant stress" (p. 74).

Based upon this observation, Tuan et al. designed a new end-region reinforcing detail that concentrated reinforcement near the beam end. Special transverse reinforcement (threaded rod or deformed bars welded to top and bottom plates) designed to resist 2% of the applied prestressing force P_i was provided within the end $h/8$ of the member. An equal amount of reinforcement was spread over the region between $h/8$ and $h/2$ from the beam end. In this way, the amount of transverse reinforcement required by AASHTO in the end $h/4$ was instead spread over the end $h/2$.

Beams reinforced with the proposed detail were reported to have smaller crack widths and lengths than those using standard details. However, stresses were higher (mean *maximum* spalling stress of 16 ksi compared to 11 ksi). Four beam end regions had maximum stresses that exceeded the AASHTO limit by as much as 30%; all were 43-in. I-beams (instrumented near the flange/web junction, as shown previously in Figure 2.35). IT-beams again experienced lower spalling stresses than did I-beams.

Tuan et al. used their strain gage readings to calculate the total transverse-bar force at prestress transfer for each beam end region. As they note, the transverse-bar force at transfer *"is not limited to steel in the end h/4 of the member"* (p. 77). Unfortunately, their instrumentation was, in the case of I-beam specimens, and so a substantial amount of extrapolation was sometimes required in the calculation of transverse-bar force at transfer (spalling force).

Though the accuracy of their reported total forces is called into question because of this extrapolative procedure, some general observations are possible. Beams with 0.6-in. strands experienced higher spalling forces (by 20%) compared to similar sections prestressed with 0.5-in. strands. The spalling force can be calculated within the end $h/4$

for all beam end regions without resorting to extrapolation. No significant difference was found between the spalling forces acting in this region for the differently-detailed beams. The mean spalling force for I-beams was 2.0% P_i, similar to the ratio found by Marshall and Mattock (1962), 1.7% P_i. In *no* cases did the spalling-force ratio exceed 3.0%.

When comparing these measured ratios of transverse-bar force at transfer of prestress to prestressing force, it is essential to recall that the AASHTO design procedure assumes a uniform stress distribution (Figure 2.32-b). As the Tuan et al. beams were instrumented in the spalling zone, their reported transverse stress distributions were more like that shown in Figure 2.32-a: linear decrease in stress with distance from member end.

Aside from Tuan et al.'s observation that crack widths and lengths were reduced with the proposed detail, the performance of the proposed detail was inferior to that of the standard detail. The *average* stress in the end-region steel (total spalling force divided by the area of transverse reinforcement resisting it) was higher, and several beam end regions with the proposed detail had *maximum* stress measurements exceeding the AASHTO stress limit. Concerns regarding constructibility were not eliminated, particularly for shallower members for which 2% P_i within *h*/8 may be more restrictive than 4% P_i within *h*/4 once minimum end cover is considered.

2.4.2.5 Crispino, 2007

Crispino conducted an experimental study of two pretensioned concrete beam end regions with the intent of controlling diagonal spalling cracking in deep I-beams (Virginia bulb tees). The study served as experimental verification of the strut-and-tie-based design approach of Davis, Buckner and Ozyildirim (2005), which was presented in Section 2.3.1.3.

Typical crack patterns for the beam used for this study are shown in Figure 2.36. Virginia DOT (VDOT) criteria for acceptable cracking are as follows:

- Diagonal cracks terminating within *h*/2
- Horizontal cracks terminating within *h*/4
- Widths less than 0.012 in. for standard service conditions

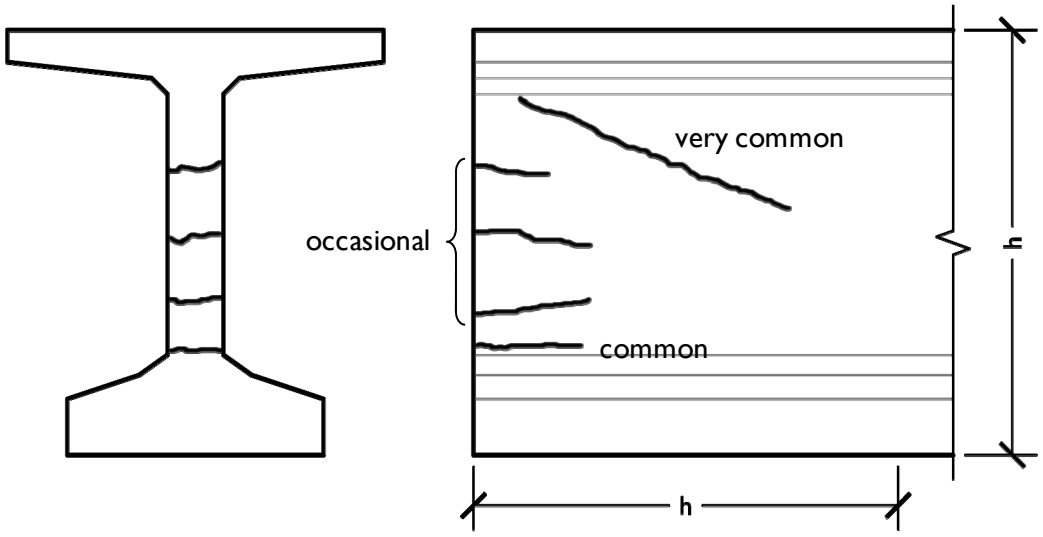

Figure 2.36 Typical crack pattern in Virginia bulb tee *(after Crispino, 2007)*

Based on a comparison of the typical cracking pattern and these criteria, it can be gathered that at the time of the Crispino study, Virginia bulb tees "very commonly" showed unacceptable cracking.

The end-region behavior of a 53-in. bulb tee constructed was examined in the course of the study. The two ends of the beam were designed using the same STM (Davis, Buckner & Ozyildirim), but used different allowable reinforcement stresses: 12 ksi or 18 ksi. The STM procedure sets up two zones of reinforcement: within *h*/4 from the beam end and between *h*/4 and 3*h*/4. The 12-ksi and the 18-ksi ends had the same

stirrup spacing in the region closest to the beam end, but different spacing in the next region: the 18 ksi-end had 20% less steel there.

Two components of the experimental program designed by Crispino deserve mention: the materials choice and the detensioning method. Lightweight self-consolidating concrete (SCC) was used. This material has a low modulus of elasticity and tensile strength relative to normal-weight concrete. For detensioning, strands were flame-cut as per standard practice in Virginia. Other studies of reinforcement strains in pretensioned beams since Marshall and Mattock (1962) have used multi-strand gradual detensioning.

Beam end regions were instrumented as shown in Figure 2.37. Strain gages were applied to the bars nearest the beam end at the bottom flange/web junction (bottom row of gages) and the predicted crack location from Gergely-Sozen analysis (second row). These bottom rows of strain gages could be said to be in the bursting zone, but their ability to measure maximum bursting strains may have been compromised by the fact that they extend only a short distance ($h/4$) into the beam. The upper sets of gages, measuring spalling strains, were positioned along the expected diagonal crack location (based on field experience). Approximately 60% of the gages functioned after transfer of prestress.

At transfer, cracks formed in both end regions. Following Itani and Galbraith (1986), Crispino reported transverse-reinforcement stresses occurring after the beam was lifted. Cracking in the lower portions of the two ends were comparable, but the 18-ksi end developed a diagonal crack above the uppermost line of gages. This diagonal crack was visible on both sides of the beam and extended 37 in. (approximately $3h/4$, exceeding the acceptance criteria by 50%).

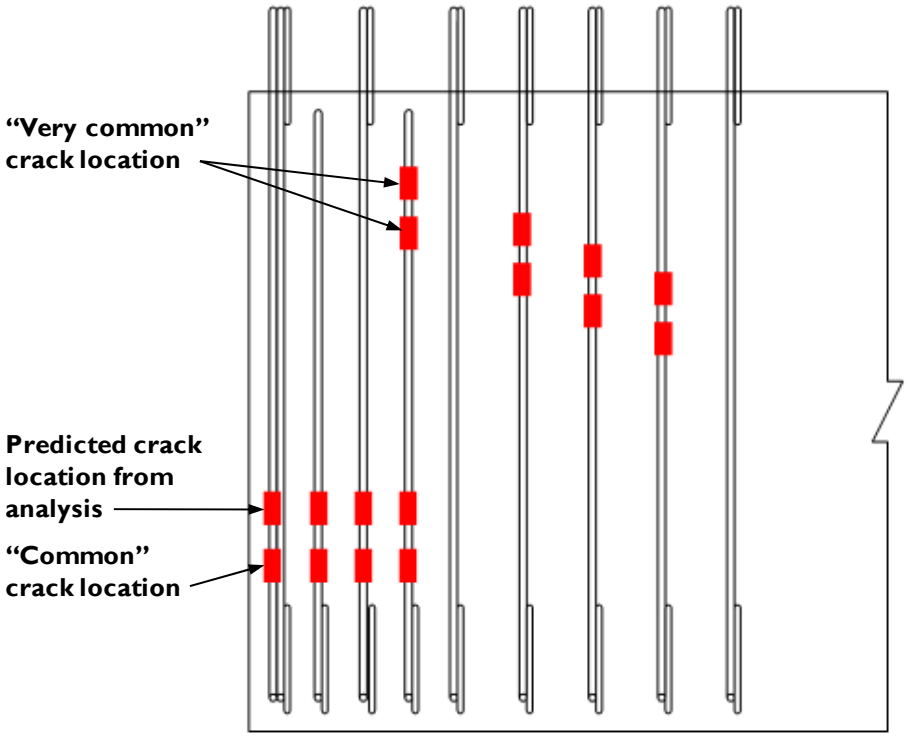

Figure 2.37 Typical gage locations *(after Crispino, 2007)*

Cracking was rather fine (maximum crack widths for the 12- and 18-ksi ends were 0.003 and 0.005 in., respectively) and no gage measured stresses exceeding the AASHTO limit (20 ksi). Crispino judged the end region detailed with a 12-ksi design stress acceptable and that with an 18-ksi design stress unacceptable based on the diagonal-crack length.

2.4.2.6 O'Callaghan, 2007

O'Callaghan completed a study of bursting and spalling in a new line of Texas bulb tees (Tx girders) while the pretensioned beams were in design development. Both end regions of four beams of varying depths (two at 28 in., and one each at 46 in. and 70

in.) were tested at transfer of prestress. The beams were prestressed using 0.6-in strand, which typically filled the 60% of the available spaces in the bottom flange.

Unlike in other recent projects, the pretensioning bed used for this study was contained within a structural laboratory (at The University of Texas at Austin). As a result of fabricating the beam in the laboratory as opposed to at a commercial precasting facility, the researchers were able to more thoroughly instrument the beam end regions. At least 32 strain gages were provided in each end region, compared to four gages in the Tuan et al. study (2004).

The beams contained an end-region reinforcing detail unique to this project. Shear reinforcement (2 – #4) at moderately close spacing (3 or 4 in.) was extended into the beam end region. In the end regions, supplemental spalling reinforcement was provided as straight #6 bars bundled with the shear reinforcement. The resulting special end-region reinforcement has an area triple that of the standard shear reinforcement (1.28 vs. 0.40 in.^{2}).

Transverse reinforcement in the beams was generally adequate based on AASHTO and PCI requirements (referred to as "spalling" reinforcement requirements), though that in the shallowest beam (Tx28) was insufficient by 15%. O'Callaghan also compared the provided transverse reinforcement to CEB-FIP requirements for bursting reinforcement. All beams had insufficient transverse reinforcement, by 100 to 200% of the provided area per this code (O'Callaghan, 2007).

Beams were instrumented in both bursting and spalling zones, typically at three depths as shown in Figure 2.38. The lowest of these lines of strain gages was at the bottom flange/web junction (just above the primary group of prestressing strands); the middle at the section centroid; and the upper at the top flange/web junction. A distance *h* into the beam was instrumented.

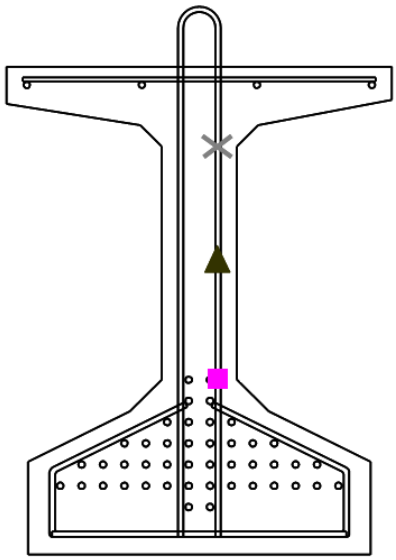

Figure 2.38 Typical gage locations *(O'Callaghan, 2007)*

Cracking in the bursting zones of the Tx girder specimens was extensive (Figure 2.39). Typically a wide crack of 0.007 to 0.009 in. formed at the bottom web/flange junction. This crack would begin a few inches into the beam and extend 30 to 40 in. For 7 of the 8 end regions, the AASHTO stress limit (20 ksi) was exceeded at this depth: in most cases, by more than one bar. Bars stressed beyond 20 ksi were located 15 to 30 in. into the beam. Near the beam end, where supplemental bundled reinforcement was provided, *no bar* was observed to exceed the stress limit. Cracks also formed in the side of the flange, but these cracks were not as wide. One beam was instrumented at this depth, but the stresses found there were much lower than those at the bottom flange/web junction.

Cracking in the spalling zone was limited to one or two fine cracks extending a few inches into the beam. The most extensive spalling cracks were seen in the deepest

beam (70 in. deep), confirming the correlation between eccentricity and spalling. Spalling stresses reached a maximum of approximately 10 ksi at mid-depth of this beam.

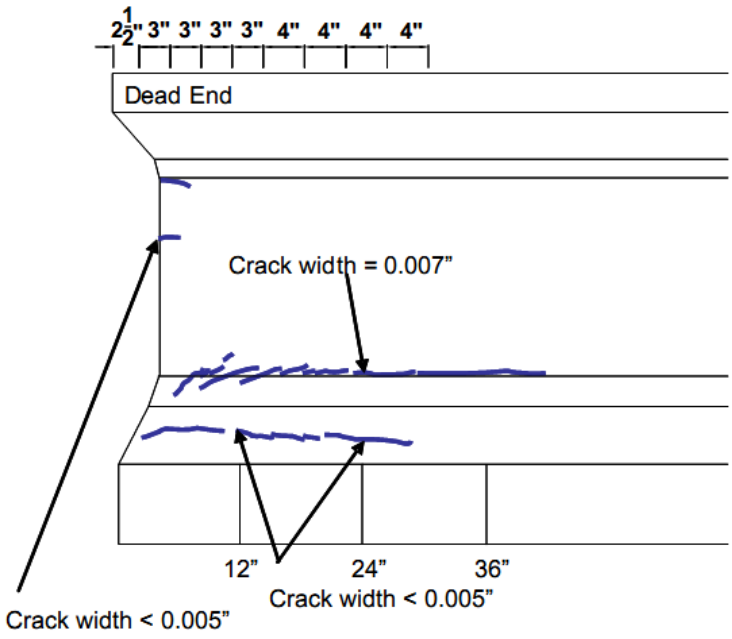

Figure 2.39 Typical crack pattern with widths *(O'Callaghan, 2007)*

For the beams of this study, bursting effects were clearly more significant than spalling effects. These beams were more highly stressed than most others, and had prestressing force applied close to the bottom flange/web junction. Perhaps most significantly, though, the beams employed gages in the bursting zone, without which the significance of the bursting stresses could have been missed.

In recognition of the high observed bursting stresses in the transverse reinforcement, O'Callaghan recommended extending the bundled straight-bar reinforcement out to one transfer length (36 in.) from the end of the beam, at which location the stresses were judged to have diminished sufficiently. This recommendation was adopted by the TxDOT in the design standards for the new beams (2007).

2.4.2.7 Smith et al., 2008

Most recently, Smith et al. attempted to measure the transverse tensile strains in a wide IT-beam (Figure 2.40). No significant strains were found in the transverse reinforcement, nor was the section observed to crack.

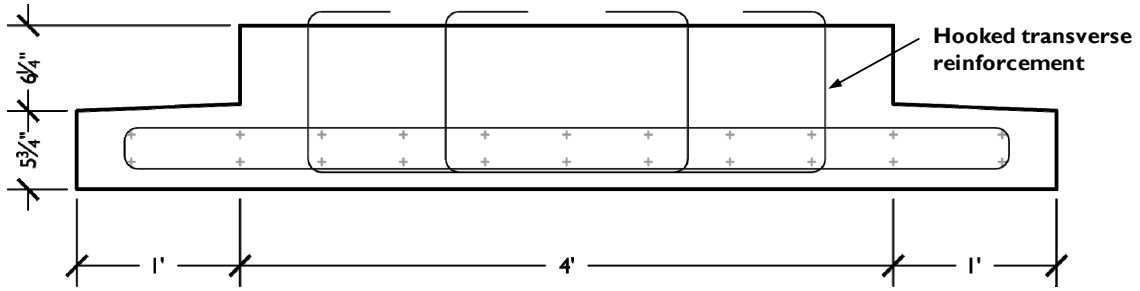

Figure 2.40 Wide IT-beam monitored by Smith et al.

2.4.2.8 Summary

Analysis of a transverse-bar bursting/spalling stress database incorporating the studies outlined in this section and Research Project 5831 is presented in Section 4.3. At present, it is sufficient to note that aside from three studies (Itani and Galbraith. 1986; Crispino, 2007; O'Callaghan, 2007), experimental studies of transverse tensile strains in end-region reinforcement have been limited to examination of spalling effects. Most measured bar strains, when converted to stresses, were below the AASHTO limit (20 ksi), though some exceeded the limit by as much as 50%. In general, the *more* end-region transverse reinforcement provided, the *lower* the measured stress in those bars.

2.5 STATE OF PRACTICE

2.5.1 Field Experience with End-Region Cracking

Fountain (1963) completed a visual evaluation of 88 prestressed concrete bridges during 1959 and 1960. Ten years after from the construction of the first prestressed

concrete bridge in the United States, the Bureau of Public Roads (BPR), PCA and PCI wished to know how bridges constructed using the new technology were performing. The vast majority of the bridges were judged to be in *"excellent"* condition (p. 43), but many were found to contain girders with some end-region cracking.

Of note were cracks *"at [member] ends and along junctions between flanges and webs"* (p. 1). Such cracking was especially prevalent in pretensioned I- and T-beam bridges in which the prestressing force was separated into two groups at beam ends. An example of this construction, an I-beam with both straight strands in the bottom flange and harped strands in the top flange and web, is shown as Figure 2.41.

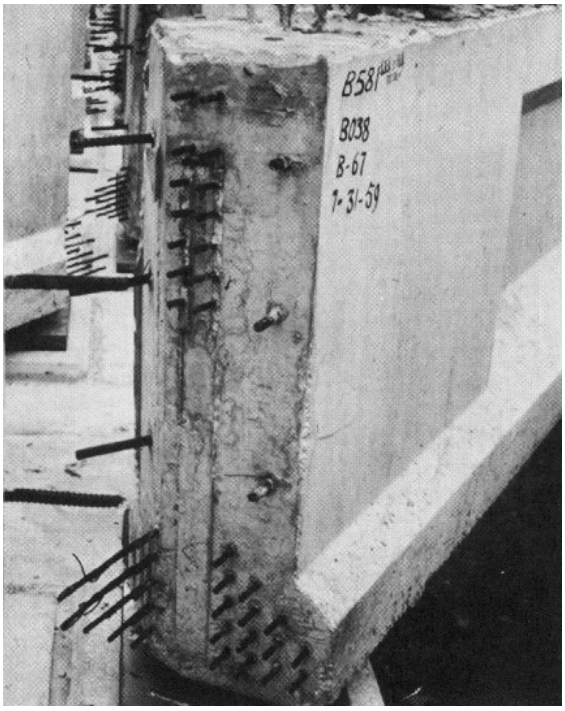

Figure 2.41 Beam with two strand groups *(Fountain, 1963)*

90% of bridges with this sort of beam (30 of 32 bridges) were found to have end-region cracking near the section centroid. The cracking was typically well-controlled by

the provided transverse reinforcement: cracks were less than 0.008 in. wide and 12 in. long. The provision of end blocks had no impact on whether a girder cracked in this pattern.

Fountain did not observe cracking near the section centroid in other bridge types. Representing the "other" category were inverted T-beam (IT-beam), box beam, and slab bridges. The field-study finding that near-centroid cracking was unlikely for IT-beams was confirmed by later experimental studies (Tuan et al., 2004; Smith et al., 2008).

Observation of horizontal cracks at flange/web junctions is also of interest. Unlike for horizontal cracking near the centroid, the occurrence of this form of cracking could not be correlated with end-region prestressing force distribution. These cracks were *"ragged and discontinuous,"* usually *"having lengths of 1 to 4 in."* (p. 21). Primarily observed at the top flange/web junction, cracks of this sort were also seen near the bottom flange. They typically appeared on both sides of girders, but Fountain expressed doubts that such cracks extended through the section breadth.

The primary causes hypothesized for horizontal flange/web cracking were fabrication-related. Many early I-sections lacked fillets. The reentrant corners then found at the flange/web junction were vulnerable to cracking due to form restraint, by the differential settlement before the concrete hardened or early-age shrinkage afterward. For beams cast in two stages—box beams in the Fountain study or U-beams and box beams both, in TxDOT Research Project 5831— another cause was hypothesized: inadequate vibration provided at the interface between concretes from the two casting stages.

A second source for typical crack patterns in pretensioned beam end regions is Gamble (1997). Over the course of field investigations for the Illinois DOT that spanned the 1970s, Gamble and his research group examined *"perhaps 100 pretensioned*

I-girders" (p. 102), the majority of which were 48 in. deep with strand groups in the top and bottom flanges.

Most of these beams had cracks just above and at the bottom flange/web junction (Figure 2.42); cracks in other locations were unusual. The upper of the two "common" cracks, Gamble noted, formed at the location predicted by Gergely-Sozen analysis. Cracks were typically less than 0.008 in. wide and did not extend 18 in. from the end of the beam. The widest crack observed was 0.016 in. Gamble judged this sort of cracking to be well controlled by the transverse reinforcement in the end region.

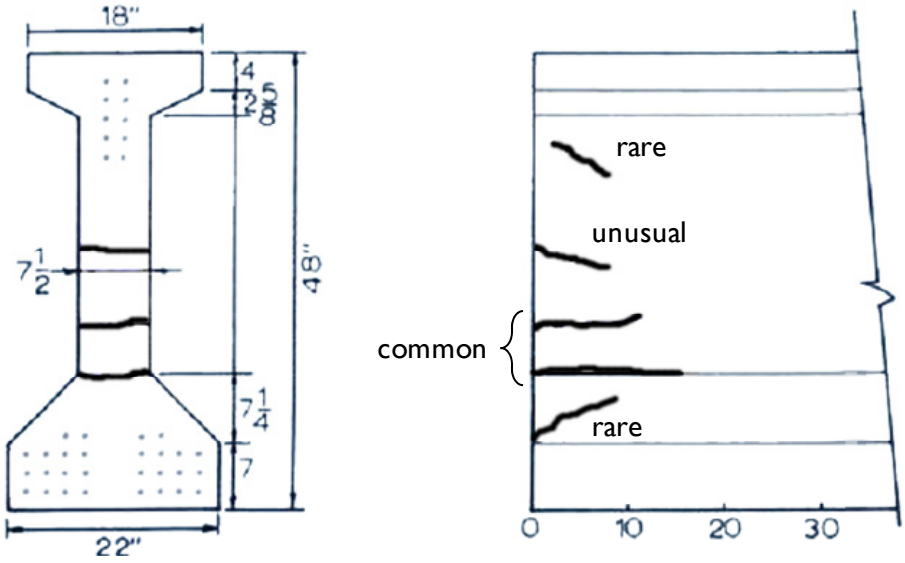

Figure 2.42 Prevalence of crack patterns noted in pretensioned I-beams
(after Gamble, 1997)

Gamble also noted that while most beam end regions cracked immediately after prestress transfer, cracks sometimes took up to two weeks to form. One group of 50 beams was analyzed for an age-crack relationship, but no correlation could be found.

Itani and Galbraith (1986) reported the results of a small survey of I-beams with rectangular end blocks. Of the 25 beams they examined in the field, all experienced end-region cracking. Most beams had two to five cracks, which were 0.008 to 0.012 in. wide.

Lastly Barrios (1994) inspected two 54-in. Texas U-beams fabricated in a precast plant for end-region cracking during a study of prestress transfer and debonding. No cracks were found at prestress transfer, but one week later diagonal cracking (Figure 2.43) was observed. The beams examined by Barrios represented typical design cases for U-beams, rather than worst-case scenarios in terms of end-region stresses: approximately 20% of the prestressing strands were debonded at the beam end.

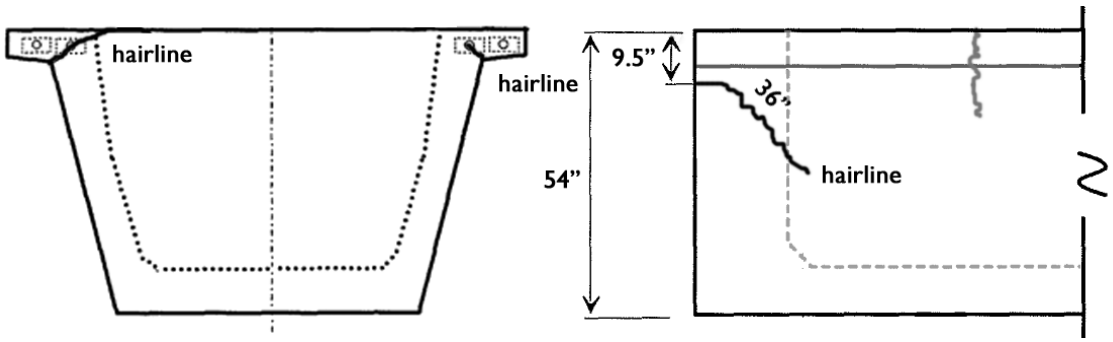

Figure 2.43 Cracking in Texas U-beam, one week after transfer *(Barrios, 1994)*

Barrios also tested confining reinforcement details, matching the standard U-beam detail (Figure 2.44-a) against a proposed detail (Figure 2.44-b). Both details included confining reinforcement at the beam end as shown in Figure 2.45. As no cracking was noted in bursting zone, the stress in the confining reinforcement was assumed to be low, and both confining details were judged to be adequate. The version with less reinforcement (Figure 2.44-a) was recommended, and remains as the current standard.

It should be noted that Barrios did not perform structural testing on the U-beams. Under shear loading, as diagonal cracks form near the bottom flange, confining

reinforcement would be activated and could then serve to delay strand bond failure, and perhaps prevent horizontal sliding-shear failure.

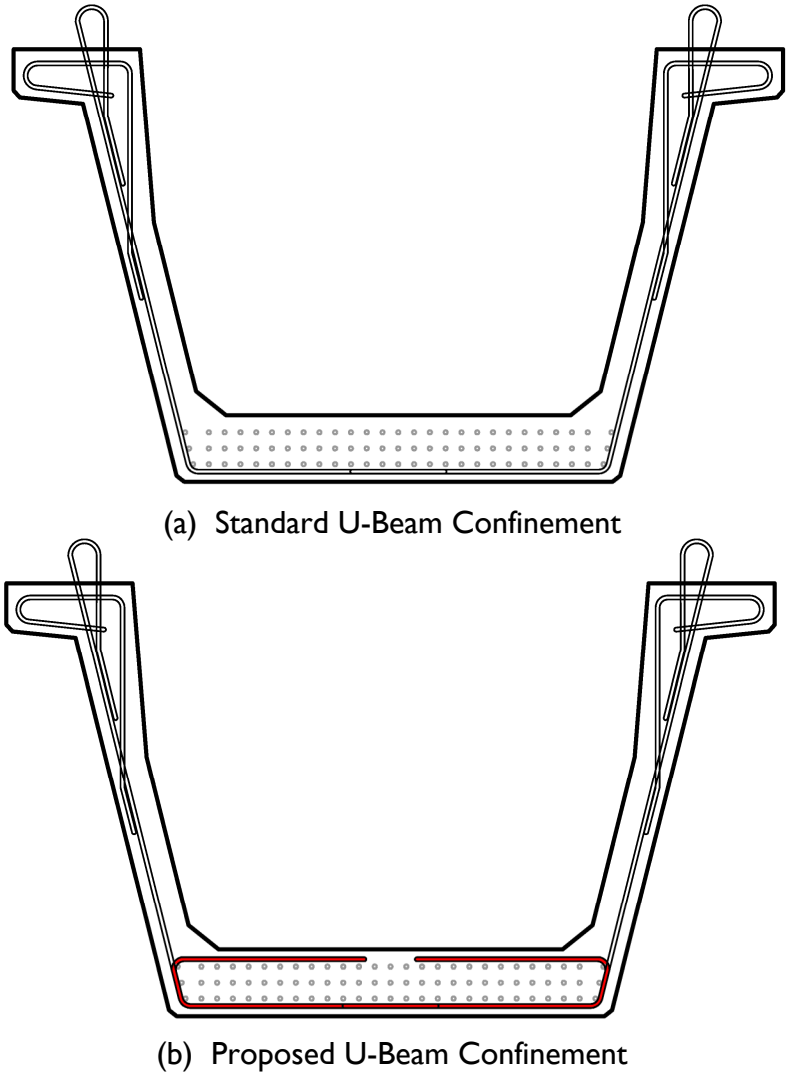

***Figure 2.44 Confining reinforcement details tested by Barrios** (1994)*

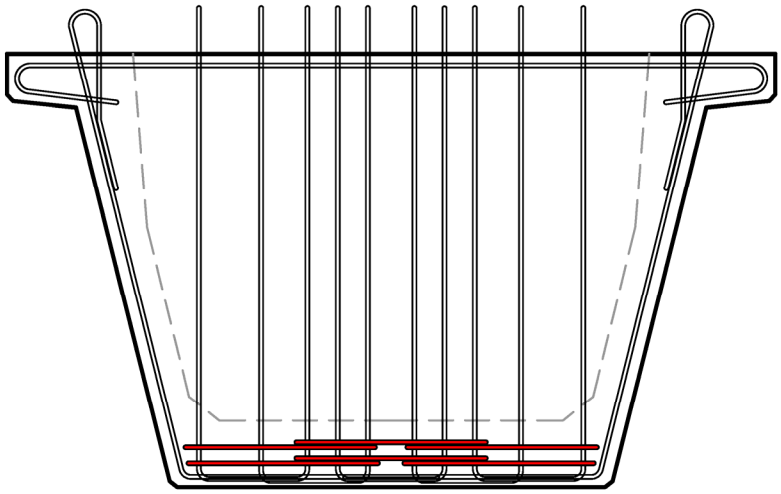

Figure 2.45 Confining reinforcement provided at end of beams with both details shown in Figure 2.44

2.5.2 Best Practices for Minimizing End-Region Cracking

The PCI Committee on Quality Control Performance Criteria put out a publication in 1985 relating precasters' experience of all sorts of cracks that might form *"during casting, stripping or shipment"* (p. 4) of pretensioned beams and columns. The document was based on a national survey of PCI members. Causes and effects were outlined for a number of crack types, along with preventative and remedial measures.

Of interest to the present investigation is the description of *"horizontal end cracks in [the] web or flange"* (p. 10). The causes of such cracks listed in the document include improper design and/or construction, as summarized in Table 2.2. Other causes listed are *not* categorized as "improper," suggesting that even with best practices, some amount of horizontal cracking is likely to occur in pretensioned concrete beams. These other causes are listed in Table 2.3.

Table 2.2 Causes of end-region cracking from improper technique per PCI report

Improper Design	**Improper Fabrication**
Too little end reinforcement Too much prestress force	During casting During transfer and stripping During handling

Table 2.3 Other causes of end-region cracking per PCI report

Cause	**Resulting Crack Location** (Figure 2.46)
Settlement of concrete	Web (a)
Differential stresses between the flange and web due to detensioning or inherent in the design	Bottom Flange/Web Junction (b)
Insufficient cover of the strand	Bottom Flange (c)

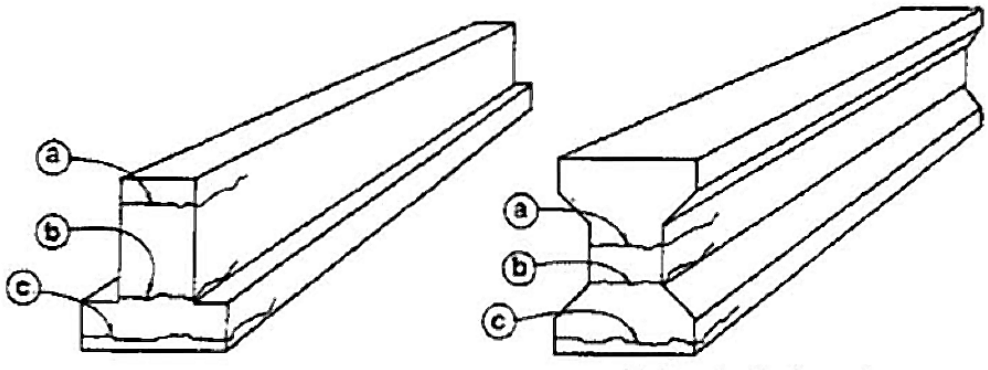

Figure 2.46 Common cracks in pretensioned beams *(PCI, 1985)*

The structural impact of such cracks, the PCI committee claimed, is *"minimal"* in most cases, noting that the end reaction of the beam effectively provides a clamping force that tries to close these cracks. The addition of superimposed dead load (e.g. roadway deck) after the beam is placed in a bridge would increase this clamping force. That said,

cracks located along lines of prestressing (Figure 2.46, crack ***c***) may cause loss of bond, which could subsequently lead to decreased shear and moment capacity near the end of the beam (PCI, 1985).

As part of an ongoing NCHRP project (18-14) investigating end-region cracking and potential repair schemes for pretensioned beams, Tadros et al. (2007) conducted a survey of DOT officials, bridge consultants and precast concrete fabricators throughout the United States and Canada. Responses were received from representatives of 37 states and provinces. Respondents were asked, based on their experience, to identify contributing causes of end-region cracking; their responses are summarized in Table 2.4.

Table 2.4 Causes of cracking summarized from national survey of bridge design/construction professionals conducted by Tadros et al., 2007

Design-Related Cracking	**Fabrication-Related Cracking**
Inadequate design of end-region reinforcement	Detensioning method
Concrete release strength (compressive/tensile)	Lifting method
Strand size, spacing and distribution	

2.5.3 Acceptable End-Region Cracking Criteria

Most pretensioned concrete beams experience some cracking in their end regions due to the combination of bursting, spalling, shrinkage, temperature and other effects. Excessive cracking, however, is typically prohibited by DOT specifications and/or practice. Different sources demarcate the boundaries between acceptable and excessive cracking differently: for example, Gamble (1997) judged a 0.016 in. wide, 18 in. long crack to be acceptable, whereas Itani and Galbraith (1986) judged a 0.005 in. wide, 15 in. long crack unacceptable.

From the survey discussed in the previous section, Tadros et al. (2007) report that most bridge professionals use crack width as the sole criterion of acceptable end-region behavior. A crack above a given width triggers a particular repair, as shown in Table 2.5.

Table 2.5 Typical DOT practice for repair of cracks in pretensioned concrete beams
(Tadros et al., 2007)

Crack Width	**Required Action**
≤ 0.007 in.	Coat with a surface sealant
0.007 to 0.025 in.	Epoxy-inject crack
≥ 0.025 in.	Beam is rejected

The 0.007 in. crack width criterion for epoxy injection can also be found in the PCI Manual for the Evaluation and Repair of Precast, Prestressed Concrete Bridge Products (2006), though for beams subject to aggressive environments. For moderate environments, this standard recommends no repairs for pretensioned beams with cracks of up to 0.012 in. wide. The CEB-FIP Model Code (1990) proposes the same crack width limit (0.30 mm or 0.012 in.) as a standard for pretensioned beams *"in the absence of any specific requirements"* (Clause 7.4.2).

The Texas DOT (TxDOT) has no official acceptable crack-width criteria, but O'Callaghan (2007) reported that end-region cracks wider than 0.010 in. are typically epoxy-injected. If a large number of wide cracks form in an end region, the beam is typically rejected.

2.6 DESIGN CODE REQUIREMENTS

Prestressed concrete design in the United States is governed by codes published by three organizations: AASHTO, ACI and PCI. The code provisions published by these

bodies relevant to pretensioned concrete beam end regions are presented, with their historical development. Provisions from one European code, the CEB-FIP Model Code (1990), are also presented.

2.6.1 AASHTO Provisions

Provisions for the design of prestressed concrete first entered the American Association of State Highway Officials (AASHO) Standard Specifications for Highway Bridges in 1961. Later that year, a set of interim specifications were released. The differences in these two versions of the same document related to end-region design are illustrative of a fundamental change in philosophy brought about by research conducted by PCA (Marshall & Mattock, 1962; Fountain, 1963).

The original 1961 AASHO Specifications prescribed the use of end blocks for all prestressed concrete members. Interestingly, the requirement for *"closely spaced"* end-region reinforcement (Section 1.13.15) was limited to post-tensioned concrete beams.

Later that year, the interim specifications (1961) eliminated the requirement for end blocks for pretensioned beams: *"For beams… where all tendons are pretensioned wires or 7-wire strand, the use of end blocks will not be required."* Instead, the interim specifications required that pretensioned concrete beams be reinforced with transverse steel. The amount of reinforcement thought necessary to control end-region cracking was prescribed by the following provision, which in slightly modified form exists in the current highway bridge code (AASHTO LRFD Bridge Design Specifications, 2009):

> *In pretensioned beams, vertical stirrups acting at a unit stress of 20,000 psi to resist at least 4 percent of the total prestressing force shall be placed within the distance of d/4 of the end of the beam, the end stirrup to be as close to the end of the beam as practicable.*

The requirement for transverse reinforcement sufficient to resist 4% of the applied prestressing force (P_i) can be considered a simplification of Marshall and Mattock's original equation, with the assumption that the beam height-to-transfer length ratio (h/l_t) be approximately equal to two (Equation 2.4).

$$A_r = 0.021 \frac{P_i}{f_s} \frac{h}{l_t} = 0.021 \frac{P_i}{f_s} (2) \approx 0.04 \frac{P_i}{f_s} \qquad \textbf{\textit{Equation 2.4}}$$

where:

A_r = *required area of transverse reinforcement near the member end*
P_i = *prestress force at transfer*
f_s = *design stress in the transverse reinforcement*
h = *depth of member*
l_t = *strand transfer length*

Fountain (1963) agreed with this characterization of the 4% P_i requirement—as coming from Marshall and Mattock—citing their research when making his recommendation for end-region reinforcement. Fountain's recommendation (below) reads very similar to the provision of the 1961 AASHO Interim Specifications.

> *Regardless of the prestressing steel pattern or computed stresses, a minimum amount of web steel sufficient to resist a total vertical tensile force equal to 4 per cent of the total initial prestress force be placed at each end of the beam between the end face and a vertical plane located one-fourth the depth of the beam from the beam end. This reinforcement should start as close to the beam end as practicable* (p. 13).

The next major change to AASHO's treatment of pretensioned beam end regions came in 1973, when confining reinforcement became mandatory. The relevant code provision reads:

> *For at least the distance d from the end of the beam, nominal reinforcement shall be placed to enclose the prestressing steel in the bottom flange. For box girders, transverse reinforcement shall be provided and anchored by extending the leg into the web of the girder* (Section 1.6.15).

It is unclear why, behaviorally, prestressing strand in the end region of a box girder (or a U-beam, essentially an untopped box girder) should require less confinement

than that in another shape. For this reason, it seems that constructibility concerns likely drove the exception.

The meaning of the term *"nominal reinforcement"* has been more precisely defined since this provision's introduction. In the current AASHTO LRFD, the provision requires confining reinforcement *"shaped to enclose the strands… not less than #3 deformed bars, with spacing not exceeding 6 in."* (Article 5.10.10.2). The exemption for box beams still exists.

The provision for transverse reinforcement in pretensioned concrete beam end regions went entirely unchanged for thirty years after its introduction – even as the organization publishing the highway bridge code changed names (from AASHO to AASHTO). Since the advent of the LRFD approach to the AASHTO code, the code provision has not escaped some change in a single edition.

In the first edition of AASHTO LRFD (1994), two changes were made to this provision: one major (and soon reversed) and the other seemingly editorial. The major change was the elimination of the reinforcement stress limit. Rather than sticking to the previous 20-ksi stress limit (aimed at crack control), the code authors allowed transverse reinforcement to be designed with stress equal to bar yield strength, not to exceed 60 ksi. The 20-ksi stress limit was restored in the next version of AASHTO LRFD, the 1996 interim specifications. The other, "editorial" change was the designation of end-region transverse reinforcement as "bursting" reinforcement, a change which likely confused some engineers. The reinforcement specified by AASHTO LRFD is to be placed very close to the beam end (within $h/4$), where *spalling* stresses, not bursting stresses, are of primary concern. As such, it seems that the term, "spalling" reinforcement, might be more appropriate.

Interim revisions to AASHTO LRFD in 2000 and 2002 changed the length of the end region in which the transverse reinforcement could be counted toward the 4% transverse tension design requirement. The 2000 interim revision changed the length from $d/4$ to $h/5$. Deep members (i.e. those likely to have high prestressing forces) typically have values of d approaching $0.9h$, so the 2000 revision likely decreased the length of the end-region design zone most for the members that required the largest amount of transverse reinforcement in that zone. Constructibility concerns are likely what drove the length of the end-region design zone back up in 2002, to $h/4$. The length of the end-region-reinforcement design zone has stayed at this value since.

The terminology used to describe end-region transverse reinforcement was changed recently (AASHTO LRFD, 2008, Interim) to "splitting" reinforcement. The change was made, according to Mertz (2008), since *" 'splitting' is generally used for pretensioned members… whereas 'bursting' is a term used more frequently for post-tensioned members"* (p. 56).

The 2008 interim specifications also reinterpret the role of the "splitting" reinforcement. While for I-beams and bulb tees, reinforcement is required only in the transverse (vertical) direction, for beams of other shapes, "splitting" reinforcement may be required in the other directions. For slabs, reinforcement is required in the lateral (horizontal) direction. For box or tub girders, including the Texas U-beam, reinforcement is required in both the transverse and lateral directions. This change seems to be based on Washington State DOT (WSDOT) standard practice (as recorded by Khaleghi, 2006) rather than the results of a specific research program. Figure 2.47 (excerpted from AASHTO LRFD) shows the two required forms of splitting reinforcement for a WSDOT trapezoidal tub girder.

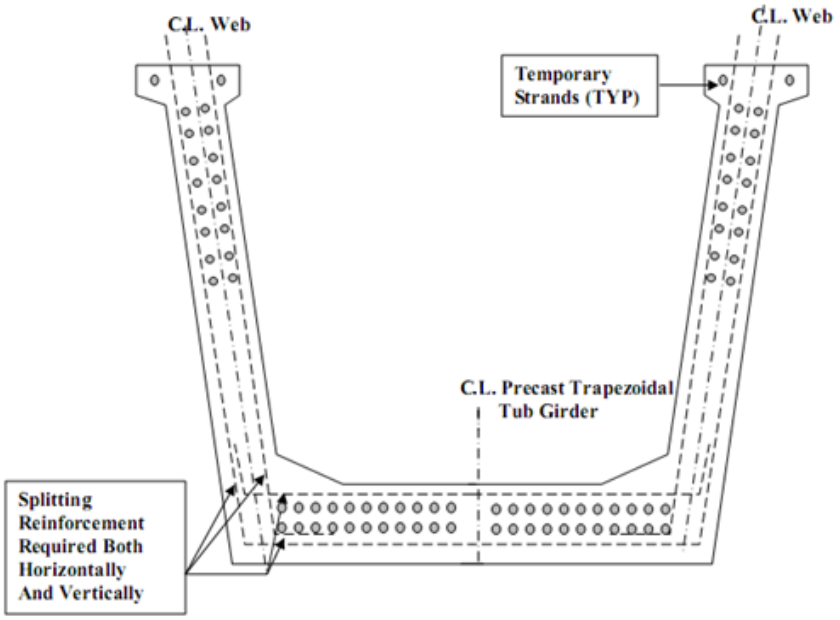

Figure 2.47 Required splitting reinforcement for a trapezoidal tub girder
(after AASHTO LRFD, 2008, Interim)

In summary, since the first mention of prestressed concrete in the AASHO code, the end-region concrete and steel requirements for pretensioned beams have changed as listed below. The majority of these changes have occurred in the past 15 years.

- End blocks were required, then not recommended;
- Requirements for confining reinforcement in the bottom flange were introduced, and then further fleshed out;
- The allowable stress in end-region reinforcement has gone from 20 ksi to yield, and back down to 20 ksi;
- The length of the zone in which the required transverse reinforcement is to be placed first decreased from $d/4$ to $h/5$, and then increased to $h/4$;
- The name given to end-region reinforcement has changed from the generic "vertical stirrups" to "bursting" reinforcement to "splitting" reinforcement; and

- The required direction for end-region reinforcement has changed from transverse only to transverse and/or lateral, depending on the section used.

2.6.2 ASCE-ACI 323 Tentative Recommendations

One of the first technical documents in the United States dealing with prestressed concrete was the Tentative Recommendations for Prestressed Concrete (1958) published by the joint ACI-ASCE committee responsible for prestressed concrete (later to be renumbered 423).

The approach to control end-region cracking in the 323 document was to provide end blocks with *"closely spaced"* transverse reinforcement, as can be seen in the following provisions from Section 214:

> *An enlarged end section, called an end block, may be required to transmit concentrated prestressing forces in a shaped member from the anchorage area to the basic cross section… [End blocks] may be needed to transmit vertical and lateral forces to supports and to facilitate end detailing… In pretensioned members with large concentrated eccentric prestressing elements, end blocks should be used…*
>
> *Reinforcing is necessary to resist tensile bursting and spalling forces induced by the concentrated loads of the prestressing steel. A reinforcing grid with both vertical and horizontal steel in the plane of the cross section should be provided directly beneath anchorages to resist spalling forces. Closely spaced reinforcement should be placed both vertically and horizontally throughout the length of the end block to resist tensile forces.*

It should be noted that the end-region stress terminology used in the Tentative Recommendations is consistent with that used in the literature (and in this thesis). Reinforcement is provided in the end region *"to resist tensile bursting and spalling forces."* That reinforcement *"directly beneath the anchorages"* (i.e. close to the member end) is *"to resist spalling force,"* not "bursting" or "splitting" forces as specified by recent versions of AASHTO LRFD (discussed in previous section).

No attempt was made in the Tentative Recommendations to quantify how "closely spaced" reinforcement needs to be to adequately control cracks. Experimental research studying end-region rebar strains would not be conducted for several years (after 1958), and without that data, the crafting of such a provision would have been difficult.

A final item of interest from this code predecessor is a provision dealing with transfer of prestress by flame-cutting. Provision 404.2.3 notes that the engineer is responsible for planning a detensioning sequence that *"[avoids] subjecting the member to unanticipated stresses"* (p. 576). How to comply with such a provision—i.e. a preferred order of flame cutting—was the subject of a study conducted by Kannel, French and Stolarski (1997).

2.6.3 ACI 318 Provisions

Between the years 1963 and 1995, the concrete building code ACI 318 contained requirements for transverse reinforcement and end blocks in prestressed concrete members that, though written in language more compatible with post-tensioning, could be read to apply to both pretensioned and post-tensioned members.

The 1963 code dealt with these requirements in Section 2614:

> *End blocks shall be provided if necessary for end bearing of for distribution of concentrated prestressing forces safely away from the anchorages to the cross section of the member…*
>
> *Reinforcement shall be provided in the anchorage zones to resist bursting and spalling forces induced by the concentrated loads of the prestressing steel.*

For ACI 318-71, the order of the provisions requiring end blocks and transverse reinforcement (Section 18.11) was interchanged, perhaps indicating growing understanding that reinforcement was often more essential to acceptable performance of the prestressed concrete beam end region than were end blocks. *"Horizontal splitting"*

was added to the list of end-region actions potentially requiring reinforcement, though, unfortunately, without definition.

In 1995, the provisions were rewritten to provide for the design of local-zone and general-zone reinforcement in post-tensioned concrete anchorage zones through the use of strut-and-tie modeling (STM); provisions could no longer be read to refer to pretensioned members.

2.6.4 PCI Recommendations

Since its 5th edition (1999), the *PCI Design Handbook* has prescribed reinforcement to resist transverse tensile stresses in pretensioned members; previous versions of the handbook offered no recommendations on the matter. The PCI provision (Section 4.2.4), essentially taken from Marshall and Mattock's recommendations (Equation 2.2), is given as Equation 2.5.

$$A_r = 0.021\frac{P_o}{f_s}\frac{h}{l_t} \qquad \textbf{\textit{Equation 2.5}}$$

where:

A_r = *required transverse reinforcement at the member end, uniformly distributed over a length h/5 from the end*
P_o = *prestressing force at transfer (after elastic losses)*
f_s = *maximum allowable stress in reinforcement, "usually assumed to be 30 ksi"*
h = *member depth*
l_t = *strand transfer length*

Two points of departure from Marshall and Mattock (1962) can be noted. First the effective prestressing force at transfer (P_o) is used rather than the initial (jacking) prestressing force (P_i). Second is the design stress used by PCI (30 ksi). While Marshall and Mattock made no direct recommendation for allowable stress, a design example in their paper (1962) uses 20 ksi, a value consistent with the AASHTO code and 50% lower than the PCI-assumed value.

No citation is provided in the PCI Design Handbook for the *de facto* increase in allowable stress for the transverse reinforcement. Writing in the PCI Journal five years after the PCI provision was adopted, Tuan et al. (2004) state that *"additional experiments are needed to investigate the possibility of reducing the splitting reinforcement with increased stress limit to 30 ksi or even 36 ksi"* (p. 81), suggesting that sufficient experimental justification for a 30-ksi design stress for transverse reinforcement did *not* exist at the time that this design provision was adopted.

2.6.5 CEB-FIP Recommendations

The CEB-FIP Model Code (1990) advocates the use of STM for the design of prestressed concrete beam end regions. However, the code contains alternative procedures based on linear analysis, to be used *"should the use of the strut-and-tie model be too problematic because of the complexity of the stress field"* or *"if the strut-and-tie model is not applicable due to lack of transverse reinforcement"* (Clause 6.9.12.1).

In the linear analysis procedures, end-region transverse forces are calculated using prism models: a symmetrical prism after Guyon (1955) for bursting and an equivalent prism similar to Gergely and Sozen (1967) for spalling. Gradual transfer of prestress to the section is accounted for in the prism length equation. Splitting force is not calculated, but rather handled by prescriptive cover and strand-spacing requirements ($>3d_b$). Standard U.S. practice (0.5- or 0.6-in. strands at 2 in. centers) complies with these splitting requirements.

2.7 DOT STANDARDS FOR U-BEAMS

Pretensioned concrete U-beams exist as standard sections in four states: Texas, Florida, Colorado and Washington. The four states' design standards are compared,

particularly in the area of required end-region reinforcement. Detailed calculations for end-region reinforcement required by various codes of practice are presented in Appendix B.

2.7.1 Texas U-Beam

The Texas U-beam was developed in the late 1980s and early 1990s, first by the Houston District of TxDOT as the trapezoidal box beam. The drive for the U-beam was primarily aesthetics: through provision of two webs, U-beams are able to be used at approximately twice the spacing of I-beams (Figure 2.48).

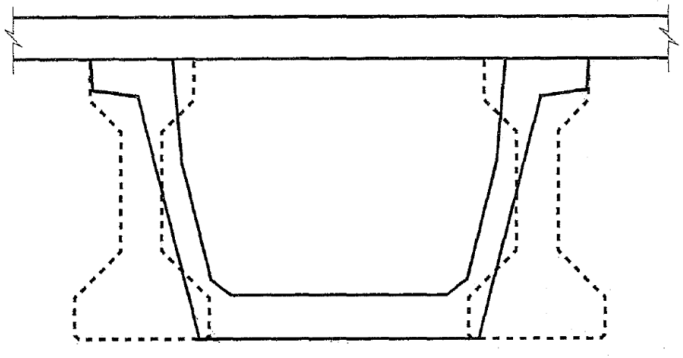

Figure 2.48 U-beam as replacement for two I-beams *(Ralls, Ybanez & Panak, 1993)*

Beams are 40 or 54 in. deep, have 5 in. webs and can be used economically for spans of up to 120 ft. Section properties are given in Figure 2.49. Two sets of beams were originally designed, the A-series, with two rows of 27 strands in the bottom flange; and the B-series, with three rows (Figure 2.50). Presently, the three-strand-row beams are standard. Strands may be placed in beam webs, but economics limit their use: the maximum economical span can be reached before the bottom flange is filled.

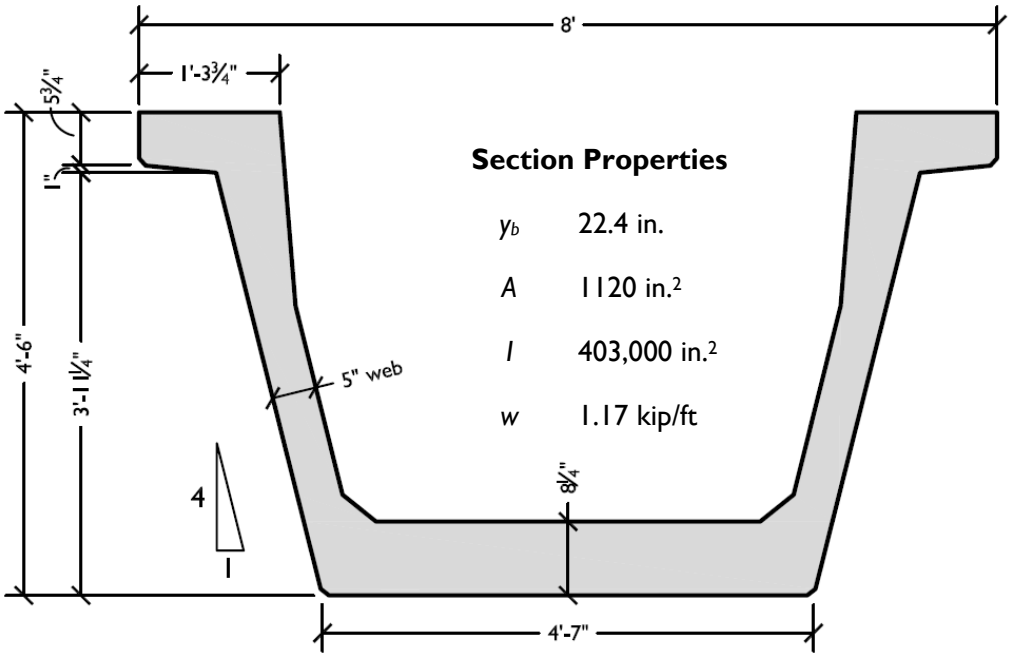

Figure 2.49 Texas/Florida U-beam section properties *(54 in. standard)*

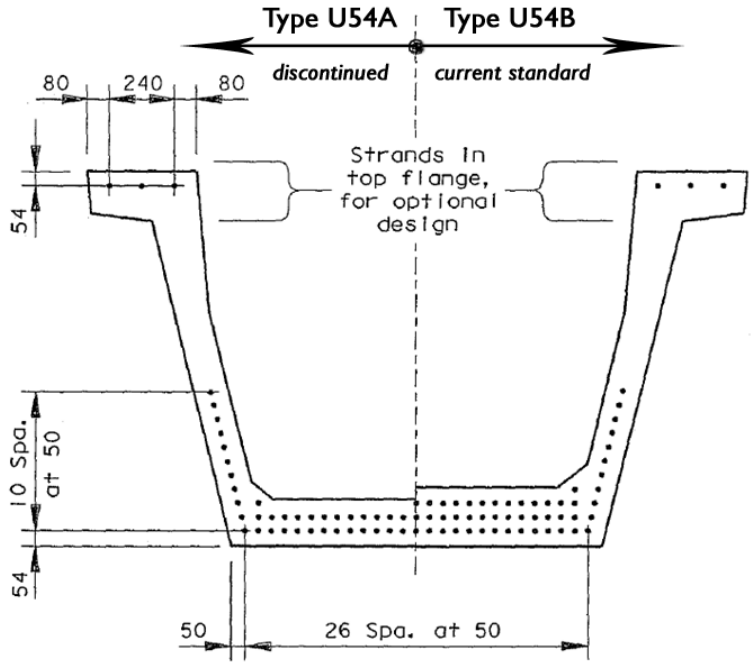

Figure 2.50 Two- & three-strand-row design standards for 54-in. Texas U-beam *(Ralls, Ybanez & Panak, 1993)*

Ralls, Ybanez and Panak (1993) state that finite element analyses for beams with square and skewed ends were conducted during design development. No details of these analyses were published, but *"no unusual behavior"* was observed (p. 27). One set of Texas U-beams were examined for end-region cracking at transfer by Barrios (1994, previously described in Section 2.5.1), but no measurements of bursting or spalling stresses were made. Since their introduction, Texas U-beams have been tested for prestress losses by Gross and Burns (2000) and Tadros et al. (2003).

End blocks are provided primarily as diaphragms: for adequate bearing area at the supports and for lateral stability of the thin U-beam webs. The end blocks also serve to distribute internal forces. In square end regions, the end-block thickness is specified as 18 in. minimum. For skewed end regions, two end-block designs are acceptable.

The design typically chosen by fabricators consists of a triangular end block, its interior face normal to the beam direction (Figure 2.51-a). For large skews, the triangular end block is massive: for a 45° skew, nearly 8 ft. long. Large end blocks are vulnerable to excessive internal curing temperatures and materials problems such as delayed ettringite formation (DEF), which can cause extensive cracking (as shown in Section 1.1). DEF may be triggered in concretes whose internal temperature exceeds 160°F (a soft conversion of the 70°C limit). While the triangular end-block design may lead to large masses of concrete at beam ends, the end block itself cannot be classified as "mass concrete" according to the TxDOT: a minimum dimension of 5 ft. in each direction is required for this designation per the TxDOT Standard Specifications (Section 420.4.14).

The other alternative consists of a smaller end block with its interior face parallel to the skew (Figure 2.51-b). For skewed ends, end-block size is specified not as the end-block thickness, but as a longitudinal distance (Figure 2.52). The specified dimension increases as a function of skew: 18 in. minimum for skews under 30° and 24 in.

minimum for greater skews. For beams with skewed ends just under 30° or for beams with the largest permissible skew (45°), the minimum end-block thickness is roughly 1 ft.

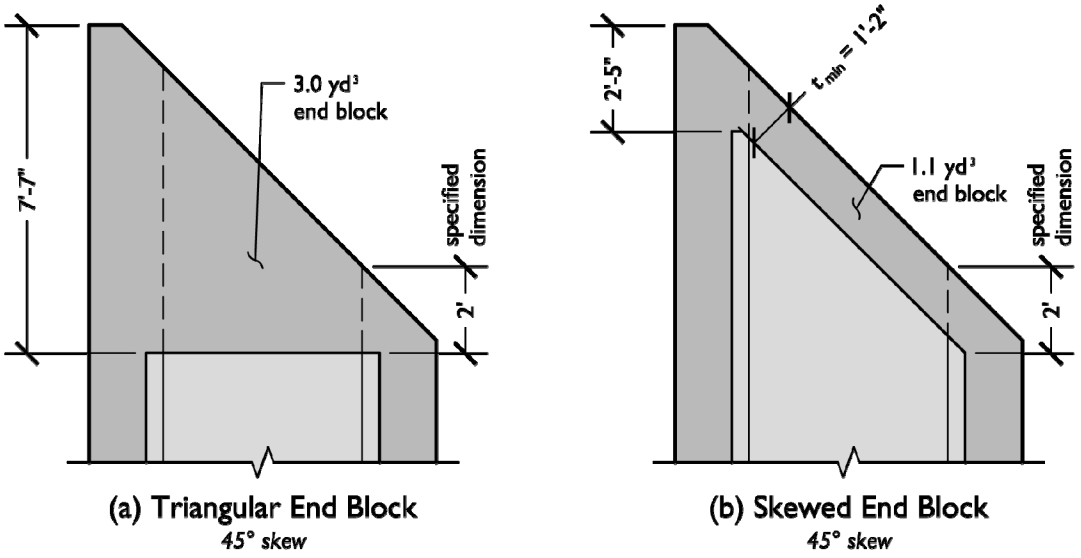

Figure 2.51 End-block design alternatives for Texas U-beam
(minimum end-block dimensions drawn for maximum skew)

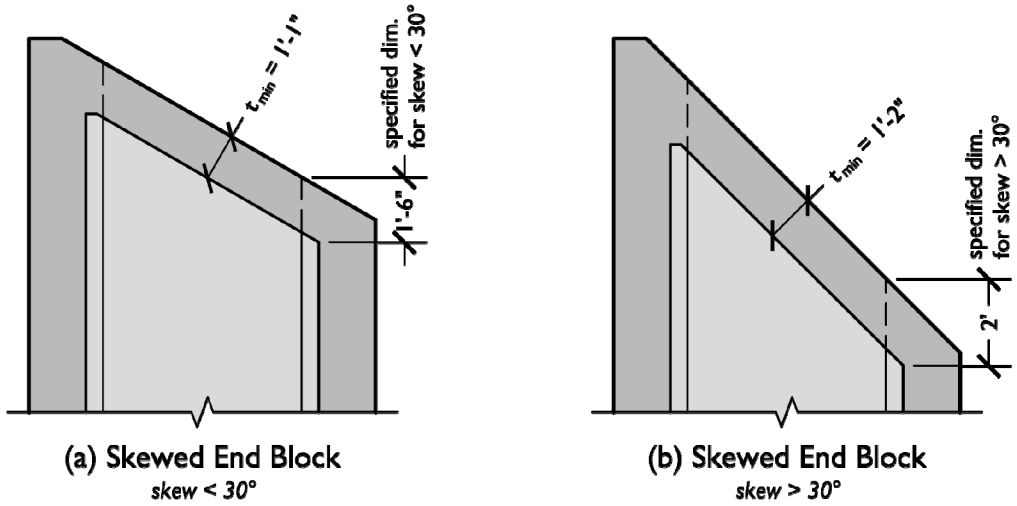

Figure 2.52 Skewed end-block dimensions for extreme cases

Transverse reinforcement in the webs of U-beams has been standardized along with the other section details (TxDOT, 2006). One #4 vertical bar is provided in each web at 4 in. spacing in the end region (end 6 ft. of the beam). Further into the beam, bar spacing may be increased, as shear considerations allow.

Within the end block, the transverse web-reinforcement is continued at close spacing. Additional transverse reinforcement is also provided near the center of the end block—within the projected area of the interior void (Figure 2.53). This reinforcement within the void projection consists of skin reinforcement at their outer (10 – #4) and inner faces (6 – #4) of the end block, with a middle layer of reinforcement (10 – #4) between the inside and outside faces, approximately 9 in. into the beam.

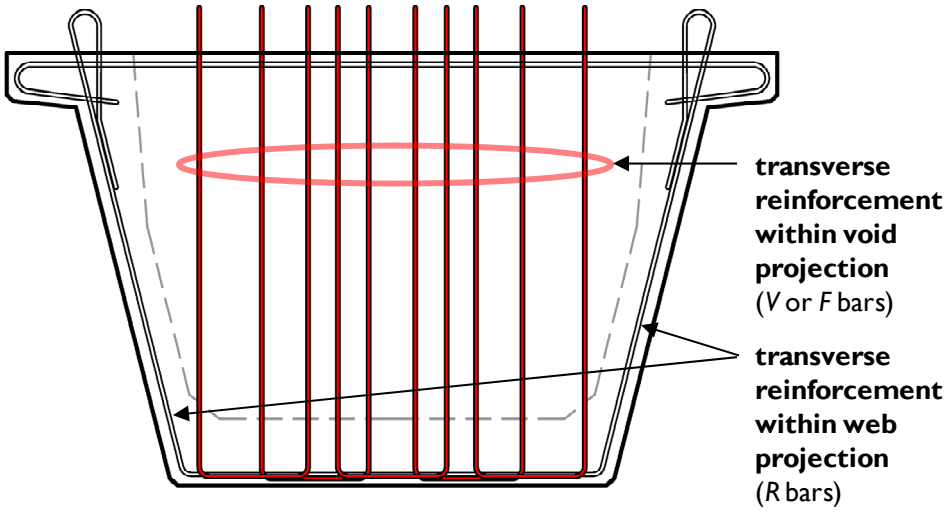

Figure 2.53 Additional transverse reinforcement near center of end block

The outer and middle layers of transverse reinforcement within the void projection lie within a distance $h/4$ from the beam end, so could be counted toward the AASHTO LRFD "splitting" reinforcement requirement (Section 2.6.1). Barrios (1994) treated the end-block reinforcement in this manner. The question of whether this

treatment (counting the transverse reinforcement near the center of the end block) is within the intent of the AASHTO LRFD is discussed further in Section 2.7.5.

2.7.2 Florida U-Beam

Adapted from the Texas standard, the U-beam has existed as a standard section in Florida since the mid-1990s. At present four depths have been standardized (ranging from 48 to 72 in), including a 54-in. section identical in cross section to the Texas U54 (show previously in Figure 2.49). Up to three rows of 26 strands can be placed in the bottom flange.

End-region transverse reinforcement within the webs of the Florida U-beam is more substantial than that in the Texas U-beam, with one #5 bar in each web at 3 in. spacing. The larger bar size and the closer spacing combine for an 85% increase for transverse web-reinforcement in the beam end region compared with the Texas standard.

Transverse reinforcement within the void-projected area of the end block is similar to the Texas U-beam (Figure 2.53), with three layers of transverse bars: one each at the outer (6 – #5) and inner faces (6 – #4) of the end block, and one between (6 – #5).

A recent Florida DOT design bulletin sets limits on the bonded prestressing force at pretensioned beam ends in order to control end-region cracking: the limits for U-beams were set such that the transverse-bar design stress is 18 ksi (Nickas, 2004). This design stress is 10% less than that prescribed by AASHTO.

At skewed ends, the end blocks used in Florida U-beams are always skewed (like Figure 2.51-b), never triangular (Figure 2.51-a). The maximum allowable skew is much less than allowed in Texas: 15° vs. 45°. End blocks are 18 in. thick, regardless of the beam skew.

2.7.3 Colorado U-Girder

The Colorado U-girder (Figure 2.54) was developed in the late 1990s for beams 48 to 84 in. deep. Webs are sloped similarly to Texas/Florida beams, but top flanges are wider. A major difference between the Colorado and Texas/Florida standard is the lack of an end block in the Colorado beam. Diaphragms are provided at various locations in the beam, but at the beam end, the diaphragms are cast integrally with the bridge bent caps (cast in place). The top flanges for the Colorado beam, shown in Figure 2.54 as much wider than those of the Texas/Florida standard, are actually of variable width dependent on beam spacing. (The widest permissible flanges are depicted in the figure.)

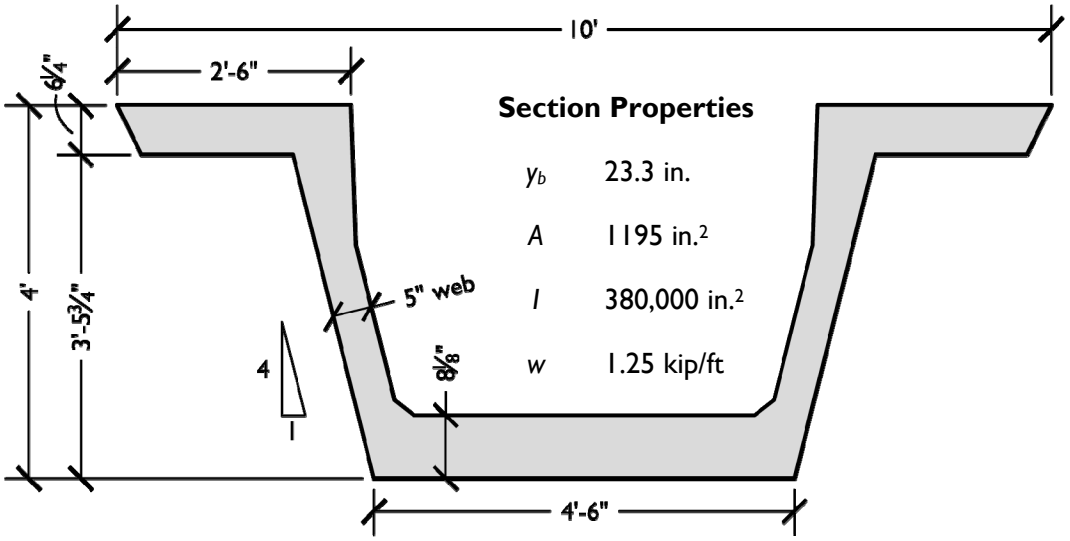

Figure 2.54 Colorado U-girder section properties
(48 in. deep, pretensioned standard)

Colorado beams may be solely pretensioned or prestressed by a combination of pretensioning and post-tensioning. If the pretensioned/post-tensioned option is chosen, a wider web width is used (7.5 or 10 in.) to accommodate the post-tensioning duct; otherwise the beam webs are similar to the Texas/Florida section (5 in. thick).

Pretensioned/post-tensioned beams have been used in horizontally curved bridges (McMullen, Elkaissi & Leonard, 2008); an example of this construction is shown in Figure 2.55.

In the pretensioned-only beam, strands may be placed in the top flanges and webs in addition to the bottom flange. Web strands may be harped (inward in addition to downward). The bottom flange may hold up to three rows of 25 strands each.

The primary end-region reinforcement consists of 4 – #4 transverse bars and 2 – #4 lateral bars are spaced at 3.3 in. This transverse and lateral reinforcement is placed with one bar on each face of the webs and bottom flange, respectively. Supplemental transverse #6 bars are installed in both webs, very close to the beam end.

Figure 2.55 Curved pretensioned/post-tensioned Colorado U-girder *(Endicott, 2005)*

2.7.4 Washington Trapezoidal Tub Girder

The Washington State trapezoidal tub girder was introduced in 2004. Tub girders are 48 to 78 in. deep and have 7-in. webs (40% thicker than the Texas/Florida standard).

In the Washington tub girder, like in the Colorado U-girder, end blocks are not necessarily provided at the ends of the precast beam (in lieu of cast-in-place end diaphragms).

Beams to be used with standard, cast-in-place decks have cross sections as shown in Figure 2.56. Partial-depth, pretensioned concrete panels are sometimes used as stay-in-place formwork, in which case the Washington beam cross section is modified slightly, to provide top flanges (similar to those in the Texas/Florida section) on which the panels might rest. This version of the tub girder was previously shown (as an excerpt from AASHTO LRFD) in Figure 2.47.

Two rows of up to 30 strands are placed in the bottom flange. Additional, harped strands may be placed in the webs, as shown in Figure 2.57. Harped-strand construction is easier for Washington beams than for Colorado beams: as Washington webs are sloped nearly twice as steep, strands need not be harped inward as far.

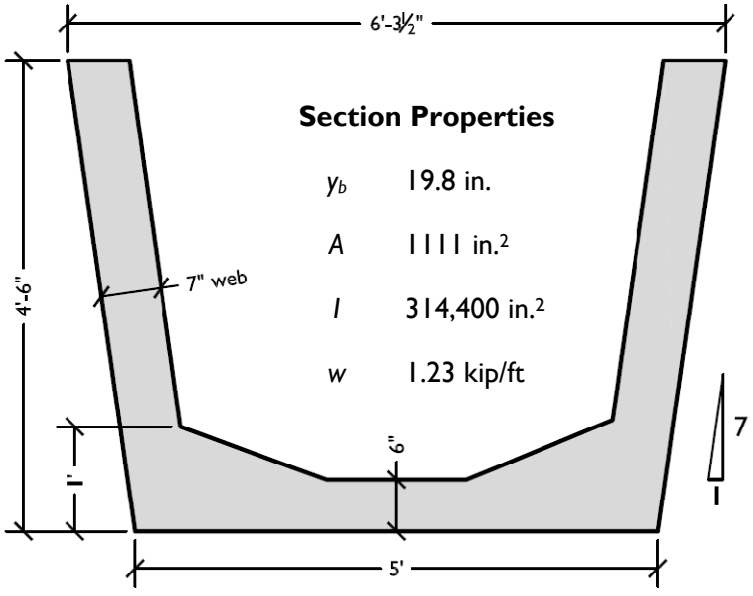

Figure 2.56 Washington trapezoidal-tub-girder section properties
(54 in. standard)

Figure 2.57 Harped strands in webs of Washington trapezoidal tub girder
(Tadros, 2005)

Primary end-region reinforcement is similar to that of the Colorado standard, but larger transverse bars are used. Typical details are for 4 – #5 transverse bars and 2 – #4 lateral bars, spaced at 3.5 in. Skews of greater than 15° are permitted; no maximum skew is shown on the standard drawings.

2.7.5 Comparison of End-Region Reinforcement

How to count the transverse reinforcement for U-beams with end blocks (Texas and Florida beams) in accordance with the applicable AASHTO LRFD provisions (section 5.10.10) is subject to some interpretation. Neither the specifications nor the commentary provided with the "splitting" reinforcement provision directly addresses the case of beams with end blocks. Rather, it is stated that *"splitting resistance is of prime importance in relatively thin portions of pretensioned members that are tall or wide, such as… the webs of tub girders"* (Article C5.10.10.1, emphasis added).

The depiction of a Washington trapezoidal tub girder accompanying the AASHTO LRFD provisions (Figure 2.58) may appear suggest that transverse "splitting" reinforcement must be provided within the webs of a given beam. It should be recalled, though, that Washington tub girders do not typically have precast end blocks.

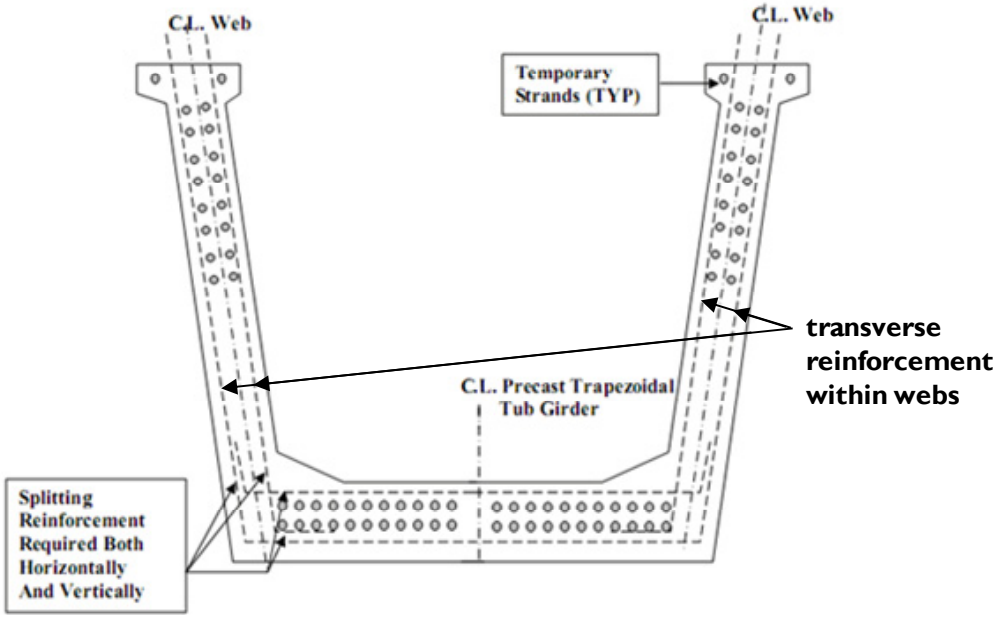

Figure 2.58 Transverse reinforcement in end region of WSDOT trapezoidal tub girder *(after AASHTO LRFD, 2008, Interim)*

In Texas and Florida U-beams, the amount of transverse reinforcement provided near the center of the end block (within the projected area of the void) is much greater than that provided near the exterior face (within the projected area of the web), as shown in Figure 2.59. If the AASHTO LRFD end region length (h/4) is considered, the Texas beam has *three times* the transverse reinforcement in the void-projected area as compared the web-projected area.

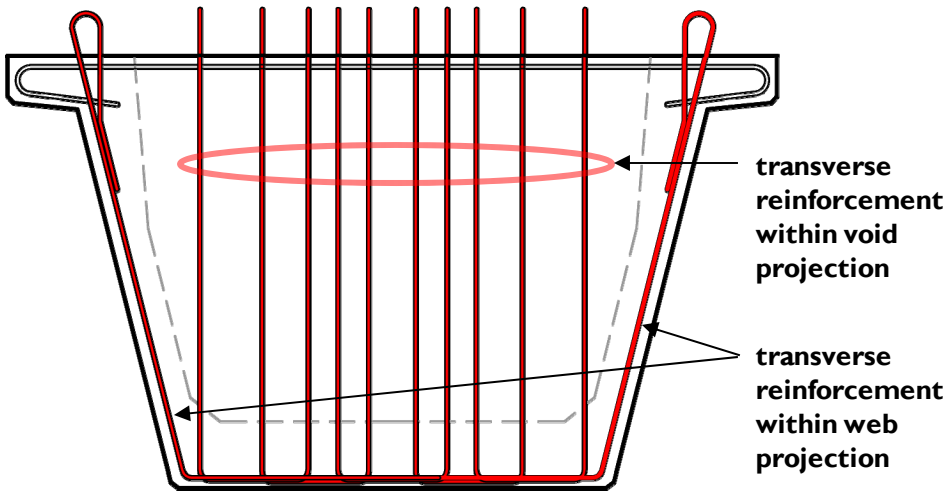

Figure 2.59 Transverse reinforcement in the end block of a Texas U-beam, divided into that provided within the projected areas of the void & the webs

In light of the ambiguities in AASHTO LRFD, and the considerable effect resulting from how the transverse reinforcement is counted, two figures—Figures 2.60 and 2.61—show the standard end-region reinforcement for the four U-beams alongside spalling and lateral bursting code requirements. The former of these considers all transverse reinforcement in end blocks; the latter neglects consideration of the reinforcement within the void projection of end blocks. This distinction only affects the counting of provided reinforcement area for the Texas and Florida beams.

For these figures, a 54-in. beam of each type was considered, with a prestressing force consistent with that used in the experimental portion (78 – 0.5-in. strands). It should be noted that the CEB-FIP Model Code (1990) does not require bursting reinforcement for this beam. For the CEB-FIP spalling reinforcement, no length is given in the code in which the required reinforcement must be placed. For the sake of comparison with the DOT standard designs, an end-region design length of $h/2$ was assumed. Calculations for amount of reinforcement required by the various codes are presented in Appendix B.

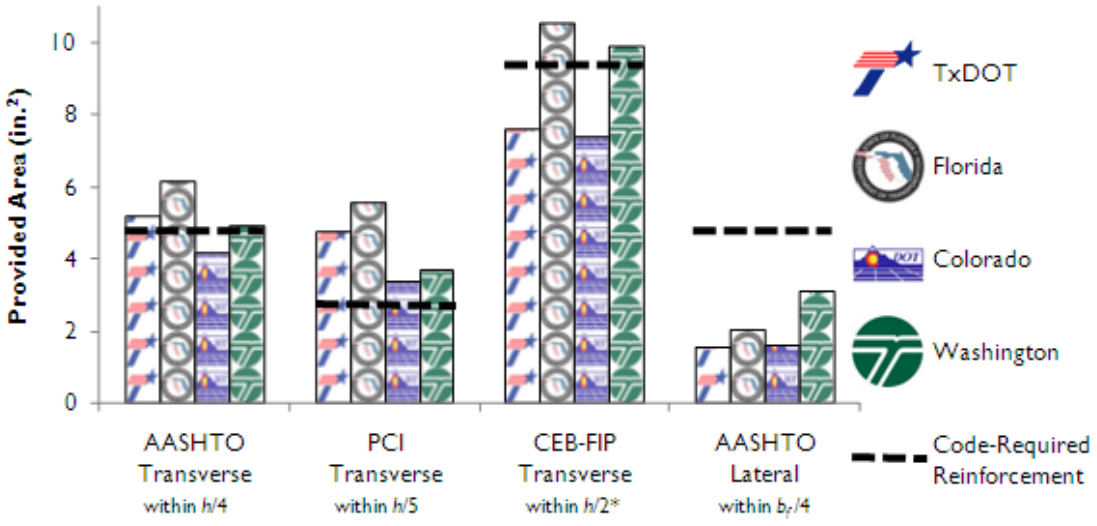

Figure 2.60 Standard end-region reinforcement for U-beams
(54 in. deep, 78 – 0.5-in. strands) ***vs. code requirements***
(counting all transverse reinforcement in end block)

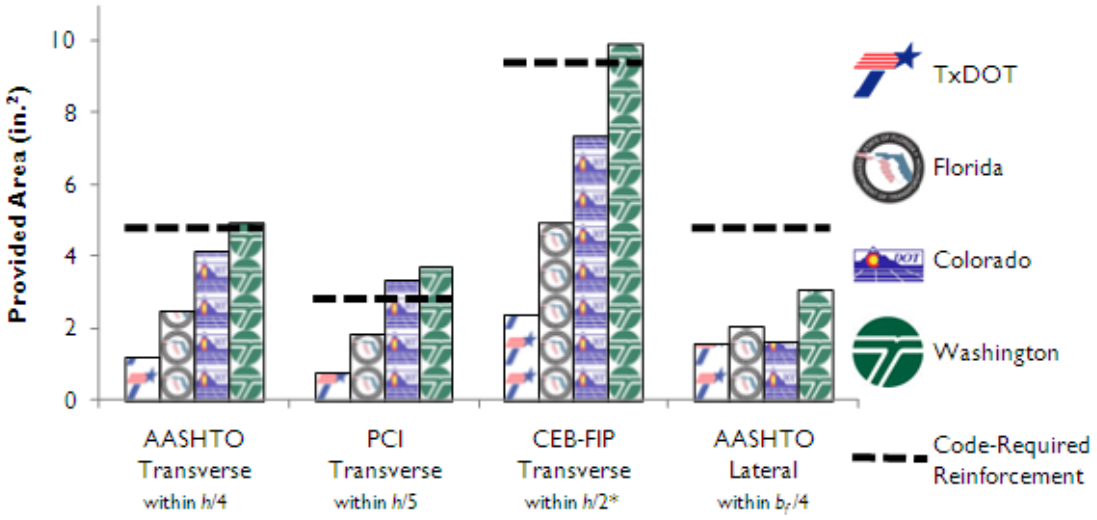

Figure 2.61 Standard end-region reinforcement for U-beams
(54 in. deep, 78 – 0.5-in. strands) ***vs. code requirements***
(neglecting transverse reinforcement within projection of void in end block)

2.8 SUMMARY

In this chapter, literature related to bursting and spalling effects in pretensioned concrete beams was reviewed. Attention was directed toward experimental test results, particularly those from studies in which end-region transverse reinforcement was instrumented. Such a scheme was used in the present study, as will be discussed, along with other aspects of the experimental program, in Chapter 3.

CHAPTER 3

Experimental Methods

3.1 OVERVIEW

Pursuant to the research aims described in Chapter 1, two 30 ft. long, pretensioned concrete U-beams were fabricated in the Ferguson Structural Engineering Laboratory of The University of Texas at Austin. Beam end regions were instrumented with strain gages on reinforcing bars in the transverse and lateral directions in order to experimentally determine the stresses generated by bursting and spalling effects.

One U-beam containing no internal instrumentation was fabricated by a precaster and inspected by the research team. This beam proved helpful in planning the instrumentation for the beams fabricated in the Ferguson Laboratory.

The organization of this chapter is as follows. First design considerations for the U-beam specimens are discussed, followed by details of the mechanical testing programs for concrete and steel-reinforcement samples. Lastly instrumentation plans and fabrication techniques are examined.

3.2 SPECIMEN DESIGN

U-beam specimen design will be detailed after a brief presentation of fundamental theory related to pretensioned concrete beams.

3.2.1 Prestressed Beam Theory

Three concepts will be presented briefly in this section: linear and nonlinear stress distributions, elastic shortening and transfer length. For thorough coverage of these and other topics, Collins and Mitchell (1997) is recommended.

3.2.1.1 Linear and Nonlinear Stress Distributions

Within the end region of a prestressed concrete beam, concentrated prestressing forces spread to the entire beam cross section. At some distance from the beam end, the internal stresses become distributed linearly, there conforming to one of the basic tenets of beam theory: the Bernoulli-Navier assumption that "plane sections remain plane." Closer to the end, however, the state of stress is "disturbed" (i.e. nonlinear). Strut-and-tie theory (Schlaich, Schäfer & Jennewein, 1987) refers to regions with linear stress distributions as B-regions, after Beam theory or in honor of Bernoulli; and regions with nonlinear stress distributions as D-regions, after the Disturbed state of stress.

Strictly speaking, no hard line divides D-regions from B-regions. Elastic analysis of a post-tensioned beam (Figure 3.1) shows the gradual transition to a linear stress distribution. In this figure, the stress distribution is linear where the stress trajectories are parallel, or about a distance *h* from the end of the beam as predicted by Saint-Vénant's principle.

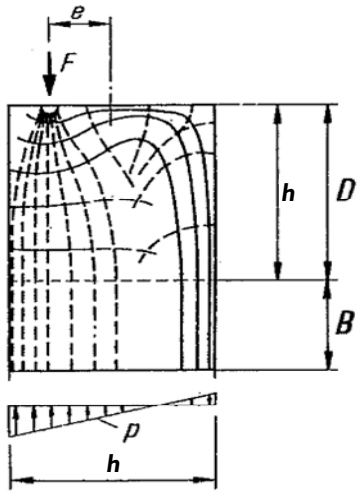

Figure 3.1 Elastic stress trajectories in a post-tensioned concrete beam, illustrating the division into D- and B-regions *(after Schlaich, Schäfer & Jennewein, 1987)*

Where the stress distribution is linear, the stresses at the extreme fibers (top and bottom) can be calculated using the basic flexural theory. Immediately after transfer of prestress, the top- and bottom-fiber stresses are as described in Equation 3.1.

$$f_{bot}^{top} = \frac{P_o}{A_g} \mp \frac{P_o\, e\, y_{bot}^{top}}{I_g} \qquad \textbf{Equation 3.1}$$

where:

f_{bot}^{top} = *stress at top* or *bottom fiber of beam, ksi*
P_o = *effective prestressing force (after elastic losses), kip*
A_g = *gross cross-sectional area, in.*^{2}
e = *eccentricity of prestressing force, in.*
y_{bot}^{top} = *distance from centroid to top* or *bottom of section, in.*
I_g = *gross-section moment of inertia, in.*^{4}

The two components of Equation 3.1 represent the axial and flexural stresses resulting from the prestressing load, respectively. An additional flexural-stress component results from the beam self-weight; however, controlling stress checks for U-beam specimens are made at the transfer length, close enough to the member end for stresses from self-weight to be negligible.

3.2.1.2 Elastic Shortening of Beam

At transfer, prestressed concrete beams shorten axially in response to the applied prestressing force. This instantaneous deformation results in a loss of prestress on the order of 10% of the initial (jacking) stress. The prestress loss due to elastic shortening calculated by AASHTO LRFD (2009, Article 5.9.5.2.3a) is as given in Equation 3.2.

$$\Delta f_{p,ES} = \frac{E_p}{E_{ci}}\, f_{cgp} \qquad \textbf{Equation 3.2}$$

where:

E_p = *elastic modulus of prestressing strand, ksi*
E_c = *elastic modulus of concrete at transfer, ksi*
f_{cgp} = *stress in concrete at depth of prestress centroid, ksi*

Empirical expressions can be used to predict modulus values from compressive-strength test results. ACI 363 (1992) provides an equation (Equation 3.3) that correlates well with measured modulus values for moderate- and high-strength concrete (3 to 12 ksi). This equation is compared to that given in ACI 318 (2008, Provision 8.5.1) in Figure 3.2. The release strength of the U-beam specimens is near the center of the range of applicability for the 363 equation.

$$E_c = 40\sqrt{1000 f_c'} + 1000 \qquad \textit{Equation 3.3}$$

where:

E_c = *elastic modulus of concrete, ksi*

f_c' = *compressive strength of concrete, ksi*

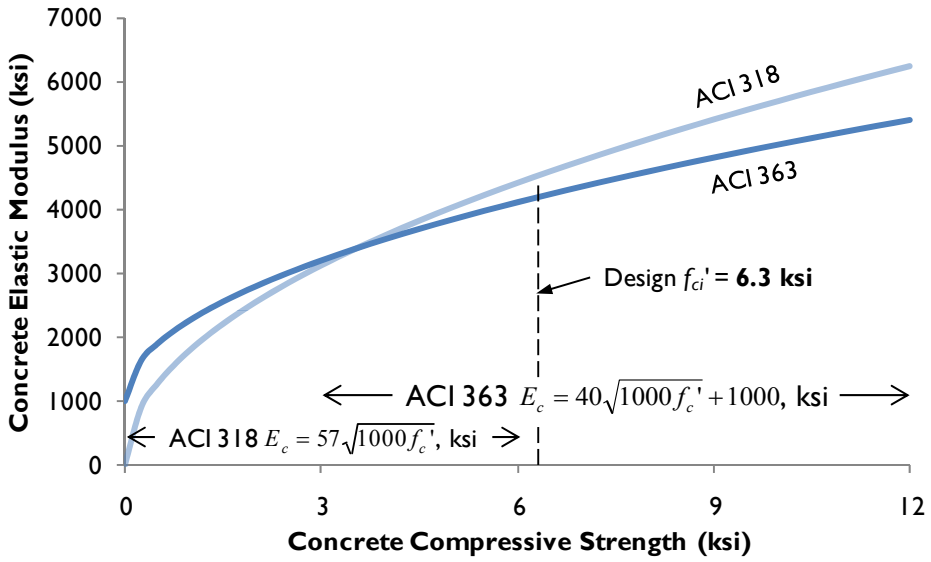

Figure 3.2 Concrete modulus equations from ACI 318 & 363

3.2.1.3 Transfer Length of Prestressing Strand

In a pretensioned concrete beam, the prestressing force is transferred from strand to concrete gradually, through bond and friction, over the transfer length of the strand. Transfer length is assumed to be proportional to the effective prestress in ACI 318

(2008, Provision 12.9.1). At prestress transfer, only losses due to elastic shortening have occurred, so the ACI 318 transfer length is as described in Equation 3.4.

$$l_t = \frac{f_{pi} - \Delta f_{p,ES}}{3} d_b \qquad \textbf{\textit{Equation 3.4}}$$

where:

f_{pi} = *initial (jacking) prestress in strand, typically* $0.75 f_{pu} = 203\ ksi$
$\Delta f_{p,ES}$ = *prestress loss from elastic shortening of beam, ksi*
d_b = *strand diameter, in.*

AASHTO LRFD (2009, Article 5.11.4.1) assumes the transfer length to be $60d_b$. If elastic losses can be assumed at 10%, the provisions are essentially equivalent as shown in Equation 3.5.

$$l_t = \frac{f_{pi} - \Delta f_{p,ES}}{3} d_b \approx \frac{0.90 f_{pi}}{3} d_b = \frac{0.90 \cdot 203\ ksi}{3} d_b \qquad \textbf{\textit{Equation 3.5}}$$

$$l_t = 61 d_b \approx 60 d_b$$

3.2.2 U-Beam Design

The intent of the specimen design was to maximize the bursting and spalling effects on the section. As discussed in the literature review, O'Callaghan (2007) found high bursting stresses and relatively low spalling stresses in transverse end-region reinforcement for tested Tx-girder bulb tees. Moderate spalling stresses (exceeding 10 ksi in one case) were found in the deepest girder tested (70 in.), however.

Marshall and Mattock's design equation for spalling reinforcement (Equation 3.6), previously discussed in Section 2.4.2.1, was used as a guide to increase spalling effects.

$$P_r = 0.021\, P_i \frac{h}{l_t} \qquad \textbf{Equation 3.6}$$

where:

P_r = *spalling force, kip*
P_i = *prestressing force (before elastic losses), kip*
h = *beam height, in.*
l_t = *transfer length, in.*

The prestressing force used was the economical maximum for U-beams: a full bottom flange of strands. (The use of a large prestressing force also served to maximize the bursting effects on the section.)

It should be noted that the Florida standard strand pattern (3 rows of 26 strands) was used, rather than the Texas pattern (3 rows of 27 strands). The Florida design was more compatible with strand pattern to be used for the Texas box beams to be tested in a later phase of this project. The purchase of two different sets of stressing plates ($50 thousand per set) was cost-prohibitive considering the budget of Research Project 5831, and the difference in structural behavior between beams with rows of 27 or 26 strands was deemed negligible for research purposes.

The height-to-transfer length ratio (h/l_t) was maximized by choosing the deeper U-beam (54-in. section rather than 40-in.) and the strands with shorter transfer lengths (0.5-in. strands used rather than 0.6-in.).

The concrete release strength was chosen based on the bottom-fiber stress from linear analysis (as discussed in Section 3.2.1.1). The stress limit for the bottom fiber was taken as $0.65f'_{ci}$, following recommendations from TxDOT Research Project 5197 (Birrcher, 2006; Schnittker, 2008).

The top-fiber stress was allowed to exceed the nominal tensile strength limit ($6\sqrt{1000f'_{ci}}$), but sufficient longitudinal reinforcement was provided in the top portion of the beam to resist the entire tensile force from prestressing with a design stress of

approximately 30 ksi (ACI 318, 2008, Provision 18.4.1). The standard U-beam design was modified slightly: 4 – #7 bars were placed in the tension zone of each web and top flange rather than 4 – #5 (Figure 3.3).

The section design for Beams 1 and 2 is summarized in Figure 3.4, with detailed calculations provided in Appendix C.

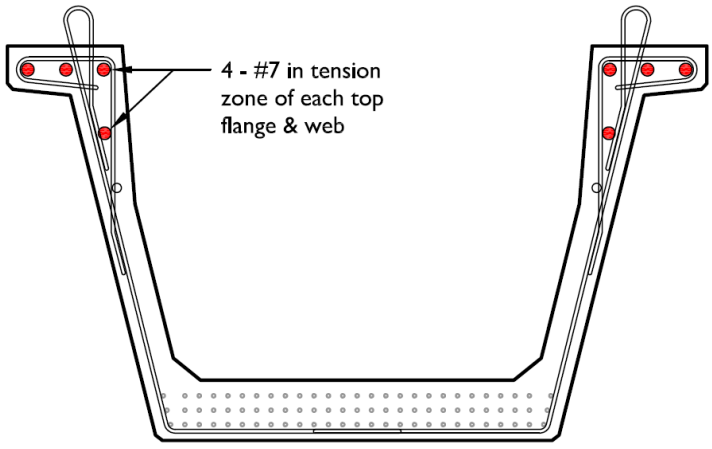

Figure 3.3 Tension-zone longitudinal reinforcement

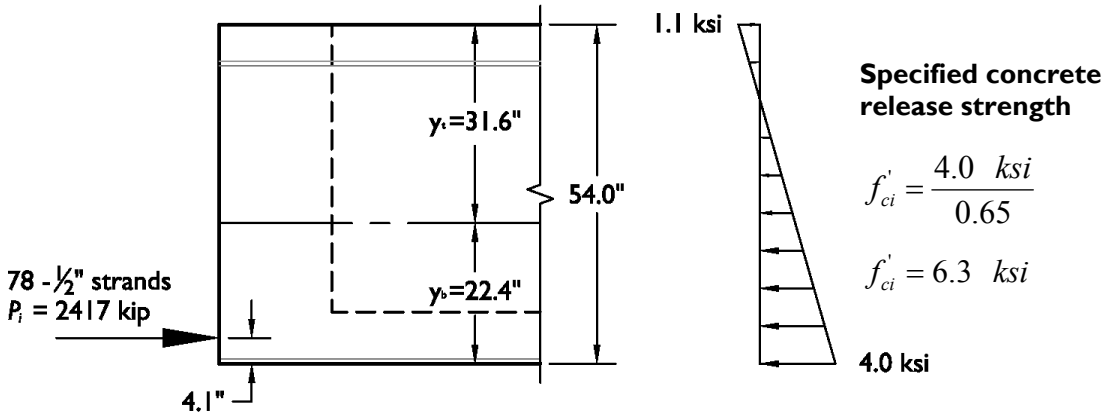

Figure 3.4 Beam 1 & 2 design summary

3.3 CONCRETE PROPERTIES

3.3.1 Concrete Mixture Design

Efficient precast concrete fabrication demands high early-strength concretes. Typically, large amounts of Type III cement (6 to 7 sacks, or 570 to 670 lb/cy) is mixed with small amounts of water (water-cement ratio, $w/c < 0.40$) so that beams can reach their release strengths (4 to 7 ksi) within 18 to 24 hours. Beams can then be released and moved from the pretensioning bed the day after casting.

Precast concrete mixes are highly engineered: much high-range water-reducer is needed for workable concrete with the low w/c used. The balance of coarse aggregate to fine aggregate may be lower than in conventional concrete (1 to 1.5:1, compared to 1.5 to 2:1) to avoid segregation while the concrete is fresh. Lastly chemical retarders are often used to prevent flash setting, especially during hot Texas summers.

Concrete made with Type III cement is not commercially available as ready-mix in the Austin area at present, likely due to insufficient demand and concerns over flash setting. A local precast concrete fabricator, Coreslab Structures, was able to provide help designing the concrete mixture proportions for application on this project, and donated the concrete, batched at their facility 15 miles north of the Ferguson Laboratory. The concrete mixture design used for both beams is shown in Table 3.1. This design is similar to high-early-strength mixtures used by Texas precast highway-beam fabricators.

The design used is a "straight-cement" concrete mixture, containing no fly ash replacement. Within the first year of this project, TxDOT mandated the use of Class F fly ash in precast concrete mixes at 25% replacement of cementitious material (Marek, 2008). The purpose of this new prescription was control of alkali-silica reaction (ASR), a slow-acting chemical reaction in which alkalis from cement and other sources interact with reactive (glassy) silica in aggregate to form an expansive gel. The provision of fly

ash changes the composition of the calcium-silicate-hydrate gel (C-S-H), the "glue" in concrete, so that the gel absorbs alkalis and prevents them from reacting with the silica (Folliard et al., 2006).

Table 3.1 Concrete mixture proportions

Material	**Detail**	**Quantity**
Cement	Alamo Grey Type III	611 lb/cy
Coarse Aggregate	¾ in. Crushed Limestone	1600 lb/cy
Fine Aggregate	River Sand	1379 lb/cy
Water Water-Cement Ratio (w/c)	—	202 lb/cy 0.33
High-Range Water-Reducer	Sika Viscocrete 2100	13 oz/Cwt
	Sikament 686	25 oz/Cwt
Retarder	Sika Plastiment	5 oz/Cwt
Slump	—	9 in.

lb/cy = pounds per cubic yard of concrete
oz/Cwt = fluid ounces per hundred-weight of cement

With shear testing for each beam to be completed within two months of casting, beam long-term behavior is not under study; the reasoning behind the TxDOT fly-ash prescription does not apply. A straight-cement mixture was used in an effort to maximize the internal curing temperature. Cement reacts quickly with water and gives off much heat during early hydration. The reaction of Class F ash, on the other hand, cannot begin until cement hydration has progressed sufficiently, so is slower-acting and contributes negligibly to early heat and strength gains (Schindler & Folliard, 2005; Wang, Lee & Park, 2009).

It was reasoned that the dimensional differences between the two end-block alternatives tested for skewed ends (large triangular and smaller skewed, shown in Figure 3.5) would lead to different maximum temperatures and temperature gradients, with the larger end blocks giving higher values of each.

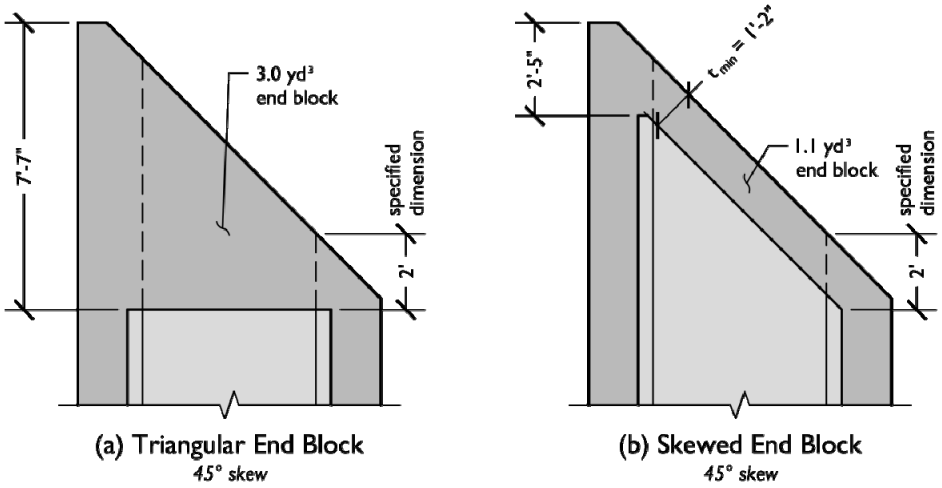

Figure 3.5 U-beam end-block design alternatives for skewed ends

3.3.2 Concrete Mechanical Testing

Concrete cylinders (4 by 8 in.) were tested in compression and under splitting tension. Compression testing was used to determine when the beam had gained sufficient strength for transfer of prestress. Splitting-tension testing was done at release to qualify the likelihood of cracking in the end regions studied for this project as compared to those in the literature.

Compressive-strength testing (Figure 3.6) was performed following ASTM C 39. Cylinders were capped at each end with an unbonded neoprene pad (within a steel retainer). Talcum powder was applied to pads to minimize friction between the pads and the cylinder ends. Loading proceeded at a controlled rate (approximately 35 psi/sec, or

0.4 kip/sec) until failure. The compressive strength was determined according to the following equation:

$$f_c' = \frac{4P}{\pi D^2} \qquad \textit{Equation 3.7}$$

where:

P = *ultimate load, kip*
D = *cylinder diameter (nominally 4 in.)*

Figure 3.6 Cylinder compressive-strength testing

As the cylinders gained strength, their observed failure mode would change. Within 15 hours after batching, cracks would form around the coarse aggregate, and cylinders would fail in the cup-and-cone mode. At later times (when the cement paste was stronger), cracks would form *through* the aggregate and cylinders would fail in shear. The release strength of 6.3 ksi was reached approximately 18 hours after batching. The 28-day compressive strength of the concrete used for the beams ranged from 9 to 11 ksi (for different batches).

Splitting tensile-strength testing (Figure 3.7) was performed following ASTM C 496. Load was applied to the length of the cylinder with thin plywood shims, at a controlled rate of less than 0.1 ksi/min (or 0.1 kip/sec).

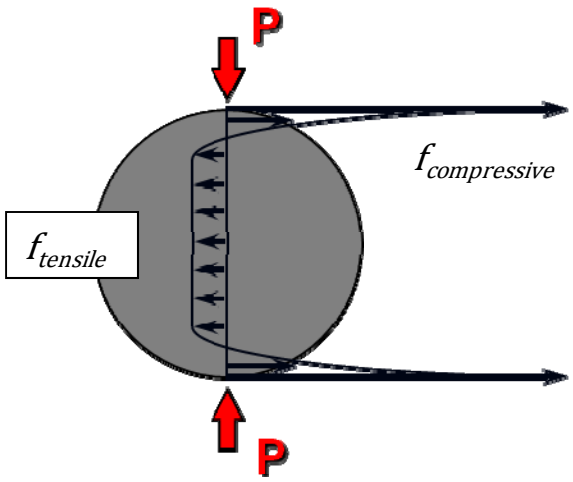

Figure 3.7 Schematic for splitting tensile-strength test *(after Tuchsherer, 2007)*

Strength was calculated as shown in Equation 3.8, which arises from elastic theory (Timoshenko & Goodier, 1934 provides a derivation). The splitting tensile strength at release was 7 to $10\sqrt{f'_{ci}}$.

$$f_{sp} = \frac{2P}{\pi DL} \qquad \textbf{Equation 3.8}$$

where:

P = *ultimate load, kip*
D = *cylinder diameter (nominally 4 in.)*
L = *cylinder length (nominally 8 in.)*

Test data from cylinder breaks along with those from other mechanical tests are reported in Appendix D.

3.3.3 Temperature-Match Curing

In order to expedite pretensioning-bed turnover, precast concrete fabricators may transfer prestress once the concrete reaches its release strength. The internal curing

temperature of a beam is much hotter than ambient conditions due to the exothermic nature of cement hydration. The heat generated from hydration fuels the reaction, as higher temperatures increase the rates of dissolution for cement compounds, and those of diffusion and dispersion for by-product ions (Folliard, 2008).

Cylinders that are "beam-cured," or placed alongside a pretensioned concrete beam to cure, clearly experience a different set of boundary conditions than a fictitious cylinder considered from within the curing beam. The maturity age of a given concrete specimen, shown conceptually in Figure 3.8, considers both the curing time and temperature, and has been linked to early-strength gains (Mindess, Young & Darwin, 2003).

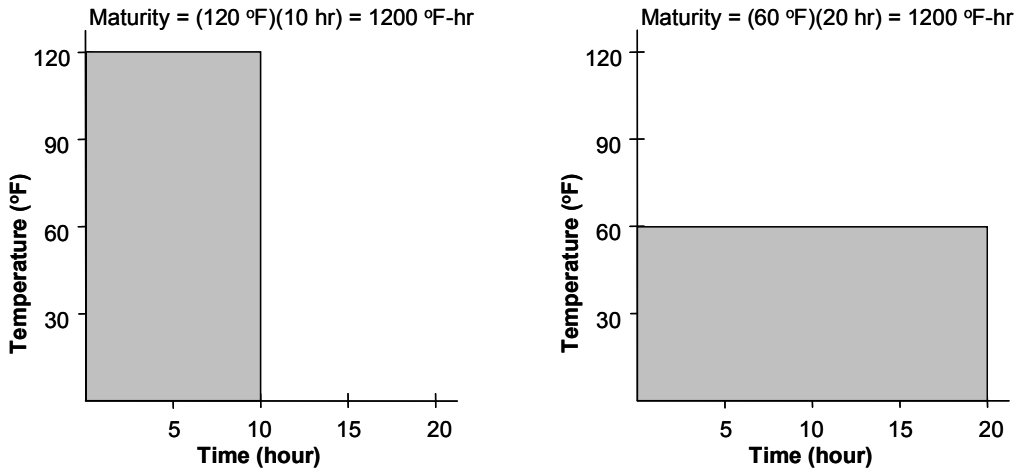

Figure 3.8 Maturity-age concept *(Kehl & Carrasquillo, 1998)*

For Research Project 5831, it was desired that the beams be released as early as they might in a precasting yard. An earlier prestress transfer means a lower-strength concrete; lower tensile strength means more extensive end-region cracking. Temperature-match curing is used by a number of Texas beam fabricators, and was used in this project.

For temperature-match curing, thermocouples are installed in a concrete beam at points of interest, and measured temperature data is relayed to a computer control system, which controls the curing temperature for the cylinder specimens. Cylinders are cast not in plastic molds, but in insulated, instrumented cylinder molds (Figure 3.9). Within the computer software (*Sure Cure*), each cylinder is set up as a slave to a given thermocouple in the beam. Heating elements in these molds are activated when the cylinder temperature lags behind the master temperature.

Figure 3.9 **Sure Cure** ***temperature-match-curing system*** *(Tuchsherer, 2007)*

Two locations of interest for the beams in this study are the "release point" and the "hot spot." The release point is a location near the bottom fiber of the beam where the temperature is likely to be low. For U-beams, the release point is located near the bottom flange/web junction 8 ft. into the beam (Holt, 2008). The hot spot in the beam was

hypothesized to be at the centroid of the end block. Since the internal curing temperature would be highest there (i.e. the maturity age greatest), the compressive strength would likely be higher than at the release point. Cylinders tracking both the release point and hot spot were tested as the beam was curing: the release point for determination of when to transfer prestress and the hot spot to provide some warning that this time was approaching.

Match-cured cylinders were also made for the "top flange," a point located near the center of top flange at one transfer length (30 in.) from the beam end. These cylinders were tested for their splitting tensile strength just after transfer of prestress. The temperature was expected to be cooler at this location compared to others further down in the section; if so, the tests would yield a lower-bound tensile strength for the concrete at transfer.

Aside from the thermocouples installed for match-curing, thermocouples were installed in beam end blocks to determine the section temperature profile, as described in Section 3.5.4.

3.4 STEEL REINFORCEMENT PROPERTIES

Mechanical testing was performed on samples of reinforcing bar and prestressing strand taken from each beam. The purpose of this testing was to verify nominal material properties assumed for the reinforcement (e.g. elastic modulus, yield strength, tensile strength); and to determine a modified elastic modulus for strain gages on strands.

3.4.1 Reinforcing-Bar Mechanical Testing

Two types of reinforcing bars were used in the beam specimens (Figure 3.10):

- Grade 60 deformed bar for all of Beam 1 and the skewed end of Beam 2, and
- Welded deformed wire for the square end of Beam 2.

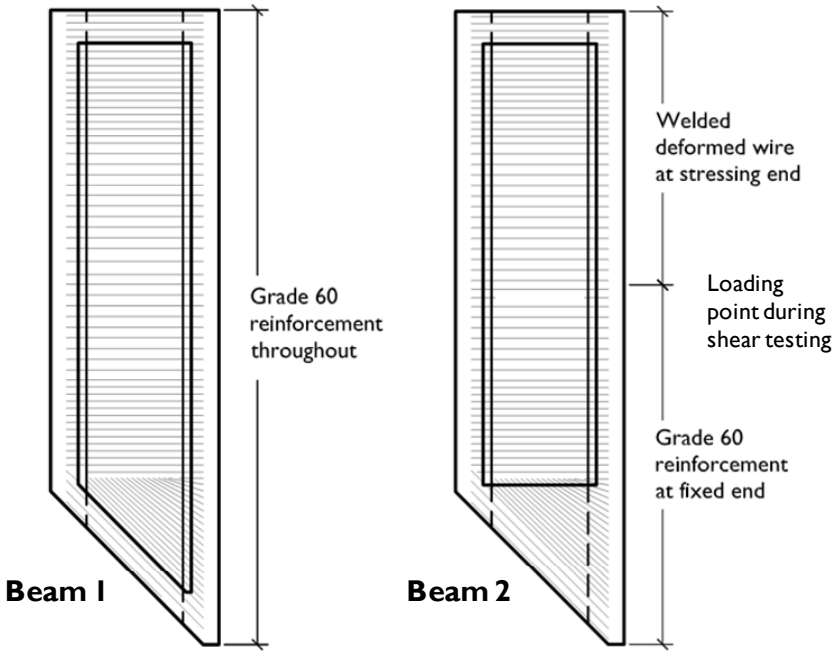

Figure 3.10 Reinforcing bar used in U-beam specimens

Tension testing was conducted on samples of Grade 60 rebar and deformed wire to verify the elastic modulus, the yield strength and the tensile strength. Bar samples were tested in a 60-kip testing machine with 16 in. free between the grips (Figure 3.11). An 8-in. extensometer mounted on the bar sample (Figure 3.12) was used for modulus testing. The loading rate was controlled at 0.1 kip/sec before yield (roughly one-quarter the maximum rate per ASTM A 615). After yield, the extensometer was removed, and the loading rate increased to 0.02 in./sec, as measured by a linear potentiometer tracking the movement of the bottom platen (rigidly connected to the top grip).

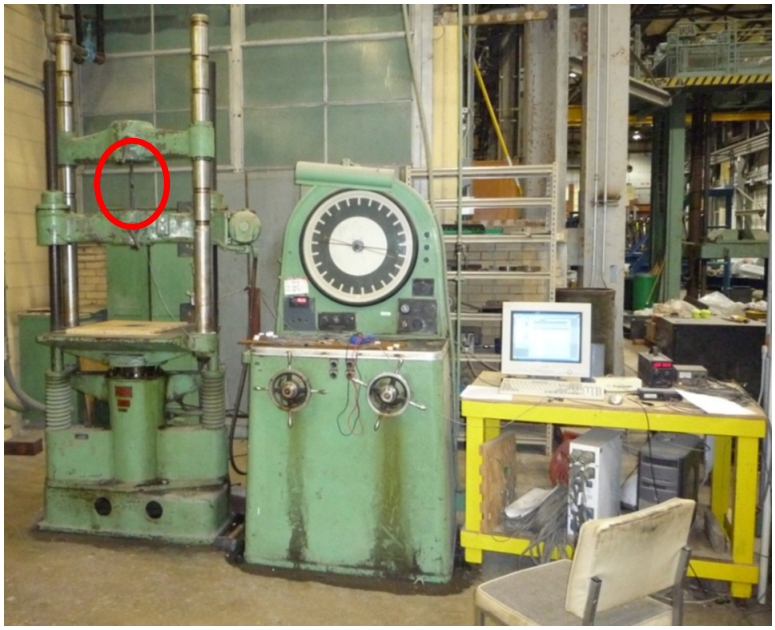

Figure 3.11 Reinforcing-bar tension testing in 60-kip test machine

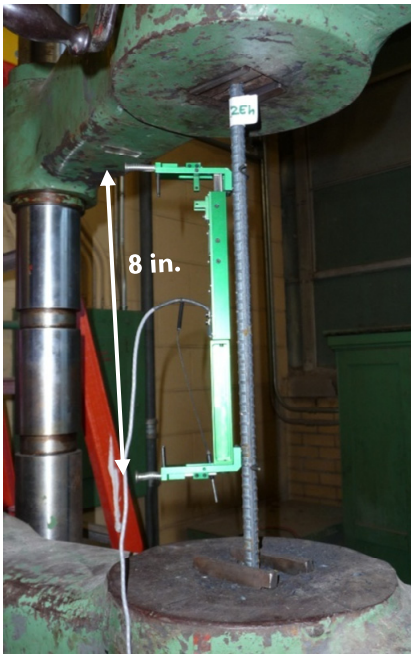

Figure 3.12 Extensometer on reinforcing-bar sample

Grade 60 rebar yielded at 65 ksi and failed at 110 ksi. Deformed wire did not show a yield plateau, but using the two-tangent method, yield strength was determined to be 85 ksi. Though deformed wire yielded at a higher stress, it failed at a lower stress, 95 ksi. The failure modes of the two bar types were different (Figure 3.13). The Grade 60 bar failed with a cup-and-cone shape after substantial necking and a gradual loss of capacity. The deformed wire failed in a brittle manner.

The measured elastic modulus was similar to the book value, 29,000 ksi. Reinforcing-bar tension test results are reported in Appendix D.

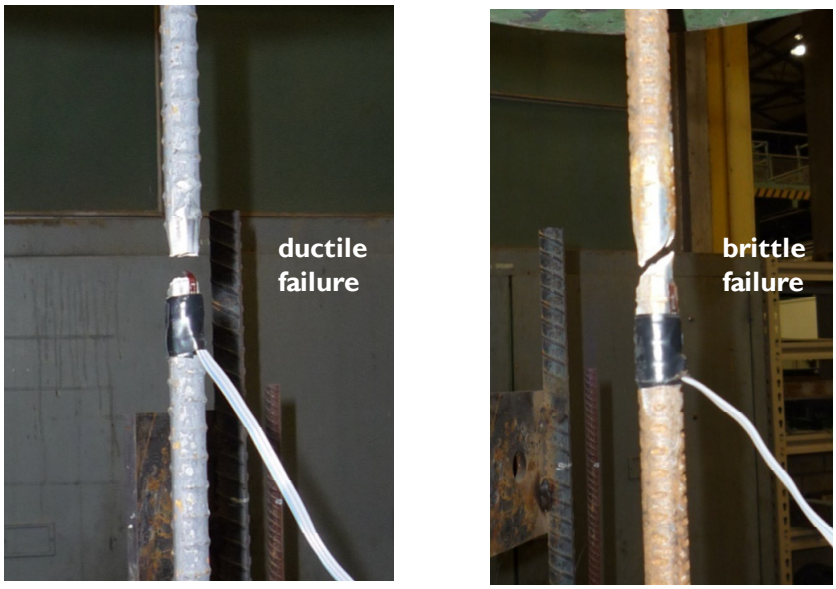

Figure 3.13 Failure modes for Grade 60 rebar (left) & deformed wire (right)

3.4.2 Prestressing-Strand Mechanical Testing

Strand testing focused on elastic-modulus testing. During stressing and release of beam specimens, strand behavior was to be examined through use of linear potentiometers and strain gages. The two sets of instruments measure different deformations: the linear potentiometers, the linear deformations; and the strain gages, the

deformation of a single wire within the seven-wire strand (approximately 10˚ off the linear axis).

Tension testing was run on 72-in. strand samples, each instrumented with a 24-in. extensometer and a strain gage (Figure 3.14). For a given load, the strain measured by the extensometer and that measured by the gage were slightly different due to the off-axis installation of the strain gage. Separate values of the elastic modulus were calculated from the extensometer data (engineering elastic modulus, Equation 3.9) and the strain gage data (modified elastic modulus, Equation 3.10).

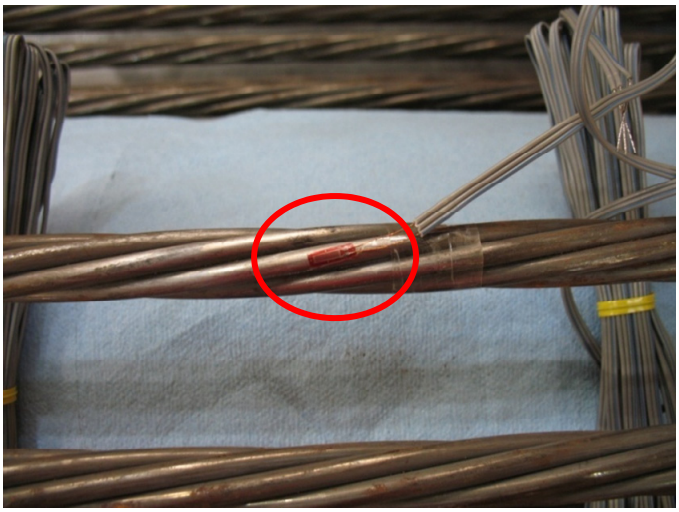

Figure 3.14 Typical strain-gage installation along pitched wire within strand
(O'Callaghan, 2007)

$$E = \frac{P_2 - P_1}{A_p}\frac{L_o}{\Delta_2 - \Delta_1} \qquad \textbf{Equation 3.9}$$

where:

$P_{1,2}$ = *load at two points (e.g. 20% and 100% of prestressing load), kip*
A_p = *strand area, nominally 0.153 in.*^{2}
$\Delta_{1,2}$ = *extensometer deformations corresponding to load points, in.*
L_o = *initial distance between extensometer contact points, in.*

$$E_{mod} = \frac{P_2 - P_1}{A_p}(\varepsilon_2 - \varepsilon_1) \qquad \textit{Equation 3.10}$$

where:

$\varepsilon_{1,2}$ = *gage strains corresponding to load points, in./in.*

Measured engineering and modified elastic modulus values were approximately 28,500 and 30,500 ksi, respectively.

Figure 3.15 Extensometer & strain gage on strand sample

Two slightly different procedures were used for testing the strand samples from the two beams. Samples for the first beam were tested to tensile failure. For such tests, ASTM A370 Annex A7 advises against gripping the strand directly: the clamping force applied to the strand could affect test results. For samples tested to failure, the strand was

cleaned and epoxied into light-gage black galvanized pipe (Figure 3.16) using a two-component epoxy (Pro-Poxy 200). Strand prepared in this manner was tested in a 600-kip testing machine until tensile failure. Failures occurred 5% above the rated tensile strength for the strand, at approximately 285 ksi. The typical failure mode involved the outer wires "unzipping" from the king wire, and is shown in Figure 3.17.

Figure 3.16 Strands epoxied into black pipe for tensile-strength testing

Though the epoxied-pipe setup reached the failure load reliably, problems were encountered along the way. The pipe would slip between the grips periodically, moving a small distance (less than 0.10 in.) and jarring the extensometer. Data collected from tests in which the strand slipped was still usable for calculating the engineering and modified elastic moduli, but the inter-test variation was greater than desired. Since the tensile-strength testing was done only to verify nominal properties, it was abandoned for the second beam in hopes of more accurately measuring the elastic modulus.

Figure 3.17 Typical strand failure mode

For the second-beam modulus testing, strands were tested with stressing chucks at each end bearing against the testing machine platens (Figure 3.18). Variation between test values of the elastic modulus decreased substantially with this procedure: the coefficient of variation was halved for the engineering and modified elastic moduli. Detailed results from mechanical testing of prestressing-strand samples are reported in Appendix D.

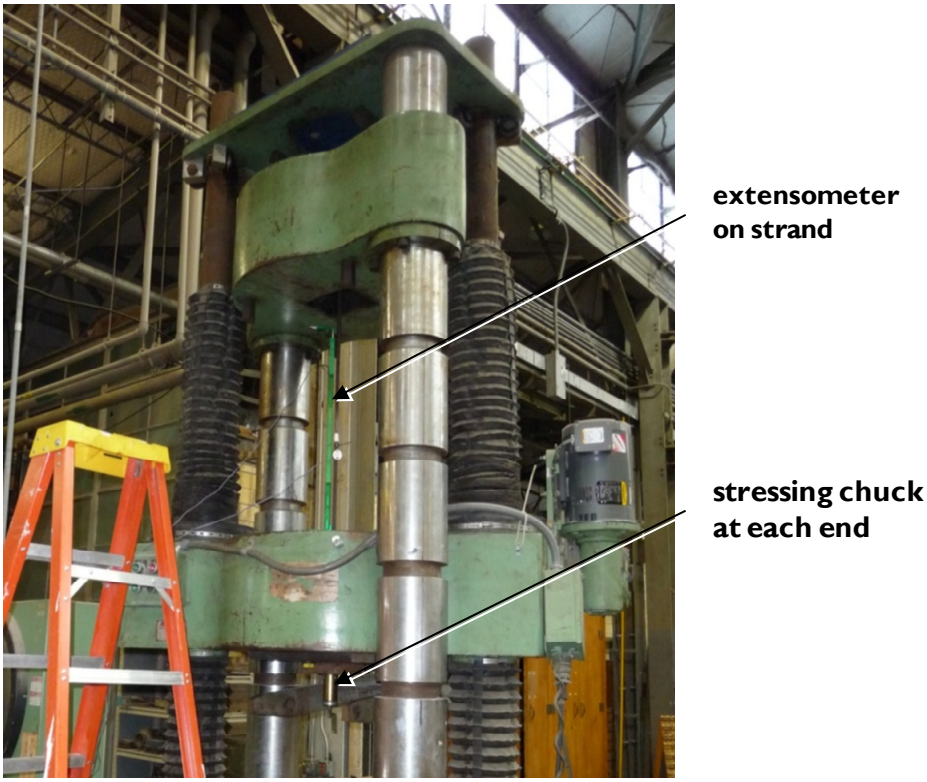

Figure 3.18 Setup used for Beam 2 elastic-modulus testing for strand

3.5 INSTRUMENTATION

3.5.1 Strain Gages on Reinforcing Bars

Strain gages on transverse and lateral reinforcement in the end region represent the primary form of instrumentation used in this study. Gages were placed on the bars near where cracks were expected to form at transfer. As mentioned previously, if a beam cracks far from the locations instrumented with strain gages, the gages are likely to "miss the crack," and return small strains. Expectations with regards to cracking were informed by observations of a precaster-fabricated U-beam (Beam 0, discussed further in Section 3.6.1), whose crack map (as received, at five months age) is shown as Figure 3.19.

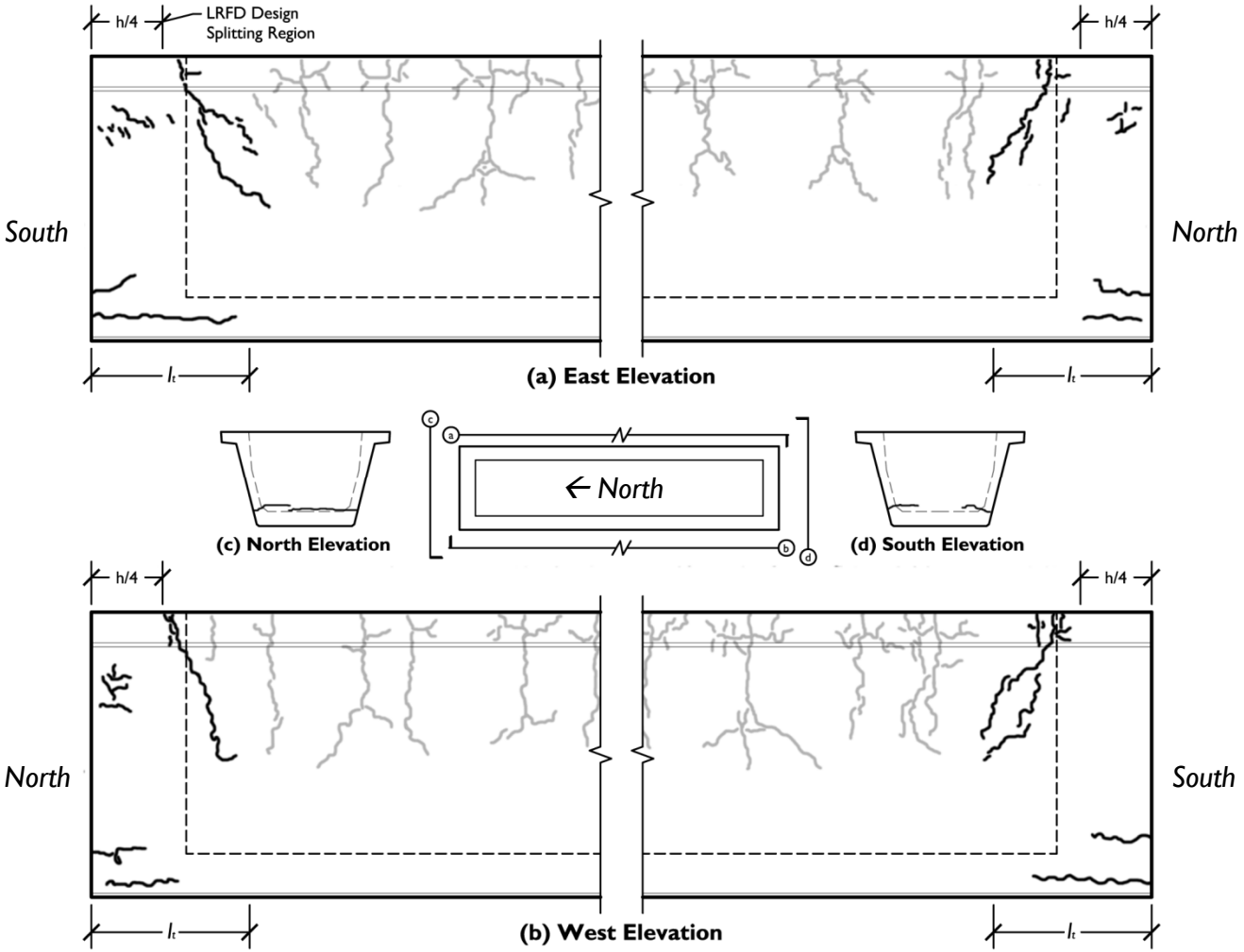

Figure 3.19 Crack map for Beam 0, as received five months after cast & release

Typically four series of strain gages were used in each end-region web. As shown in Figure 3.20, these series include the following:

- Three sets of strain gages mounted on transverse reinforcement, and
    - Gages measuring spalling strains at the top of the web
    - Gages measuring spalling strains at middle of the web (section centroid)
    - Gages measuring bursting strains at the bottom of the web
- One set of strain gages mounted on lateral reinforcement.
    - Gages measuring lateral bursting strains in the bottom flange

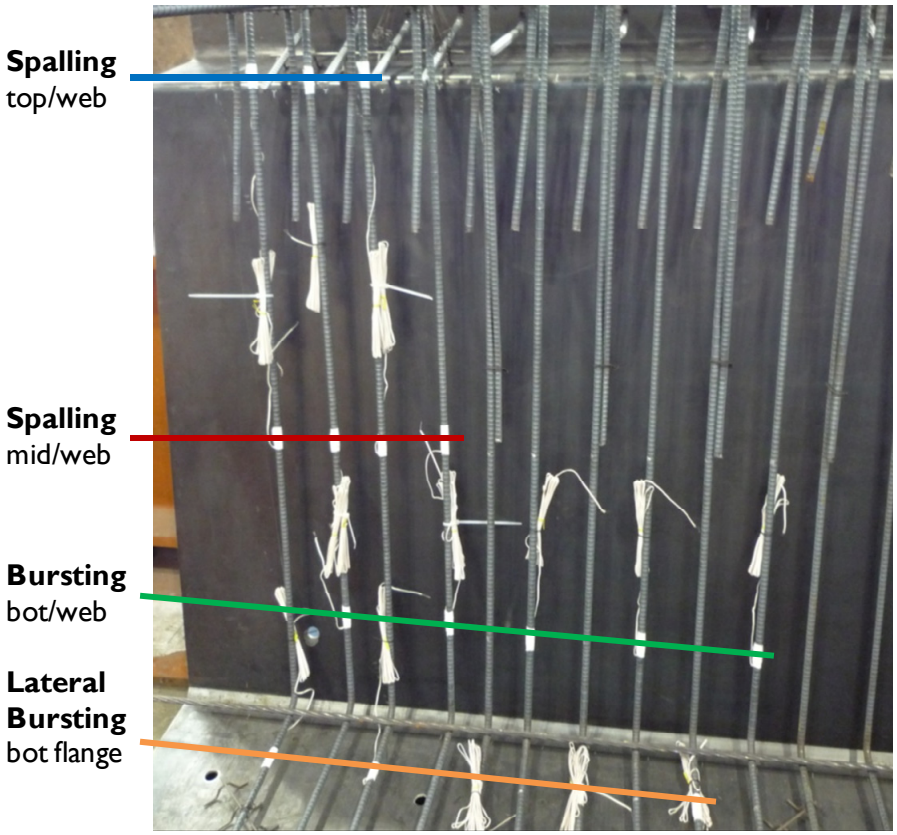

Figure 3.20 Typical strain-gage placement in beam end-region

Beam 1 also included an additional strain gage series on transverse bars, measuring bursting strains at the centroid of the prestress (bottom flange, midheight). Strain data from this series was similar to that acquired from the strain gages at the bottom of the web (located just 5 in. away), so the prestress-centroid strain gages were discontinued.

Within the end block, strain gages were typically applied to the transverse bars within the projected area of the webs (*R* bars); but not to the transverse bars within the projected area of the void (Figure 3.21).

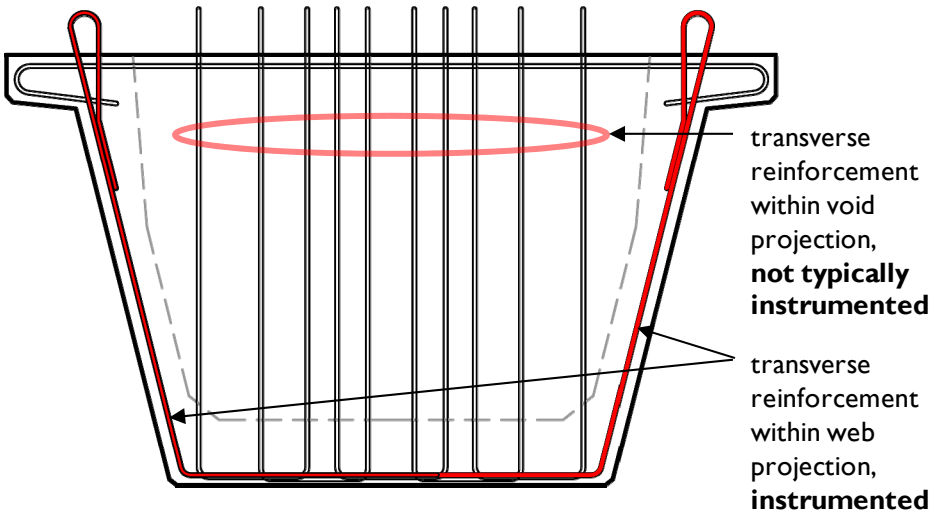

Figure 3.21 Instrumentation for transverse reinforcement within end block

Strain gages used on reinforcing bar were 6-mm WFLA foil gages from Tokyo Sokki Kenkyujo (TML). These gages had a pre-bonded silicone pad sufficient to provide waterproofing and cushioning during casting. Strain gages were applied as follows. Bar deformations at the desired gage location were removed through grinding and sanding (ending with fine-grit sanding wheels) using a rotary tool. Weak acid/base solutions (Vishay Micromeasurements) were used to remove surface dust and mill-scale. Lastly the

strain gage was applied to the bar using cyanoacrylate strain-gage adhesive (*CN*, TML). Electrical tape was wrapped around the gage and bar to decrease the likelihood of gage peel-off. Gages were checked immediately after installation through use of a multimeter, with a resistance reading just over 120 ohms indicating good electrical connections.

3.5.2 Strain Gages on Prestressing Strands

Strain gages were installed on prestressing strand for use during tensioning (measuring initial prestrain) and detensioning (assessing transfer length and effective prestressing force after transfer). As a part of the fabrication process, gages were installed on a given strand row after that row had been strung through the beam and given a nominal tension (3 kip) through monostrand jacking. The gages used were 5-mm FLA foil gages (TML).

The strain-gage installation procedure for strands follows. The outer wire on which the gage was to be installed was prepared using fine sandpaper and weak acid/base solutions. The strain gage was then positioned along the wire using clear tape. The tape peeled back, cyanoacrylate adhesive was used to attach the gage to the strand. Two coatings were applied to protect the gage during casting. These coatings were, in order of application, microcrystalline wax (*W-1*, TML) and heat-shrink coating tape (*CT-D16*, TML).

Figure 3.22 shows strain gages being installed on strands within the large triangular end block of Beam 2. When installation is completed, the strain gages appear as shown in Figure 3.23.

Figure 3.22 Strand strain-gage installation process (Beam 2, 45°-skewed end)

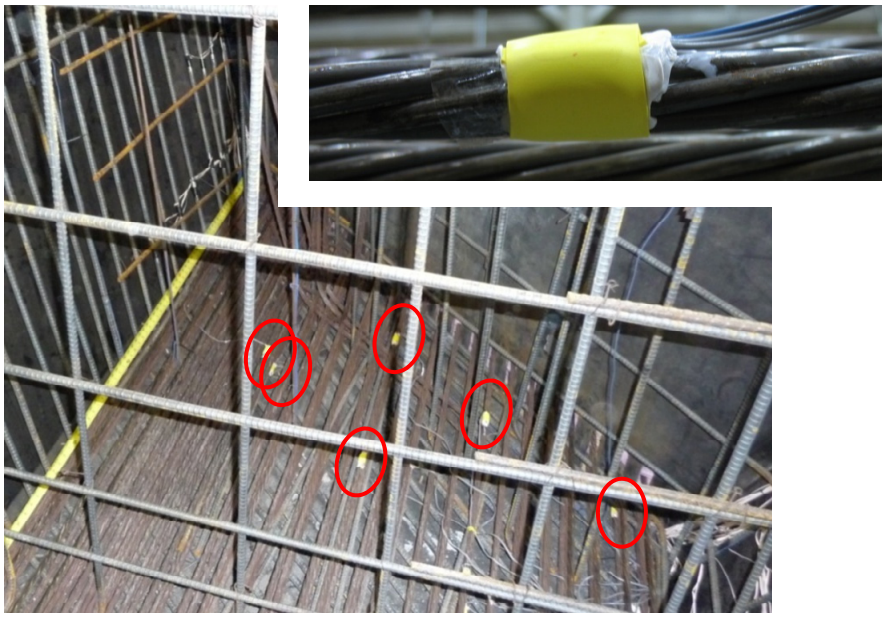

Figure 3.23 Completed strand strain gaging *(inset from O'Callaghan, 2007)*

Since one purpose of the strain gages installed on strands was to verify the code transfer length (30 in.), the distance along a strand from where it entered the beam to its

gage location was varied. Gages were placed within, at and beyond the transfer length. An example of the strain-gage installation plan is shown as Figure 3.24.

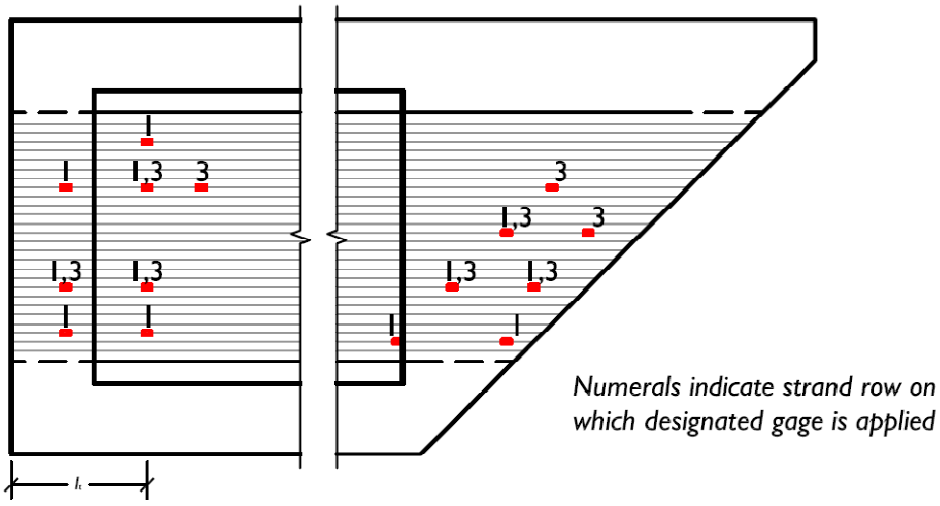

Figure 3.24 Strand strain-gage locations (Beam 2)

3.5.3 Data-Acquisition Systems

Because of the large number of strain gages to be used on both reinforcing bar and strand, two data-acquisition systems (DAQs) were used. Different bridges are required for strain gages as compared to other instrumentation (e.g. linear potentiometers, load cells, pressure transducers). Most of the quarter-bridges (used to connect strain gages) at a DAQ located at the south end of the pretensioning bed. The north-end DAQ was split between quarter-bridges (strain gages) and half-bridges (other instrumentation). Because of the distance between the strain gages within the beam and the DAQs, lead-wire extensions were used. Lead wires from strain gages from a particular series (e.g. transverse bursting) from one corner of a beam specimen were collected together, then extended to an interface board (Figure 3.25). The interface board was connected to the bridges, which were plugged into the DAQ.

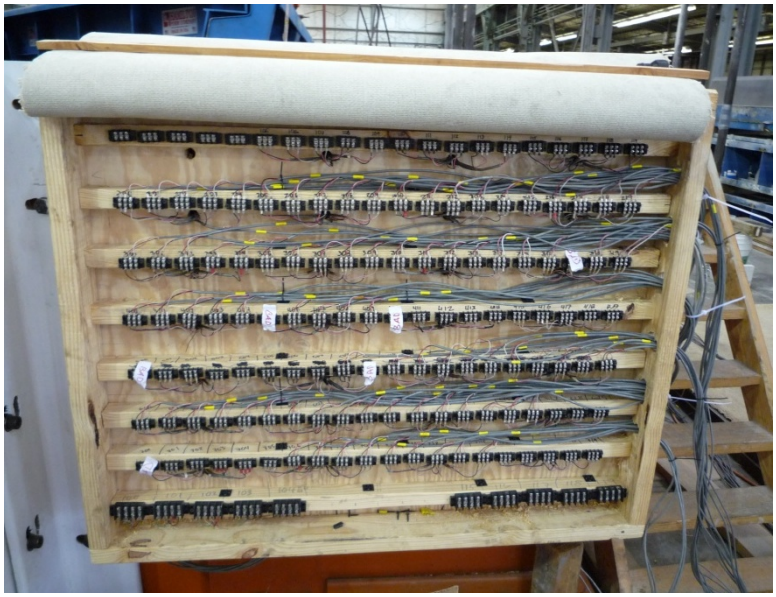

Figure 3.25 Interface board used to connect strain-gage leads to quarter-bridges

A total of 215 channels (over the north and south DAQ) were available for use during testing, but a few were out of operation. Malfunctioning channels were identified through testing at the bridges and interface board. Channels were short-circuited, and the resulting voltage recorded at the DAQ would be noted. For quarter- and half-bridges, channels were checked as shown in Figures 3.26 and 3.27, respectively.

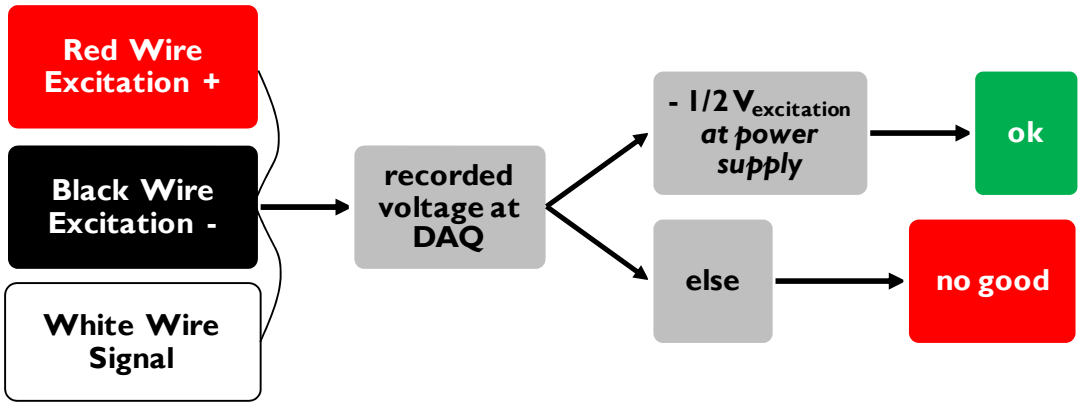

Figure 3.26 Heuristic for checking quarter-bridge channels

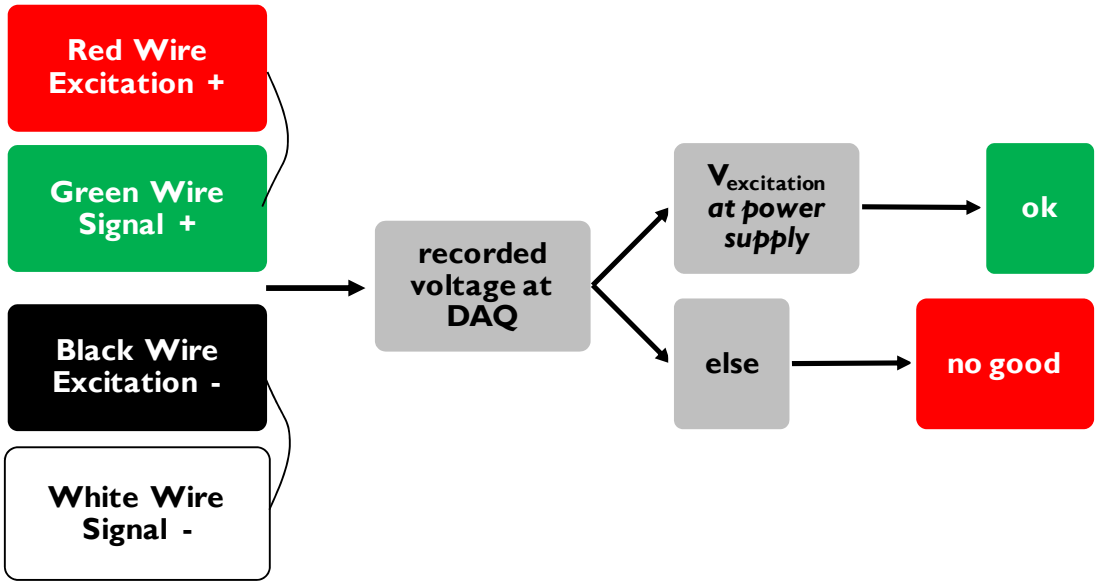

Figure 3.27 Heuristic for checking half-bridge channels

3.5.4 Thermocouples in Concrete

Thermocouples were used for two purposes:

- as components in the temperature-match curing system used to create cylinder specimens with similar temperature time histories as desired locations within the beam specimens; and
- to measure the temperature profile within the end blocks.

A typical thermocouple installation is shown in Figure 3.28.

Cylinders were match-cured to three locations within the beam: the release point (8 ft. from end at bottom flange/web junction), the hot spot (centroid of end block at the skewed end) and the top flange (center of flange at one transfer length from end). More detail on the thermocouples used for match-curing was given in Section 3.3.3.

Typical temperature readings for a section without an end block (40-in. I-beam) is shown in Figure 3.29. This figure shows three stages of cement hydration: the initial dormant period, then a quick rise in temperature followed by a slow cool down. The

beam has a "hot spot" (measurement location 6, center of bottom flange), but its temperature curve is indistinguishable from others until the downward-sloping portion of the curve is reached.

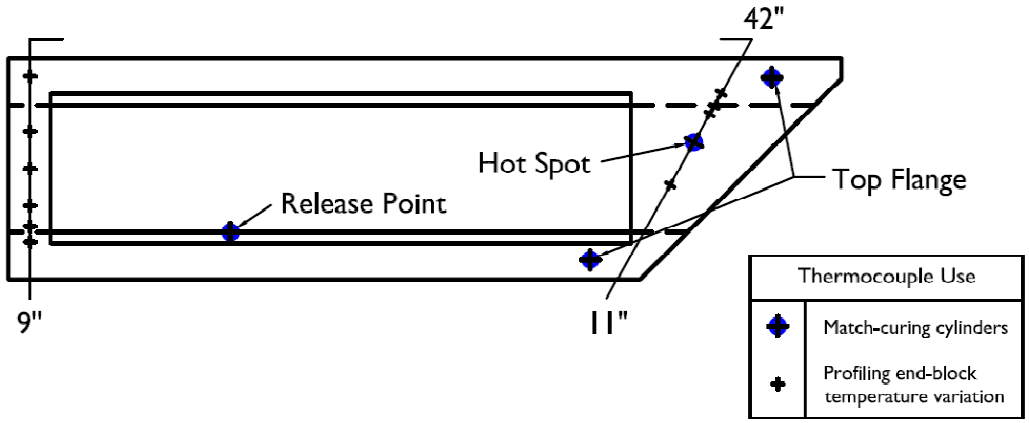

Figure 3.28 Typical thermocouple instrumentation (Beam 2)

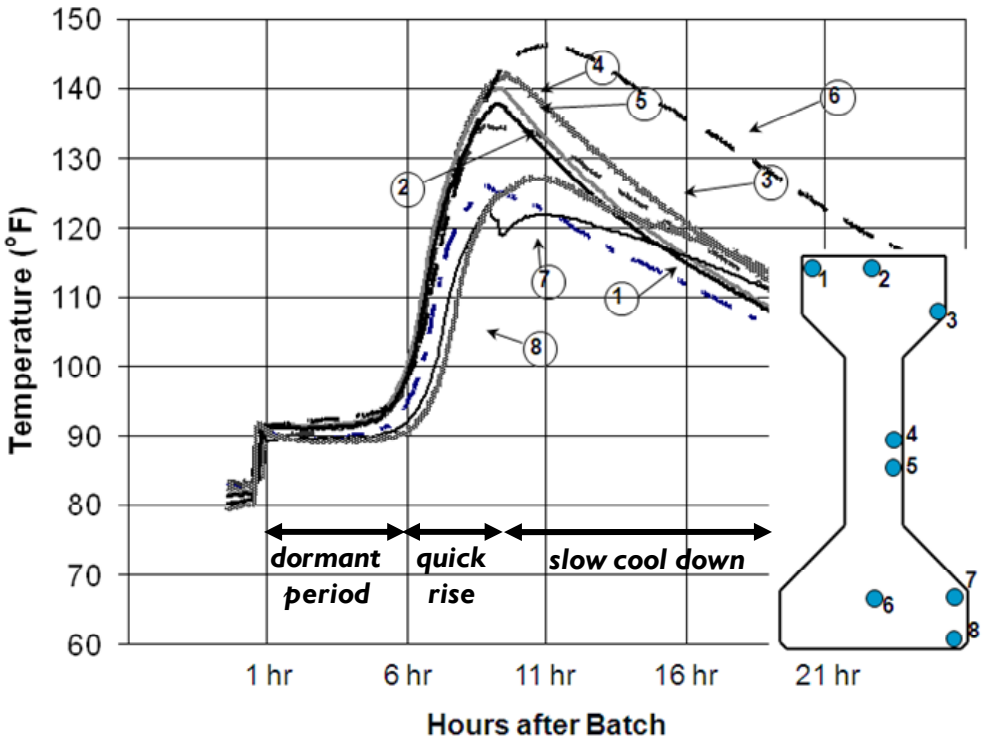

Figure 3.29 Typical thermocouple data *(after Tuchscherer, 2007)*

For the beams in this study, special interest was paid to the maximum temperature and the temperature variation with the 45˚-skewed end blocks. The two design alternatives require different volumes of concrete: the large triangular end block is three times the size of the other design (Figure 3.5). All end blocks were instrumented with thermocouples throughout a cross section crossing their centroid. Typical thermocouple locations are shown in Figure 3.30. Spacing of thermocouples varied from 10 to 24 in.

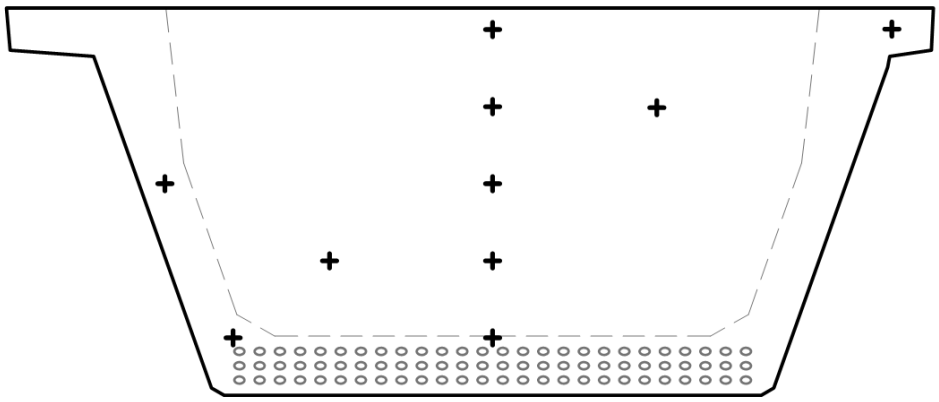

Figure 3.30 Thermocouple placement in small skewed end block (Beam 1)

All thermocouples consisted of copper and constantan wires (Type T, Omega). Thermocouples measure temperature using the electrostatic potential between the two metals, which varies as a known function of temperature. Thermocouples were prepared by stripping the wire sheathing and twisting the wire ends together at a measurement location. Thermocouples whose data was to be recorded by the match-curing system were plugged into the system's wireless transponder. Data from other thermocouples were recorded using a Campbell Scientific *C21X* datalogger. A multiplexer was used to increase the channel capacity of the datalogger. Care was taken to prevent the thermocouple wires from touching at points other than the intended measurement location.

3.6 BEAM FABRICATION

3.6.1 Beam Casting at Precast Concrete Plant

Before U-beams were fabricated at the Ferguson Laboratory, the research team observed the casting of a 30 ft. long U-beam at Bexar Concrete Works, a major precast-concrete fabricator based in San Antonio. This beam was constructed with widely-spaced transverse reinforcement as part of an effort to determine the shear strength of the U-beam near its midspan. Shear reinforcement was spaced at 8 in. and 18 in. at the two beam ends, respectively.

U-beams are cast in two stages, monolithically. After concrete is placed in the bottom flange (Figure 3.31), with care to ensure adequate vibration around the strands (Figure 3.32), a steel interior-void form is lowered into place (Figure 3.33). The interior void has polystyrene spacers attached to each end to facilitate the removal of the void form before transfer. After the interior-void form is secured into place with cross-form hangers, concrete placement proceeds, with the webs, top flanges and end blocks filled around the void form (Figure 3.34). Lastly the top surface is finished (Figure 3.35).

Some time must pass between the first and second stages of the cast for the interior void to be placed. As long as the bottom-flange concrete is still plastic (allowing the concretes from the two stages to be inter-mixed through vibration) , casting is allowed to proceed. TxDOT quality-assurance staff report that a 60- to 90-min. delay between the first and second stage is typical.

Figure 3.31 Placing concrete using sidewinder (concrete buggy)

Figure 3.32 Consolidating bottom-flange concrete using internal vibrators & external form vibrators *(not shown)*

Figure 3.33 Installing the interior-void form

Figure 3.34 Filling the webs and end blocks around the interior-void form, held in place with hangers

Figure 3.35 Finishing the top surface

The beam fabricated at Bexar Concrete Works (Beam 0) was observed only during casting. Five months later, when it was transported to the Ferguson Laboratory, crack mapping was done for the beam elevations. The as-received crack map for Beam 0, shown previously as Figure 3.19, proved valuable while planning strain-gage placement for the beams fabricated in the laboratory, as discussed in Section 3.5.1.

3.6.2 Pretensioning Facility

Beams were fabricated within the Ferguson Laboratory using a pretensioning bed constructed by O'Callaghan. The bed is a self-reacting frame designed for a 2500-kip maximum prestressing force, and can accommodate specimens approximately 40-ft. in length. A set of four 800-kip hydraulic rams are used for the multi-strand tensioning and gradual detensioning. More details on the frame construction and properties are provided in O'Callaghan (2007).

In order to use a pretensioning bed designed for I-beams to fabricate U-beams, some modifications to the bed were required. The existing bulkheads at the stressing and fixed ends were neither wide enough nor contained an appropriate strand pattern for U-beams, so new plates were purchased to replace them.

Figure 3.36 FSEL pretensioning bed *(O'Callaghan, 2007)*

The new bulkheads were 12 in. thick, A36 steel plates measuring 91 by 52 in. in section. This thickness was deemed appropriate based on FEA suggesting that, at 12 in. thickness, the bulkhead would not yield during U-beam or box-beam fabrication. The plates were drilled with ¾-in. through-holes to match the U-beam and box-beam strand patterns. The stressing-end bulkhead was mounted on 8-in. angles, which rested on steel plates. Polytetrafluoroethylene (PTFE) sheets were epoxied on both sides of the angle/plate interface to allow the bulkhead to slide during stressing (Figure 3.37).

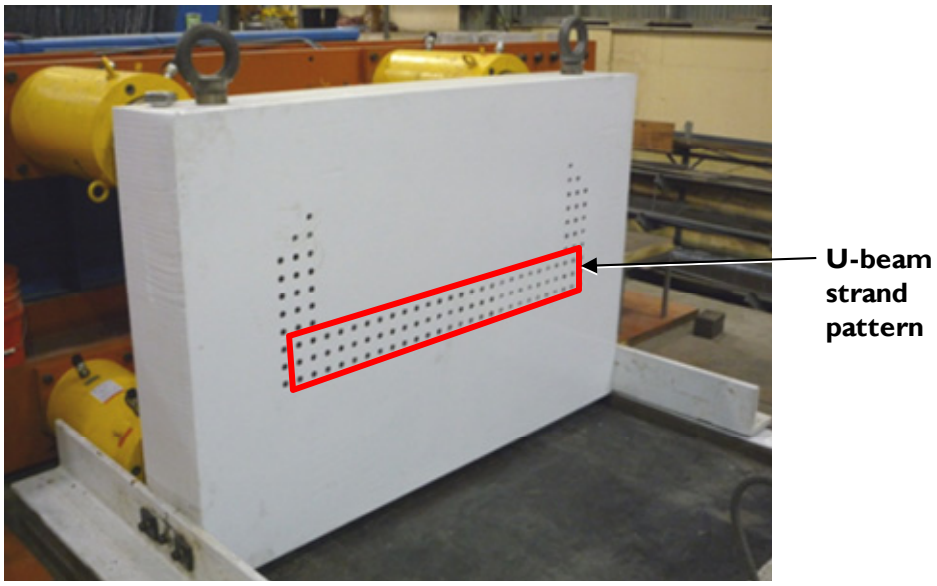

Figure 3.37 Wider bulkhead in place at stressing end

Custom U-beam steel forms were designed and fabricated by Hamilton Form. The side forms differ from typical designs in that the custom forms are tapered (Figure 3.38) for better fit within the existing pretensioning bed. Steel beam headers were used; wooden headers are typically used at precast fabrication facilities. With the provided formwork, a variety of beams could be constructed, with square ends or skewed ends (20° or 45°) and with either end-block detail (triangular or skewed) at the skewed ends.

The formwork set up for a beam with one square end (near end) and one 45°-skewed end (far) is shown in Figure 3.39.

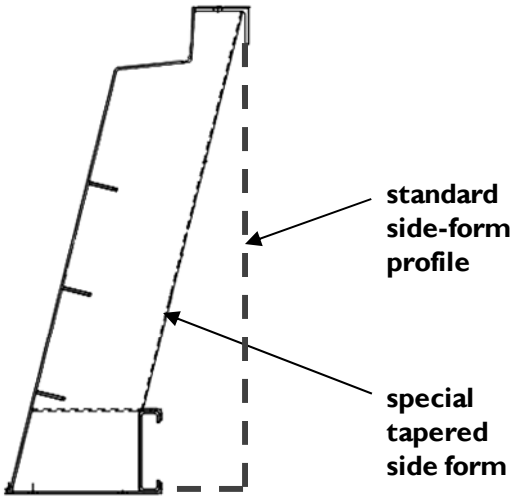

Figure 3.38 Special tapered side form fabricated by Hamilton Form

Figure 3.39 U-beam formwork in pretensioning bed

Some modifications were made to the form headers (Figure 3.40) in order to make the removal of the header after prestress transfer easier.

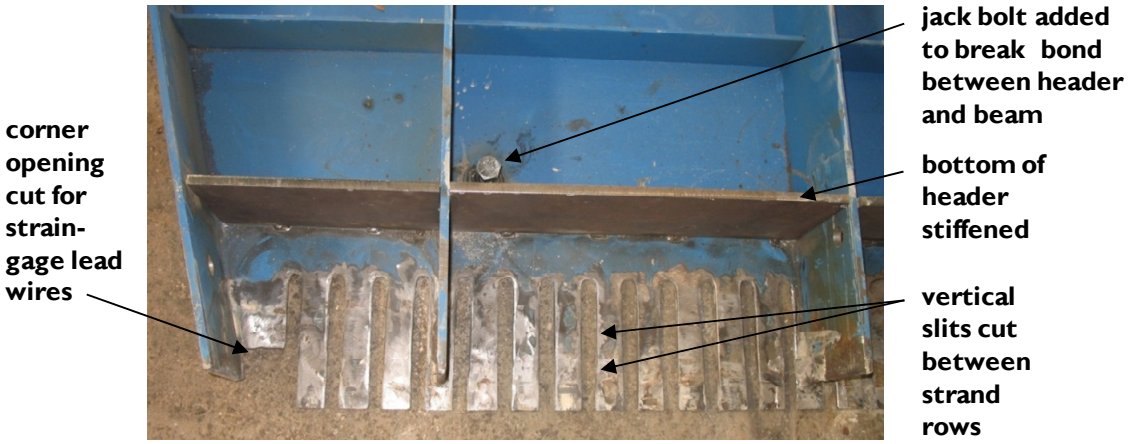

Figure 3.40 Modifications to beam header

3.6.3 Strand Tensioning

After reinforcing bars were positioned throughout the beam and strain gages installed in regions of interest (e.g. end-region transverse bars), strands were installed, pulled by hand through one bulkhead, along the length of the beam, and out the far bulkhead. With stressing chucks placed on each strand, strands were stressed individually to a nominal tension (3 kip) for strain-gage installation. One row of strands was installed at a time (Figure 3.41), with a pause to install the gages for that row before proceeding to the next. Strain-gage installation procedures were discussed in detail in Section 3.5.2.

After all strand rows and associated gages were installed, the prestressing strands were ready for full tensioning. A few hours before the beam was cast, strands were stressed to approximately 203 ksi (31 kip per strand). First the rams were retracted slightly, letting off the initial tension (used for gaging) from the strands. The rams were then extended, pushing the stressing-end bulkhead away from the prestressing frame and stretching the strands. Since the centroid of the prestressing force did not correspond with the bulkhead center (between ram supports), different hydraulic pumps were used for the top and bottom sets of rams.

Figure 3.41 Strands installed, tensioned to nominal stress for instrumentation

During tensioning, the applied prestressing force was measured by three methods:

- Ram pressure: Pressure in the hydraulic lines connecting pump and rams (measured by pressure transducer and dial gauges);
- Strand elongation: displacement of stressing-end bulkhead less the axial shortening of the prestressing frame (measured by linear potentiometers at both ends of the frame); and
- Strain in select strands (measured by strain gages mounted on strand outer wires).

At several points before full tensioning, stresses measured by the three methods were compared and the bulkhead was checked for levelness.

For 31 kip tension in the strands, the stressing-end bulkhead was displaced approximately 4.75 in.: 4.5 in. of strand elongation (as given by Equation 3.11) and 0.25 in. of prestressing-frame shortening.

$$\Delta = \frac{P_i L_o}{E_p A_p} = \frac{31.0\ kip \cdot 612\ in.}{27800\ ksi \cdot 0.153\ in.^2} = 4.46\ in. \qquad \textbf{\textit{Equation 3.11}}$$

where:

P_i = *desired prestressing force (31 kip per strand)*
L_o = *initial free length of strand (approximately 51 ft. = 612 in.)*
E_p = *strand engineering elastic modulus (27800 ksi for Beam 1)*
A_p = *total strand area (0.153 in.^{2} per strand)*

The movements of the bulkheads at both ends of the beam were monitored with linear potentiometers as shown in Figure 3.42.

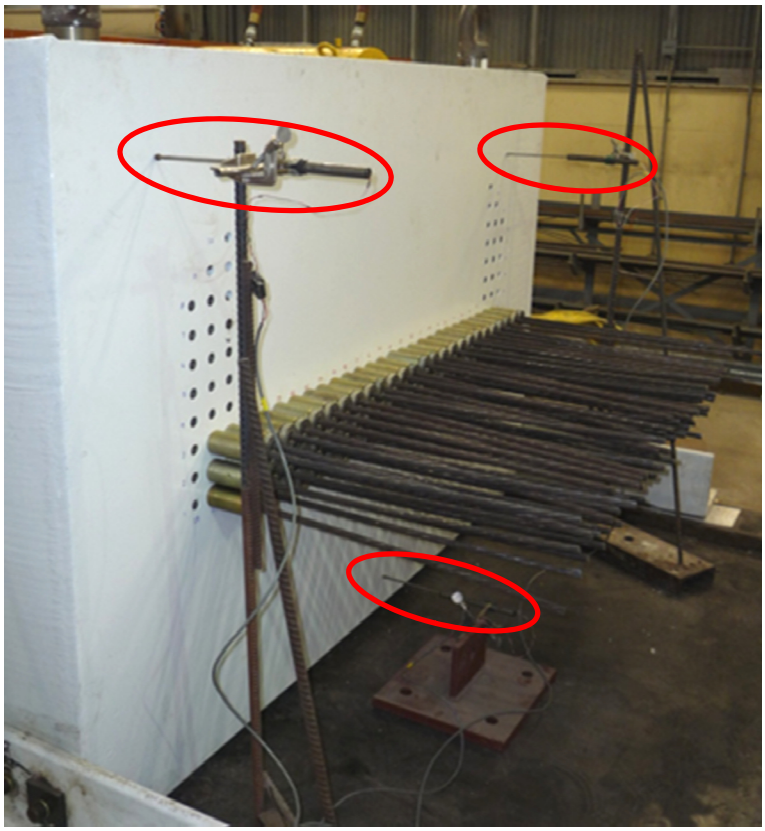

Figure 3.42 Linear potentiometers (circled) used to monitor strand elongation

Correspondence between the values of prestressing force measured by the different methods was good (3.7% mean discrepancy between methods) and less than the 5% code maximum (ACI 318, 2008, Provision 18.20.1). Precision improved during the second beam cast, with the error halved (1.4% discrepancy). The reported prestressing force applied for each beam represents the mean prestressing force associated with measurements of ram pressure and strand elongation.

3.6.4 Beam Casting

After the strands were fully tensioned, the beams could be cast. A similar procedure to that observed at the precast-beam fabricator (Section 3.6.1) was used; a few particulars of the casting process used at the Ferguson Laboratory are noted.

Concrete for the U-beams was provided by Coreslab Structures, as previously discussed in Section 3.3.1. After batching, this concrete was loaded into mixing trucks rented from a local ready-mix concrete provider and transported to the laboratory (approximately 15 miles). Because of the journey, and concerns about concrete flash-setting in the trucks, chemical retarder (5 oz/Cwt) was incorporated in the concrete mixture design (Table 3.1).

When the concrete trucks arrived at the laboratory, the concrete slump was measured as shown in Figure 3.43. High-slump concrete (9 in. goal) was desired for easy placement of the concrete, particularly in the bottom flange, congested by the large number of prestressing strands used. If trucks arrived with low-slump concrete, water and/or superplasticizer could be mixed in before placement.

A large number of cylinders were cast alongside the beams (Figure 3.44). A total of 48 cylinders were match-cured to locations in the beam, with the majority corresponding to the “release point” and “hot spot” locations (described previously in

Section 3.3.3). Additional cylinders were cured under ambient conditions; most of these were used for strength testing conducted days and weeks after transfer.

Figure 3.43 Slump testing

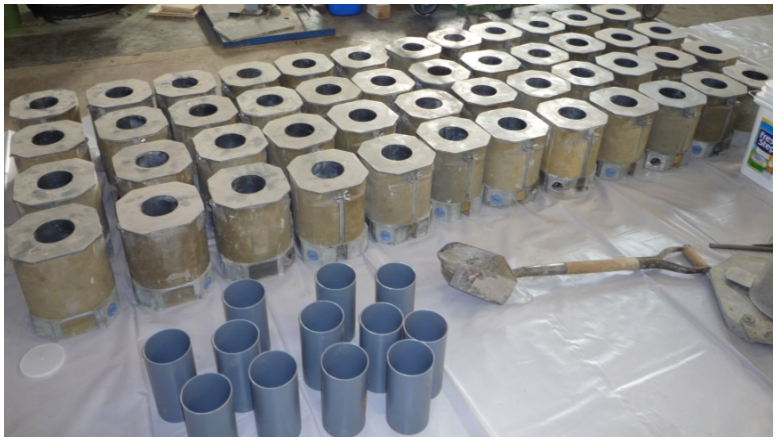

Figure 3.44 Cylinder molds set out for beam cast
(plastic molds for cylinders cured under ambient conditions, metal insulated molds for match-cured cylinders)

Figures 3.45 to 3.50 show the fabrication of a laboratory-cast U-beam. Several hours after the beam was finished (allowing time for the bleed water to appear and evaporate), it was covered with a polypropylene sheet to decrease moisture loss and minimize early-age shrinkage cracking.

Figure 3.45 Placing concrete in the bottom flange

Figure 3.46 Consolidating bottom-flange concrete using internal vibrators & external form vibrators

Figure 3.47 Moving interior void into position after bottom flange is cast

Figure 3.48 Positioning interior-void hangers

Figure 3.49 Casting end block (and webs) around the interior void

Figure 3.50 Placing concrete in large triangular end block (Beam 2, 45°-skewed end)

3.6.5 Transfer of Prestress

Starting 8 hours after the beam cast, match-cured cylinders (from the release point and the hot spot) were tested under compression. As the measured compressive strength for cylinders match-cured to the release point approached the release strength, the interior void was removed from the beam (Figure 3.51).

When the concrete release strength was achieved, the strands were detensioned gradually (over the course of several minutes) as shown in Figure 3.52. The beam was removed from the forms within the next few days, and crack pattern resulting from transfer was noted.

Figure 3.51 Removing interior void form in preparation for transfer

Figure 3.52 Detensioning by gradually decreasing pressure in stressing rams

3.6.6 Moving the Beam

Moving U-beams (beam weights in excess of 40 kip) within the laboratory was no trivial task. A stiffened W30 steel section with three-ply, 10-in. nylon slings was used (Figure 3.53). Consideration of the centroid of the combined spreader-and-concrete-beam system was necessary for balance: the centroid for a U-beam with a 45º-skewed end was as much as 18 in. off-center along the longitudinal axis and 3 in. off laterally.

Figure 3.53 Lifting Beam 0 from delivery truck

3.7 SUMMARY

Methodology used in the experimental program was explained in this chapter; experimental results, their significance and recommendations arising from them will be discussed in Chapter 4.

CHAPTER 4

Results & Discussion

4.1 OVERVIEW

As discussed in Chapter 3, two full-scale 54 in. deep U-beams were fabricated in order to evaluate the behavior of the current TxDOT standard end-region reinforcing details. Results from end-region studies are presented, with focus on experimentally determined transverse-bar stresses at prestress transfer. A database of past bursting and spalling studies (53 beam end regions), in which transverse-reinforcement strains were also monitored at transfer, was assembled. Data from the U-beam specimens (four end regions) was analyzed in the context of this experimental database, and trends are identified. Preliminary recommendations specific to the Texas U-beam end-region reinforcement are made. Details recommended in this section will be tested at transfer and under shear loading in the next phase of TxDOT Research Project 5831.

4.2 EXPERIMENTAL RESULTS FROM RESEARCH PROJECT 5831

4.2.1 Stresses Inferred from Measured Strains

As experimentally determined stresses in transverse and lateral reinforcing bars are essential components to this study, a description on how raw strain-gage output was converted to the reported stresses is given below.

Strain time histories were recorded for 12 to 30 hours after prestress transfer for the gages mounted on reinforcing bars. A properly functioning strain gage (90% of gages installed) behaved as follows. Soon after transfer, the gage registered a sudden rise in strain. After 5 to 15 min., the measured strains began a slow, linear increase

(1 ksi/12 hours). Typical strain time histories for two gages—one reading low strains and another high—are shown in Figure 4.1.

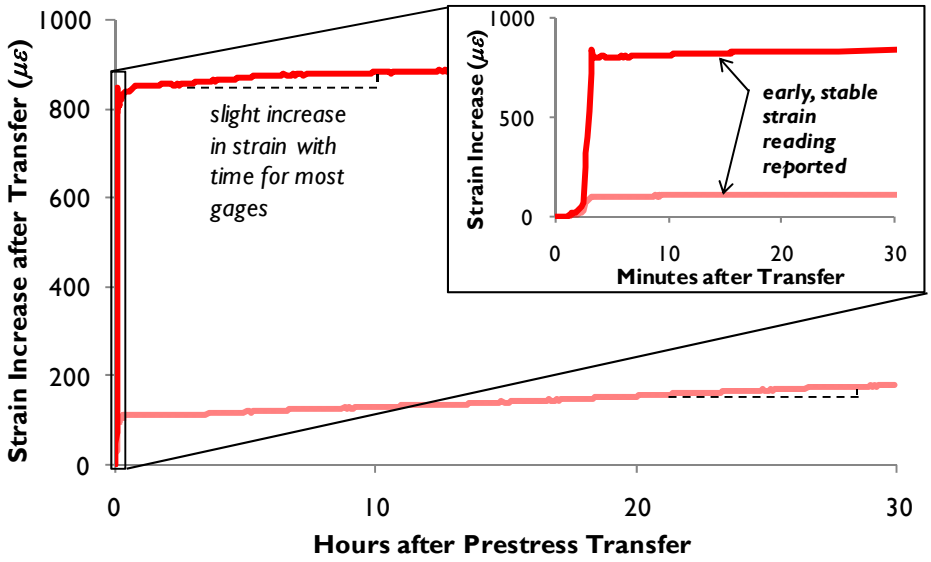

Figure 4.1 Strain time histories for two gages

The time-dependent increase in measured bursting/spalling strains observed for this project is similar to a finding of Arthur and Ganguli (1965). In their experimental study of concrete surface strains in end regions of pretensioned I-beams without web reinforcement (discussed in Section 2.4.1.5), tensile strains across cracks were observed to increase with time. Itani & Galbraith (1986), however, reported that foil strain gages, as used in Research Project 5831, are not reliable for long-term measurements (Section 2.4.2.3). Since the potential time-dependent strain rises could not be reliably separated from time-dependent instrumentation error, the stresses reported are those based on stable strain readings soon after prestress transfer. The use of such strain readings also provides continuity with some past studies of bursting and spalling stresses in transverse reinforcement (Marshall & Mattock, 1962; Tuan et al., 2004).

The strain time history for each gage was thus reduced to a single metric, typically by taking the strain value measured some 15 min. after transfer. This strain was multiplied by the nominal elastic modulus of the steel reinforcement (29,000 ksi) to generate the stress reported.

4.2.2 Beam 1 Results

4.2.2.1 Beam 1: Cast & Release

The cast and release of Beam 1 is summarized in Figure 4.2. For descriptions of each step in this process, refer to Chapter 3.

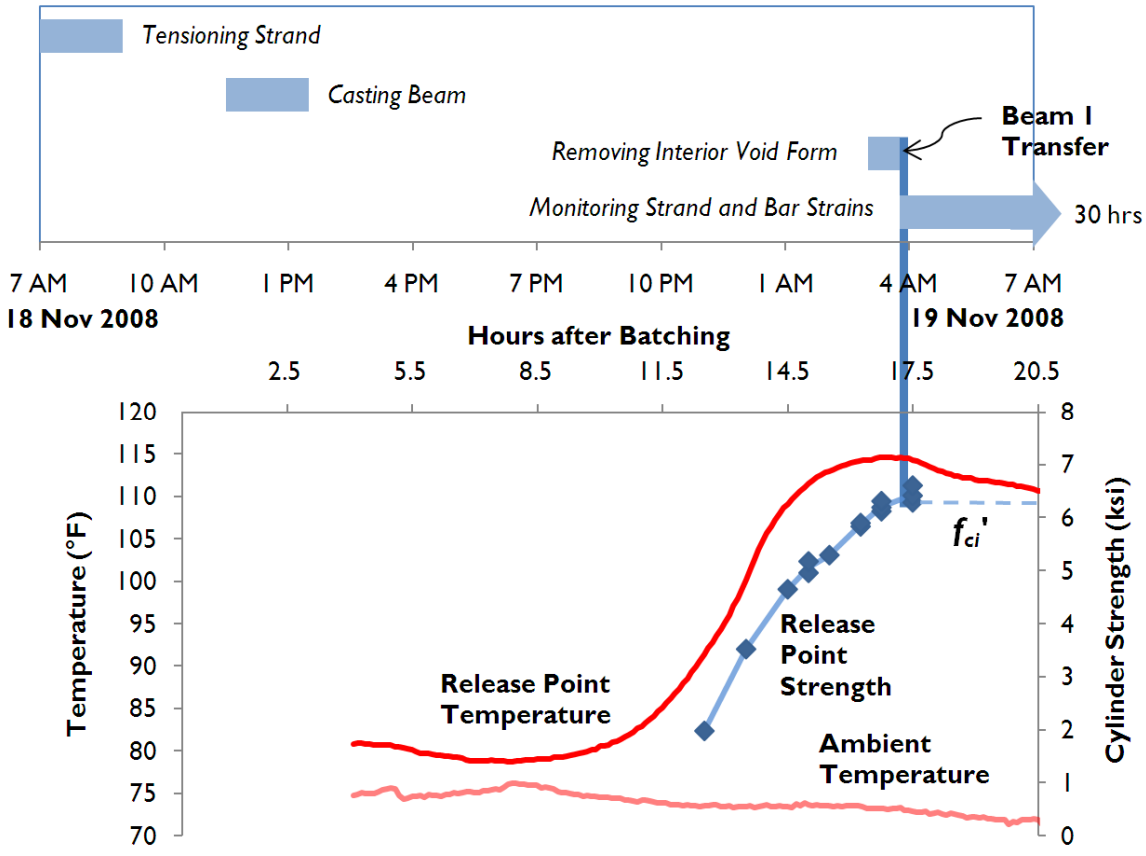

Figure 4.2 Beam 1 cast & release timeline with key events

The prestressing force for Beam 1 was measured by three methods (Table 4.1) with good correlation between the various measurements. The value of prestressing force used for subsequent calculations represents the mean of the measured values from methods (a) and (b), ram pressure and strand elongation, and was within 1% of the target value (Table 4.2).

Table 4.1 Beam 1 as-measured prestress

Method	**Prestress (ksi)**	**Deviation from (a)**
(a) Ram Pressure	196.9	—
(b) Strand Elongation	205.5	+ 4.4%
(c) Strain in Strands	190.8	- 3.1%

Table 4.2 Beam 1 applied prestressing force compared with target value

Method	**Prestress (ksi)**	**Prestressing Force (kip)**
Average of (a) and (b)	201.2	2401
Target	202.5	2417

The compressive strength of the cylinders match-cured to the release point was 6.4 ksi, or very nearly the target release strength (6.3 ksi). The bottom-fiber stress at transfer was $0.63f'_{ci}$.

Cracking occurred in the beam end regions (horizontal and diagonal cracks) and along the top edge of the beam (vertical cracks), immediately after prestress transfer. End-region cracks were typically hairline, with widths of 0.005 in. or less except at one location near the top flange/web junction at the skewed end (Location *1A* in Figure 4.3).

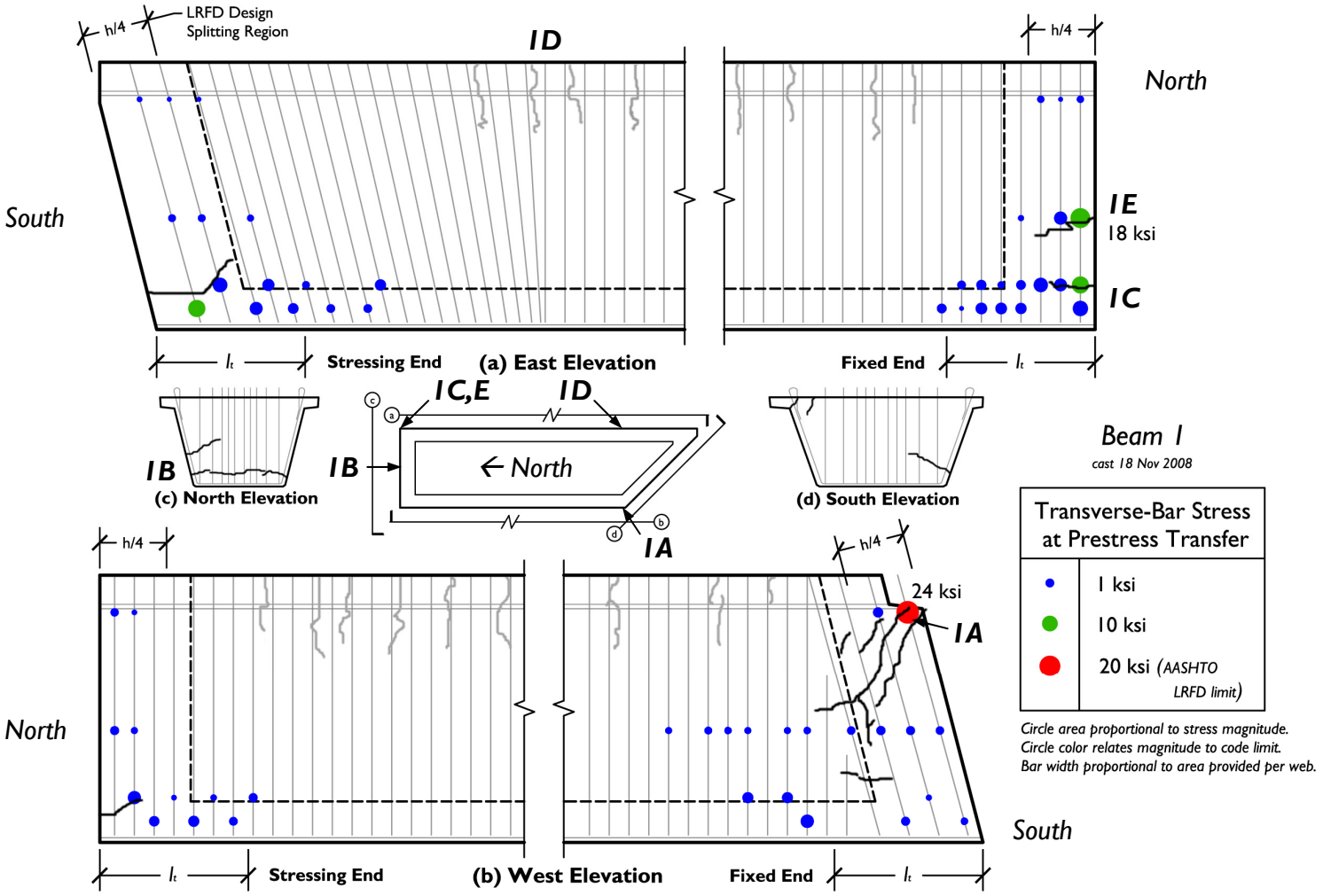

Figure 4.3 Beam 1 transverse-bar bursting & spalling stresses, with cracking from transfer

Horizontal cracks in both the bursting and spalling zone wrapped around the beam ends, and seemed to engage the end-block transverse reinforcement, especially at square end (Location *1B*). Flexural cracks from the top edge of the beam began 3 ft. from the beam end (outside the beam end region). These cracks were 0.025 in. in width or less, with most measuring 0.010 in.

4.2.2.2 Beam 1: Strand Stresses

At transfer, gages on prestressing strands recorded decreases in strain, from which, through multiplication by an experimentally determined modulus (determined through testing reported in Section 3.4.2), the prestress loss at instrumented sections can be inferred. Prestress losses are represented in Figure 4.4 by circle area.

Losses, subtracted from the initial prestress, give effective prestress. Within the transfer length, the effective prestress increases with distance into the beam. As the effective prestress stabilizes 30 in. into the beam (Figure 4.5), the experimentally determined transfer length matches the code value (30 in. for both the ACI 318 and AASHTO LRFD equations, as discussed in Section 3.2.1).

The prestress loss measured one transfer length into the beam can be taken as the prestress loss from beam elastic shortening. The average values at the stressing and fixed ends were similar (22 and 23 ksi, Figure 4.4) and comparable with the code-predicted value (25 ksi, reported in Appendix C). Past studies of prestress losses in Texas U-beams (Gross & Burns, 2000; Tadros et al., 2003) have similarly shown the elastic-shortening loss provisions to be accurate.

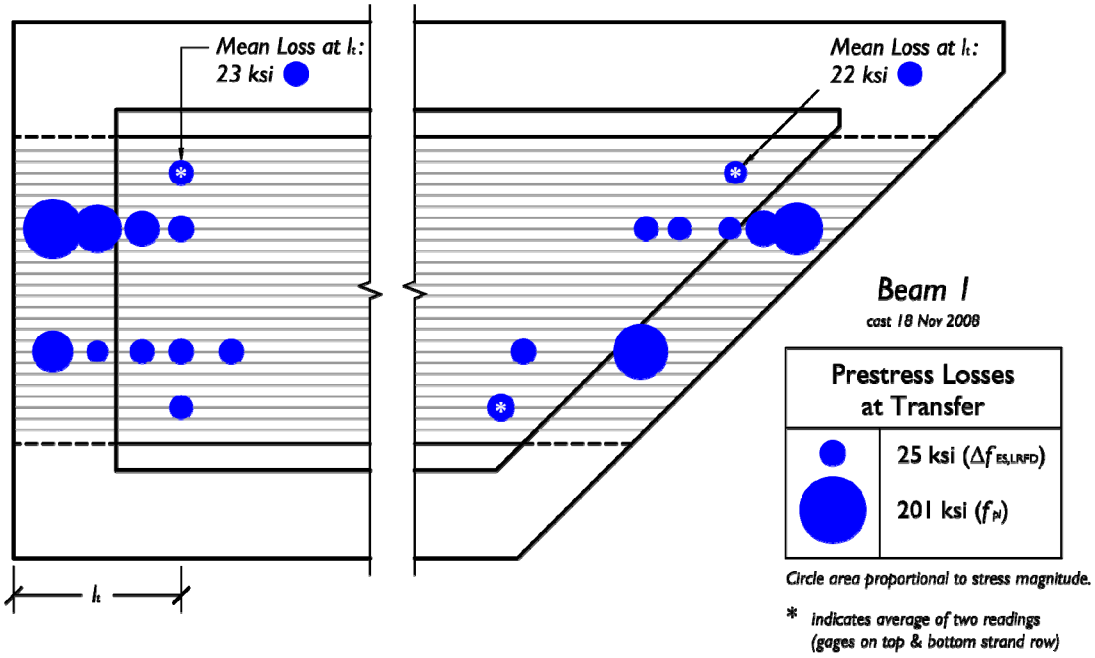

Figure 4.4 Beam 1 prestress losses in instrumented strands, after transfer

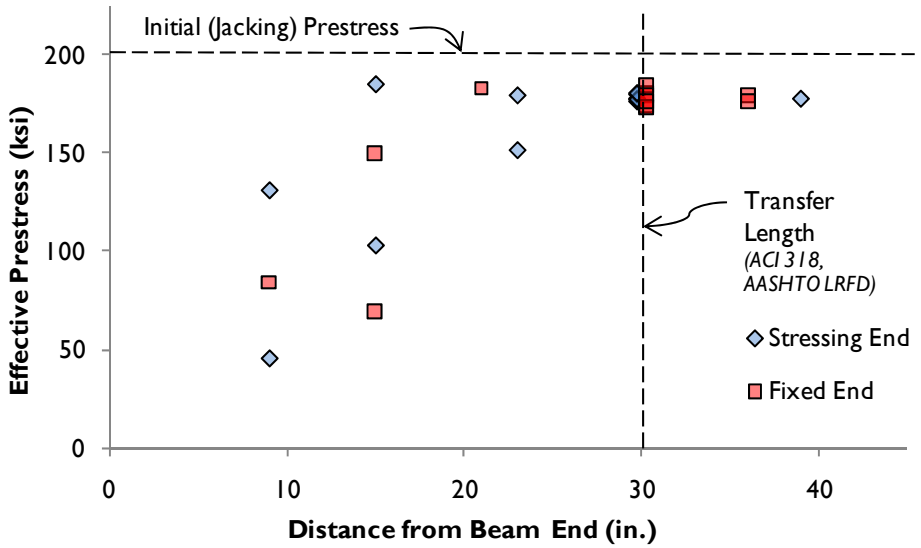

Figure 4.5 Beam 1 effective prestress & distance from beam end, after transfer

4.2.2.3 Beam 1: Transverse-Bar Bursting & Spalling Stresses

Bursting and spalling stresses in transverse reinforcement are shown in Figure 4.3. The circles in this figure represent stress values, and are superimposed on Beam 1 end-region elevations at the location of their associated strain gage. Circle area is proportional to the stress measurement; its color relates the stress measurement to the AASHTO design maximum, 20 ksi. Crack patterns from transfer are also shown on the beam elevation.

Measured stresses were low compared to the AASHTO limit in general. Transverse-bar stresses typically decreased with distance from the beam end, even in the bursting zone. Reasonable correlation can be seen between the presence of a visible crack and the measurement of moderate stresses (at least 8 ksi) or higher. Nevertheless, at some locations where cracking was noted, stresses were relatively low (e.g. Location *1C*, Figure 4.3).

For one gage located at the top flange/web junction (Location *1A*), stresses exceeded the AASHTO limit (thus is represented by a red dot in Figure 4.3). The high stress was measured adjacent to long, wide cracks (20 to 30 in., 0.020 in.). This cracking was exacerbated, if not caused, by the large skew. Across the beam width from this location (at Location *1D*), the prestressing force from the strands was fully transferred to the section: the provided bond length (90 in.) exceeded the transfer length by a factor of three. The cracks at the top flange/web junction extended from the top corner of the end block (at Location *1A*), then to run diagonally across the web.

The only other location where the measured transverse-bar stress approached the AASHTO limit was mid-depth at the square end of the beam (Location *1E*, Figure 4.3). By 1 hour after transfer, readings from this gage surpassed the 20-ksi limit stress. The

crack adjacent to this location was not notably wide or long, and seemed to engage multiple bars.

4.2.2.4 Beam 1: Lateral-Bar Bursting Stresses

Bursting stresses in lateral bars near the square end of the beam were typically less than 10 ksi in magnitude, as shown in Figure 4.6. In no cases did the lateral bursting stresses exceed the AASHTO limit (20 ksi).

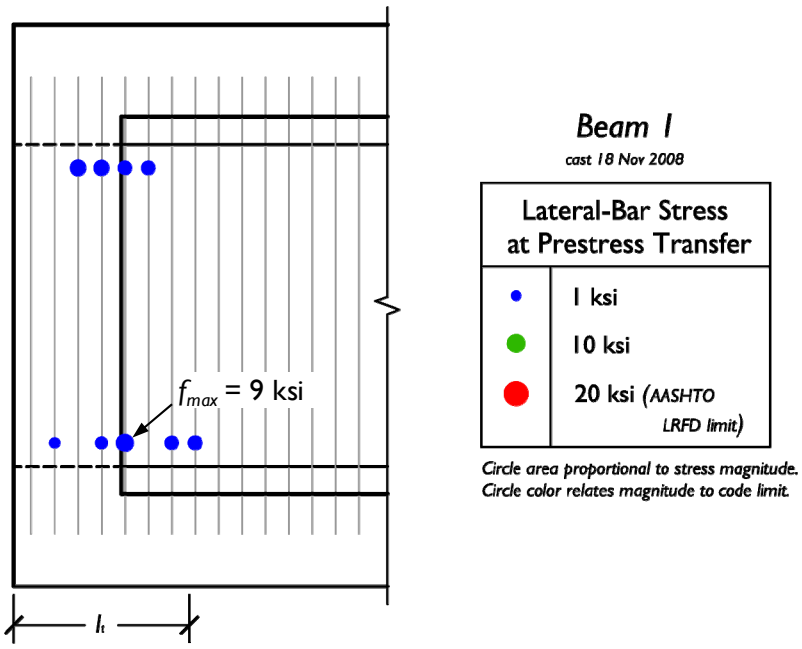

Figure 4.6 Beam 1 lateral-bar bursting stresses

An attempt was made to measure the lateral bursting stresses at the skewed end; however the strain gages, oriented at 45° to the strand, picked up a component of the prestressing force. This interpretation is supported by the observed increase in compressive strains with distance into the beam until the transfer length was reached. The prestressing force, then, was effective in suppressing any bursting effects that existed in the gage direction.

4.2.2.5 Beam 1: End-Block Temperature Profile

The temperature variation within the Beam 1 end blocks at the time of prestress transfer is represented by Figure 4.7. The figure was generated by linearly interpolating between measured temperature values (at thermocouples) with the ambient temperature imposed as a boundary condition a nominal distance from the beam edge. As the iso-temperature lines are based on an interpolative procedure, Figure 4.7 provides a *qualitative* indication of temperature between thermocouple locations (marked with crosses).

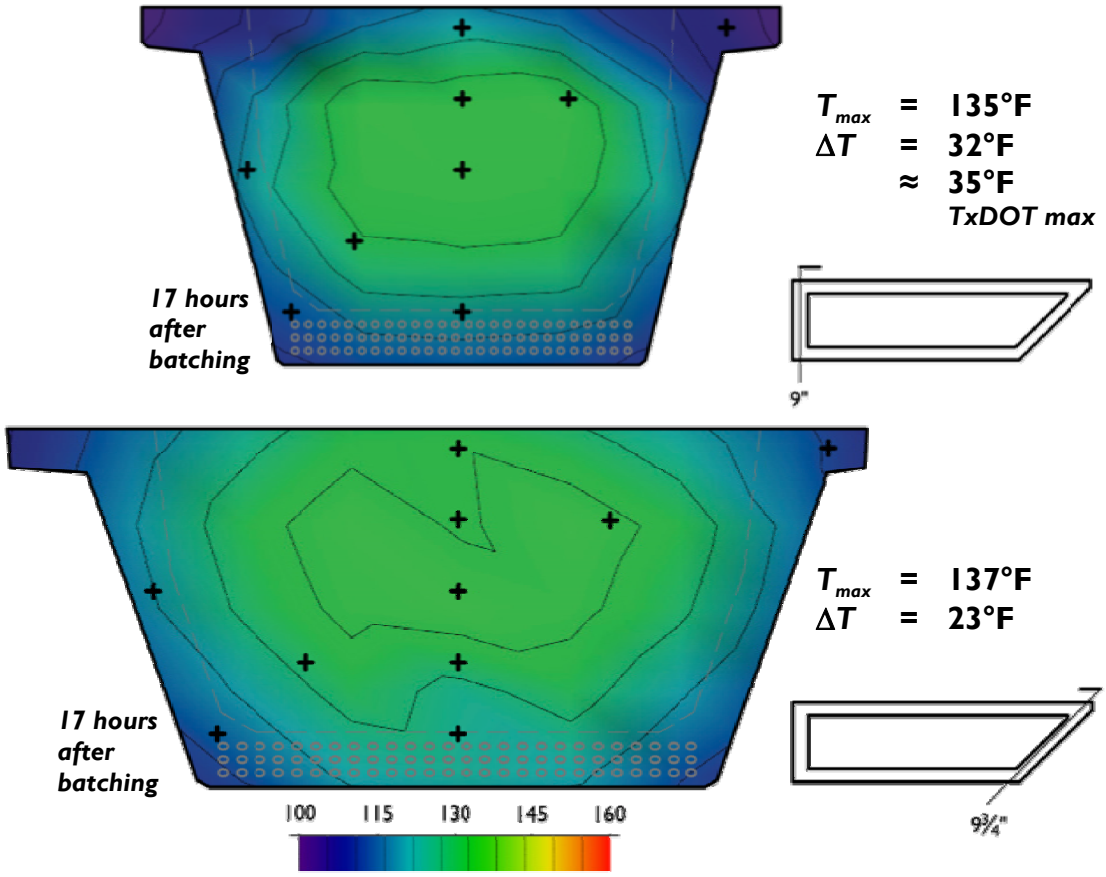

Figure 4.7 Beam 1 end-block temperature profiles, at transfer of prestress

The temperatures in the end blocks at transfer are relatively uniform near the section centroid. A temperature differential of 32°F exists, though, in the square end block (between the end-block-centroid and top-flange measurement locations). This temperature differential can be compared with the TxDOT maximum for mass concrete (35°F), though U-beam end blocks do not technically meet the definition for mass concrete (too small), as discussed in Section 2.7.1. Temperature profiles for all end blocks are compiled in Appendix E.

4.2.3 Beam 2 Results

Beam 2 was fabricated similarly to Beam 1, with the exception of the end-block detail used at the skewed end. The design alternative favored by Texas precasters (large triangular end block) was used in Beam 2.

4.2.3.1 Beam 2: Cast & Release

The cast and release of Beam 2 is summarized in Figure 4.8. It should be noted that though the two beams were cast three months apart, ambient temperatures were similar: 75 to 80°F (as shown in Figures 4.2 and 4.8).

The first portion of concrete batched (Truck 1) arrived at the laboratory with poor workability (3 in. slump). Water was added to the concrete (32 lb/cy) to achieve the target slump (9 in.), increasing the water-cement ratio slightly (from 0.33 to 0.38). No water was added to the other concrete (Truck 2) as it had sufficient workability. Truck 1 concrete was placed in the bottom flange and skewed end block; Truck 2 concrete was placed in the webs, square end block and top flanges.

The prestressing force for Beam 2, reported in Tables 4.3 and 4.4, was within 1% of the target value.

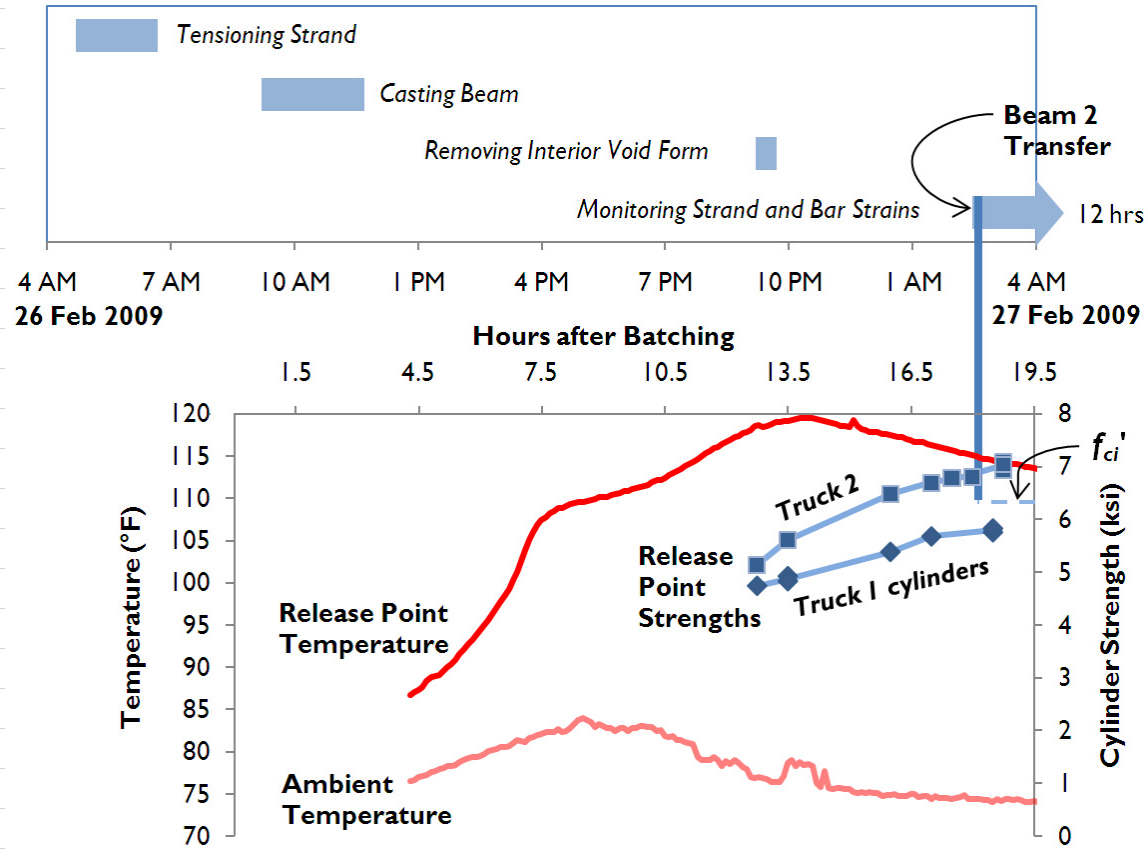

Figure 4.8 Beam 2 cast & release timeline with key events

Table 4.3 Beam 2 as-measured prestress

Method	Prestress (ksi)	Deviation from (a)
(a) Pressure at Rams	202.6	—
(b) Strand Elongation	205.8	+ 1.6%
(c) Strain in Strands	200.1	- 1.2%

Table 4.4 Beam 2 applied prestressing force compared with target value

Method	Prestress (ksi)	Prestressing Force (kip)
Average of (a) and (b)	204.2	2437
Target	202.5	2417

The beam was released when the average cylinder strength of the concretes from both trucks, match-cured to the release point, corresponded to the target release strength. Per standard TxDOT practice, the release-point thermocouple was placed at the bottom flange/web junction (Section 3.3.3), where the two concretes would have mixed during placement. The actual bottom-fiber stress active at transfer was $0.64f'_{ci}$.

As in Beam 1, horizontal and diagonal cracks formed in the beam end regions and vertical cracks formed along the top edge of the beam at transfer of prestress. Unique to Beam 2 were the diagonal cracks in the bursting zone, in the direction of shear stresses from beam self-weight (Location *2A* in Figure 4.9). End-region cracks were typically hairline except for one location near the top flange/web junction (Location *2B*), analogous to the location of wide cracking in Beam 1 (Location *1A* in Figure 4.3). Both bursting and spalling cracks wrapped around the beam ends like in Beam 1, particularly at the square end (Location *2C*). Flexural cracking, too, was similar to Beam 1.

4.2.3.2 Beam 2: Strand Stresses

Prestress losses and effective prestress for Beam 2 are shown in Figures 4.10 and 4.11. The elastic-shortening loss was determined to be slightly higher at the square end (29 ksi) than at the skewed end (22 ksi). The average of these two experimentally determined values corresponds well with the value predicted by AASHTO LRFD (25 ksi). The code transfer length (30 in.) was also verified.

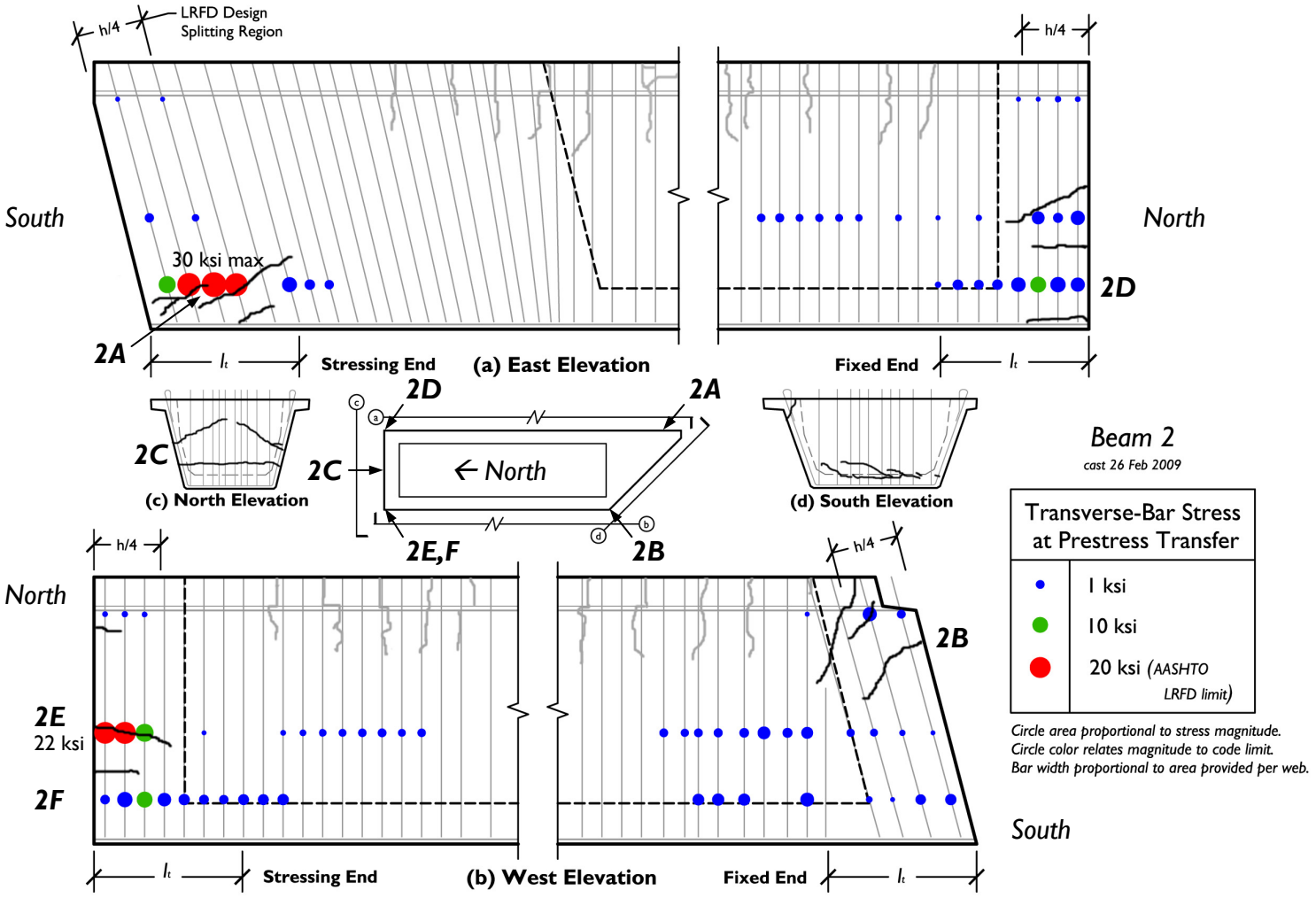

Figure 4.9 Beam 2 transverse-bar bursting & spalling stresses, with cracking from transfer

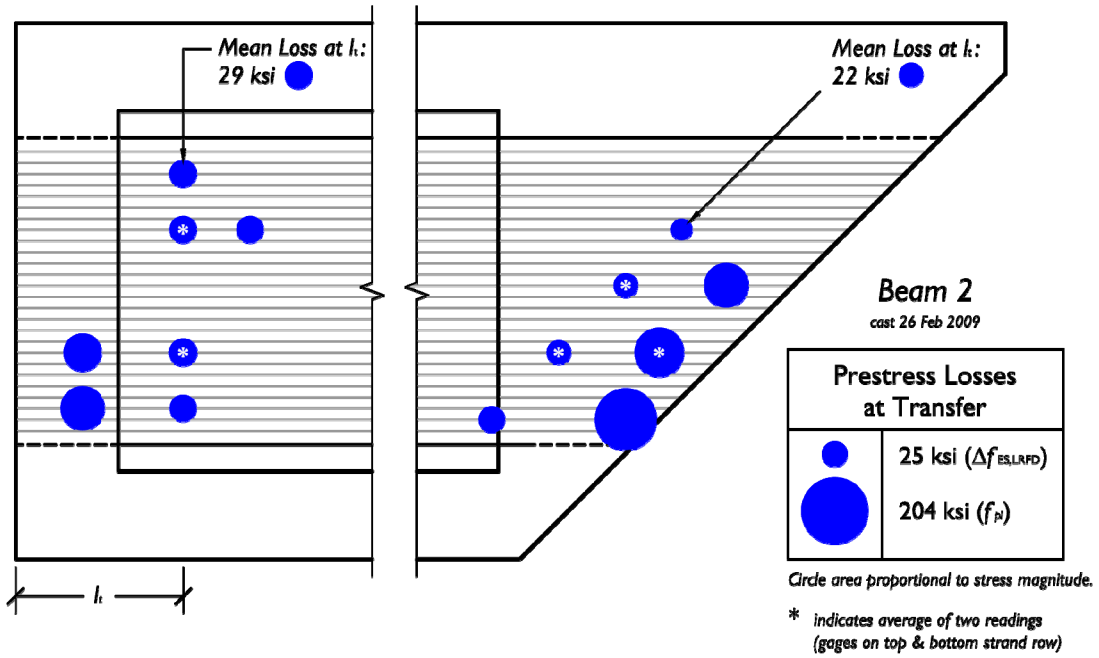

Figure 4.10 Beam 2 prestress losses in instrumented strands, after transfer

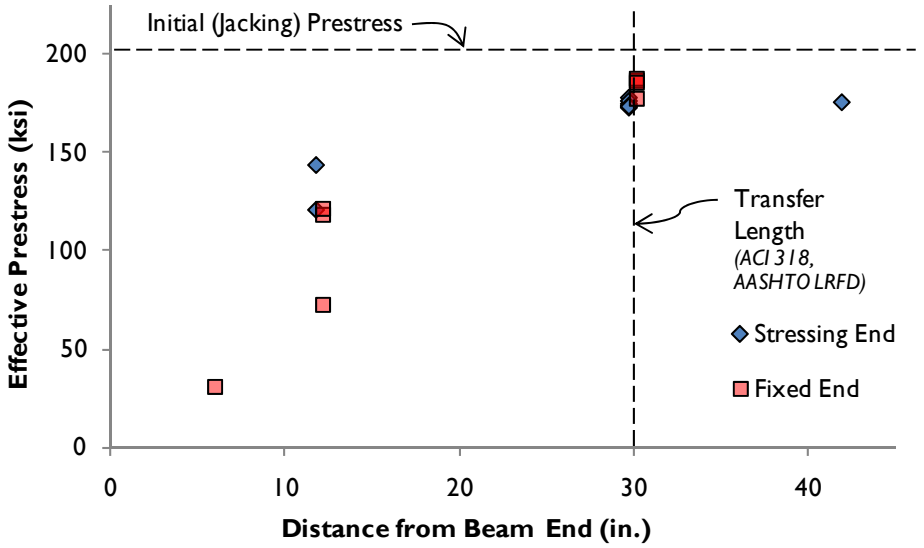

Figure 4.11 Beam 2 effective prestress & distance from beam end, after transfer

4.2.3.3 Beam 2: Transverse-Bar Bursting & Spalling Stresses

Bursting and spalling stresses in transverse reinforcement and crack patterns from transfer for Beam 2 are shown in Figure 4.9.

Measured stresses were somewhat higher than in Beam 1, but still low compared to the AASHTO limit (20 ksi) in general. Spalling-zone stresses decreased with distance from the beam end as observed in Beam 1. However, in three bursting zones of Beam 2 (Locations *2A, 2D* and *2E* in Figure 4.9), measured stresses peak at the third bar from the beam end. This behavior (stresses that reach their maximum some distance into the beam) is characteristic of bursting.

As for Beam 1, reasonable correlation exists between visible cracking and moderate to high stresses in reinforcement. In some locations (e.g. Location *2D*), cracks formed between lines of gages; there stresses in the transverse reinforcement closer to the cracks (than the instrumented locations) are expected to be higher than those measured.

The AASHTO stress limit was surpassed for multiple bars in both the spalling and bursting zones. Near mid-depth at the square end of the beam (Location *2F* in Figure 4.9), spalling stresses in the first two bars averaged 22 ksi (10% beyond the AASHTO limit). A crack 15 in. in length, but less than 0.005 in. in width, formed along the line of these strain gages.

More interesting is the location in which bursting stresses exceeded the AASHTO limit (Location *2A*). Here stresses peaked at 30 ksi, 50% past the code limit. Stresses dissipated to nominal levels by one transfer length (30 in.) into the beam. The adjacent cracks formed diagonally from the corner of the beam, in the same direction as shear cracks. It should be noted that these high bursting stresses were measured within the large triangular end block. Whatever beneficial effect that the large end block may have had in

terms of force distribution seems to have been trumped by the additional stresses from temperature, shrinkage and self-weight effects present at the time of prestress transfer.

4.2.3.4 Beam 2: Lateral-Bar Bursting Stresses

As in Beam 1, relatively constant lateral-bursting stresses were found (Figure 4.12), all below the AASHTO stress limit of 20 ksi. Limited cracking (hairline) on the underside of the beam along its length was noted.

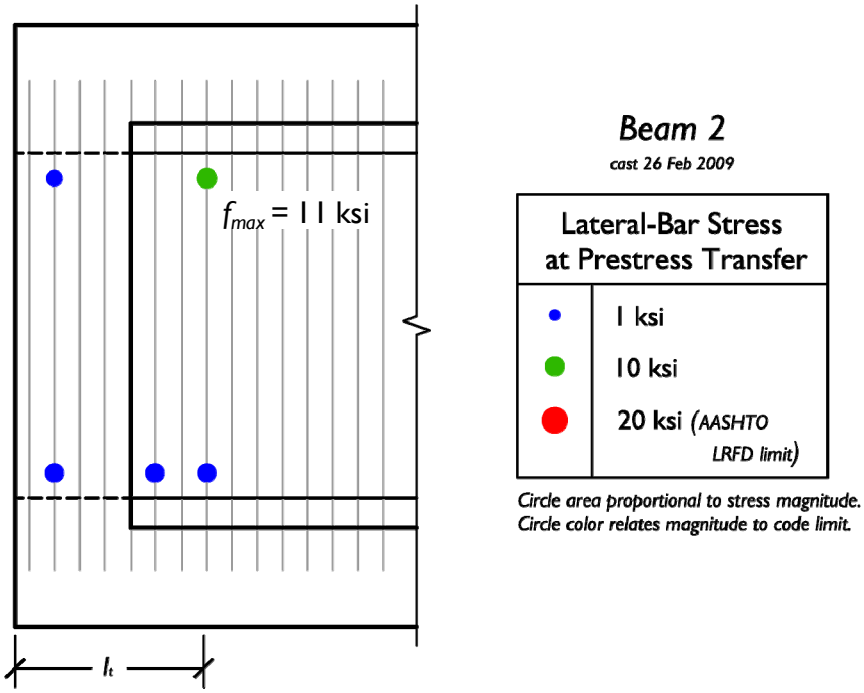

Figure 4.12 Beam 2 lateral-bar stresses

4.2.3.5 Beam 2: End-Block Temperature Profile

The large triangular end block at the skewed end of Beam 2 registered higher internal curing temperatures than the small skewed end block of Beam 1. The temperature profile (Figure 4.13) shows the center of the beam was very hot compared to

the outer edge. As noted in Section 4.2.2.5, this profile should be read qualitatively between temperature-measurement points.

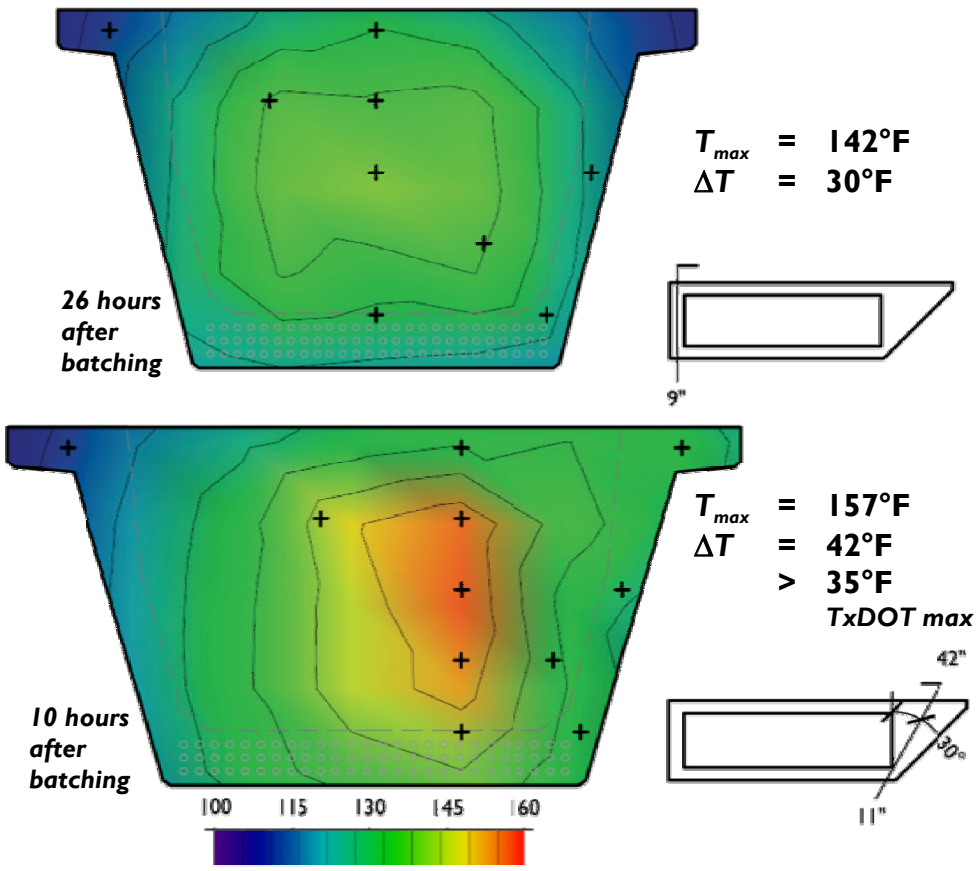

Figure 4.13 Beam 2 end-block temperature profiles, at transfer of prestress

The end-block-centroid ("hot spot") temperature was just below the threshold temperature for delayed ettringite formation (DEF), 160°F, at transfer of prestress. Figure 4.14 shows that the hot spot continued to increase in temperature after transfer, reaching the DEF threshold 6 hours after transfer. The TxDOT maximum allowable temperature in beams using concrete mixtures with no supplemental cementitious materials (SCMs), 150°F, was surpassed 4 hours before transfer. It should be noted that these temperature

limits were only exceeded at locations near the center of the large triangular end block; the maximum temperature at the release point was approximately 120°F.

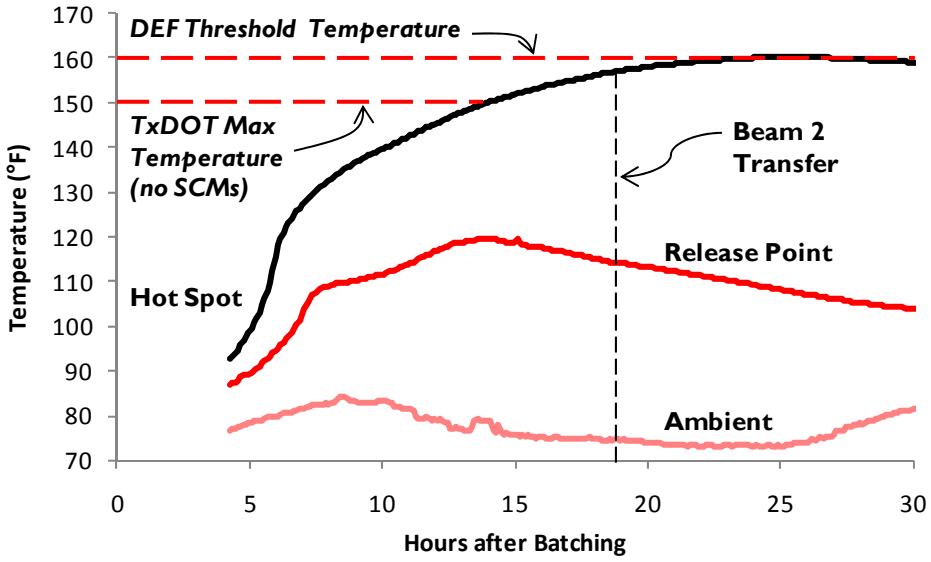

Figure 4.14 Temperature time variation with temperature limits (Beam 2)

The difference in internal temperature variation between the two end-block designs for the skewed end (small skewed in Beam 1; large triangular in Beam 2) can be seen best by examining temperature profiles not at prestress transfer, but rather at the time when the internal temperature differential reached its maximum (Figure 4.15).

For Beam 1, this time was 8 hours after transfer. The temperature within the beam was relatively uniform, but the top and bottom corners were approximately 30°F cooler than the end-block centroid. For Beam 2, the maximum temperature differential came 8 hours *before* transfer. Concrete near the centroid of the large triangular end block had clearly begun hydration—its temperature had surpassed 140°F—some hours ahead of the concrete near the beam exterior surface (just above the ambient temperature). The 55°F

temperature differential observed in Beam 2 greatly exceeded the 35°F allowable temperature differential for mass concrete.

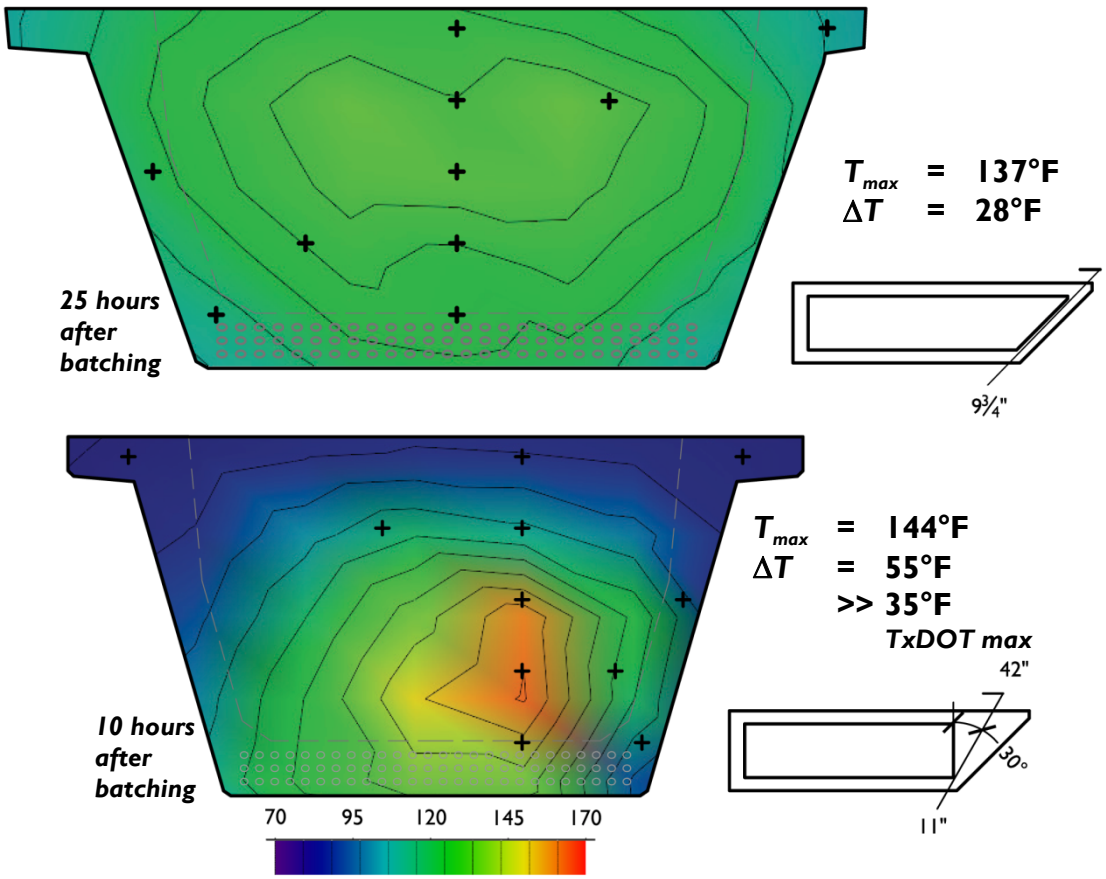

Figure 4.15 Temperature profiles for two end-block alternatives for skewed ends at time of maximum temperature differential (Beams 1 & 2)

4.3 DATABASE OF BURSTING & SPALLING STRESSES IN TRANSVERSE BARS OF PRETENSIONED BEAM END REGIONS

In order to place the findings of the present study in context, it was helpful to view data from Beams 1 and 2 alongside those from past studies in which bursting and

spalling stresses were measured in transverse reinforcing bars within the end regions of pretensioned concrete beams.

4.3.1 Studies of Bursting & Spalling

Past studies included in the transverse-bar bursting and spalling stress database, previously discussed in Section 2.4.2, are listed in Table 4.5.

Table 4.5 Specimens examined in past studies of bursting and/or spalling stresses

Source	Year	End-Region Type	Number of Strain-Gage Lines
Marshall & Mattock	1962	14 I-beams	Single
Itani & Galbraith	1986	3 I-beams	Multiple (3 or 4)
Tuan et al. *	2004	18 I- and 8 IT-beams	Single
Crispino	2007	2 I-beams	Multiple (4)
O'Callaghan	2007	8 I-beams	Multiple (3 or 4)

* *For additional information on the layout of transverse reinforcement in these specimens, Tadros, Yehia and Jongpitaksseel (2003) was consulted.*

While all these studies investigated stresses in transverse reinforcement at transfer of prestress, they did so by slightly different methods. Notable among the methodological differences is the number of distinct strain-gage lines (along the beam length) used within the end region. In the case of beam end regions instrumented with all their strain gages in a single line, in order for the maximum transverse stress to be measured, a researcher would need to know *a priori* the maximum-width crack locations in a pretensioned beam specimen. When the inherent randomness of cracking in concrete is considered, it becomes clear that the use of multiple lines of strain gages is more likely to yield higher measurements of stress. The additional gages do not induce high stresses, but rather allow for their measurement.

Most studies of transverse-bar stresses at transfer have been conducted using a single strain-gage line per specimen; these studies focused on spalling behavior. Studies examining bursting behavior have also included strain gages in the spalling zone. As such, a disparity exists between the database size for spalling and bursting behavior, as shown in Figure 4.16. Spalling behavior was measured for each beam end region included in the database (57), bursting behavior for 30% of them (17 of 57 end regions).

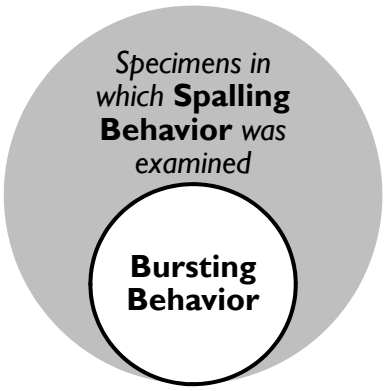

Figure 4.16 Proportion of database in which bursting & spalling behaviors were examined

Because of differences between studies and randomness in material properties, high variation is expected between specimens. The primary purpose of the database is to examine general trends in behavior, to assess the conservatism of existing design equations rather than develop new ones.

4.3.2 Assembly of Database

For specimens in the literature, section properties, material properties and prestressing strand patterns were readily available. From these properties, the top- and bottom-fiber stresses at prestress transfer could be determined. The transverse reinforcement layout was also inputted in the database. For the U-beam specimens, all

transverse reinforcement contained within end blocks was considered. As shown in Figure 4.17, end-block transverse reinforcement consisted of vertical bars within the projected area of the void, and angled bars within the projected area of the webs.

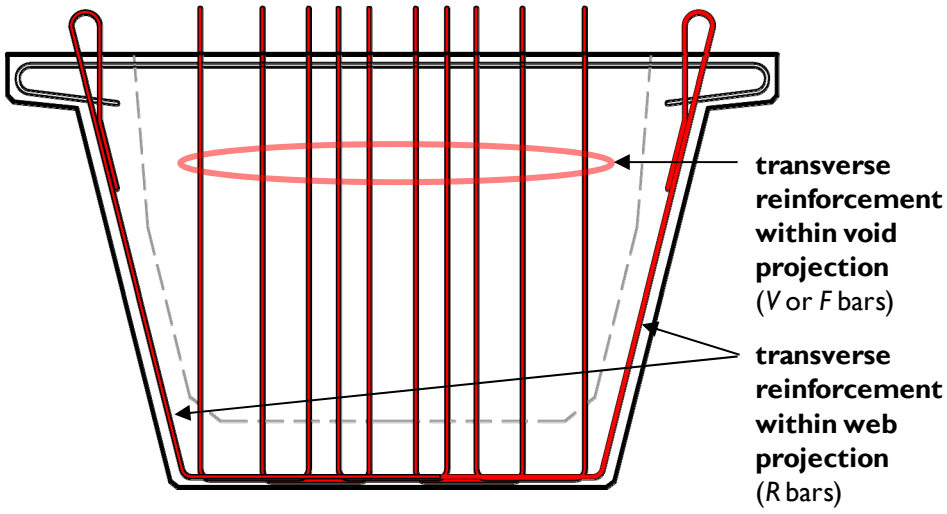

Figure 4.17 Transverse reinforcement within the U-beam end block

Transverse-bar bursting/spalling strain variation was available for 45 of the 57 beam end regions in the database; for the others—all from Marshall & Mattock (1962)—only the total bursting/spalling force was available. The transverse-bar strain data was converted to bursting and spalling stresses assuming a nominal elastic modulus (29,000 ksi) for the reinforcing bar.

Bursting and spalling stresses for these 45 beam end regions are summarized in figures similar to Figure 4.3 and Figure 4.9, showing stresses in transverse reinforcement at transfer as well as crack patterns. These figures are collected in Appendix A.

Not every end-region bar was instrumented for most studies, so stresses were interpolated linearly between locations of measurement. In the case of studies in which strains were reported from multiple gage lines (e.g. strain gages in both the bursting and

spalling zones), linear interpolation was performed independently for each line of strain gages. The maximum measured stress per bar was used to compute the total bursting/spalling force for each beam end region. In addition, the maximum measured bursting or spalling stress in each end region was noted.

4.3.3 Total Bursting/Spalling Force in the Beam End Regions

As every beam included in the database were instrumented to a distance $h/4$ from the beam end, the total transverse-bar bursting/spalling force summed within the region extending to $h/4$ could be computed without incurring error from extrapolation. This end-region length corresponds to that considered in AASHTO LRFD design. Figure 4.18 shows the total bursting/spalling force within $h/4$ as a function of the prestressing force applied at the beam end.

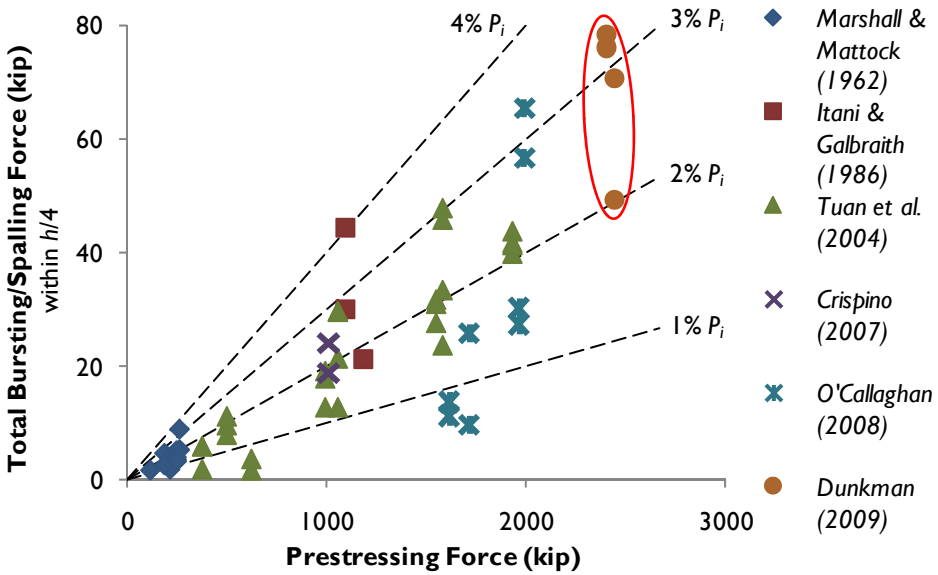

Figure 4.18 Total transverse-bar bursting/spalling force & prestressing force
(U-beam specimens circled)

Based on Figure 4.18, the 4% P_i design "splitting" force assumed by AASHTO LRFD appears to be a conservative limit on the transverse force actually imparted on an end region at transfer of prestress. Approximately 90% of instrumented beam end regions (51 of 57) were subject to bursting/spalling forces of less than 3% P_i at transfer. Beam section geometry may play a slight influence on the total bursting/spalling force (Figure 4.19), but the limited number of non-I-beam specimens prevents stronger conclusions from being made.

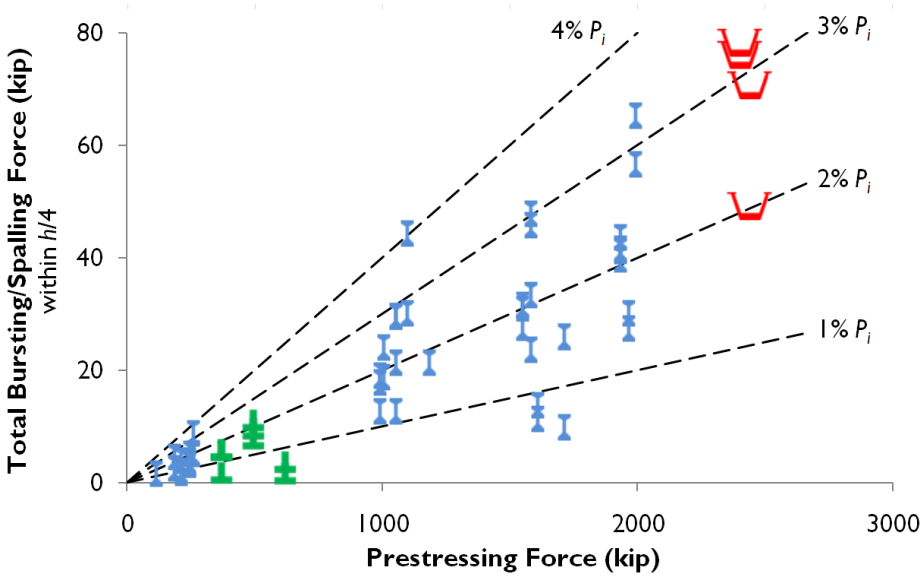

Figure 4.19 Total transverse-bar bursting/spalling force & prestressing force, with section geometry for beam end-region specimens emphasized

Figure 4.19 shows U-beams subject to moderate to high transverse forces at transfer of prestress, compared to the other specimens in the database. The moderate to high bursting/spalling forces match up with the multiple instances of bursting or spalling stresses significantly beyond the AASHTO limit (up to 50% beyond).

It should be noted, however, that the total transverse-bar bursting/spalling force is a measure of the *average* bursting/spalling stress in the transverse reinforcement

multiplied by the provided area, and thus gives no indication of the *maximum* bursting/spalling stress in a given end region. Low bursting/spalling forces could mean either low average stresses in reinforcement (good end-region behavior) or insufficient reinforcement coupled with high average stresses (poor behavior).

4.3.4 Maximum & Average Bursting/Spalling Stresses in Beam End Regions

As noted previously (Section 2.4.2.1), measured stress in reinforcement correlates with crack width. Crack width serves as the primary criterion by which DOTs accept a pretensioned concrete beam (acceptance criteria discussed in Section 2.5.3). While such criteria may not specify whether they are to be applied to a maximum or average crack width, it is reasonable that a pretensioned-beam inspector, after measuring a high maximum crack width, would be concerned with other items than recording measurements along the less-wide portions of the crack and computing an average width. Since *maximum* crack widths are then likely used most often to gauge behavior in the precast plants, *maximum* bursting/spalling stresses measured by strain gages on transverse bars may be used to evaluate the behavior of a given end region.

It is appropriate to compare the magnitude of both maximum and average transverse-bar bursting and spalling stresses with the AASHTO stress limit of 20 ksi. This stress limit, it should be noted, serves as both the maximum and average allowable stress for the transverse reinforcement. The uniform stress variation assumed by AASHTO LRFD for transverse bars is not always seen in actual beams, though. Typical spalling behavior, for example, consists of a non-uniform transverse-bar stress variation: one that decreases linearly with distance from the beam end (Marshall & Mattock, 1962).

Uniform and linearly-decreasing transverse-bar stress variations carry with them different maximum-to-average stress ratios within the end-region length considered:

- 1:1 for a uniform stress (depicted in Figure 4.20-a)
- 2:1 for a linearly decreasing stress (Figure 4.20-b)

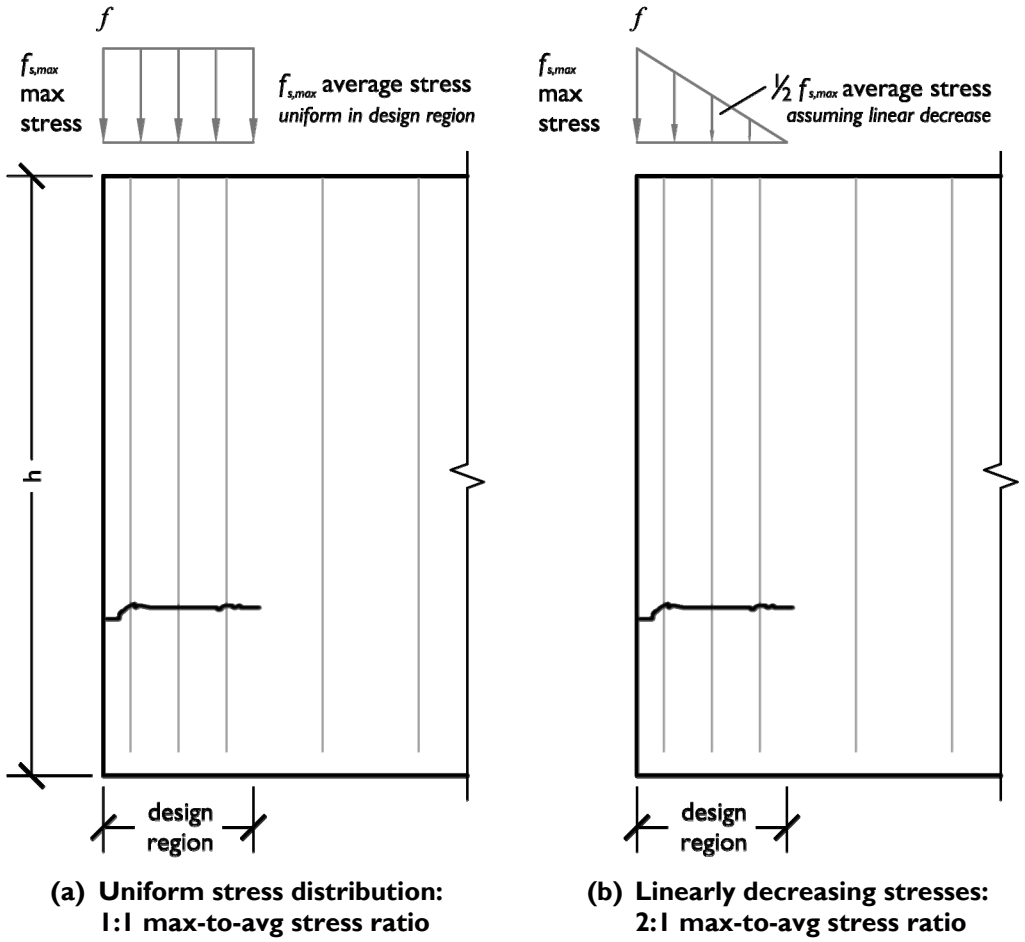

Figure 4.20 Assumed end-region transverse-bar stress distributions & associated maximum-to-average stress ratios

Figure 4.21 shows the maximum bursting/spalling stress in each beam end region compared with their average stress (within the *h*/4 region). The average stress in the

transverse reinforcement can be calculated readily from the total transverse-bar bursting/spalling force, shown previously in Figures 4.18 and 4.19.

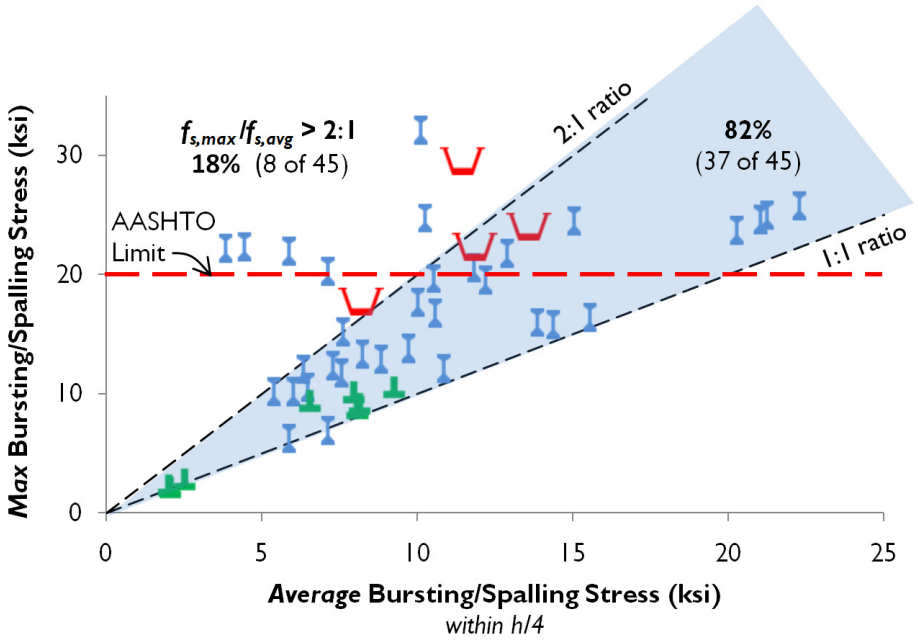

Figure 4.21 Maximum transverse-bar bursting/spalling stress compared with average within h/4 design region

It can be seen that most specimens (82% of beam end regions), regardless of their cross section, lie between the lines defined by 1:1 and 2:1 maximum-to-average stress ratios. The uniform transverse-bar stress variation (1:1 stress ratio) is clearly a design idealization: approached by a few specimens, but not generally the case.

A parallel can be drawn between these measured reinforcement stresses and crack width data. The maximum-to-average crack-width ratio assumed by the CEB-FIP Model Code (1978) is 1.7, which compares favorably with the median maximum-to-average stress ratio in transverse reinforcement, 1.6.

4.3.5 Contributing Factors to High Maximum Bursting/Spalling Stress

Four factors were found to weigh heavily toward high maximum transverse-bar bursting/spalling stresses: average bursting/spalling stress in transverse reinforcement; amount of transverse reinforcement; bottom-fiber stress near beam end; and prestressing-strand type.

First, revisiting Figure 4.21, it can be seen that higher average stresses in transverse reinforcement are correlated with high stress maxima. Figure 4.22 shows that most specimens (60%) with average bursting/spalling stresses greater than 10 ksi had maximum bursting/spalling stresses that exceeded the 20-ksi AASHTO limit. Less than 20% of those with average stresses less than 10 ksi exceeded the stress limit. Three of the four U-beam end regions were subject to average bursting/spalling stresses of greater than 10 ksi; the same three end regions had maximum stresses exceeding 20 ksi.

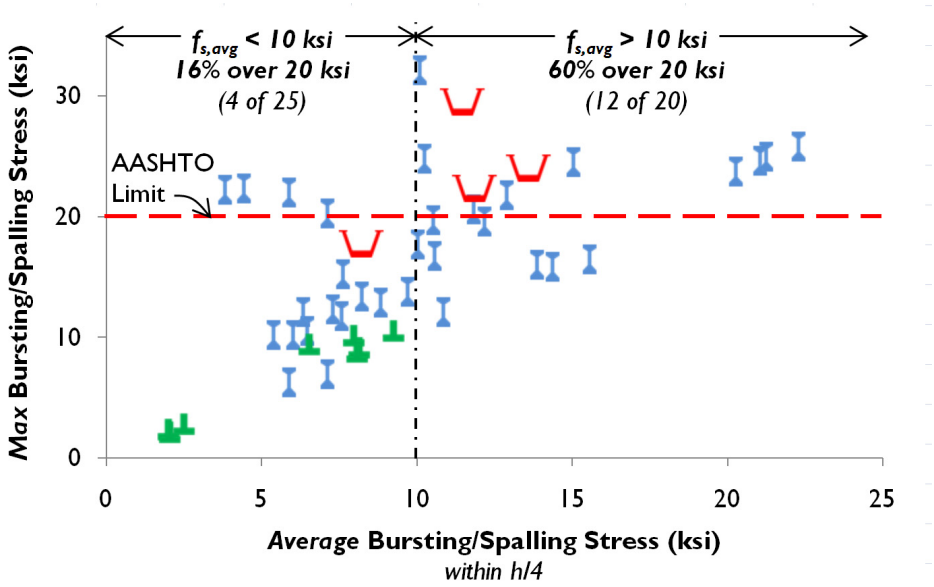

Figure 4.22 Contribution of high average bursting/spalling stress in transverse reinforcement to high maximum bursting/spalling stress

The amount of transverse reinforcement provided in an end region was also found to influence maximum transverse-bar stresses at transfer of prestress. The specimens in the database were split between those meeting and those not meeting the AASHTO LRFD requirement for transverse reinforcement within the *h*/4 design length. Half of beams not meeting the code requirement had a maximum bursting/spalling stress exceeding the 20-ksi limit; a quarter of those meeting the code exceeded the limit (Figure 4.23).

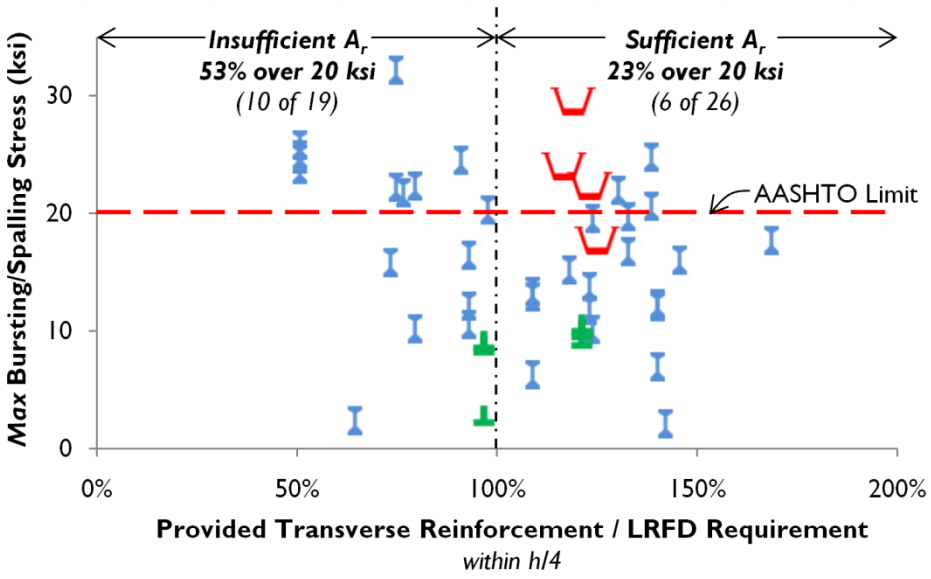

Figure 4.23 Contribution of reinforcement provided within end h/4 region
(normalized by that required by AASHTO LRFD)
to high maximum transverse-bar bursting/spalling stress

The effect of bottom-fiber stress on maximum transverse-bar bursting/spalling stress appears to be quite strong (Figure 4.24), but is moderated by the fact that approximately 60% (8 of 14) of the specimens subject to high sectional stresses also had LRFD-insufficient transverse reinforcement in their end-regions. Still nearly 80% of specimens with bottom-fiber stresses greater than 3.6 ksi (i.e. 60% allowable compressive

stress ratio multiplied by a typical release strength, 5 ksi) exceed the AASHTO stress limit, while less than 10% of those with lower bottom-fiber stresses exceed the limit.

Read another way, Figure 4.24 is instructive to future research efforts. Beams subject to low bottom-fiber stresses are relatively insensitive to quantity of provided transverse reinforcement in the end region. If the purpose of an experimental program is to develop a prescription for an adequate amount of end-region reinforcement for a particular beam, beam specimens should be tested subject to high bottom-fiber stresses. The bottom-fiber stress applied to the U-beam specimens, 4.0 ksi, appears adequate for these purposes.

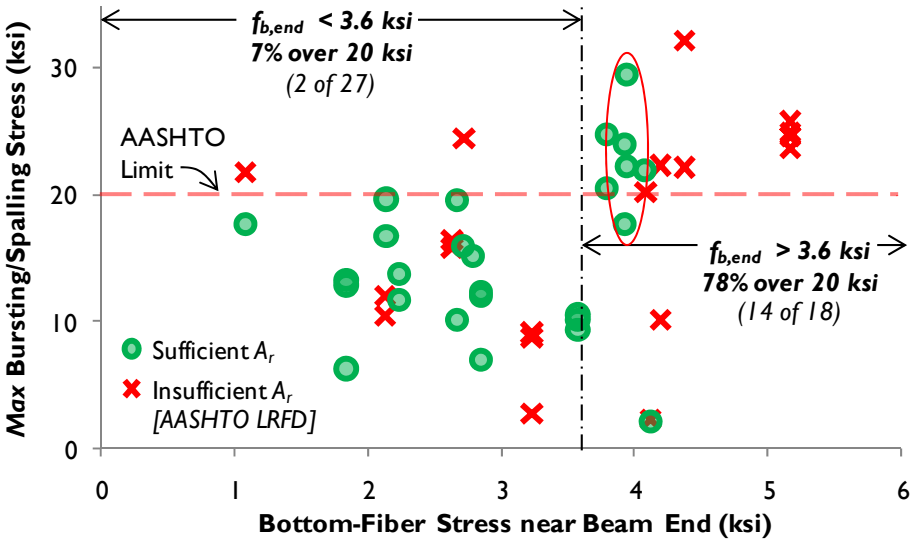

Figure 4.24 Contribution of bottom-fiber stress near beam end to high maximum transverse-bar bursting or spalling stress
(U-beam specimens circled)

Lastly strand type has some influence on maximum transverse-bar bursting or spalling stress: over 50% of specimens using 0.6-in. strand (11 of 20 beam end regions)

exceeded the AASHTO stress limit, compared to roughly 20% of those with 0.5-in. strand (5 of 23).

It should be noted that two of these factors identified in this section to contribute to high maximum bursting/spalling stress, inadequate transverse reinforcement and large strand diameter, were listed as causes of cracking in a recent survey of bridge design and construction professionals (Table 2.4).

4.3.6 Evaluation of AASHTO LRFD & PCI Design Equations

Though the design equations for transverse end-region reinforcement in AASHTO LRFD and the PCI Design Handbook were likely based on the same source (Marshall & Mattock, 1962), they have slightly different formulations. The equation in AASHTO LRFD sets the design transverse force proportional to prestressing force, while that of PCI sets the design force proportional to the prestressing force *divided by* the height-to-transfer length ratio [$P_r/(h/l_t)$]. Linear regression conducted on these two design models (Figure 4.25 and Figure 4.26) yielded similar correlation, indicating that neither is significantly better for design purposes. Such a conclusion runs counter to viewpoints expressed by Tuan et al. (2004), and is adequate justification the continued use of the simpler AASHTO LRFD design equation.

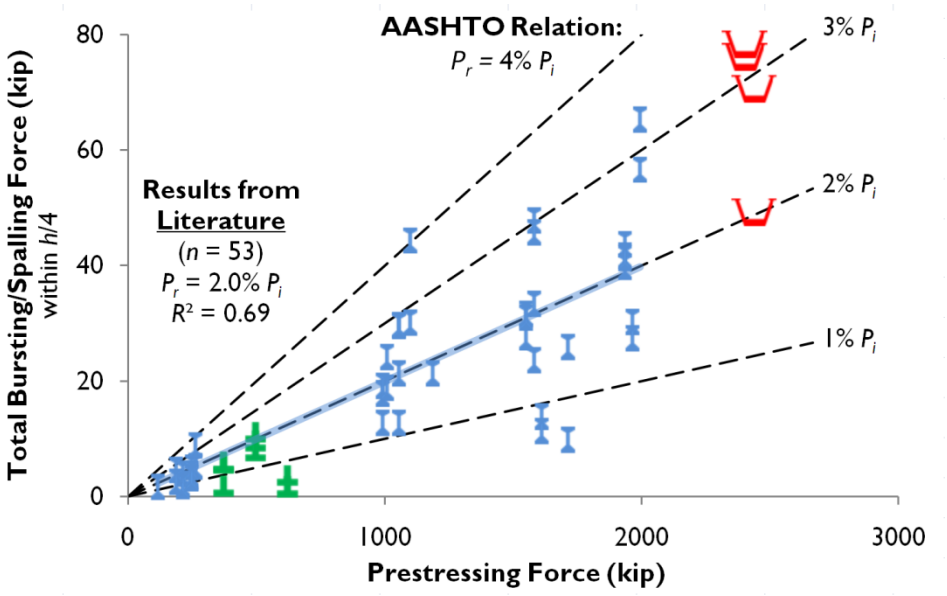

Figure 4.25 Relation between total transverse force & prestressing force [AASHTO LRFD]

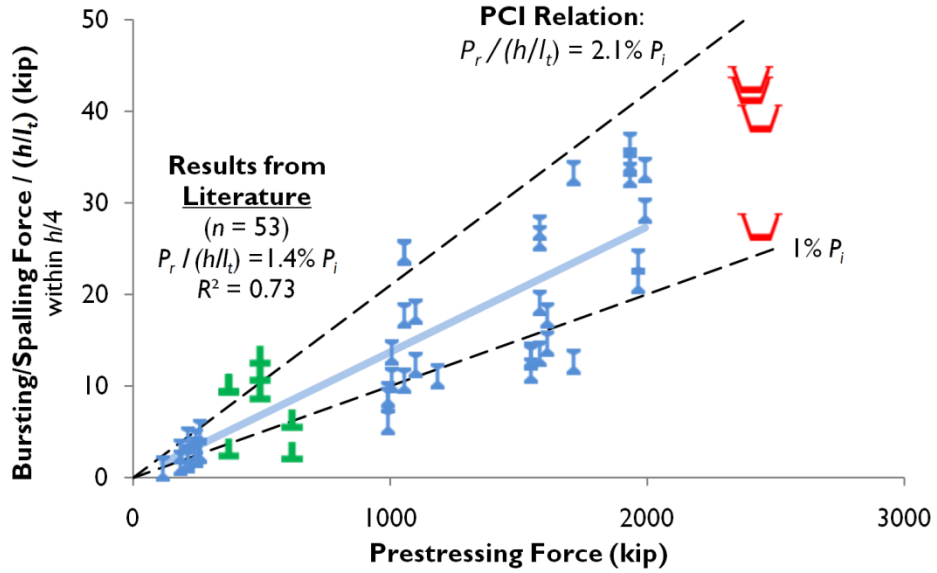

Figure 4.26 Relation between total transverse force, divided by beam height-to-transfer-length ratio, & prestressing force [PCI]

4.3.7 Concluding Remarks on Database Analysis

As mentioned previously, for the majority of beam end regions studied (40 of 57), spalling behavior was examined without adequate instrumentation to assess bursting behavior. Discussion above focused on the LRFD end region (the end $h/4$ of a beam), rather than distances further into the beam in which bursting stresses reach their maximum. That the transverse-reinforcement design procedure stipulated in AASHTO LRFD tends to keep maximum bursting and spalling stresses below 20 ksi should not be interpreted as an indication that the AASHTO-provided reinforcement is all that is required for good end-region behavior. Crispino (2007) and O'Callaghan (2007) have both identified the need for reinforcement outside the $h/4$ region in bulb tees: the former due to spalling behavior, and the latter due to bursting behavior. Unfortunately, at this time, too few studies have examined transverse-bar stresses sufficiently further into the beam to provide for a reasonable meta-analysis of bursting behavior.

Lastly, it should be noted that the assumption of a 20-ksi average stress for transverse reinforcement is inappropriate if a single instance of a transverse-bar stress exceeding 20 ksi is intolerable for crack-control reasons. If, however, the 20-ksi limit was set primarily in consideration of average reinforcement stresses and average crack widths, then exceeding the stress limit in limited circumstances (e.g. for one bar in a highly stressed end region) may be considered acceptable performance by some engineers.

4.4 RECOMMENDATIONS

Based on the experimental results for the two U-beam specimens viewed in light of the literature, recommendations for the U-beam bursting and spalling reinforcement are made in this section.

4.4.1 Recommended Texas U-Beam Reinforcing Details for Testing

One of the tasks in TxDOT Research Project 5831 was to recommend better end-region reinforcement details and to test these new details, as discussed in Section 1.1. As the project is only partly complete (Year 2 of 5), the details here recommended are of a preliminary nature and may undergo changes as testing continues in the coming months.

The high transverse-bar stresses measured in both the bursting (Beam 2) and spalling zones (Beams 1 and 2), coupled with the inadequate web reinforcement compared to other DOT standards, lead to the recommendation to provide additional transverse reinforcement in the U-beam standard design. The addition of this reinforcement would help to control cracking at transfer of prestress, and could improve shear performance.

An end-region detail presently under consideration is shown in Figure 4.27. The two main components of this detail are additional transverse reinforcement, bundled with the existing steel and installed at the interior face of the web; and thickened webs in the end region. While the web would be thickened primarily for shear purposes, the additional concrete could decrease average transverse-bar stresses slightly by carrying a portion of the transverse stress between cracks.

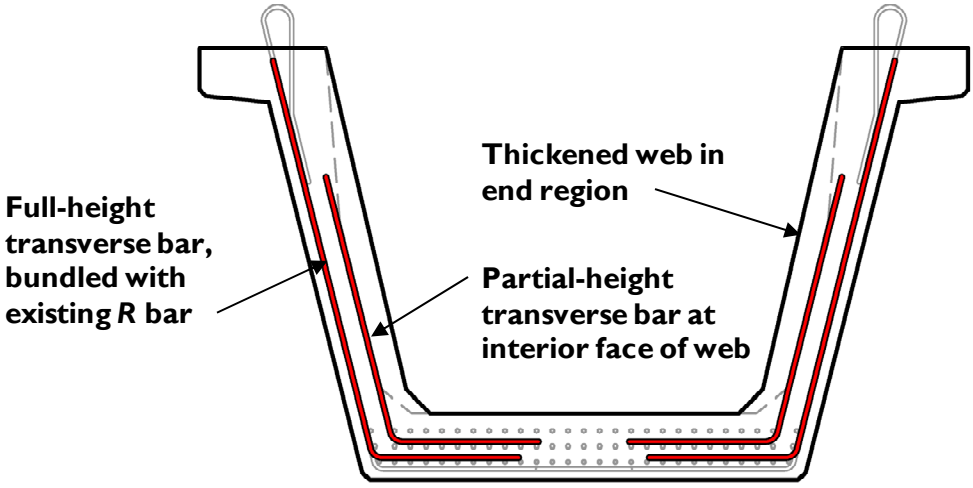

Figure 4.27 Proposed end-region detail (cross-section)

The additional steel should be extended through the spalling zone (near the beam end) into the bursting zone, as shown in Figure 4.28. While the maximum bursting stresses were measured closer to 20 in. into the beam (two-thirds of the transfer length for these specimens), it is conservatively recommended to extend the supplemental reinforcement out to one transfer length from the beam end. As 0.6-in strand is the largest commonly used in Texas beams, it would be safe to use 36 in. as the end-reinforcing zone based on bursting and spalling considerations. Shear demands, however, may require the special detailing to be extended further into the beam.

Lateral end-region reinforcement in the bottom flange, though substantially less than that required by AASHTO LRFD (Section 2.7.1), was not observed to experience high stresses, nor was severe longitudinal cracking noted in the bottom flange. As such, no supplemental lateral reinforcement is recommended based on bursting and spalling considerations.

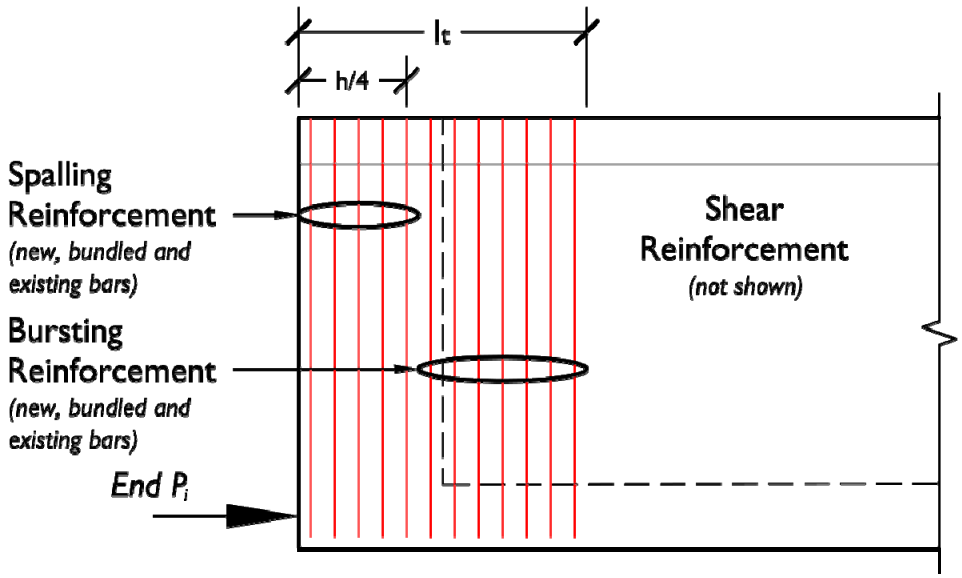

Figure 4.28 Proposed end-region detail (elevation)

Though two end-block designs were tested (large triangular or small skewed end block) for skewed ends, no trend in the measured bursting and spalling stresses could be linked to the end-block design chosen. Neither end block seems to provide superior performance at transfer.

4.4.2 Special Considerations for Bursting Reinforcement

One method presently employed by TxDOT to control transverse cracking (as well as meet stress checks) is selective debonding of prestressing strands. This practice merits discussion as it relates to design of transverse reinforcement and shear capacity. Debonding decreases the transverse force near the beam end by decreasing the prestressing force there applied. Willis (1963) indicated that debonding has been common practice to control cracking in Texas beams since the early 1960s. It is sometimes performed empirically at the fabricator's discretion: if a pretensioned concrete beam shows end-region cracking necessitating repairs, subsequent beams of similar design

(e.g. others for the same project) would have some (or more) strands debonded at the beam end.

TxDOT design specifications permit up to 75% debonding at the beam end, though fewer strands are typically debonded in U-beams (20 to 40%). While debonding may improve end-region serviceability, it is done to the detriment of shear strength. Under shear loading, bonded prestressing strands work as a tension tie near supports: the fewer bonded strands provided, the less the tie capacity.

As presently directed on the standard drawings, debonding in U-beams proceeds from the outermost strands inward, skipping adjacent strands. This order makes sense in I-beams, in which the strands near the center are both in the web and above the bearing pad. The last strands to be debonded in this out-to-in pattern are those most crucial to the shear response of the member. For U-beams, the strands beneath the webs and above the bearing pad are still important in shear, but are in different locations. The standard debonding order should be changed to reflect this fact.

The practice of debonding strands fundamentally changes the behavior of a prestressed concrete beam. No longer is the prestressing force applied entirely at the beam end, so it follows that the bursting forces are no longer confined to the end region. Instead, bursting reinforcement should be provided at each section in which a new portion of the prestressing force is applied, in quantities sufficient to resist the transverse force associated with that portion of the prestressing force. An example of this design concept is shown in Figure 4.29.

Similar to the situation of beams with debonded strands is that of beams with dapped ends. In the dapped-end case, *no* strands are bonded at the beam end. It is clear that bursting reinforcement should be provided beyond the dap rather than at the member end.

At present, AASHTO LRFD (2009) lacks language requiring transverse reinforcement (except as per shear demands) beyond a distance *h*/4 from the beam end. In Texas U-beams and to a dramatic extent in bulb-tee Tx girders (O'Callaghan, 2007), the need for bursting reinforcement beyond this region has been shown. In beams with debonded strands or dapped ends, bursting reinforcement should be provided wherever force is transferred from prestressing strands to concrete, even if that be a great distance from the beam end.

4.5 SUMMARY

In Chapter 4, experimental results for the testing of U-beams at prestress transfer were discussed, with special attention paid to the measured stress variation in end-region transverse reinforcement. Results from the four U-beam end regions were laid against the backdrop of a database of transverse-bar stress test results. From the database, some contributing factors to high bursting and spalling stresses were identified. Lastly preliminary recommendations were made for U-beam end-region detailing primarily focused on additional transverse reinforcement. In the following chapter, the work conducted will be summarized and the primary conclusions reported.

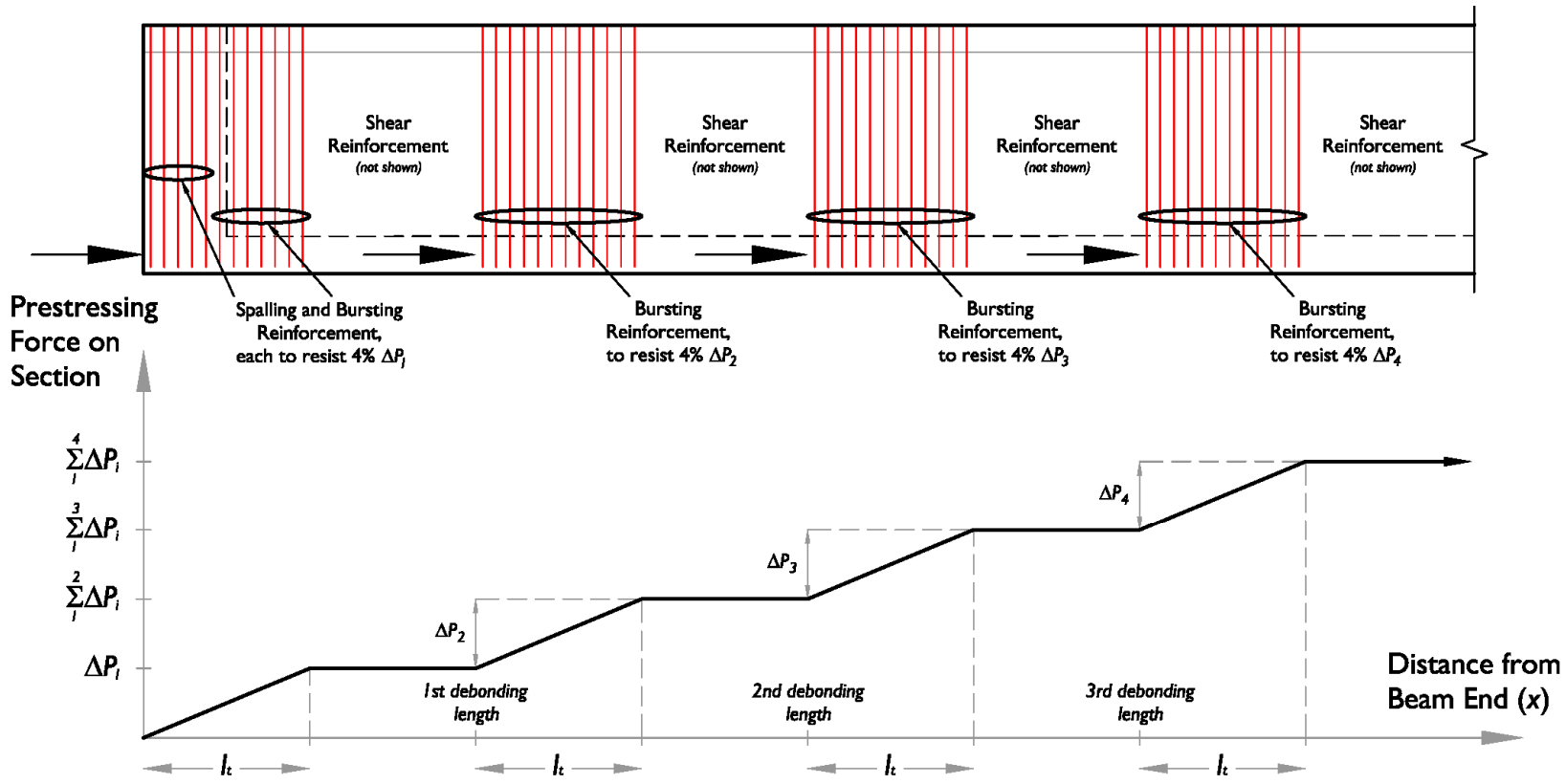

Figure 4.29 Design of bursting & spalling reinforcement in a U-beam with debonded strand

CHAPTER 5

Conclusions

5.1 SUMMARY OF RESEARCH PROGRAM

An experimental study of bursting and spalling behavior in pretensioned concrete U-beams, conducted as part of TxDOT Research Project 5831, is reported in this thesis. Two full-scale U-beam specimens were fabricated at the Ferguson Structural Engineering Laboratory of The University of Texas at Austin, with their end regions instrumented with strain gages on reinforcing bars and prestressing strands, and thermocouples in concrete end blocks. These specimens were designed to represent the worst-case scenario for bursting and spalling stresses in U-beams.

U-beams were cast following procedures observed at a precast concrete plant and meeting TxDOT standards. Prestress was transferred as soon as the measured compressive strength of the concrete, match-cured to a TxDOT-standard release point within the beam, reached the release strength (corresponding to a bottom-fiber stress at transfer of $0.65f'_{ci}$ near the beam end). At transfer of prestress, horizontal and diagonal cracks formed in the end regions of the U-beams. Strain increases in transverse and lateral reinforcing bars were measured, and converted to bursting or spalling stresses; strain decreases in prestressing strands were used to calculate prestress losses.

Bursting and spalling stresses measured in the U-beam specimens were analyzed alongside those in an experimental database of past studies of pretensioned concrete beams in which end-region transverse reinforcement was instrumented at prestress transfer. This database contains 57 specimens (i.e. beam end regions) in which transverse-bar force at transfer was reported—or could be calculated. Most of these specimens (40 of 57) came from studies in which spalling effects (and not bursting

effects) were examined. Several factors contributing to measurements of high transverse-bar bursting or spalling stresses were identified. Lastly recommendations were made with regard to U-beam end-region reinforcement and bursting design in special cases (debonding and dapped ends).

5.2 CONCLUSIONS

From the experimental and analytical studies conducted for TxDOT Research Project 5831, the following conclusions can be made:

1. Though most strain gages on end-region reinforcing bars indicated low bursting and spalling stresses (less than about 5 ksi), some returned much higher readings. Experimentally determined stresses in both the bursting zone (Beam 2) and spalling zones (Beams 1 and 2) surpassed the limit set by AASHTO LRFD (20 ksi) by as much as 50%. The high bursting and spalling stresses provide a basis for proposed design changes in the end-region details.
2. Contributing to the high maximum transverse-bar stresses at prestress transfer (based on database analysis) were two factors applicable to the U-beam specimens tested: high average transverse-bar bursting/spalling stress in the end region and high bottom-fiber stress near the beam end.
3. Placed in context of U-beam design standards of other state DOTs, Texas U-beams have little transverse reinforcement in their webs. Much transverse reinforcement, however, is provided within the end blocks, especially near the center of the section.
4. The provision of additional transverse reinforcement in U-beam webs is recommended. This reinforcement may take the form of new bars near the interior web face and bundled bars near the exterior, to extend to a distance of at least 36 in. from the beam end. Proposed changes to the end-region reinforcing details will be

tested at transfer and under shear loads in the near future under Research Project 5831, with these test results determining the adequacy of such details.

5. Measured stresses in bottom-flange lateral bars never exceeded the AASHTO limit (20 ksi), despite the fact that the reinforcement provided in this zone was 30% of that required by AASHTO LRFD. As the recent code change (2008) requiring "splitting" reinforcement in this zone seems to have been based on Washington State DOT standard practice rather than the results of a specific research program, the code requirement may be overly conservative. Similar results from other beam types (e.g. box beams, as planned in later portions of Research Project 5831) would be necessary to substantiate these findings, however.
6. No trend in the measured bursting and spalling stresses could be linked to the end-block design alternative (large triangular or small skewed end block) chosen for the skewed end; neither end block can be recommended as providing superior performance at prestress transfer. Should the finding of structural equivalence be replicated in shear testing and further bursting/spalling testing, the small skewed end block may be recommended for temperature-related reasons.
7. Bursting reinforcement should be provided in all locations at which strands first bond to concrete, be they near the beam end as in the usual case, or further from the beam end in the case of debonded strands or dapped ends. With limited experimental work thus far conducted examining the effects of different levels of bursting reinforcement, it is recommended that bursting reinforcement should be designed similarly to the "splitting" reinforcement in AASHTO LRFD, to resist 4% of the applied prestressing force (or increment of applied prestressing force newly bonded at that section) with an allowable design stress of 20 ksi for the transverse reinforcement.

5.3 RECOMMENDED FUTURE RESEARCH

Continued development and testing of new transverse-reinforcement details for U-beams and box beams will be the next steps for Project 5831. Limited study of bursting and spalling stresses in beams with debonded strands has also begun under the auspices of the project; however, it seems that the subject may be deserving of a more intensive treatment. One reason often given (PCI, 1985; Itani & Galbraith, 1986; Tadros et al., 2007) for why bursting and spalling stresses are not necessary to consider for beams in service is the beneficial clamping effect of the beam reaction in the region close to the support. For beams with debonded strands, a significant portion of the prestressing force may be transferred in locations far from the end support.

Work with bursting and spalling database has made it clear that members of different cross sections can behave differently at transfer. Increasing the database size by conducting more tests on pretensioned beams with extensively-instrumented end regions would be invaluable to the understanding of bursting and spalling behavior. As noted in the previous section, particularly lacking are tests of pretensioned beams with varying levels of bursting reinforcement. As bulb tees members have proved particularly vulnerable to cracking problems, their use in such a study would be natural.

Continued study of lateral bursting stresses will also be interesting. As noted previously, requirements for bottom-flange lateral reinforcement in wide pretensioned concrete members were recently added to AASHTO LRFD (2008). Should U-beams and other members with much less than the LRFD-required lateral reinforcement continue to show serviceable lateral bursting zones, there may be cause to readdress this provision. An extreme case for lateral bursting, in which the lateral-bar stress in a beam with debonded strands would be measured between widely-spaced, bonded strand groups, would be valuable to investigate for the purposes of code calibration.

APPENDIX A

Database of Transverse-Bar Bursting & Spalling Stresses in Pretensioned Beam End Regions

Over the course of TxDOT Research Project 5831, a database of similar tests—ones in which bursting and spalling were assessed through use of strain gages on transverse reinforcement in pretensioned concrete beam end regions—was assembled from available sources from the literature. These sources (Marshall & Mattock, 1962; Itani & Galbraith, 1986; Tuan et al., 2004; Crispino, 2007; O'Callaghan, 2007) were discussed individually in Section 2.4.2.

Of the 57 beam end regions examined in these works and in Research Project 5831, transverse-bar stresses at prestress transfer were available for 45. Beams studied were mostly I-beams (80%), although inverted T-beams and U-beams were also studied. Detailed discussion of this database can be found in Section 4.3.

The following figures show circles representing stress values superimposed on elevations of the beam end region in which they were measured. Circles are placed at the location at which stresses were measured (i.e. both on the instrumented bar and at the correct height, except as noted); their area is proportional to the stress measurement. The color of the circles relates the stress measurement to the 20 ksi stress allowable for reinforcement within pretensioned concrete anchorage zones (AASHTO LRFD Bridge Design Specifications, 2009).

Typical spalling behavior involves by high measured stresses in transverse bars close to the beam end, decreasing quickly with distance into the beam, reaching negligible values within $h/4$. Typical bursting behavior involves high measured stresses further into the beam. Bursting stresses typically increase with distance into the beam

until the maximum stress is achieved. Stresses then decrease, likely within one transfer length from the beam end.

Crack patterns from prestress transfer, available for one-third of the specimens, are provided on the beam elevations. Reasonable correlation can be seen between the crack locations and reinforcing-bar stress measurements. The transverse reinforcement is drawn with variable line thickness, proportional to the bar area (with heavier lines indicating greater area).

Beam cross-sections give information on the prestressing strand pattern (at the instrumented member end) and transverse-reinforcement shape, as well as section geometry.

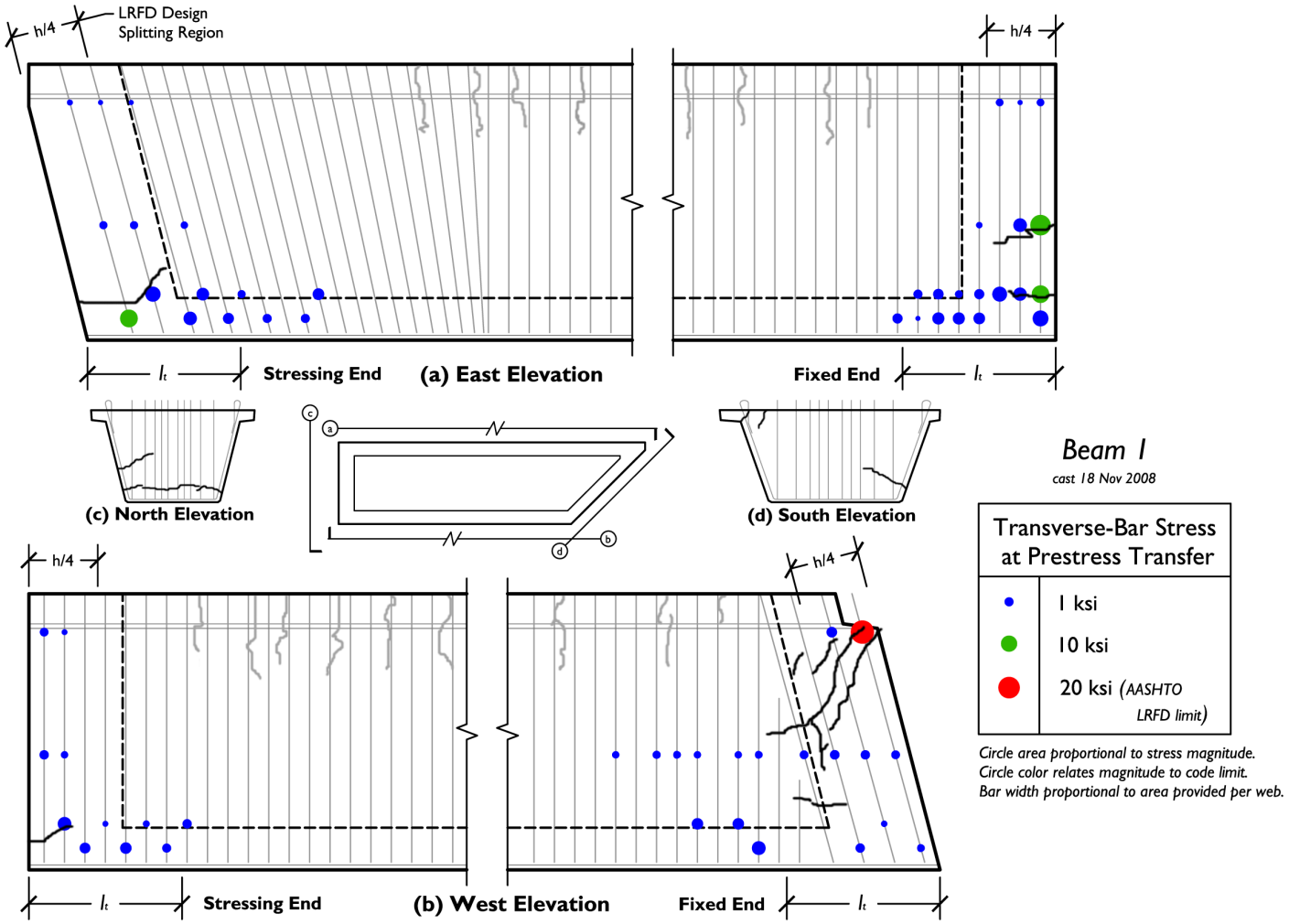

Figure A.1 U-beam with skewed end block

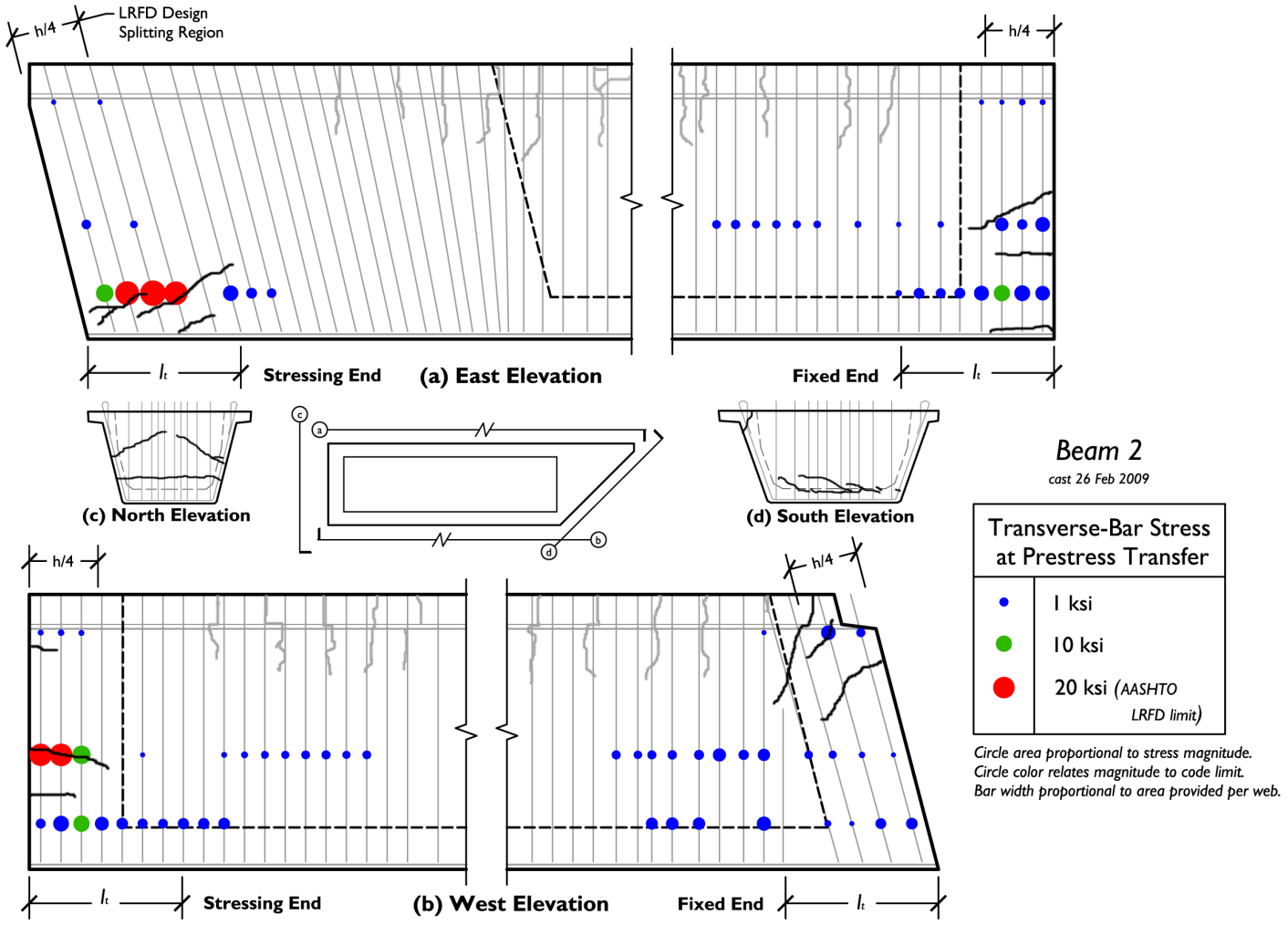

Figure A.2 U-beam with triangular end block

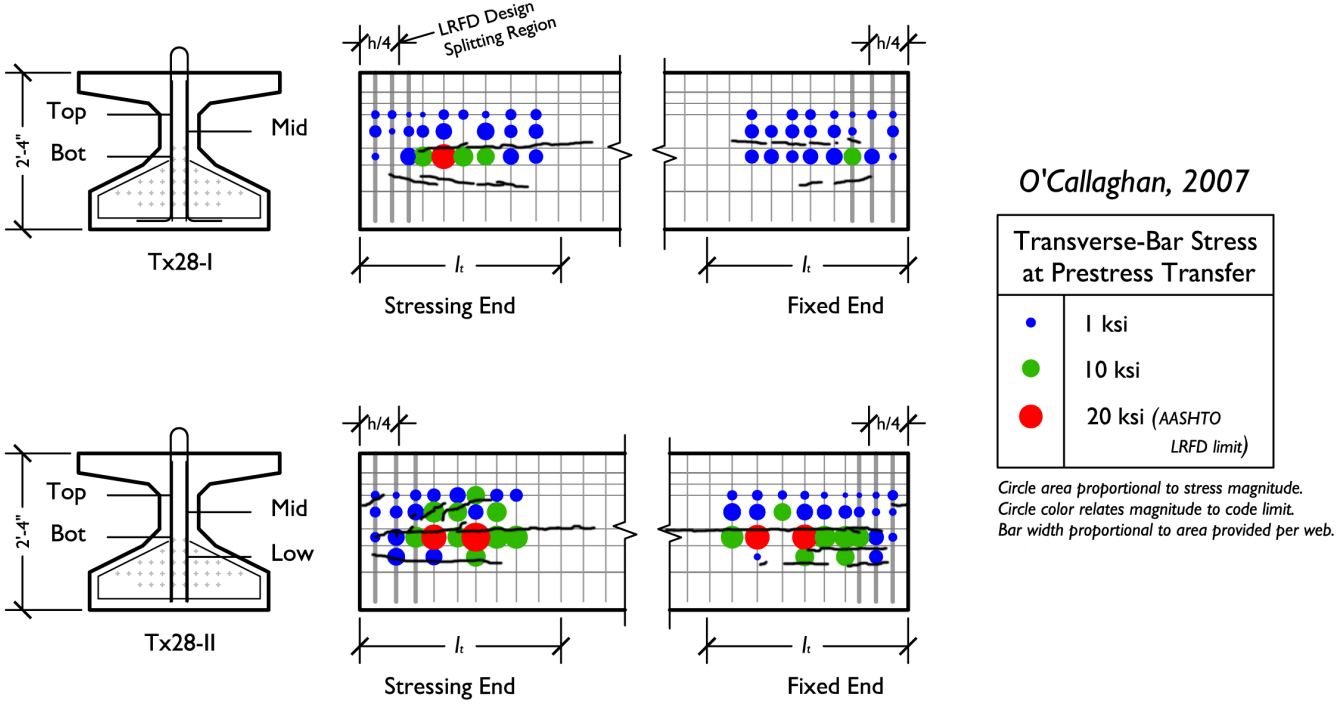

Figure A.3 Shallow Texas bulb tees (Tx girders)

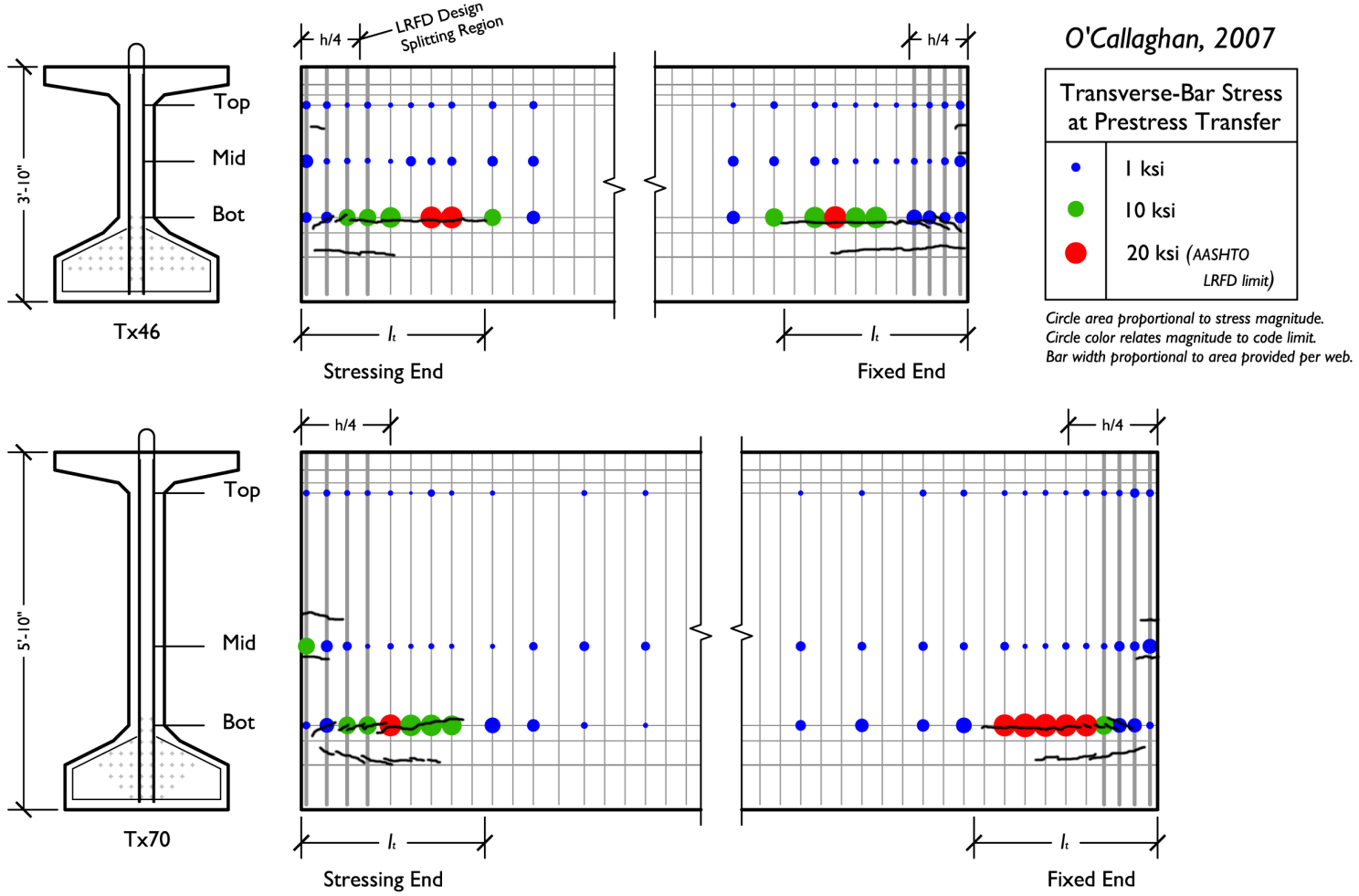

Figure A.4 Deep Texas bulb tees (Tx girders)

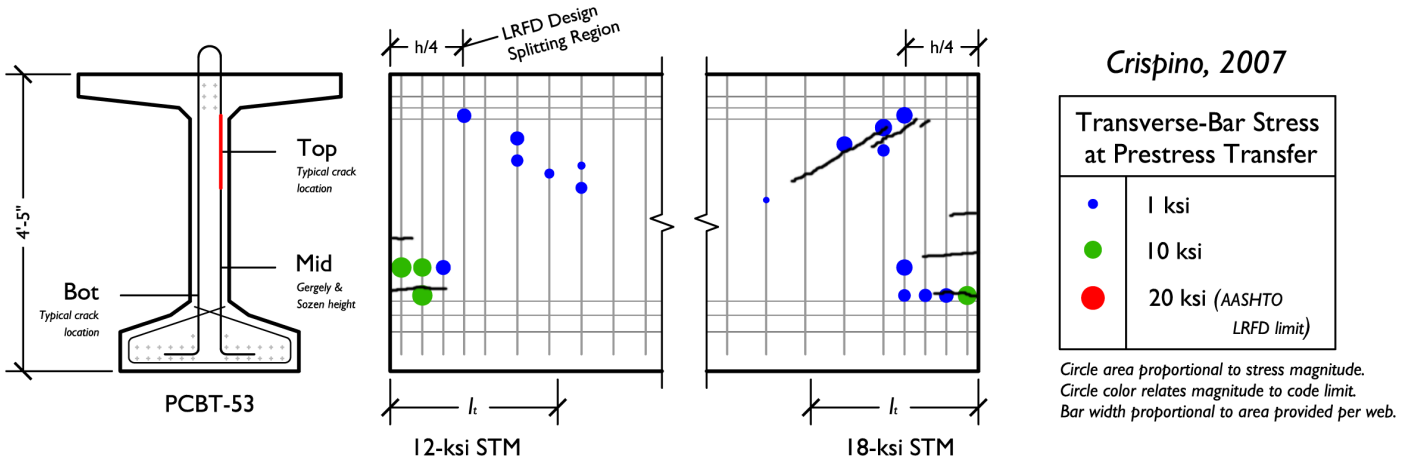

Figure A.5 Lightweight-concrete Virginia bulb tee (PCBT girder)

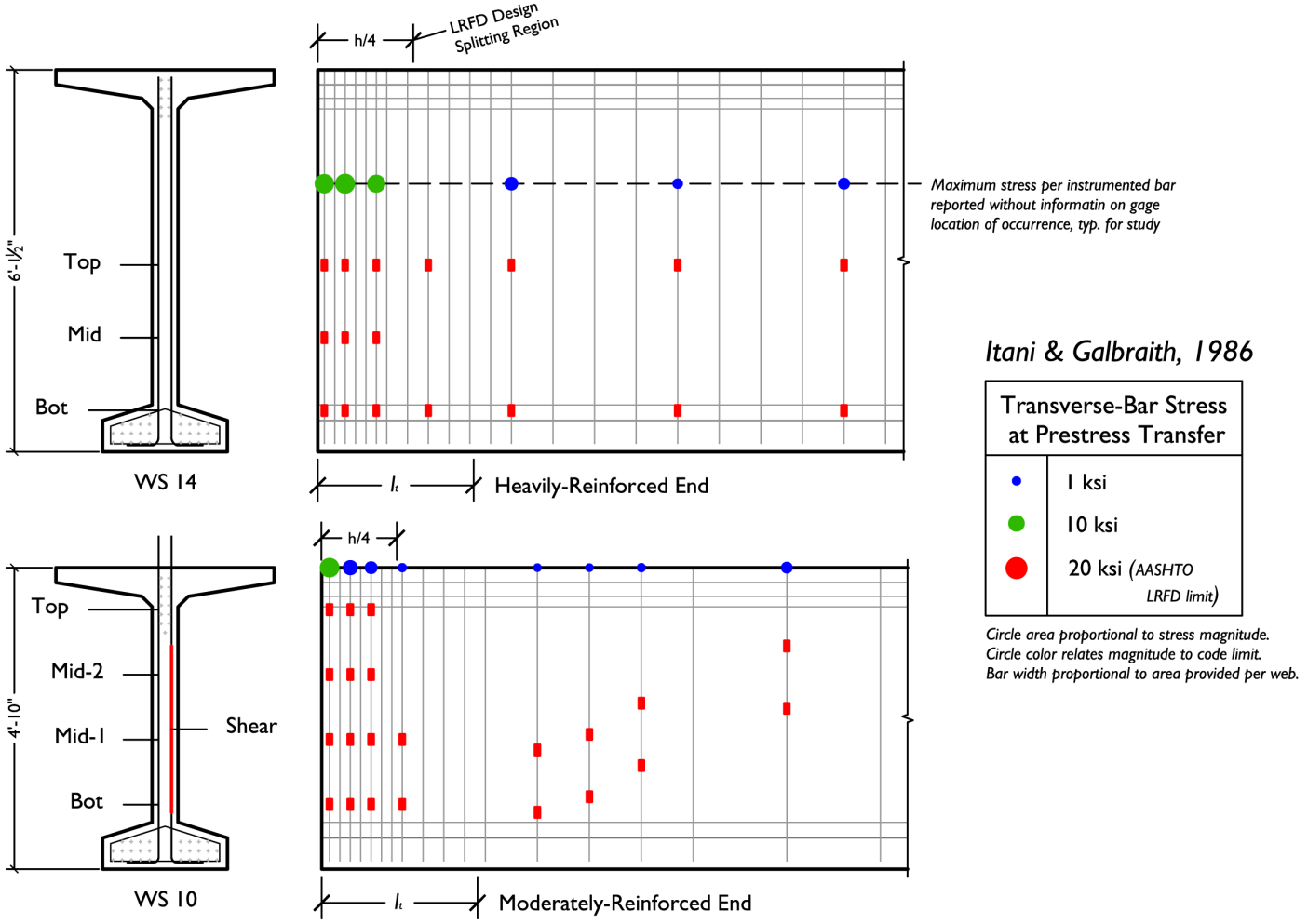

Figure A.6 Washington bulb tees (WS girders)

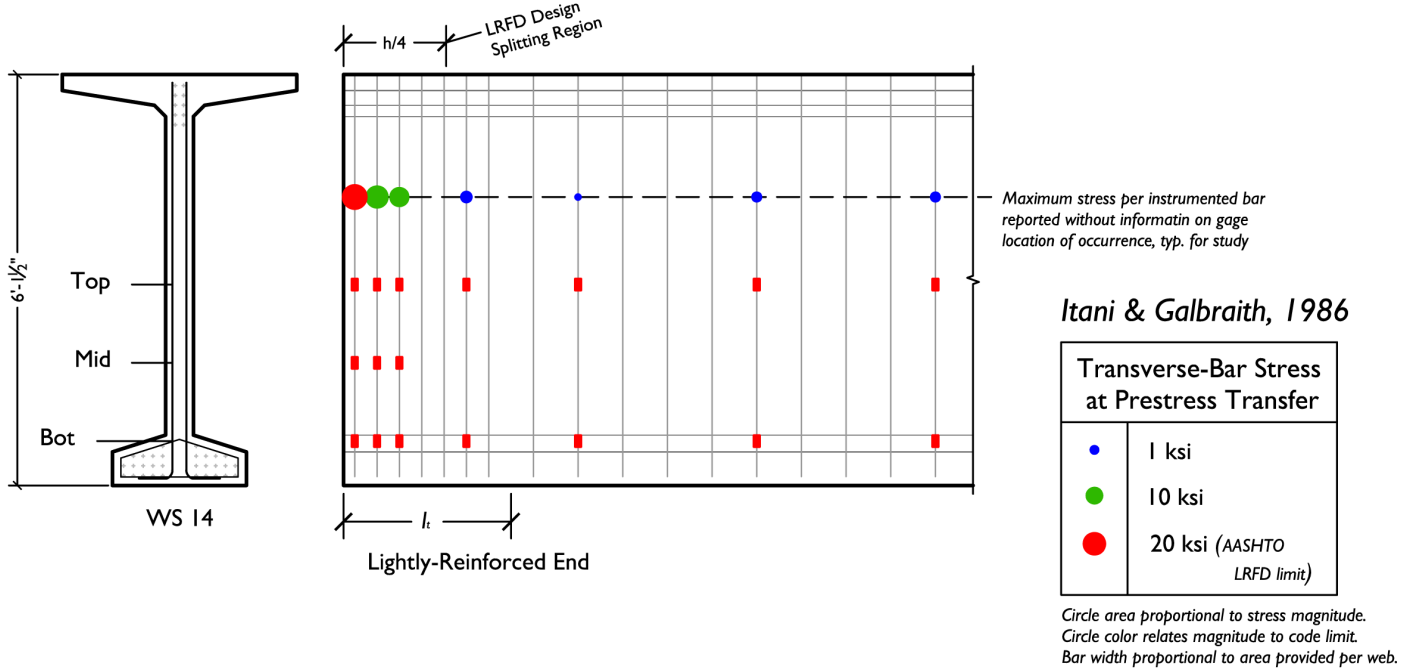

Figure A.7 Washington bulb tee (WS girder)

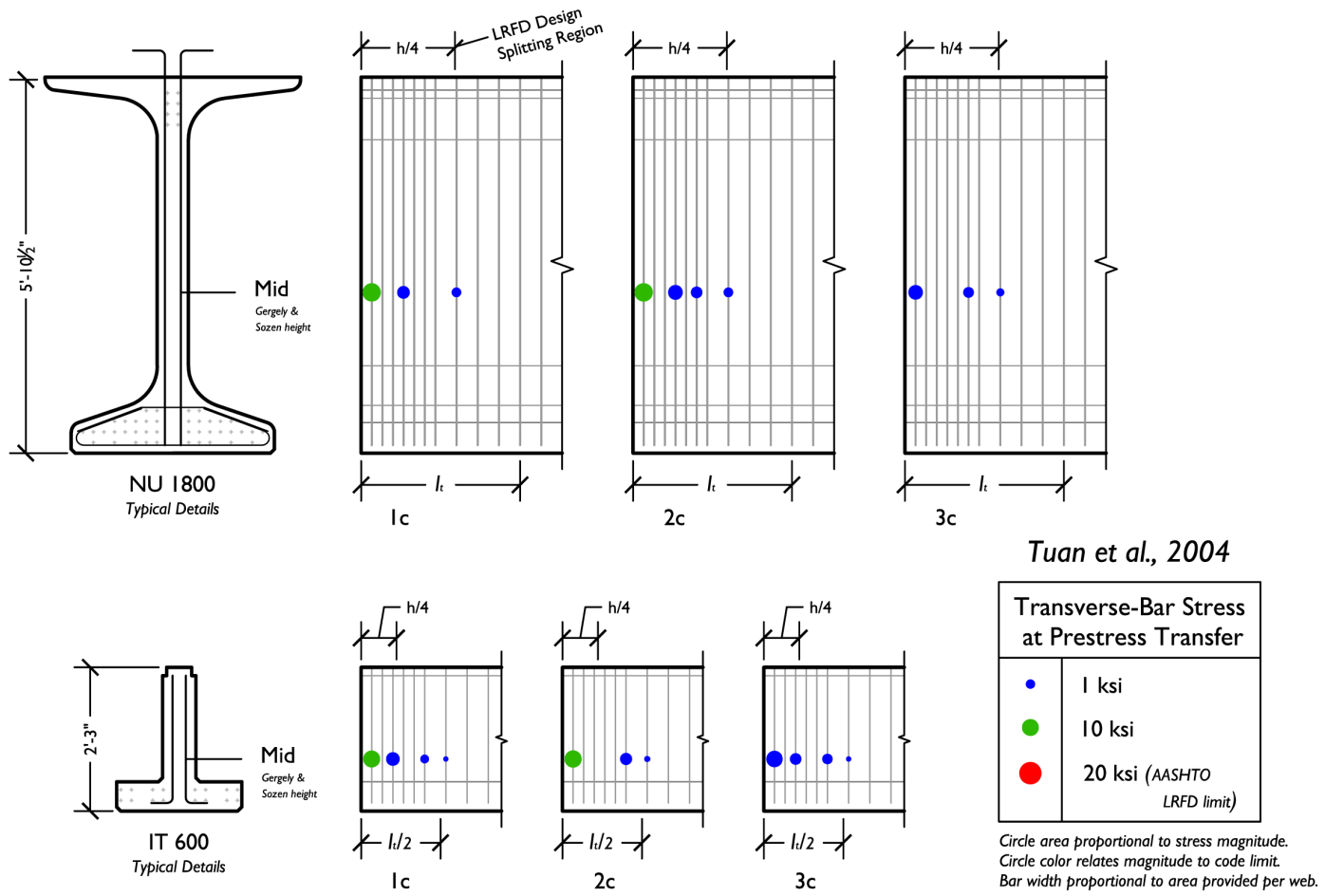

Figure A.8 Deep Nebraska bulb tees and inverted tees (NU and IT girders), typical reinforcing details

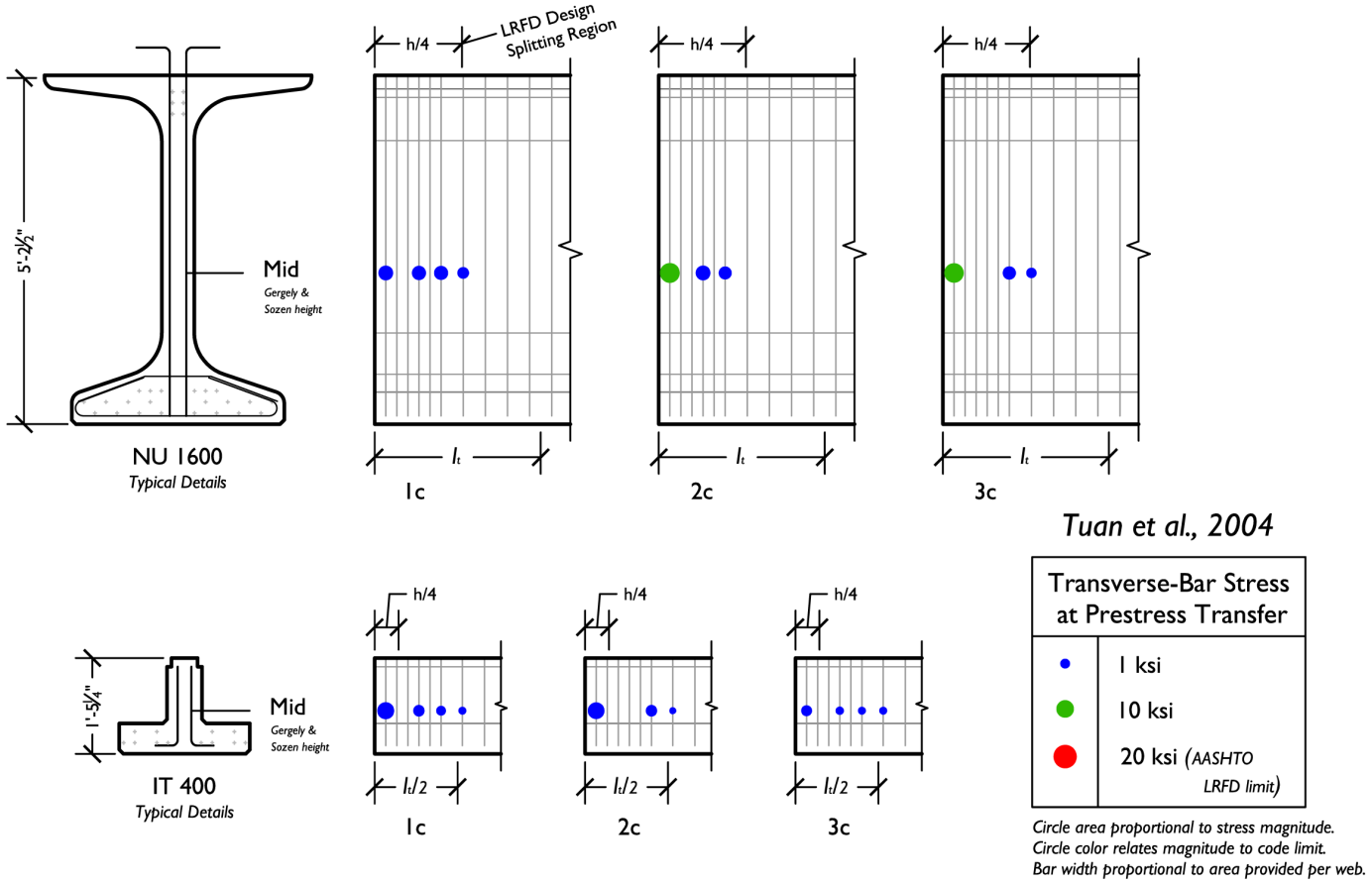

Figure A.9 Nebraska bulb tees and inverted tees (NU and IT girders), typical reinforcing details

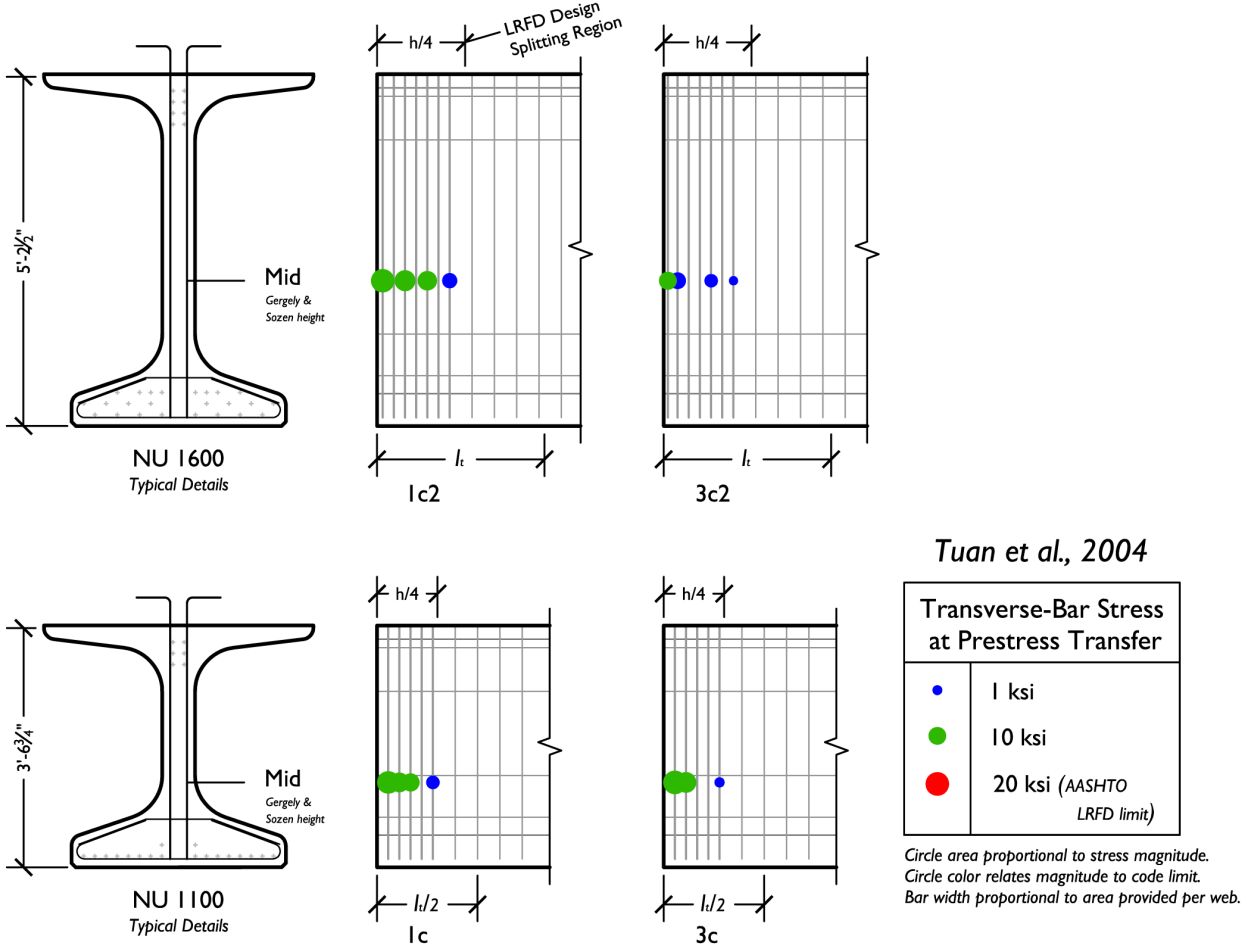

Figure A.10 Nebraska bulb tees of two depths (NU girders), typical reinforcing details

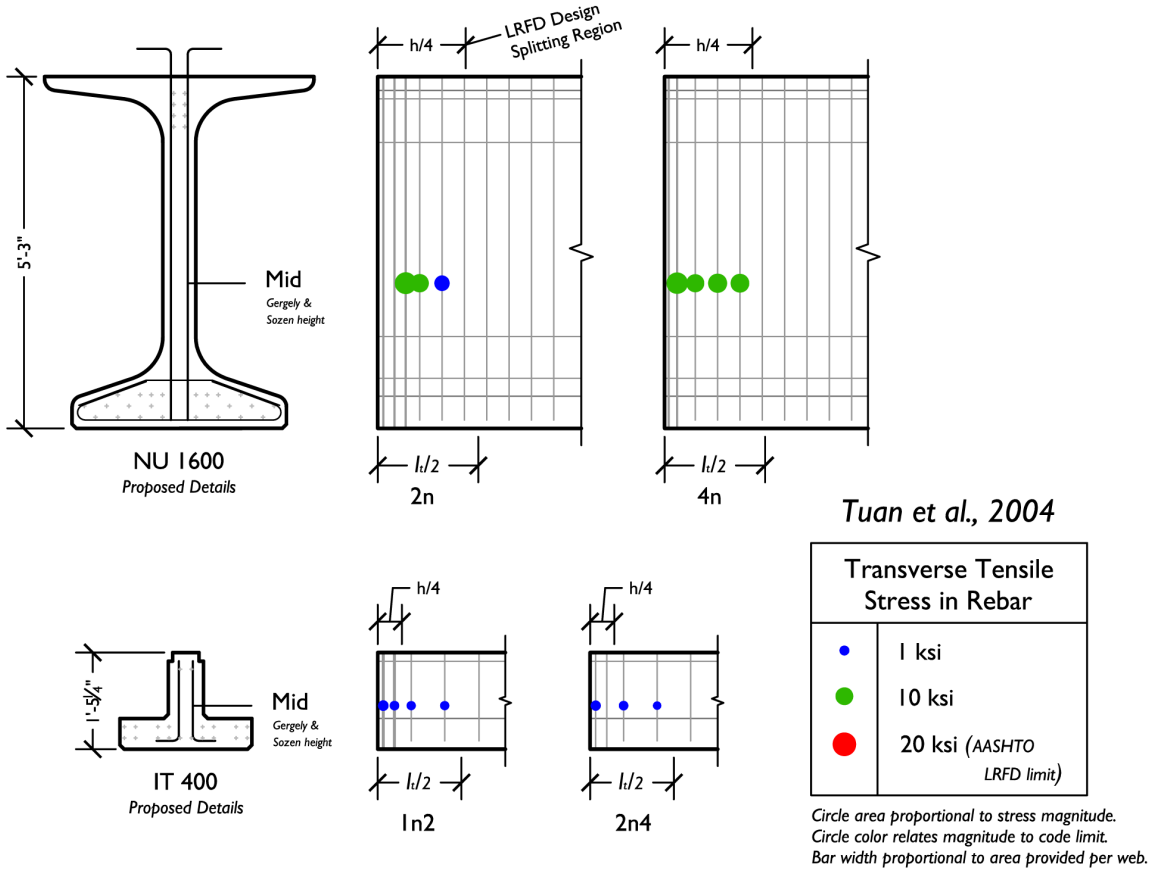

Figure A.11 Nebraska bulb tees and inverted tees (NU and IT girders), proposed reinforcing details

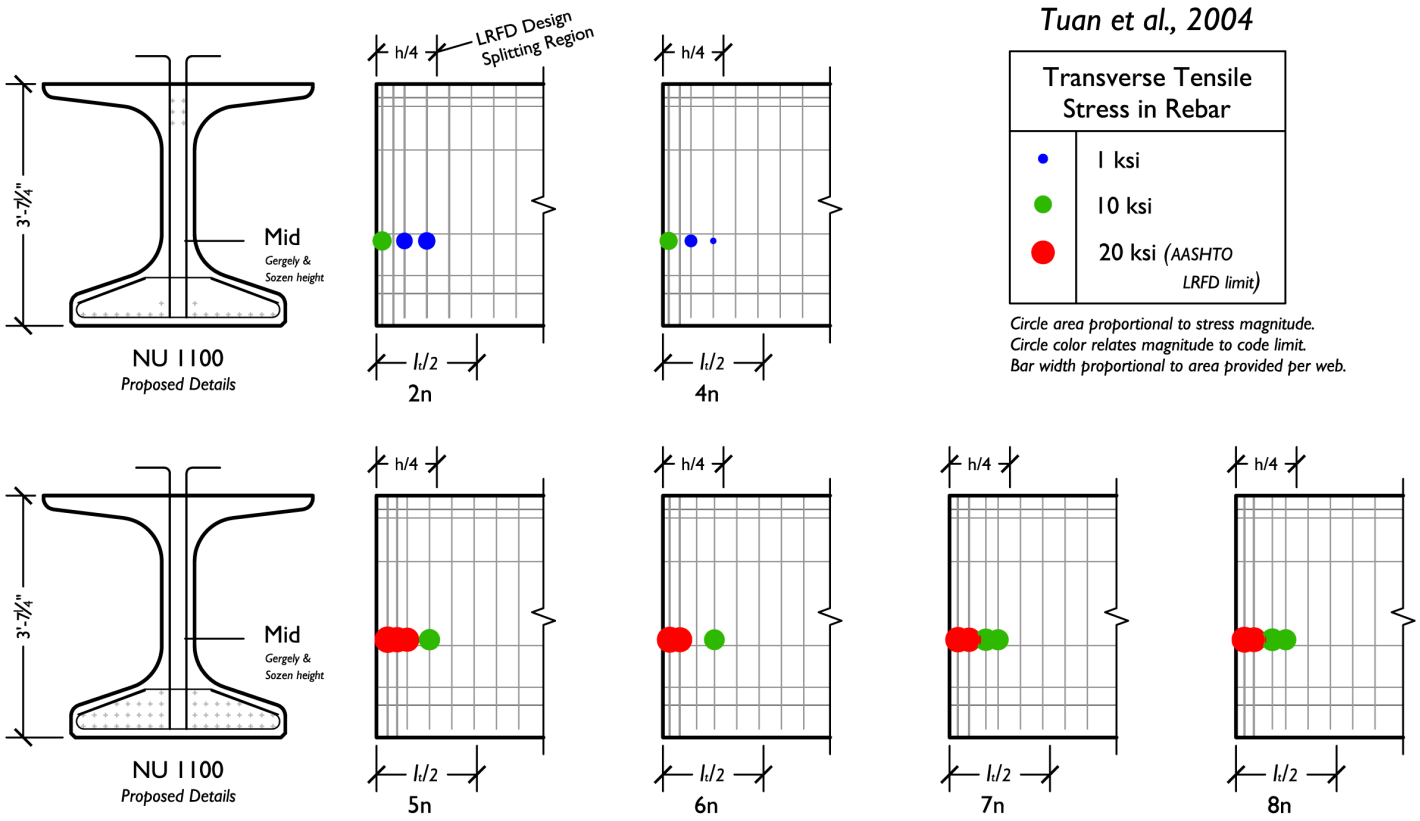

Figure A.12 Shallow Nebraska bulb tees (NU girders), proposed reinforcing details

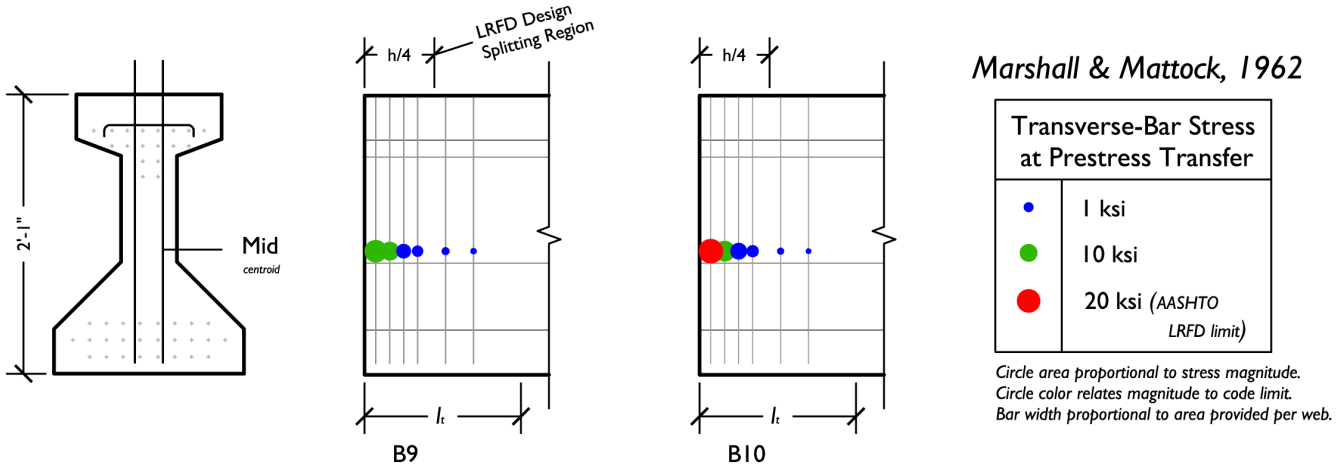

Figure A.13 Shallow I-beams

APPENDIX B

Calculations of Code-Required End-Region Reinforcement for U-Beam Specimens

B.1 AASHTO LRFD (2009) END-REGION REINFORCEMENT (ARTICLE 5.10.10.1)

$$A_r = 0.04 \frac{P_i}{f_s} = 0.04 \frac{2417\ kip}{20\ ksi} = 4.83\ in.^2 \qquad \textit{Equation B.1}$$

where:

A_r = required area of transverse reinforcement within h/4 from member end, and lateral reinforcement within b_f/4 from end
P_i = prestress force at transfer
f_s = design stress in the transverse reinforcement, not to exceed 20 ksi

B.2 *PCI DESIGN HANDBOOK* (2004) TRANSVERSE REINFORCEMENT (SECTION 4.2.4)

$$A_r = 0.021 \frac{P_i}{f_s} \frac{h}{l_t} = 0.021 \frac{2417\ kip}{30\ ksi} \frac{54}{30} = 3.05\ in.^2 \qquad \textit{Equation B.2}$$

where:

A_r = required area of transverse reinforcement within h/5 from member end
P_i = prestress force at transfer
f_s = design stress in the transverse reinforcement, not to exceed 30 ksi
h = depth of member
l_t = strand transfer length

B.3 CEB-FIP MODEL CODE (1990) BURSTING AND SPALLING REINFORCEMENT

B.3.1 Concrete Tensile Strength (Clause 2.1.3.3.1)

$$f_{ctk} = 0.138\ ksi \left(\frac{f_{ck}}{1.45\ ksi}\right)^{2/3} = 0.138\ ksi \left(\frac{6.3}{1.45}\right)^{2/3} \qquad \textit{Equation B.3}$$

$$f_{ctk} = 0.367\ ksi$$

where:

f_{ctk} = concrete tensile strength (5th percentile)
f_{ck} = concrete compressive strength at transfer of prestress

$$f_{ctd} = \frac{f_{ctk}}{1.5} = \frac{0.367\ ksi}{1.5} = 0.245\ ksi$$ *Equation B.4*

where:

f_{ctd} = lower-bound concrete tensile strength

$$f_{ctm} = 0.203\ ksi \left(\frac{f_{ck}}{1.45\ ksi}\right)^{2/3} = 0.203\ ksi \left(\frac{6.3}{1.45}\right)^{2/3}$$ *Equation B.5*

$$f_{ctm} = 0.541\ ksi$$

where:

f_{ctm} = concrete tensile strength (mean)

$$f_{ct,fl} = f_{ctm} \frac{1 + 1.5\left(\frac{h}{3.94\ in.}\right)^{0.7}}{1.5\left(\frac{h}{3.94\ in.}\right)^{0.7}}$$

$$f_{ct,fl} = 0.541\ ksi\ \frac{1 + 1.5\left(\frac{54}{3.94}\right)^{0.7}}{1.5\left(\frac{54}{3.94}\right)^{0.7}}$$ *Equation B.6*

$$f_{ct,fl} = 0.598\ ksi$$

where:

$f_{ct,fl}$ = concrete tensile strength in flexure (mean)

h = depth of member

B.3.2 Bond Strength (Clause 6.9.11.2)

$$f_{bpd} = \eta_{p1}\eta_{p2}f_{ctd} = 1.2 \cdot 1.0 \frac{0.367}{1.5} = 0.293\ ksi \qquad \textit{Equation B.7}$$

where:

η_{p1} = factor considering the type of prestressing tendon:
η_{p1} = 1.4 for indented or crimped wires, and
$\boldsymbol{\eta_{p1} = 1.2}$ for 7-wire strands

η_{p2} = factor considering the position of the tendon:
η_{p2} = 1.0 for all tendons with an inclination of 45-90˚
(with respect to the horizontal),
$\boldsymbol{\eta_{p2} = 1.0}$ for all horizontal tendons which are up to 10 in. from the bottom or at least 12 in. below the top of the concrete section, and
η_{p2} = 0.7 for all other cases.

B.3.3 Basic Anchorage Length (Clause 6.9.11.3)

$$l_{bp} = \frac{A_{sp}}{\varphi\pi}\frac{f_{ptd}}{f_{bpd}} = \frac{7}{36} \cdot 0.5\ in. \frac{270\ ksi/1.15}{0.293\ ksi} = 77.8\ in. \qquad \textit{Equation B.8}$$

where:

$A_{sp}/\varphi\pi$ = φ /4 for tendons with a circular cross-section, and
$\boldsymbol{7\varphi/36}$ for 7-wire strands

f_{ptd} = lower-bound tensile strength, $f_{ptk}/1.15$, where
f_{ptk} is the strand tensile strength (5th percentile)

f_{bpd} = bond strength

B.3.4 Transmission Length (Clause 6.9.11.4)

$$l_{bpt} = \alpha_8 \alpha_9 \alpha_{10} l_{bp} \frac{\sigma_{pi}}{f_{pd}} = 1.0 \cdot 0.5 \cdot 0.5 \cdot 77.8\ in. \frac{180\ ksi}{203\ ksi} \qquad \textit{Equation B.9}$$

$$l_{bpt} = 17.3\ in.$$

where:

α_8 = factor considering release method:
$\boldsymbol{\alpha_8 = 1.0}$ for gradual release, and
α_8 = 1.25 for sudden release.

α_9 = factor considering action to be verified:
α_9 = 1.0 for moment and shear capacity, and
$\boldsymbol{\alpha_9 = 0.5}$ for transverse stresses in anchorage zone.

α_{10} = factor considering bond:
$\boldsymbol{\alpha_{10} = 0.5}$ for strands, and
α_{10} = 0.7 for indented or crimped wires

l_{bp} = basic anchorage length

σ_{pi} = stress in strands just after release (i.e. after elastic losses)

f_{pd} = strand design stress

B.3.5 Bursting Force (Clause 6.9.12.2)

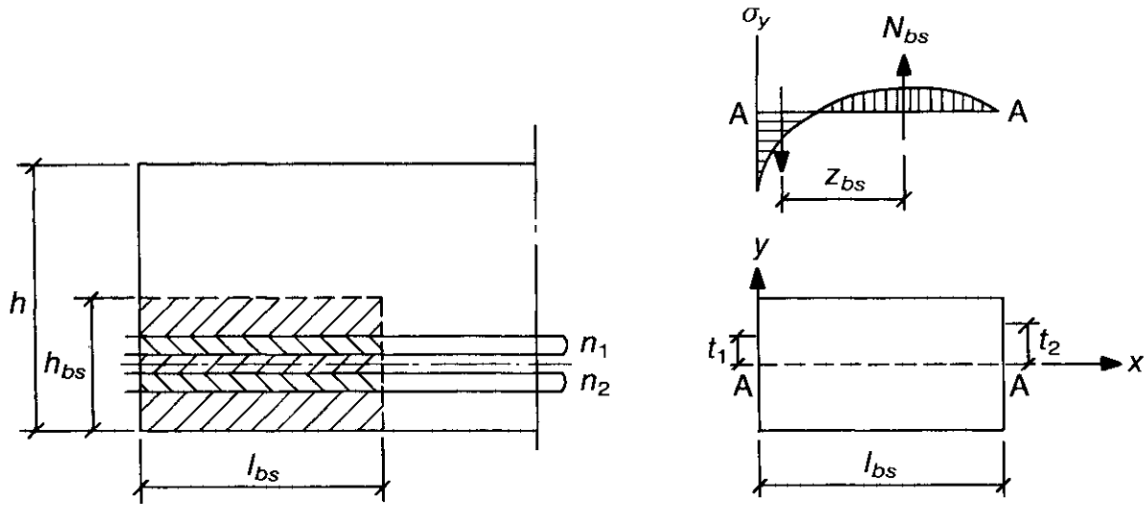

Figure B.1 Symmetrical prism model for CEB-FIP bursting provisions (CEB-FIP MC 1990)

$$l_{bs} = \sqrt{{h_{bs}}^2 + 0.6{l_{bpt}}^2} = \sqrt{8.25^2 + 0.6 \cdot 17.3^2}\ in.$$

Equation B.10

$$l_{bs} = 15.7\ in.$$

where:

l_{bs} = symmetrical prism length (as tendons are anchored by bond)
h_{bs} = prism height (twice the distance from prestress centroid to bottom fiber)
l_{bpt} = transmission length

$$N_{bs} = \frac{0.5(n_1 + n_2)t_1 - n_1 t_1}{z_{bs}} \gamma_1 F_{sd}$$

$$N_{bs} = \frac{0.5(39 + 39\,)2.14\ in. - 39 \cdot 2\ in.}{0.5 \cdot 15.7\ in.} 1.1 \cdot 31\ kip \qquad \textit{Equation B.11}$$

$$N_{bs} = 23\ kip$$

where:

N_{bs} = bursting force
t_1 = distance between the centroid of the tendons above the prestress centroid to the prestress centroid
t_2 = distance between the centroid of the concrete stress block above the prestress centroid to the prestress centroid
n_1, n_2 = number of tendons above and below prestress centroid
z_{bs} = internal moment arm, $0.5l_{bs}$, where l_{bs} is the prism length
γ_1 = partial safety factor against tendon overstressing
F_{sd} = design force per strand

$$\sigma_{bs} = \frac{2N_{bs}}{b_{bs} l_{bs}} = \frac{2 \cdot 23\ kip}{(57.1\ in.)(15.7\ in.)} = 0.051\ ksi \qquad \textit{Equation B.12}$$

where:

σ_{bs} = bursting stress
b_{bs} = prism breadth (at prestress centroid)

Since $\sigma_{bs} < f_{ctd}$, the bursting force can be resisted adequately by the concrete. Cracking in the bursting zone is not predicted, and no bursting reinforcement need be provided.

B.3.6 Spalling Force (Clause 6.9.12.3)

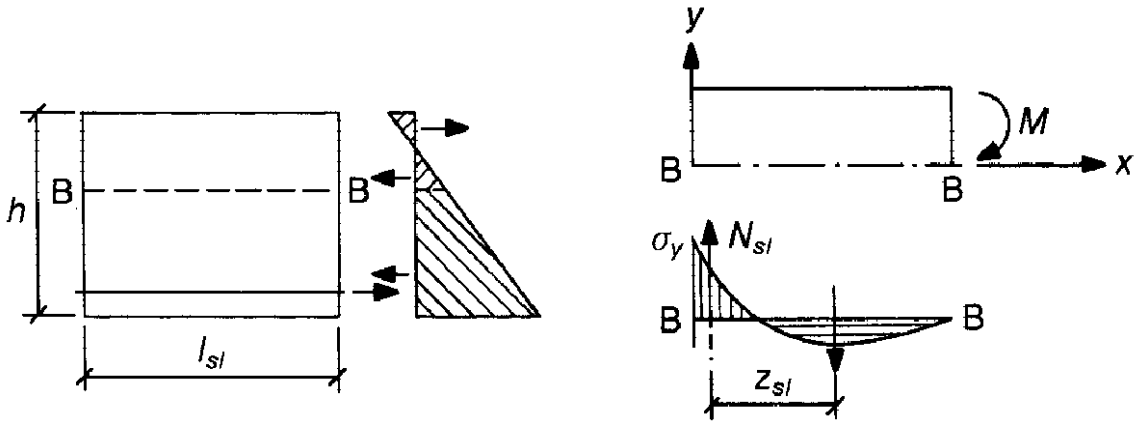

Figure B.2 Model for CEB-FIP spalling provisions (CEB-FIP MC 1990)

$$l_{sl} = l_{bs} = 15.7\ in. \qquad \textit{Equation B.13}$$

where:

l_{sl} = equivalent prism length (same definition as symmetrical prism length, l_{bs}, considered in bursting)

$$N_{sl} = \frac{M_{sl}}{z_{sl}} = \frac{4000\ kip \cdot in.}{0.5 \cdot 15.7\ in.} = 509\ kip \qquad \textit{Equation B.14}$$

where:

N_{sl} = spalling force

M_{sl} = moment in top portion of beam shown in Figure B.2 as *M*, and calculated using sectional analysis (results shown in Figure B.3) *(Calculating the moment in the top portion of the beam is equivalent to calculating the unbalanced moment in the bottom portion of the beam, as done in the Gergely-Sozen method.)*

z_{sl} = internal lever arm, $0.5l_{sl}$

$$\sigma_{sl} = \frac{8N_{sl}}{b_{sl}l_{sl}} = \frac{8 \cdot 509\ kip}{(10.3\ in.)(15.7\ in.)} = 25.1\ ksi \qquad \textit{Equation B.15}$$

where:

σ_{sl} = spalling stress

b_{sl} = prism breadth

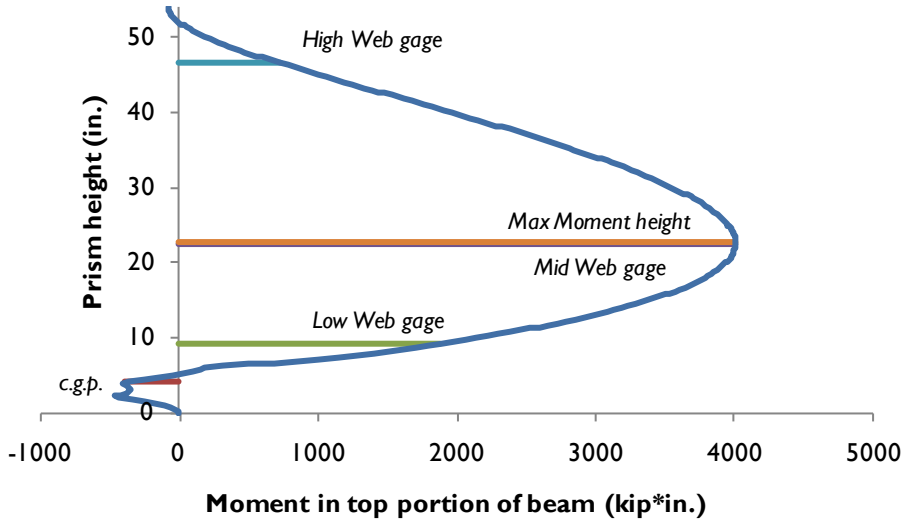

Figure B.3 Unbalanced moment considering bottom portion of beam only

Since $\sigma_{sl} >> f_{ct,cl}/1.5 = 0.399 \quad ksi$, spalling reinforcement is necessary.

$$A_{r,sl} = \frac{N_{sl}}{f_{sy}} = \frac{509 \quad kip}{60 \quad ksi} = 8.48 \quad ksi \qquad \textit{Equation B.16}$$

where:

$A_{r,sl}$ = spalling reinforcement, to "*be put parallel to the end face in its close vicinity*"

f_{sy} = steel yield strength

APPENDIX C

Specimen Design Calculations

C.1 Linear Stress Distribution

Assume prestress losses from elastic shortening total 10% of the initial prestressing force. (Calculations are iterative.)

$$P_i = n_p f_{pi} a_p = 78 \cdot 202.5\ ksi \cdot 0.153\ in.^2 \qquad \textit{Equation C.1}$$

where:

n_p = number of prestressing strands in section
f_{pi} = initial (jacking) prestress in strands
a_p = area per strand (0.5- in. diameter)

$$f_{bot} = \frac{P_o}{A_g} + \frac{P_o\ e\ y_{bot}}{I_g}$$

$$f_{bot} = \frac{0.9 \cdot 2417\ kip}{1120\ in.^2} + \frac{0.9 \cdot 2417\ kip \cdot 18.2\ in. \cdot 22.4\ in.}{403{,}000\ in.^4} \qquad \textit{Equation C.2}$$

$$f_{bot} = 4.14\ ksi$$

where:

f_{bot} = stress at bottom fiber of beam
P_o = effective prestressing force after elastic losses, assumed as 90% P_i
A_g = gross cross-sectional area
e = eccentricity of prestressing force
y_{bot} = distance from centroid to bottom of section
I_g = gross-section moment of inertia

$$f_{top} = \frac{P_o}{A_g} - \frac{P_o\ e\ y_{top}}{I_g}$$

$$f_{top} = \frac{0.9 \cdot 2417\ kip}{1120\ in.^2} - \frac{0.9 \cdot 2417\ kip \cdot 18.2\ in. \cdot 31.6\ in.}{403{,}000\ in.^4} \qquad \textit{Equation C.3}$$

$$f_{top} = -1.16\ ksi$$

where:

f_{top} = stress at top fiber of beam
y_{top} = distance from centroid to top of section

C.2 CONCRETE RELEASE STRENGTH

A bottom-fiber stress limit of $0.65f'_{ci}$ (TxDOT Research Project 5197) and a top-fiber stress limit of $6\sqrt{1000f'_{ci}}$ (ACI 318, 2008, Provision 18.4.1) are to be applied.

$$f'_{ci} = \frac{f_{bot}}{0.65} = \frac{4.14\ ksi}{0.65} = 6.4\ ksi \qquad \textit{Equation C.4}$$

where:

f'_{ci} = concrete release strength

$$f_{top} = -1.16\ ksi < -6\sqrt{1000f'_{ci}} = -0.48\ ksi \qquad \textit{Equation C.5}$$

The top-fiber stress limit is not satisfied, so *"additional bonded reinforcement… shall be provided in the tensile zone to resist the entire tensile force with the assumption of an uncracked section"* (ACI 318, Provision 18.4.1).

$$h_{tz} = \frac{f_{top}}{f_{bot} - f_{top}} h = 11.9\ in. \qquad \textit{Equation C.6}$$

where:

h_{tz} = height of tension zone

$$T_{tz} = -\int_{h-h_{tz}}^{h} f\,dy = 195\ kip \qquad \textit{Equation C.7}$$

where:

T_{tz} = tension in top portion of beam to be resisted by longitudinal reinforcement

f = stress in concrete, as a function of depth

$$f_{s,tz} = \frac{T}{A_{s,tz}} = \frac{195\ kip}{4.80\ in.^2} = 41\ ksi \qquad \textit{Equation C.8}$$

where:

$f_{s,tz}$ = stress in tension-zone longitudinal reinforcement

$A_{s,tz}$ = provided longitudinal reinforcement, 4 – #7 in each top flange/web *(double the tension-zone reinforcement compared to TxDOT standard)*

Allowable stress for tension-zone reinforcement at transfer range from 30 ksi (ACI 318, 2008, Provision 18.4.1) to 60 ksi (PCI Design Handbook, 2004, Section 4.2.2.2). Flexural cracking at the top of the beam was not expected to interfere with measurements of transverse-bar strains, as explained in Section 3.2.2.

C.3 PRESTRESS LOSSES FROM ELASTIC SHORTENING OF BEAM

$$f_{cgp} = f_{bot} - \frac{(y_{bot} - e)}{h}(f_{bot} - f_{top})$$

$$f_{cgp} = 4.14\ ksi - \frac{4.1}{54}5.30\ ksi \qquad \textit{Equation C.9}$$

$$f_{cgp} = 3.74\ ksi$$

where:

f_{cgp} = stress in concrete at depth of prestress centroid
h = beam height

$$E_{ci} = 1260\sqrt{f'_{ci}} + 1000 = 1260\sqrt{6.4} + 1000 = 4160\ ksi \qquad \textit{Equation C.10}$$

where:

E_{ci} = elastic modulus of concrete at release

$$\Delta f_{ES} = \frac{E_p}{E_{ci}} f_{cgp} = \frac{28500}{4160}3.74\ ksi = 25.6\ ksi \qquad \textit{Equation C.11}$$

where:

E_p = elastic modulus of prestressing strand

$$\frac{\Delta f_{ES}}{f_{pi}} = \frac{25.6}{202.5} = 12.6\% \qquad \textit{Equation C.12}$$

Actual prestress losses from elastic shortening exceed assumed losses (10%). After a few iterations, convergence is reached, and design values are as shown in Table C.1

Table C.1 Specimen Design for Beams 1 & 2

Parameter	Design Value
Concrete release strength, f'_{ci}	6.3 ksi
Bottom-fiber stress, f_{bot}	4.04 ksi
Top-fiber stress, f_{top}	-1.14 ksi
Height of tension zone, h_{tz}	11.9 in.
Tension in top portion of beam, T_{tz}	190 kip
Stress in tension-zone longitudinal reinforcement, $f_{s,tz}$	40 ksi
Stress in concrete at depth of prestress centroid, f_{cgp}	3.65 ksi
Concrete elastic modulus at release, E_{ci}	4210 ksi
Prestress losses from elastic shortening, Δf_{ES}	24.8 ksi
Prestress loss ratio, $\Delta f_{ES}/f_{pi}$	12.2%

APPENDIX D

Concrete and Reinforcement Mechanical Test Results

D.1 Concrete Strength Results

D.1.1 Beam 1

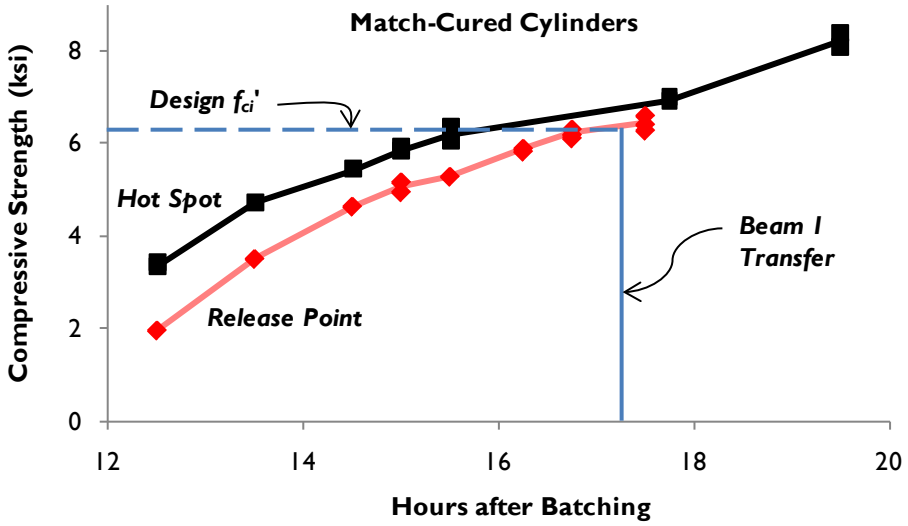

Figure D.1 Beam 1 match-cured cylinder compressive strengths

Table D.1 Beam 1 match-cured cylinder compressive strengths

Hours after Batching	Release Point f_c' (ksi)	
12.5	1.98	1.98
13.5	3.53	3.53
14.5	4.66	4.66
15	4.97	5.07
15	5.18	
15.5	5.30	5.30
16.25	5.84	5.87
16.25	5.90	
16.75	6.13	6.22
16.75	6.20	
16.75	6.32	
17.5	6.29	6.44
17.5	6.42	
17.5	6.61	

Hours after Batching	Hot Spot f_c' (ksi)	
12.5	3.34	3.38
12.5	3.41	
13.5	4.74	4.74
14.5	5.44	5.44
15	5.91	5.87
15	5.83	
15.5	6.08	6.23
15.5	6.38	
17.75	6.92	6.96
17.75	6.99	
19.5	8.39	8.24
19.5	8.09	

Table D.2 Beam 1 match-cured cylinder splitting-tensile strength at release

Hours after Batching	Top Flange f_{sp}' (ksi)	
18	0.79	0.77
18	0.83	
18	0.68	

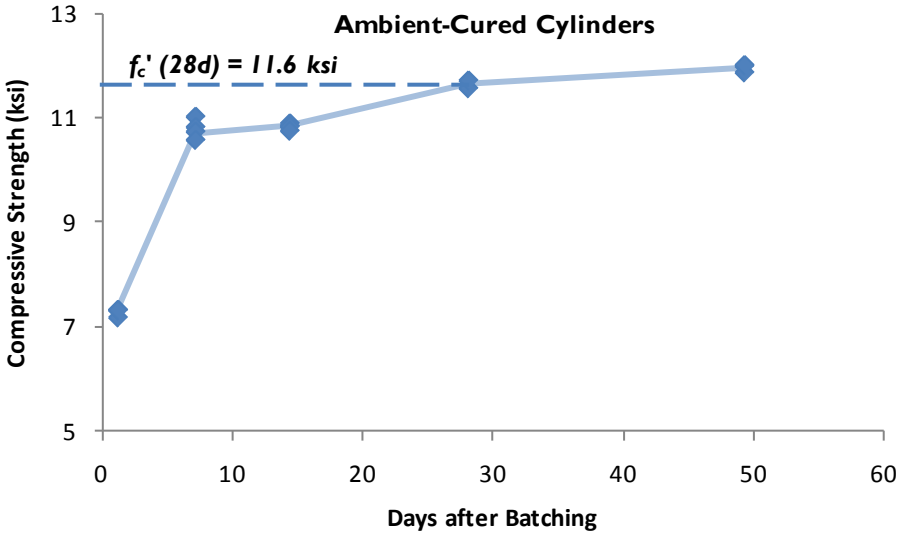

Figure D.2 Beam 1 ambient-cured cylinder compressive strengths

Table D.3 Beam 1 ambient-cured cylinder compressive strengths

Days after Batching	Ambient f_c' (ksi)	
1.1	7.19	7.30
1.1	7.34	
1.1	7.34	
1.1	7.34	
7.1	11.03	10.80
7.1	10.83	
7.1	10.74	
7.1	10.58	
14.3	10.90	10.84
14.3	10.85	
14.3	10.84	
14.3	10.76	
28.1	11.57	11.65
28.1	11.72	
49.3	11.99	11.96
49.3	11.87	
49.3	12.02	

D.1.2 Beam 2

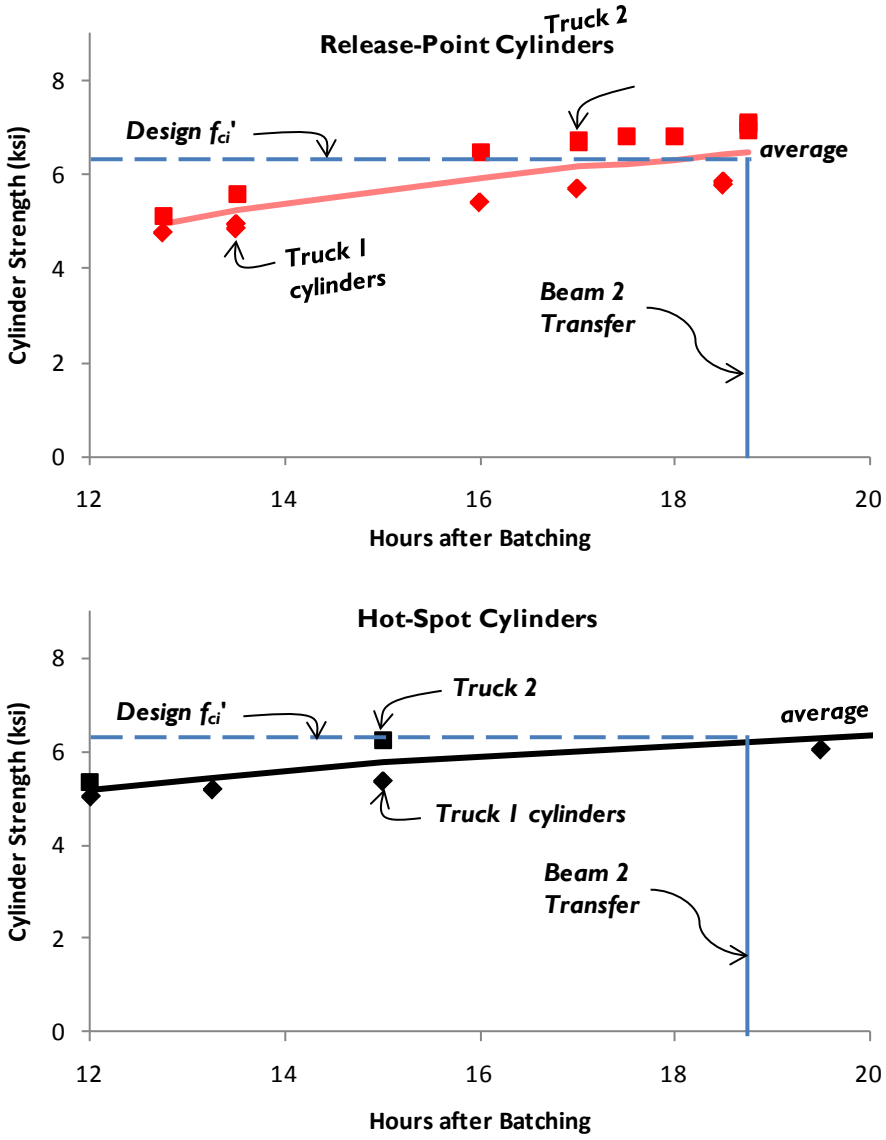

Figure D.3 Beam 2 match-cured cylinder compressive strengths

Table D.4 Beam 2 match-cured cylinder compressive strengths

Hours after Batching	Truck	Release Point f_c' (ksi)	
12.75	1	4.74	4.74
12.75	2	5.13	5.13
13.5	1	4.93	4.93
13.5	2	5.61	5.61
13.5	1	4.83	5.11
16		5.39	
16	2	6.49	6.49
17	1	5.68	5.68
17	2	6.70	6.77
17.5		6.80	
18		6.81	
18.5	1	5.76	5.80
18.5		5.83	
18.75	2	6.95	7.03
18.75		7.10	
18.75		7.05	

Hours after Batching	Truck	Hot Spot f_c' (ksi)	
12	1	5.05	5.05
12	2	5.34	5.34
13.25	1	5.20	5.28
15		5.37	
15	2	6.25	6.25
19.5	1	6.05	6.79
31		7.27	
31		7.06	
31	2	8.23	8.08
31		7.93	

Table D.5 Beam 2 match-cured cylinder splitting-tensile strength at release

Hours after Batching	Truck	Top Flange f_{sp}' (ksi)	
18	1	0.540	0.545
18		0.540	
18		0.570	
18		0.530	
18	2	0.600	0.600
18		0.600	

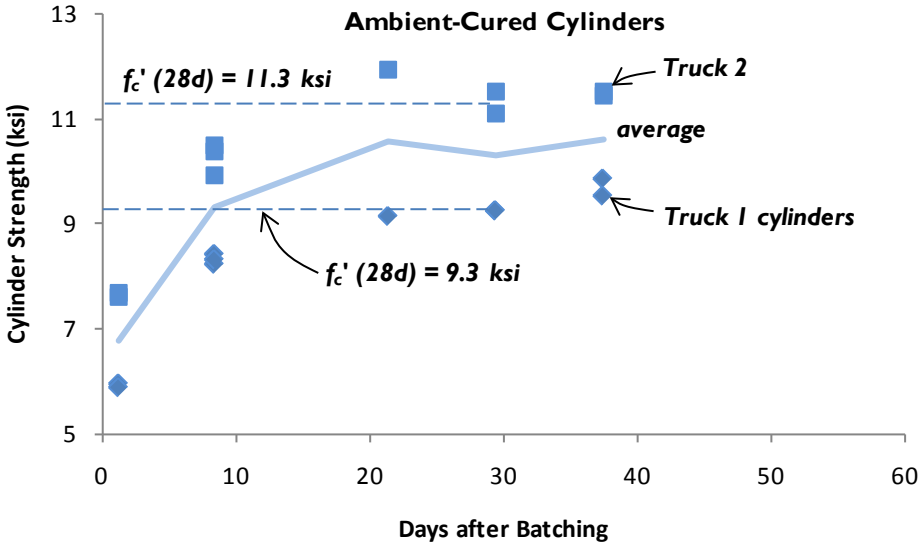

Figure D.4 Beam 2 ambient-cured cylinder compressive strengths

Table D.6 Beam 2 ambient-cured cylinder compressive strengths

Days after Batching	Truck	Ambient f_c' (ksi)	
1.2	1	5.95	5.92
1.2		5.88	
1.2	2	7.70	7.66
1.2		7.62	
8.4	1	8.24	8.33
8.4		8.43	
8.4		8.32	
8.4	2	9.93	10.27
8.4		10.50	
8.4		10.38	
21.4	1	9.15	9.15
21.4	2	11.94	11.94
29.4	1	9.25	9.26
29.4		9.26	
29.4	2	11.53	11.32
29.4		11.11	
37.4	1	9.87	9.70
37.4		9.54	
37.4	2	11.51	11.48
37.4		11.46	
42.3	1	9.70	9.70
42.3	2	12.25	12.06
42.3		11.87	

D.2 Reinforcing-Bar Modulus & Strength Results

Table D.7 Grade-60-rebar moduli, yield & tensile strengths

Beam	Sample	E_s (ksi)	f_{sy} (ksi)	f_{su} (ksi)
1	A	--	61	101
1	B	--	65	93
2	A	--	61	101
2	B	--	67	109
2	C	--	66	108
2	D	30,700	68	111
2	E	28,200	65	109
2	F	28,100	65	109
2	G	29,100	66	110
mean		29,000	65	106
c.o.v.		4.2%	3.7%	5.6%

Table D.8 Deformed-wire moduli, yield & tensile strengths

Beam	Sample	E_s (ksi)	f_{sy} (ksi)	f_{su} (ksi)
2	A	--	87	96
2	B	--	87	96
2	C	--	88	97
2	D	31,100	80	97
mean		31,100	86	96
c.o.v.		--	4.8%	0.5%

D.3 PRESTRESSING-STRAND MODULUS & STRENGTH RESULTS

Table D.9 Prestressing-strand elastic moduli & tensile strengths (Beam 1)

Beam	Strand Row	Sample	E_p (ksi)		f_{pu} (ksi)
			Engineering	Modified	
1	1	A	28,100	29,900	--
1	1	B	27,800	29,300	--
1	2	C	27,300	30,100	--
1	2	D	27,300	29,300	281
1	3	E	28,500	--	291
1	3	F	28,000	31,300	291
mean			27,800	30,000	287
c.o.v.			1.7%	2.8%	2.0%

Table D.10 Prestressing-strand elastic moduli (Beam 2)

Beam	Strand Row	Sample	E_p (ksi)		f_{pu} (ksi)
			Engineering	Modified	
2	2	A	28,900	31,100	--
2	2	B	28,700	30,400	--
2	2	C	29,100	31,200	--
2	2	D	28,800	30,600	--
2	3	E	28,500	30,400	--
2	3	F	28,400	30,900	--
mean			28,700	30,800	--
c.o.v.			0.9%	1.1%	--

APPENDIX E

End-Block Temperature Profiles

E.1 BEAM 1

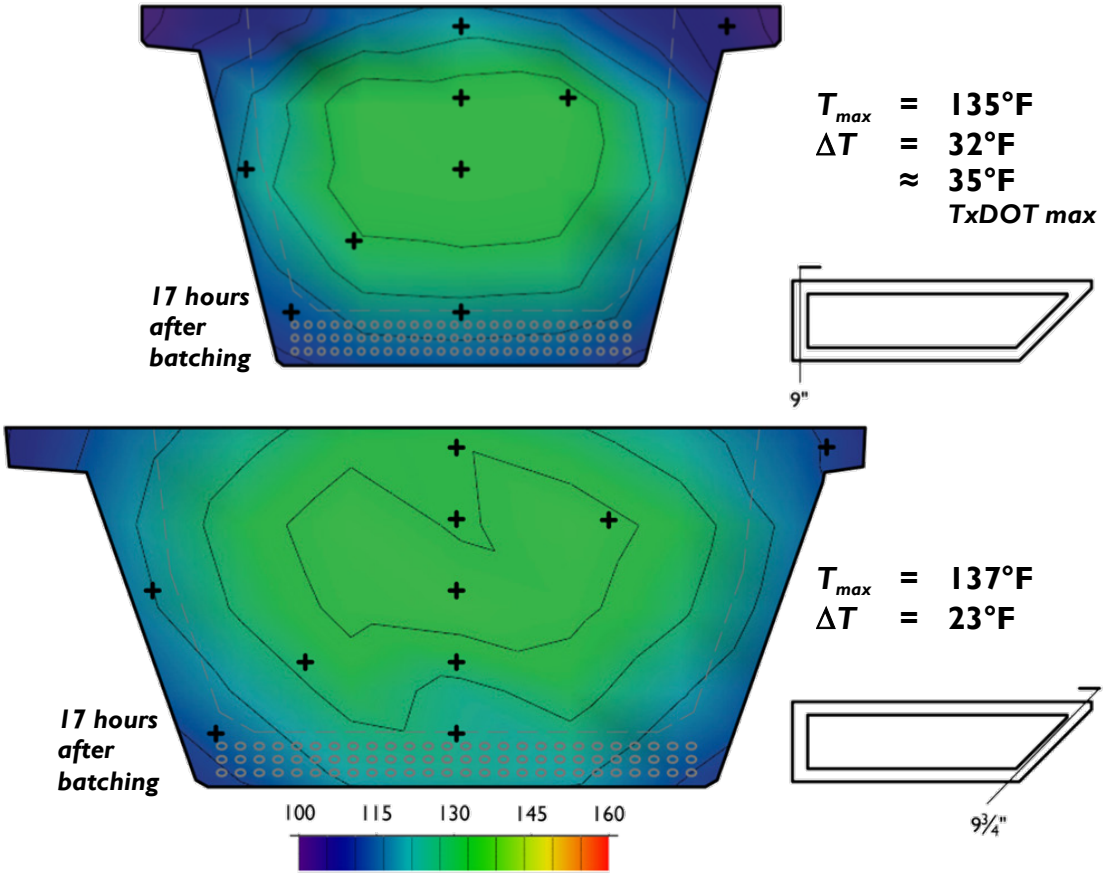

Figure E.1 Beam 1 temperature profiles, at transfer of prestress

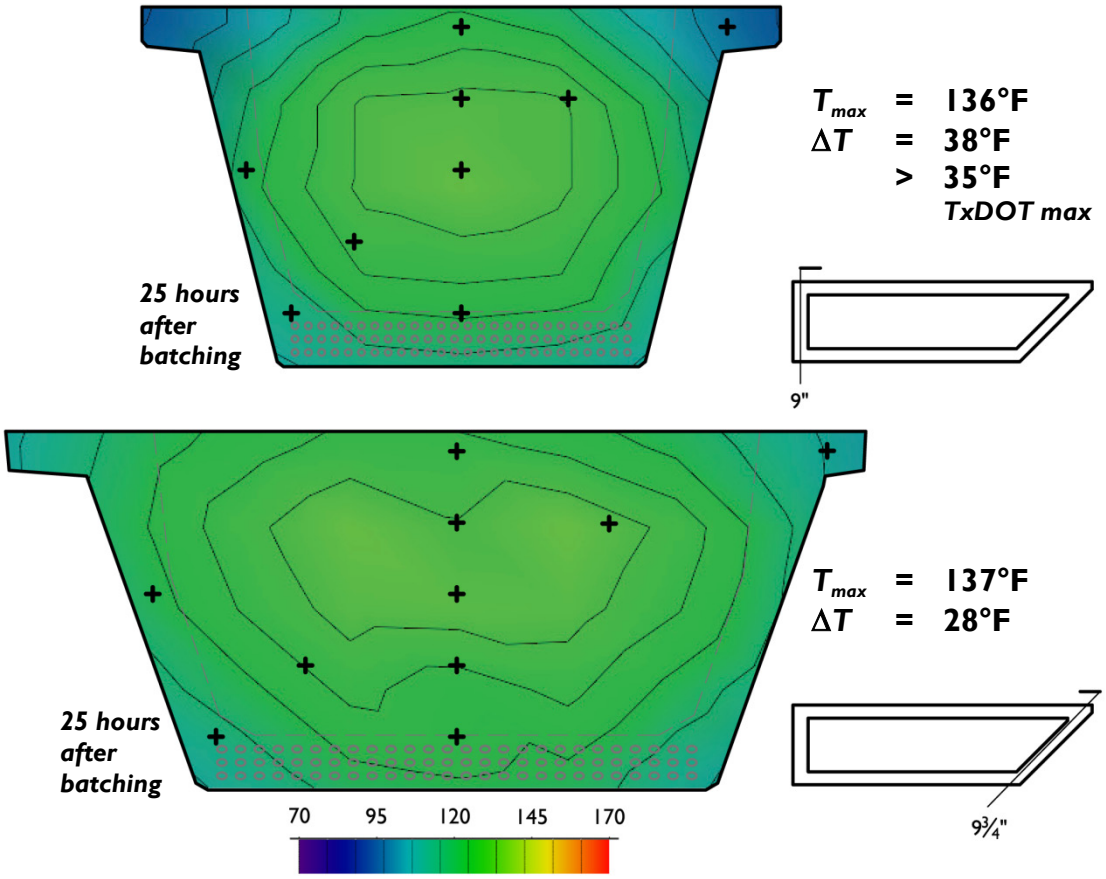

Figure E.2 Beam 1 temperature profile at time of maximum temperature differential

E.2 BEAM 2

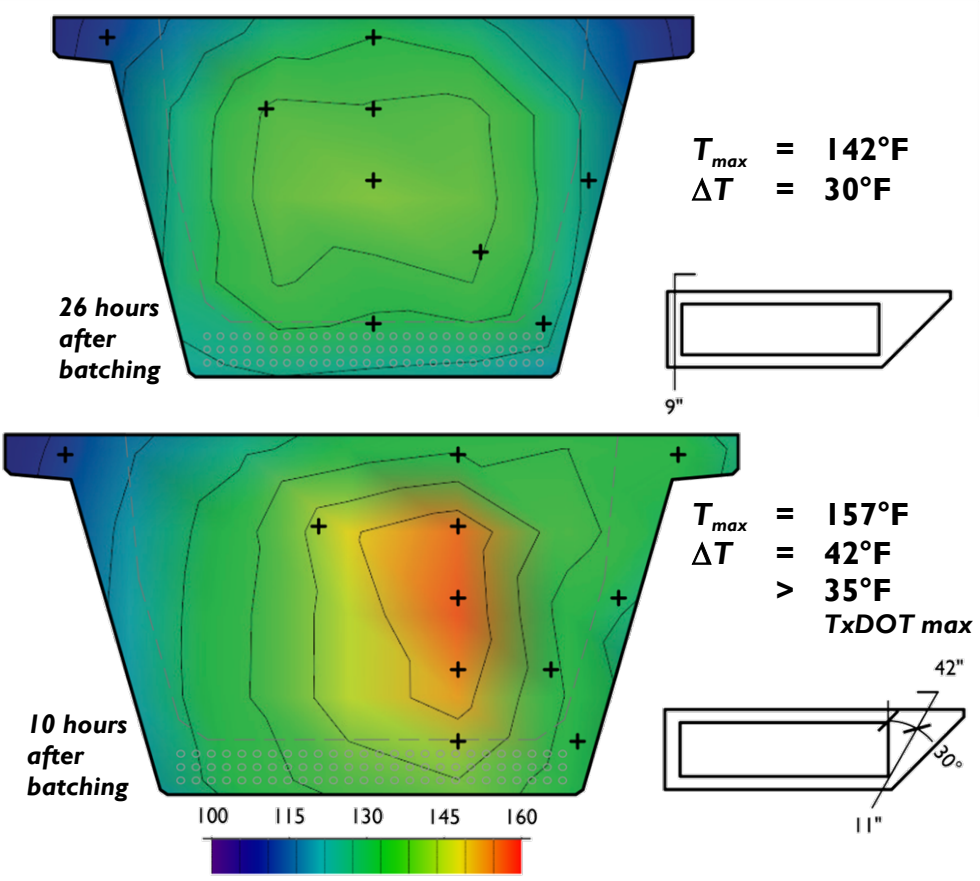

Figure E.3 Beam 2 temperature profile, at transfer of prestress

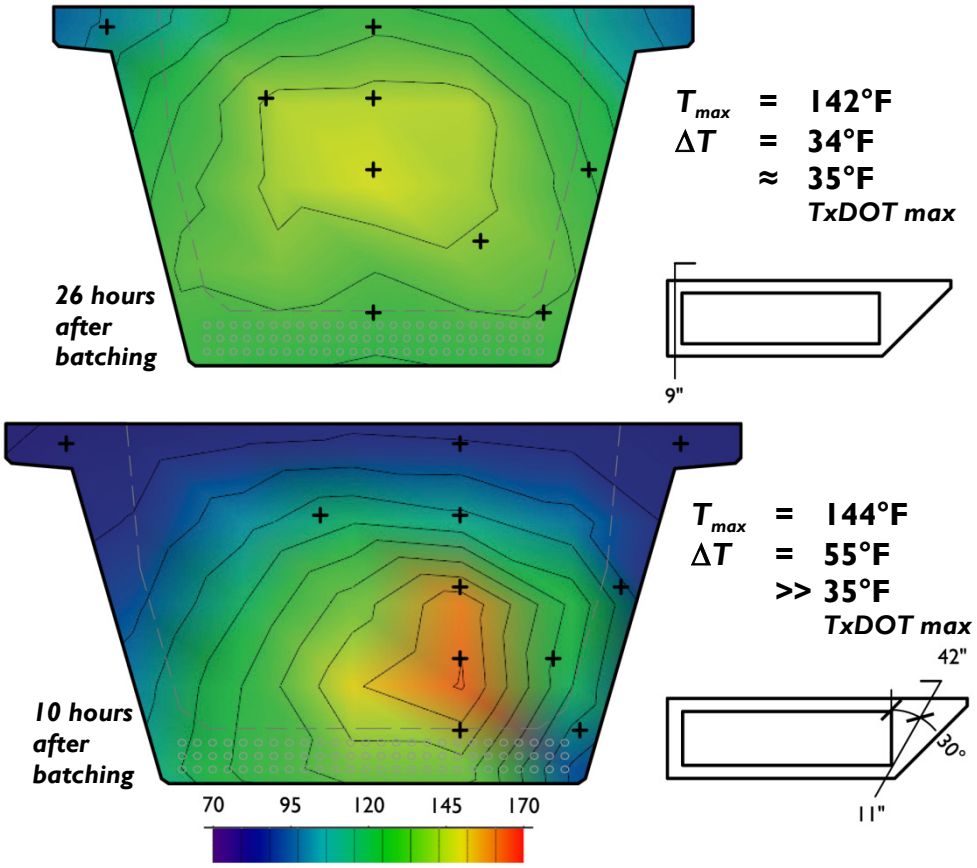

Figure E.4 Beam 2 temperature profile at time of maximum temperature differential

REFERENCES

REFERENCED STANDARDS

American Association of State Highway and Transportation Officials or Equivalent (Washington)

Standard Specifications for Highway Bridges 8th ed (1961).

Standard Specifications for Highway Bridges 8th ed., Interim (1961).

Standard Specifications for Highway Bridges 11th ed (1973).

AASHTO LRFD Bridge Design Specifications 1st ed (1994).

AASHTO LRFD Bridge Design Specifications 1st ed., Interim (1996).

AASHTO LRFD Bridge Design Specifications 2nd ed., Interim (2000).

AASHTO LRFD Bridge Design Specifications 2nd ed., Interim (2002).

AASHTO LRFD Bridge Design Specifications 4th ed., Interim (2008).

AASHTO LRFD Bridge Design Specifications 4th ed., Interim (2009).

American Concrete Institute, Committee 318 (Farmington Hills, MI)

Building Code Requirements for Reinforced Concrete and Commentary (1963).

Building Code Requirements for Reinforced Concrete and Commentary (1971).

Building Code Requirements for Structural Concrete and Commentary (1998).

Building Code Requirements for Structural Concrete and Commentary (2008).

American Concrete Institute, Other Committees

ACI Committee 224 (1972), "Control of Cracking in Concrete Structures," *ACI Journal*, Vol. 69, No. 12, pp. 717-752.

ACI-ASCE Joint Committee 323 (1958), "Tentative Recommendations for Prestressed Concrete," *ACI Journal*, Vol. 54, No. 1, pp. 545-578.

ACI Committee 363 (1992), *Report on High-Strength Concrete*, 55 pp.

American Society for Testing and Materials (West Conshohooken, PA)

A 36 Specification for Carbon Structural Steel.

A 615 Standard Specification for Deformed and Plain Carbon-Steel Bars for Concrete Reinforcement.

C 39 Standard Test Method for Compressive Strength of Cylindrical Concrete Specimens.

C 143 Standard Test Method for Slump of Hydraulic-Cement Concrete.

C 192 Practice for Making and Curing Concrete Test Specimens in the Laboratory.

C 496 Standard Test Method for Splitting Tensile Strength of Cylindrical Concrete Specimens.

Department of Transportation Standard Drawings

Florida DOT (2008), *Florida U 54 – Standard Details*.

Texas DOT (2006), *Prestressed Concrete U-Beam Standards*.

Texas DOT (2007), *Prestressed Concrete I-Girder Standards*.

Washington State DOT (2007), *Precast Trapezoidal Tub Girder Details* and *Trapezoidal Tub S-I-P Deck Panel Girder Details*.

Fédération Internationale du Béton or Equivalent (Lausanne, Switzerland)

CEB-FIP Model Code (1978).

CEB-FIP Model Code (1990).

Precast and Prestressed Concrete Institute (Chicago)

PCI Committee on Quality Control Performance Criteria (1985) "Fabrication and Shipment Cracks in Precast or Prestressed Beams and Columns," *PCI Journal*, Vol. 30, No. 3, pp. 2-27.

PCI Design Handbook 5th ed (1999).

PCI Design Handbook 6th ed (2004).

PCI Manual for the Evaluation and Repair of Precast, Prestressed Concrete Bridge Products (2006).

Texas Department of Transportation (Austin)

Bridge Design Manual – LRFD (2009).

Making and Curing Concrete Test Specimens, Tex-447-A (2004).

CITED REFERENCES

Arthur, P.D. & Ganguli, S. (1965), "Tests on End-Zone Stresses in Pre-Tensioned Concrete I Beams," *Magazine of Concrete Research*, Vol. 17, No. 51, pp. 85-96.

Barrios, A.O. (1994), *Behavior of High Strength Concrete Pretensioned Girders During Transfer of Prestressing Forces*, Thesis, The University of Texas at Austin, 146 pp.

Base, G.D. (1958), *An Investigation of Transmission Length in Pre-Tensioned Concrete*, Cement and Concrete Association Research Report No. 5, 29 pp.

Birrcher, D.B. (2006), *Effects of Increasing the Allowable Compressive Stress at Release of Prestressed Concrete Girders*, Thesis, The University of Texas at Austin, 285 pp.

Bleich, F. (1923), "Der Gerade Stab mit Rechteckquerschnitt als ebenes problem" (A Straight Rod with a Rectangular Cross-Section as a Plane Problem), *Der Bauingeneur*, No. 9, pp. 304-307.

Breen, J.E. et al. (1994), *Anchorage Zone Reinforcement for Post-Tensioned Concrete Girders*, NCHRP Report 356, National Academy Press, Washington, 204 pp.

Bungey, J.H. & Millard, S.G. (1996), *Testing of Concrete Structures* 3rd ed., Chapman & Hall, London, 286 pp.

Collins, M.P. & Mitchell, D.A. (1997), *Prestressed Concrete Structures*, Response Publications, Toronto, 766 pp.

Crispino, E.D. (2007), *Anchorage Zone Design for Pretensioned Bulb-Tee Bridge Girders in Virginia*, Thesis, Virginia Polytechnic Institute and State University, Blacksburg, VA, 155 pp.

Davis, R.T.; Buckner, C.D. & Ozyildirim, C. (2005), "Serviceability-Based Design Method for Vertical Beam End Reinforcement," *Proceedings of PCI National Bridge Conference*, Palm Springs, CA, 16-19 Oct 2005.

Endicott, W.A. (2005), "A Fast Learning Curve," *Ascent*, Vol. 10, No. 3, pp. 36-49.

Folliard, K.J. et al. (2006), *Preventing ASR/DEF in New Concrete: Final Report*, Center for Transportation Research Report 0-4085-5, The University of Texas at Austin, 234 pp.

Folliard, K.J. (2008), Lecture Notes from *Advanced Concrete Materials*, CE 393, The University of Texas at Austin, Fall 2008.

Fountain, R.S. (1963), *A Field Inspection of Prestressed Concrete Bridges*, Portland Cement Association, Skokie, IL, 50 pp.

Gamble, W.L. (1997) "Comments on 'Release Methodology of Strands to Reduce End Cracking in Pretensioned Concrete Girders' by Kannel, French & Stolarski," *PCI Journal*, Vol. 42, No. 4, pp. 102-103.

Gergely, P.; Sozen, M.A. & Siess, C.P. (1963), *The Effect of Reinforcement on Anchorage Zone Cracks in Prestressed Concrete Members*, University of Illinois Structural Research Series No. 271, 170 pp.

Gergely, P. & Sozen, M.A. (1967), "Design of Anchorage Zone Reinforcement in Prestressed Concrete Beams," *PCI Journal*, Vol. 12, No. 4, pp. 63-75.

Gross, S.P. & Burns, N.H. (2000), *Field Performance of Prestressed High Performance Concrete Highway Bridges in Texas*, FHWA Report FHWA/TX-05/9-508/589-2, 655 pp.

Guyon, Y. (1955), *Prestressed Concrete* 2nd ed. (English translation), F.J. Parsons, London, 543 pp.

Hawkins, N. (1966), "The Behaviour and Design of End Blocks for Prestressed Concrete," *Civil Engineering Transactions*, Vol. 8, No. 1, pp. 193-202.

Holt, J. (2008), TxDOT, Personal Communications.

Huang, D. & Shahawy, M. (2005), "Analysis of Tensile Stresses in Transfer Zone of Prestressed Concrete U-Beams," *Transportation Research Record*, No. 1928, pp. 134-141.

Itani, R.Y. & Galbraith, R.L. (1986), *Design of Prestressed Concrete Girders Without End Blocks*, WSDOT Report WA-RD 81, 119 p.

Iyengar, K.T.S.R. (1962), "Two-Dimensional Theories of Anchorage Zone Stresses in Post-Tensioned Prestressed Beams," *ACI Journal*, Vol. 59, No. 10, pp. 1443-1466.

Kannel, J.; French, C. & Stolarski, H. (1997), "Release Methodology of Strands to Reduce End Cracking in Pretensioned Concrete Girders," *PCI Journal*, Vol. 42, No. 1, pp. 42-54.

Kapur, J. & Wilson, D. (2008), "Concrete Bridges in Washington State," *Aspire*, Vol. 1, No. 3, pp. 46-48.

Khaleghi, B. (2006), *Splitting Resistance of Pretensioned Anchorage Zones*, WSDOT Design Memorandum, 23 Dec 2006.

Krishnamurthy, D. (1970), "The Effect of the Method of Prestress Transfer on the End-Zone Stresses and Transmission Length of Pre-Tensioned Beams," *Indian Concrete Journal*, Vol. 44, No. 3, pp. 110-117.

Lenschow, R.J. & Sozen, M.A. (1965), "Practical Analysis of the Anchorage Zone Problem in Prestressed Beams," *ACI Journal*, Vol. 62, No. 79, pp. 1421-1439.

Leonhardt, F. (1964), *Prestressed Concrete Design and Construction* 2nd ed. (English translation), Wilhelm Ernst und Sohn, Berlin, 677 pp.

Lin, T.Y. & Burns, N.H. (1981), *Design of Prestressed Concrete Structures* 3rd ed., John Wiley & Sons, New York, 646 pp.

Marek, M.A. (2008), *Special Statewide Provision 424-01 (04), "Precast Concrete Structures (Fabrication)"*, TxDOT Special Provision and/or Specification Change Memorandum 17-08, 14 May 2008.

Marshall, W.T. & Mattock, A.H. (1962), "Control of Horizontal Cracking in the Ends of Pretensioned Prestressed Concrete Girders," *PCI Journal*, Vol. 7, No. 10, pp. 56-75

McMullen, M.L.; Elkaissi, J.I. & Leonard, M.A. (2008), "Long-Span Precast U-Girders in Colorado," *Aspire*, Vol. 2, No. 3, pp. 64-66.

Mertz, D.R. (2008), "AASHTO LRFD: 2008 Interim Changes, Part 1," *Aspire*, Vol. 2, No. 1, p. 56.

Mindess, S.; Young, J.F. & Darwin, D. (2003), *Concrete* 2nd ed., Prentice Hall, Upper Saddle River, NJ, 644 pp.

Nickas, W.N. (2004), *FDOT Structures Design Guidelines: Concrete Release Strength and Maximum Bonded Prestress*, FDOT Temporary Design Bulletin C04-01, 3 Feb 2004.

Nolan, S.J. (2004), *Bursting Forces in FDOT Prestressed Beams*, Presentation for FICE/FDOT Design Conference, Orlando, Aug 2004.

O'Callaghan, M.R. (2007), *Tensile Stresses in the End Regions of Pretensioned I-Beams at Release*, Thesis, The University of Texas at Austin, 265 pp.

Ralls, M.L.; Ybanez, L. & Panak, J.J. (1993), "The New Texas U-Beam Bridges: An Aesthetic and Economical Design Solution," *PCI Journal*, Vol. 38, No. 5, pp. 20-29.

Sanders, D.H. (1990), *Design and Behavior of Anchorage Zones in Post-Tensioned Concrete Members*, Dissertation, The University of Texas at Austin, 574 pp.

Sargious, M. (1960), *Beitrag zur Ermittlung der Hauptzugspannungen am Endauflager vorgespannter Betonbalken* (Contribution to the Investigation of Principal Tensile Strains in Prestressed Concrete Beam End Regions), Dissertation, University of Stuttgart (Germany).

Sarles, D. & Itani, R.Y. (1984), "Effect of End Blocks on Anchorage Zone Stresses in Prestressed Concrete Girders," *PCI Journal*, Vol. 29, No. 6, pp. 100-114.

Scott, N.L. (2004), "Reflections on the Early Precast/Prestressed Concrete Industry in America," *PCI Journal*, Vol. 49, No. 2, pp. 20-33.

Schindler, A.K. & Folliard, K.J. (2005), "Heat of Hydration Models for Cementitious Materials," *ACI Materials Journal*, Vol. 102, No. 1, pp. 24-33.

Schlaich, J.; Schäfer, K. & Jennewein, M. (1987), "Toward a Consistent Design of Structural Concrete," *PCI Journal*, Vol. 32, No. 3, pp. 74-150.

Schnittker, B.A. (2008), *Allowable Compressive Stress at Prestress Transfer*, Thesis, The University of Texas at Austin, 225 pp.

Sievers, H. (1956), "Über den Spannungszustand in Bereich der Ankerplatten von Spanngliedem in vogespannten Stahlbetonkonstmctionen" (Stress Condition in the Vicinity of Anchorage Plates of Prestressed Tendons in Prestressed Concrete Struchual Units), *Der Bauingenieur*, Vol. 31, No.4, pp. 134-135.

Smith, M. et al. (2008), *Monitoring and Analysis of Mn/DOT Precast Composite Slab Span System (PCSSS)*, MnDOT Report MN/RC 2008-41,110 pp.

Stone, W.C. & Breen, J.E. (1984), "Behavior of Post-Tensioned Girder Anchorage Zones," *PCI Journal*, Vol. 29, No. 1, pp. 64-107.

Stone, W.C. & Breen, J.E. (1984), "Design of Post-Tensioned Girder Anchorage Zones," PCI Journal, Vol. 29, No. 2, pp. 28-61.

Tadros, M.K. (2005), *Past, Present and Future of Precast Prestressed Concrete Bridges in the U.S.*, Presentation for First Brazilian Meeting on Integration of Research-Design-Production in the Field of Precast Concrete, São Paulo, Nov 2005.

Tadros, M.K. et al. (2003), *Prestress Losses in Pretensioned High-Strength Concrete Bridge Girders*, NCHRP Report 496, Transportation Research Board, Washington, 63 pp.

Tadros, M.K. et al. (2007), *Evaluation and Repair Procedures for Precast/Prestressed Concrete Girders with Longitudinal Cracking in the Web*, NCHRP 18-14 Interim Report, Transportation Research Board, Washington, DC, 120 pp.

Tadros, M.K.; Yehia, S.A. & Jongpitaksseel, N. (2003), *Prestressed Beam End Reinforcement and Camber*, Nebraska Department of Roads Project SPR-PL-1 (038) P536, Lincoln, 145 pp.

Thorson, N. (1955), "Use of Large Tendons in Pre-Tensioned Concrete", *ACI Journal*, Vol. 52 No. 2, pp. 649-659.

Timoshenko, S.P. & Goodier, J.N. (1934, 1970), *Theory of Elasticity*, McGraw-Hill, New York, 567 pp.

Tuan, C.Y. et al. (2004), "End Zone Reinforcement for Pretensioned Concrete Girders," *PCI Journal*, Vol. 49, No. 3, pp. 68-82.

Tuchsherer, R. (2007), *Tensile Stress Limit for Prestressed Concrete at Release*, Presentation for Prestressed Concrete, CE 383P Course, The University of Texas at Austin, 5 Nov 2007.

Uijl, den J.A. (1983), *Tensile Stresses in the Transmission Zones of Hollow-Core Slabs Prestressed with Pretensioned Strands*, Delft University of Technology Report 5-83-10 (Stevin Laboratory Report SR-49), 110 pp.

Wang, X.Y.; Lee, H.S. & Park, K.B. (2009), "Simulation of Low-Calcium Fly Ach Blended Cement Hydration," *ACI Materials Journal*, Vol. 106, No. 2, pp. 167-175.

Willis, L.K. (1963), "Discussion of 'Control of Horizontal Cracking in the Ends of Pretensioned Prestressed Concrete Girders' by Marshall and Mattock," *PCI Journal*, Vol. 8, No. 2, pp. 76-79.

Yettram, A.L. & Robbins, K. (1969), "Anchorage Zone Stresses in Axially Post-Tensioned Concrete Members of Uniform Rectangular Section," *Magazine of Concrete Research*, Vol. 21, No. 67, pp. 103-112.

Yettram, A.L. & Robbins, K. (1971), "Anchorage Zone Stresses in Axially Post-Tensioned I-Section Members with End Blocks," *Magazine of Concrete Research*, Vol. 23, No. 74, pp. 37-42.

Zieliński, J. & Rowe, R.E. (1960), *An Investigation of the Stress Distribution in the Anchorage Zones of Post-Tensioned Concrete Members*, Cement and Concrete Association Research Report No. 9, 32 pp.

Zieliński, J. & Rowe, R.E. (1962), *The Stress Distribution Associated with Groups of Anchorages in Post-Tensioned Concrete Members*, *Cement and Concrete Association Research Report* No. 13, 39 pp.

VITA

David Andrew Dunkman was born 25 August 1984 in Cincinnati, OH to Bob and Ruth Dunkman. Spending his childhood in the western suburban Chicago, Dunkman attended Northwestern University (Evanston, IL), where he was awarded his Bachelor of Science in Civil Engineering *cum laude* in June 2007. During the final year of his undergraduate work (June 2006 to August 2007), Dunkman interned with Wiss, Janney, Elstner Associates. In August 2007, he moved from Illinois to Texas, to pursue a graduate education in Civil Engineering (Structures) at The University of Texas at Austin, and began work at the Ferguson Structural Engineering Laboratory.

This thesis was typed by the author.